A systematic investigation of sulphide scale formation and inhibition

Bader Ghazi Alharbi

Submitted for the Degree of Doctor of Philosophy

Institute of GeoEnergy Engineering

School of Energy, Geoscience, Infrastructure and Society

Heriot-Watt University

January 2020

Abstract

This thesis presents an investigation of the formation, inhibition and interaction of iron sulphide (FeS), zinc sulphide (ZnS) and lead sulphide (PbS) scales. Several scale inhibitors were tested for their inhibition efficiency against these scales, including a selection of commonly used scale inhibitors (SIs), such as phosphonates and polymers, as well as proprietary high molecular weight sulphonated co-polymers. An extensive series of sulphide scale formation and ion displacement experiments were also carried out using slightly modified experimental sequences in the testing procedures. The purpose of these latter experiments was to establish whether the precise details of the experiment, such as the sequence of scale formation, affected the overall efficiency of the SI.

Of the tested SIs, only two showed reasonable promise for inhibiting all three sulphide scales, while some polymeric scale inhibitors prevented the deposition of ZnS and PbS in 3.5 wt% NaCl but failed to inhibit FeS. The impact of pH, temperature, salinity and scale inhibitor concentration on the inhibition efficiency and particle size of inhibited scale was also investigated. Increasing the pH and salinity had a detrimental impact on the performance of one of the proprietary scale inhibitors *i.e.* SI-3.

None of the tested phosphonate scale inhibitors showed any field-appropriate inhibition effect on any of the sulphide scales. On the other hand, some tested polymeric scale inhibitors did inhibit ZnS and PbS, but none of them prevented the deposition of FeS; however, a significant reduction in the particle size of the FeS was observed for some SIs. In the presence of SI-1 (polyphosphino carboxylic acid, PPCA), it was noted that scale inhibitor "consumption" (i.e. the SI was removed from the solution) took place for ZnS and PbS solutions but not in FeS solutions.

It was seen to be easier to inhibit ZnS and PbS when they formed concurrently rather than by subsequent formation of PbS then ZnS. In cation displacement experiments, PbS deposition was prevented provided that the preformed ZnS was inhibited.

Dedication

To my father soul, and my mother for their love and continuous support.

To my wife Mashael Alharbi for her love and patience.

To my children Nader and Naser

Acknowledgements

First of all, I would like to thank my supervisor Professor Ken Sorbie for his supervision, guidance and encouragement throughout my PhD study. Also, my gratitude is extended to Dr Alexander Graham for supervision and informative discussions.

I would like to appreciate the constructive feedback from Professor Eric Mackay, Dr Lorraine Boak and Mike Singleton.

Special thanks go to Wendy McEwan, Lorraine Boak and Katherine McIver in the FAST Analytical Team at Heriot-Watt University are thanked for performing ICP-OES analysis. Katherine McIver is also thanked for training me how to perform the scale inhibition experiments.

Jim Buckman and Alexander Graham are thanked for support with use of the ESEM facility at Heriot-Watt University.

Norah Aljeaban and Yaser Al-Duailej are acknowledged for their advice and help.

Saudi Aramco for sponsoring my PhD.

Ghaithan Al-Muntashari and my advisor Ben Williams are thanked for their support.

I would also like to thank Heather O'Hara for the administrative support.

Lastly, I would like to thank all the members of the FAST group (past and present) for making my experience in Heriot-Watt University filled with joy.

Research Thesis Submission

Name*:*	Bader Ghazi Alharbi		
School:	Energy, Geoscience, Infrastructure and Society		
Version: *(i.e. First, Resubmission, Final)*	Final Submission	Degree Sought:	Doctor of Philosophy (PhD) Petroleum Engineering

Declaration

In accordance with the appropriate regulations I hereby submit my thesis and I declare that:

1) the thesis embodies the results of my own work and has been composed by myself
2) where appropriate, I have made acknowledgement of the work of others and have made reference to work carried out in collaboration with other persons
3) the thesis is the correct version of the thesis for submission and is the same version as any electronic versions submitted*
4) my thesis for the award referred to, deposited in the Heriot-Watt University Library, should be made available for loan or photocopying and be available via the Institutional Repository, subject to such conditions as the Librarian may require
5) I understand that as a student of the University I am required to abide by the Regulations of the University and to conform to its discipline.
6) I confirm that the thesis has been verified against plagiarism via an approved plagiarism detection application *e.g.* Turnitin.

** Please note that it is the responsibility of the candidate to ensure that the correct version of the thesis is submitted.*

Signature of Candidate*:*		Date:	01/16/2020

Submission

Submitted By *(name in capitals):*	
Signature of Individual Submitting:	
Date Submitted:	

For Completion in the Student Service Centre (SSC)

Received in the SSC by *(name in capitals):*			
Method of Submission *(Handed in to SSC; posted through internal/external mail):*			
E-thesis Submitted (mandatory for final theses)			
Signature:		Date:	

Table of Contents

List of Figures

List of Tables

Publications

Al-Harbi, B.G., Graham, A. and Sorbie, K. 2018. Iron Sulphide Inhibition and Interaction with Zinc and Lead Sulphide. SPE Production and Operations 1-13.

Al-Harbi, B.G., Graham, A. and Sorbie, K. 2018. Laboratory Investigation of Zinc and Lead Sulphide Inhibition. SPE International Conference and Exhibition on Formation Damage Control, Lafayette, USA, 7-9 Feb. (This paper is currently undergoing peer-review for the SPE Production and Operations Journal).

Al-Harbi, B.G., Alduailej, Y., Graham, A. and Sorbie, K. 2018. Systematic Investigation of Iron Sulphide and Iron Hydroxide Inhibition. NACE 2018.

Al-Harbi, B. G., Graham, A. J. and Sorbie, K. S. 2017. Zinc and Lead Interactions in Combined Sulphide Scales. SPE International Conference on Oilfiled Chemistry, Montgomery, Texas, USA, 3-5 April.

Graham, A.J., **Al-Harbi, B.G**., Singleton, M.A., *et al*., 2017. Cation Exchange in Sulphide Scales. RSC Chemistry in the Oil Industry symposium, Manchester, UK, 6-8 November.

Chapter 1

Introduction and Literature Review

1.1 Background and motivation

There are several types of inorganic scale experienced in the oil and gas industry but the most common are sulphates, such as calcium sulphate, barium sulphate, strontium sulphate and carbonates, such as calcium carbonate and iron carbonate. Iron sulphides (FeS) are also commonly experienced, especially associated with corrosion-driven iron generation in the presence of H_2S gas. Less common, but of increasing concern, are zinc sulphide (ZnS) and lead sulphide (PbS), which are often referred to as "exotic" scales.

The sulphide scales ZnS and PbS have been observed in high temperature high pressure (HT/HP) oil and gas fields. Their deposition can pose safety hazards and have serious economic consequences, including reduction in well productivity, and may require the implementation of an effective scale mitigation and removal strategy. HT/HP fields are prone to critical changes in temperature and pressure and, in addition, they usually have high salinity brines; indeed, they are often referred to as HP/HT/HS systems. When these factors vary together, they tend to trigger the formation of inorganic scales including sulphides. Apart from the role of temperature and salinity in scale formation, these HT/HS conditions negatively impact scale inhibitor performance due to chemical degradation or interference from the high salinity/hardness of the brines.

Several variables have been tested and reported in the literature to ascertain their impact on the inhibition efficiency for conventional scales. This includes the impact of pH and temperature, as well as the concentration of ions such as barium, calcium and magnesium. Some research studies have further discussed the effect of heavy scaling metals, such as Zn and Fe, on the performance of scale inhibitors.

On the other hand, much of the sulphide-focused literature has exclusively sought to understand scale inhibition, rather than formation, and has tended to tackle the sulphide problem for specific fields and therefore specific conditions. There is therefore a lack of detailed understanding of factors controlling Fe, Zn and Pb sulphide precipitation and inhibition behaviour; *i.e.* factors such as pH, temperature, brine salinity, cation/sulphide molar ratio and metal-to-metal interaction. In addition, there are no published studies looking at the consumption of scale inhibitor(s) in sulphide scale solutions, although barium sulphate SI consumption studies have been published (Shaw and Sorbie 2013). This scale inhibitor consumption could likely impact the inhibition for other scales including conventional scales. It has also been found that the manner of SI consumption

gives some indication of the actual mechanism of inhibition (Shaw and Sorbie 2013). Systematic investigation of these factors is crucial to sulphide precipitation prediction, treatment design and development of scale inhibitors and dissolvers.

1.2 Research objectives

The central objective of this thesis was to investigate the formation and inhibition of FeS, ZnS and PbS as single scales or as mixed scales over a wide range of parameters including pH, temperature, salinity and cation/sulphide molar ratios. In addition, the formation of sulphide scales by cation exchange from pre-formed scales was examined in the context of inhibition mechanism and efficiency, which included the effect of physicochemical variables and the resultant size of the particles formed. The possible loss of inhibitor via "consumption" was also studied for both inhibited and uninhibited cases. Finally, a limited number of dynamic filter-blocking tests were performed to compare the static and dynamic formation/inhibition of the sulphide scales.

1.3 Literature Review

Inorganic scale deposition can pose safety hazards and have serious economic consequences. Additionally, costly operations might be required to remove and control the scales. Different types of inorganic scale have been reported as forming in several locations including the reservoir, in the wellbore and in topside process facilities. The scales form when incompatible fluids are comingled or the equilibrium is disrupted as a consequence of changes in ion concentrations, temperature, pressure and/or pH during fluid injection and production.

There are several types of inorganic scale such as sulphate scales, carbonate scales and iron sulphide (FeS), zinc sulphide (ZnS) and lead sulphide (PbS), where the latter two scales are frequently referred to as "exotic scales".

Halite (NaCl) scale forms more commonly in high temperature gas fields containing high salinity brine (Frigo *et al.* 2000; Wylde and Slayer 2013). Such fields are prone to critical declines in temperature leading to halite deposition as its solubility is proportional to temperature. Besides the role of temperature, halite can deposit due to brine evaporation into the gas phase as a result of pressure decrease (Smith and Przybylinski 2006; Wylde and Slayer 2013; Ho *et al.* 2014).

Changes in temperature or pressure, and subsequent increase in pH, result in formation of calcite ($CaCO_3$) and/or siderite ($FeCO_3$) mineral scales, as the solubility of these scales decreases with increasing pH (Nasr-El-Din *et al.*, 2004). Barite ($BaSO_4$), celestite ($SrSO_4$), anhydrite ($CaSO_4$) and gypsum ($CaSO_4.2H_2O$) can form by similar mechanisms, in addition to mixing of incompatible fluids at the appropriate conditions *e.g.* co-mingling of seawater (sulphate rich) with formation water (rich in Ba, Sr and/or Ca) (Allaga *et al.*, 1992; Al-Khaldi *et al.*, 2011). Barite can also be introduced to the formation as a consequence of drilling fluid invasion as the barite is widely used as weighting material in drilling fluids. Oddo *et al.*, 1991 reported that calcium sulphate precipitated as a consequence of mixing seawater over-flush with spent HCl/HF acid. Chelating agents such as ethylene diamine tetra acetic acid (EDTA) and diethylene triamine penta acetic acid (DTPA) are commonly used for barite dissolution while acids are used for calcite treatment (Nasr-El-Din *et al.*, 2004; Jordan and Williams, 2016).

1.3.1 Sulphide scales

Sulphide scales have very low solubilities (see Table 1.1) and thus their precipitation is virtually inevitable under conditions often encountered in oilfield systems. The solubility of FeS, ZnS and PbS increases with increasing salinity and decreases with increasing pH. By increasing the temperature, the solubility of FeS decreases, while the solubilities of both ZnS and PbS, in contrast, increase (Barrett and Anderson, 1988; Shuler *et al.*, 2000; Verri *et al.*, 2017).

Table 1.1 The approximate solubility products of sulphide scales.

Scale Type	Equilibrium constants (K_{eq})	Reference
Pyrite (FeS_2)	8.51×10^{-26}	Chase *et al.*, 1985
Mackinawite (Fe_9S_8)	2.88×10^{-18}	
Pyrrohtite (Fe_7S_8)	2.7×10^{-19}	
Lead(II) Sulphide	3.8×10^{-28}	Reviewed by Okocha and Sorbie, 2013
Zinc(II) Sulphide	2.03×10^{-25}	

Different types of scales often form in the same reservoir or even in the same well (Nasr-El-Din *et al.*, 2002; Franco *et al.*, 2010; Wang *et al.*, 2013; Wang *et al.*, 2016; Salman *et al.*, 2007). Based on simulation results for the Khuff reservoir, iron oxide and barite are likely to deposit in the producing string while calcium carbonate and iron sulphide can deposit in the producing string as well as at the sand face (Franco *et al.*, 2010). In some production wells within the Elgin and Franklin Fields, $CaCO_3$ was found to deposit at depths between 2000 and 5400m, while ZnS and PbS formed at

depths over 2000 m (Baraka-Lokmane *et al*., 2015). Chemical analysis of samples from a choke showed the presence of PbS, ZnS, FeS, calcium carbonate and sodium chloride (Orski *et al*., 2007). Scale samples collected from fields within the North Sea were identified as ZnS, PbS and barium sulphate (Jordan *et al*., 2000). Chemical analysis of scales collected from the field revealed that the predominant scale was PbS with some ZnS, $CaCO_3$ and FeS (Dyer *et al*., 2006).

1.3.2 Sources of scaling metals (Fe, Zn and Pb)

Various levels of Zn and Pb have been detected in the formation waters of fields within the North Sea and the Gulf of Mexico (Jordan *et al*., 2000; Lopez *et al*., 2005; Saidoun *et al*., 2016; McCartney *et al*., 2016). Up to 150 ppm Pb has been detected in produced water from the Dutch Rotliegend and Kupferschiefer sediments (Hartog *et al*., 2002). Pb and Zn levels were measured to be 50 and 150 ppm, respectively, in formation water collected from fields in the North Sea (Orski *et al*., 2007). It has also been reported that fields in the Gulf of Mexico have Pb and Zn concentrations up to 70 and 245 ppm, respectively (Kharaka *et al*., 1987). The Pb and Zn levels detected in formation water collected from different locations in the Culzean field were remarkably higher than other published data. Pb and Zn concentrations are 172 ppm and 452 ppm respectively (McCartney *et al*., 2016). Zn and Pb can be also introduced to produced water from metal based pipe dopes. Some pipe dopes consist mainly of Zn and contain up to 30 wt% Pb in addition to copper and graphite (Mathis et al., 2013). XRD analysis of two dope samples revealed that drill pipe and casing dopes contained 48 % Zn and 24 % Pb respectively (Nasr-El-Din et al., 2002). Also, Nasr-El-Din et al (2002) reported that the Zn and Pb concentration peaked at 301 mg/L and 45 mg/L respectively after acid pickling treatment.

ZnS and PbS have been observed in many wells despite the Zn, Pb and sulphide concentrations being very low. For example, in the presence of only 2 ppm H_2S and Zn ions introduced from zinc bromide completion fluid, a significant amount of ZnS was deposited in an oil field in the North Sea UK sector (Biggs *et al*., 1992). ZnS deposited on a crude oil cooler and HP-hydrocyclones in fields within the Norwegian sector of the North Sea where the formation water contained 20 to 25 ppm H_2S and 40 to 70 ppm Zn (Jordan *et al*., 2000). In the Gulf of Mexico, ZnS and PbS deposition was encountered in the presence of 25 ppm H_2S, 50 ppm Zn and 5 ppm Pb (Lopez *et al*., 2005).

Unlike Zn and Pb, Fe can be introduced to the produced water by several mechanisms including the dissolution of formation rocks such as siderite ($FeCO_3$), corrosion products from production tubing and/or from well stimulation treatments, such as acidisation. The main source of iron sulphide that re-precipitated in the formation is the dissolved iron sulphide during acid treatment (Walker *et al.*, 1991). Produced water samples from Marcellus and Bakken formations were found to carry up to 300 ppm Fe and levels of over 400 ppm were reported in fields in the Gulf of Mexico (Shen *et al.*, 2012, Peng *et al.*, 2015, Kharaka *et al.*, 1987). Thousands of ppm of Fe have been measured in flow back brine after acid treatment (Gougler *et al.*, 1985; Nasr-El-Din *et al.*, 2002). Therefore, it is essential to identify the source and type of iron in order to properly design the appropriate treatment method, *e.g.* corrosion inhibition and/or scale inhibition/dispersion.

Table 1.2 Fe, Zn and Pb concentrations detected in formation or produced waters

Field	Zn (ppm)	Pb (ppm)	Fe (ppm)	Reference
Dutch Rotliegend and Kupferschiefer sediments	-	150		Hartog et al., 2002
North Sea	150	50		Orski et al., 2007
Gulf of Mexico	245	70	400	Kharaka et al., 1987
Culzean field	452	172		McCartney et al., 2016
Gulf of Mexico	50	5		Lopez et al., 2005
Norwegian sector of North Sea	40-70	-		Jordan et al., 2000
Marcellus and Bakken			300	Shen et al., 2012

1.3.3 Sulphide scale formation

FeS, ZnS and PbS scales can form according to the following reactions:

$$HS^- + Fe^{2+} \rightarrow FeS + H^+ \quad (1.1)$$

$$HS^- + Zn^{2+} \rightarrow ZnS + H^+ \quad (1.2)$$

$$HS^- + Pb^{2+} \rightarrow PbS + H^+ \quad (1.3)$$

PbS and ZnS can also be formed by the reaction of lead and zinc compounds with more soluble sulphide scales *e.g.* ZnS or FeS, (see equations 1.4-1.6) depending on the

conditions, including alkalinity, temperature and mechanical disturbance (Cheng Long *et al*., 2008 Cheng Long and Youcai, 2009; Graham *et al*., 2017).

$$Pb^{2+} + ZnS \rightarrow PbS + Zn^{2+} \quad (1.4)$$

$$Pb^{2+} + FeS \rightarrow PbS + Fe^{2+} \quad (1.5)$$

$$Zn^{2+} + FeS \rightarrow ZnS + Fe^{2+} \quad (1.6)$$

Further complications may arise due to secondary precipitation events in the presence of other counter ions, such as sulphate and chloride. Many solubility values of lead sulphate are reported in the literature but according to Clever and Johnston (1980) the recommended value is 1.461 x 10^{-4} mol/L, which is equivalent to 30 ppm Pb. On the other hand, lead chloride is more soluble in water (K_{sp}= 1.7 x 10^{-5}, *i.e.* 3356 ppm Pb) but this Pb solubility decreases with increasing chloride contents due to the common ion effect of chloride. Nonetheless, above certain concentrations of chloride, the solubility of lead significantly increases as a result of favourable formation of soluble lead chloride complexes *i.e.* $PbCli^{2-i}$ where i = 1 to 4 (Holdich and Lawson 1987). $PbCO_3$ was also detected alongside $CaCO_3$ in lab samples when Pb and Ca were mixed with sulphide and bicarbonate solution (Okocha and Sorbie, 2014).

Laboratory results and field data showed that iron sulphide can undergo crystalline transformations from sulphur-deficient to sulphur-rich iron sulphide when conditions permit (Nasr-El-Din *et al*., 2000; Ford *et al*., 1992; Kvarekval *et al*., 2003). In addition to solution pH and aqueous speciation, the conversion from iron monosulphides to pyrite depends on the surface oxidation state of pre-formed iron monosulphides (Wilkin and Barnes, 1996). This study revealed that pyrite formed in oxygen free iron monosulphides solutions provided that the solutions are aged with zero valent sulphur namely polysulphides and colloidal elemental sulphur. In oxidized iron monosulphides solutions, pyrite formed regardless of the type of sulphide species. In Khuff gas wells, two distinct layers of scale have been observed (Kasnick *et al*., 1989; Nasr-El-Din *et al*., 2000; Franco *et al*., 2010; Wang *et al*., 2013; Wang *et al*., 2016). The outer layer *i.e.* adjacent to tubular, was predominantly composed of siderite and ferric compounds such as akaganeite (FeO(OH,Cl)) and goethite (FeO(OH)). The inner layer was predominately iron sulphide, which is less soluble than the other iron compounds. Therefore, this layer formed when ferric compounds and siderite were exposed to H_2S according to the following reactions:

$$Fe_2O_3 + 3H_2S \rightleftarrows 2FeS + S_{(0)} + 3H_2O \quad (1.7)$$

$$2FeOOH + 3H_2S \rightleftarrows 2FeS + S_{(0)} + 4H_2O \quad (1.8)$$

The main form of Fe in the reservoir environment is ferrous iron (Fe^{2+}), however Fe can exist in the oxidized ferric (Fe^{3+}) form. Ferrous iron is not considered to be a serious problem *per se*, as long as there is no sulphide in the system. Ferric iron, on the other hand, can precipitate as iron hydroxide $(FeOH)_3$ when pH increases above 1 according to equation 9 (Taylor *et al*., 1999). In the presence of sulphide, which is a reducing agent, Fe^{3+} can be converted to Fe^{2+} according to equation 10 below (Smith *et al*., 1969; Przybylinski, 2001).

$$Fe^{3+} + 3OH^- \rightleftarrows Fe(OH)_3 \quad (1.9)$$

$$2HS^- + 2Fe^{3+} \rightleftarrows HS_2^- + 2Fe^{2+} + H^+ \quad (1.10)$$

1.3.4 Sulphide scale dissolution

Scale inhibition is generally preferred to scale removal after the mineral scale has deposited. However, scale removal may be required in cases where the scale has already formed, or when it is more economical to remove the scale frequently (chemically or mechanically) rather than using scale inhibitor treatments. Hydrochloric acid (HCl) has been applied historically to remove sulphide scales with variable success rates (Mirza and Prasad, 1999; Bittner *et al*., 2000; Nasr-El-Din and Al-Humaidan, 2001; Nasr-El-Din *et al*., 2000; Berry *et al*., 2012; Franco *et al*., 2010).

It is common practice to evaluate sulphide dissolvers based on the weight of the scale before and after the dissolution. However, this method was found to be inaccurate in some cases due to precipitation of additives (Nasr-El-Din *et al*., 2000). Some researchers tracked the progress of the reaction by monitoring the Fe or Zn concentrations by ICP in addition to weight loss (Nasr-El-Din *et al*., 2000; Jordan *et al*., 2000; Wylde *et al*., 2016). Lab results showed that 8.06 M HCl (29.4 wt% HCl) dissolved 94.8% of galena ore (PbS) within 120 min at 80°C, where the solid/acid ratio was 10 g/L (Baba and Adekola, 2012). The galena dissolution in HCl was found to increase with increasing temperature and acid concentration and it decreased with increasing particle size and solid/acid ratio. Elemental sulphur and lead chloride were detected in the post-leaching residues.

At 20°C, the dissolving power of 15% HCl was higher than that of formic-acetic acid mixture and low molecular weight polymer acid (Jordan *et al*., 2000). Berry *et al*., 2012 reported on ZnS dissolution experiments and field data using HCl as a standalone fluid or with additives. Several factors played a significant role in the dissolution of ZnS. The solubility of ZnS in HCl decreases with increasing pressure and ZnS/acid ratio. In addition, the impact of using oxidizers such as sodium hypo-chlorite and hydrogen peroxide was evaluated, where the latter outperformed the other oxidizers. Nonetheless, there are drawbacks associated with the use of HCl, such as safety hazards resulting from H_2S generation along with the associated increases in corrosion rates. Although some additives can tackle these problems, they can adversely affect the performance of HCl (Nasr-El-Din *et al*., 2000). Both corrosion inhibitors and H_2S scavengers have been seen to create a film on the scale, which reduced the reaction with HCl and thus these additives should be carefully evaluated in order to obtain the optimal application concentration. Several chemicals have been evaluated for FeS scale dissolution in one study (Leal *et al*., 2007). Three different scale samples were used (1) calcite, pyrrhotite, siderite and akaganeite, (2) predominantly pyrrohtite, and (3) dominate types are pyrrohtite and marcasite. 28% HCl and low pH DTPA-5% HCl solutions outperformed the other chemicals. High pH EDTA dissolved 56.6% and 11% of sample 1 and 2, respectively at the same conditions, which was attributed to the difference in the scale composition. 15% HCl acid and 15% HCl-DTPA were used to remove the scale from gas producers in Saudi Arabian carbonate reservoirs. The scale was successfully removed from the tubing while the treatment was partially successful in the production liner as a consequence of pH increase and iron scale re-precipitation occurred as the acid reacted with the carbonate rock.

Other studies have shown that many iron sulphide scale dissolvers have low scale dissolving power compared to HCl (Wang *et al*., 2013; Wang *et al*., 2016; Chen *et al*., 2016). Several scale dissolvers were developed in an attempt to overcome the limitations of HCl (Wang *et al*., 2013; Hafiz *et al*., 2017; Elkatatny, 2017; Yap *et al*., 2010; El Hajj *et al*., 2015). Some of those dissolvers showed promising results for iron sulphide, even for the lowest solubility forms *i.e.* pyrite and marcasite.

Wang *et al*., 2013 conducted an extensive evaluation of 10 chemicals at 185°F and 250°F with mixing ratio 2 g scale: 20 ml dissolver. As expected, low pH chemicals had

the highest dissolving power but one of the high pH chemicals (pH of 7.5) dissolved 1.25 g of FeS and the corrosion rate was negligible compared to the low pH chemicals.

Hafiz *et al*., 2017 evaluated three chemicals at ambient conditions:

Chemical A: polymers functionalized with carboxylic, hydroxyl, aromatic hydroxyl, aryl sulphonate, and amino groups;

Chemical B: a blend of tetrakis-hydroxymethyl-phosphonium sulphate (THPS); and

Chemical C: 50% chemical A:50% chemical B) for FeS dissolution.

The FeS samples were prepared in the lab by mixing sodium sulphide and iron chloride which would yield small FeS particles. 10 g of the FeS was mixed with 10, 20 and 30 ml of each dissolver. The higher the FeS/chemical ratio was, the lowest the dissolving power. The dissolving power of these chemicals was small *e.g.* the highest FeS dissolution was achieved when 10 g was reacted with 30 ml chemical C where 1.04 g was dissolved.

Elkatatny, 2017 tested different organic acids (maleic, glutamic, succinic and gluconic acids), chelating agents (EDTA and DTPA), mixture of these chemicals, in addition to a new dissolver for field scale sample (55 wt% pyrrhotite, 21 wt% calcite, 8 wt% pyrite and 6 wt% troilite) at 125°C with mixing ratio 2 g scale: 20 g dissolver. The chelating agent outperformed the organic acids while the new dissolver, which consists of organic acid and minerals acid, had the highest dissolution *i.e.* 80 wt%.

Wylde *et al*., 2016 developed a new FeS dissolver, which is based on a carboxylate copolymer. 50 ml of the chemical was mixed with 5 g of the scale and each chemical was tested against marcasite, pyrite, pyrrhotite, troilite and 5 field scale samples. The performance of the new dissolver was comparable to 7.5% HCl and outperformed 30% active THPS and 25% acetic acid; however, THPS dissolved more troilite than HCl or the new dissolver. 7.5% HCl dissolved 20, 41, 70 and 23% of Marcasite, Pyrite, Pyrrohtite and Troilite respectively. On the other hand, 68, 36, 75 and 64% of these scales were dissolved in the new dissolver. Whereas the new dissolver and HCl both showed a high dissolving power against iron sulphide and the other scale such as $CaCO_3$, THPS performed better against iron sulphide samples.

Mahmoud *et al*., 2015 developed a new dissolver consisting of DTPA and a converter such as potassium carbonate, caesium carbonate or caesium formate. The authors reported the experimental data for pyrite dissolution at 70°C using a new dissolver, DTPA, low pH biodegradable chelating agent (BDCA) and 20 wt% HCl. The new dissolver (DTPA + potassium carbonate) dissolved 85% while the DTPA dissolved 45%. In the new dissolver, the pyrite was converted to iron carbonate, which is soluble in DTPA. The low pH chelating agent and HCl dissolved 35% and 20% respectively.

Chen *et al*., 2016 evaluated several FeS dissolvers including a newly developed high pH dissolver (alkaline dissolver) at 125°C with mixing ratio 3 g pyrrohtite:30 ml dissolver. As expected, the low pH dissolvers showed better dissolution capability as HCl dissolved 1.95 g and the strong acid dissolved 1.33 g. The alkaline dissolver had a comparable dissolving power to THPS and higher dissolving power than some dissolvers with pH 2 and 7. However, the alkaline dissolver had lower corrosion rate than the low pH dissolvers and THPS.

Wang *et al*., 2018 evaluated 6 FeS dissolvers at 100, 125 and 150°C with mixing ratio 3 g scale:30 ml dissolver. Pyrrohtite rock and three field samples comprising various compositions of iron monosulphides, iron disulphides, iron oxyhydroxide and carbonates, were used in this study. 15% HCl showed higher dissolving power compared to these dissolvers. The dissolving power of some tested chemicals increased with increasing the temperature. In addition, some dissolvers softened the hard iron sulphide deposits, which could be a scale removal mechanism.

1.3.5 Sulphide scale inhibition

Scale inhibitors can be introduced to the produced fluids, hence prevent the scale formation and deposition, by two ways. Scale inhibitors can be continuously injected at the wellhead or downhole to protect the topside facilities and the wellbore but not the reservoir. Also, scale inhibitors can be squeezed into the formation and subsequently the scale inhibitor is released continuously at concentrations greater than the minimum inhibitory concentrations (Kerver *et al*., 1969; Kerver and Heilhecker, 1969; Miles, 1970; Oddo *et al*., 1997; King and Warden, 1989). As shown in Figure 1.1, this process typically involves three stages: injecting a pre-flush or spearhead (0.1 scale inhibitor in KCl or seawater) to clean and cool the formation prior to the main stage, then the scale inhibitor solution (5% - 20% volume in KCl or seawater) and over-flush of inhibited

KCl or seawater to displace the main treatment deeper in the formation (Mackay and Jordan, 2003).

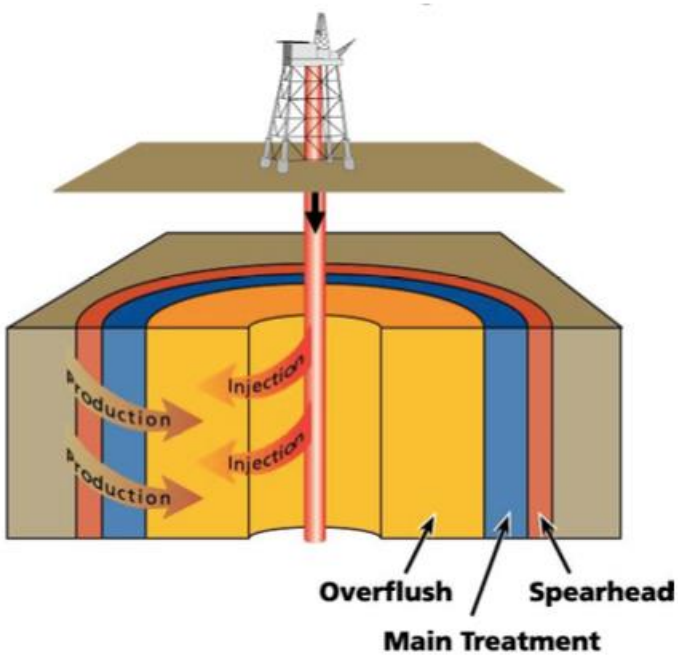

Figure 1.1 Schematic scale inhibitor process (After Mackay and Jordan, 2003).

Scale inhibitors have been widely used to prevent the precipitation or the deposition of conventional scales, such as barium sulphate and calcium carbonate, as well as sulphide scales. Sorbie and Laing, 2004 discussed the inhibition mechanism for PPCA, DETPMP and PVS in addition to the impact of pH, temperature and the concentrations of calcium and magnesium. DETPMP and PVS function mainly by crystal growth and nucleation inhibition, respectively. The inhibition mechanism of PPCA is intermediate between nucleation and crystal growth. There are 5 PO_3H_2 groups in DETPMP whereas only 1 POOH is present in PPCA and thus the impact of Ca and Mg on the inhibition efficiency in DETPMP solutions is more critical than PPCA. Shaw and Sorbie, 2012 concluded that the pH has a significant effect on the inhibition efficiency of some scale inhibitors. The inhibition efficiency of HMTPMP, DETPMP and EDTMPA for barium sulphate increased with increasing the pH. This is in line with the inhibition efficiency of DETPMP reported by Sorbie and Liang, 2004 and that is attributed to the speciation degree of DETPMP at this pH level; the more dissociated forms of these phosphonates inhibit barite more efficiently. By contrast, the inhibition efficiency of PPCA was less sensitive to pH.

The presence of small amounts of Zn ions (0.28 to 1.4 ppm) was found to significantly improve the inhibition efficiency for barium sulphate of some scale inhibitors such as BHPMP and DTPMP and to less extent the polymeric carboxylate scale inhibitors (Kan *et al*., 2009). The complex of transition metal ions with amine group of polyamino-polyphosphonates seems to be the most likely cause of the synergic effect. On contrary to the role of Zn, the presence of Fe, albeit small amount *i.e.* 5 ppm, has a negative impact on the inhibition efficiency for calcium carbonate of polycarboxylic acid, aminotri(methylene phosphonate) acid, carboxy methelene inulin (Shen *et al*., 2012). The presence of 250 ppm Fe had a negative impact on the performance of only polymeric scale inhibitor in dynamic testing for conventional scales namely carbonates and sulphates (Jordan *et al*., 2000).

Tortolano *et al.* (2014) developed a new methodology to investigate ZnS and ZnS alongside $CaCO_3$ formation and inhibition at high temperature. According to this study, the presence of ZnS is found to accelerate $CaCO_3$ formation which subsequently had a negative impact on the inhibition of co-deposition. However, some inhibitors used in this study were effective for inhibiting ZnS/$CaCO_3$ scale. The inhibition mechanism is reported to be nucleation and growth inhibition as well as dispersion. Okocha and Sorbie, 2014 examined the $CaCO_3$ crystal in presence of sulphide scale and scale inhibitor *i.e.* PPCA. First, to establish a base case the $CaCO_3$ was formed on a stainless steel surface and in the bulk solution and the corresponding SEM results showed that the $CaCO_3$ formed in the bulk and on the metal surface is different which is in a good agreement with other published findings (Chen 2005; Hasson *et al*., 1996). In presence of ZnS, $CaCO_3$ crystals were not distorted but less amount of $CaCO_3$ deposited on the metal surface compared to the base case, see Figure 1.2 a and b. Despite both $CaCO_3$ and ZnS being formed in the bulk, only $CaCO_3$ were identified on the metal surface suggesting that the ability of ZnS and $CaCO_3$ to adhere to the metal surface is different. Unlike co-precipitation with ZnS, $CaCO_3$ crystals, formed alongside PbS, were distorted as shown in Figure 1.2 c.

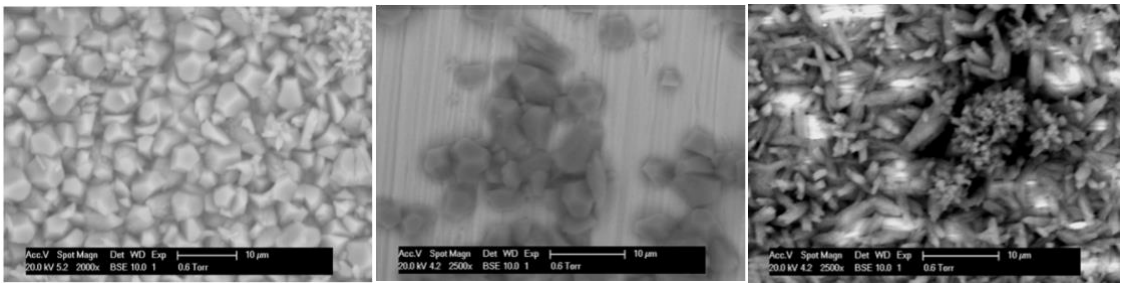

Figure 1.2 $CaCO_3$ deposit on the metal surface at 24 h (a) single $CaCO_3$, (b) co-precipitated with ZnS, (c) co-precipitated with PbS.

Russek *et al.*, 2018 examined the performance of different scale inhibitor (including polymeric and phosphorous based scale inhibitors) against $CaCO_3$ and the impact of pre-existing FeS on the inhibition. Three products (one polymeric SI and two phosphorous containing SIs) performed slightly better in the presence of pre-existing FeS, and an example is shown in Figure 1.3. By contrast, pre-existing FeS had a detrimental impact on the performance of the other scale inhibitors as the inhibition efficiency dropped significantly *e.g.* the inhibition efficiency was nearly 30 and 100% with and without FeS respectively using one of the phosphorous SIs.

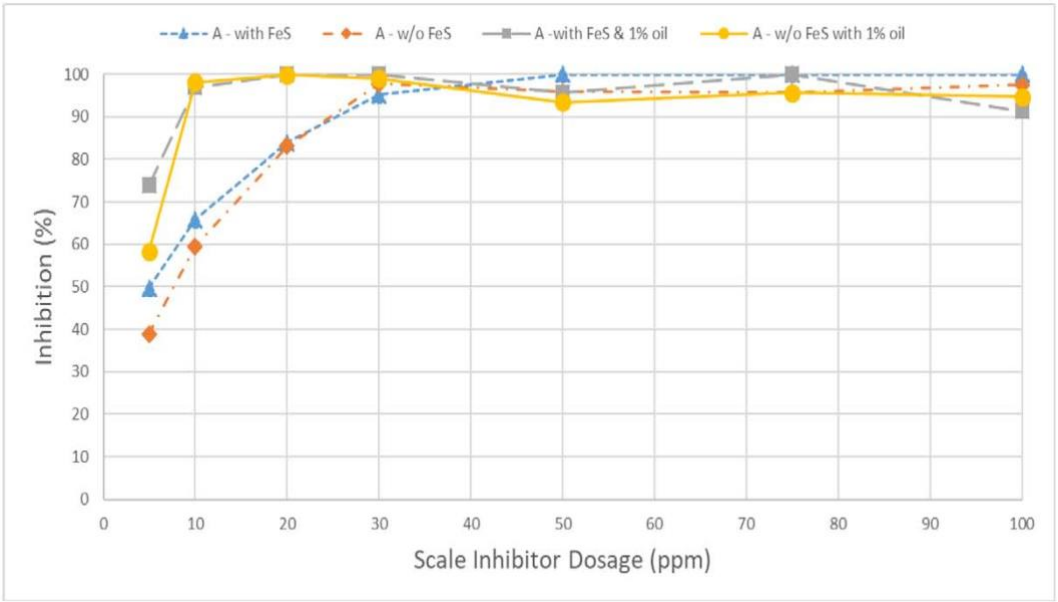

Figure 1.3 Efficiency of polymeric scale inhibitor (after Russek *et al.*, 2018).

Iron chelating agents proved to be effective in preventing precipitation of iron compounds in sweet (CO_2-rich) wells, however they were less effective in sour (H_2S-rich) wells. It has also been shown that using an iron-chelating agent combined with a sulphide-controlling agent can prevent the re-deposition of iron sulphide (Walker *et al.*,

1991). There are many research studies on the factors that affect the performance of scale inhibitors.

Hydroxyethylacrylate/acrylate copolymer SI was tested in two wells having severe ZnS deposition. The tested SI prevented ZnS deposition and hence the pumps had been working for several months without failure. In addition, produced water analysis showed that the Zn ions concentration nearly doubled after the treatment (Emmons and Chesnut, 1988).

Several scale inhibitors as well as two chelating agents were tested against ZnS scale using a static inhibition method (Collins and Jordan, 2001). Unlike common scales, *i.e.* sulphate and carbonate minerals, higher SI concentrations were required to prevent ZnS. It was found that chelating agents could prevent ZnS formation provided that their concentrations are proportional to the Zn ions concentration. Depending on the type of scale inhibitor, the scale inhibition can be attributed to threshold scale inhibition, low pH solution or chelating. Polymeric scale inhibitors outperformed the other tested inhibitors and the prevention mechanism was found to be threshold inhibition. The effectiveness of phosphonate SI can be attributed to threshold scale inhibition and to a lesser extent low solution pH. Jordan *et al*., (2000) reported that low molecular weight polymer was able to control ZnS deposition when used for topside treatment by continuous injection. In addition, polymeric scale inhibitors were found to be more effective than phosphonate scale inhibitors for this purpose.

Lopez *et al*., (2005) compared the performance of different potential sulphide scale inhibitors including commercial and proprietary polymeric species using an anaerobic tube-blocking apparatus at 166°C and saline formation water (*i.e.* Cl ~135,057). In this work, two concentrations of sulphide were used *i.e.* 25 and 50 ppm while Zn and Pb concentrations were 50 ppm and 5 ppm, respectively. The brines were prepared without bicarbonate and sulphate to ensure that the pressure increase in the tube-blocking system would be due only to ZnS and PbS precipitation. The proprietary SI and polymeric SI provided better Zn/Pb sulphide inhibition compared to other commercial sulphide SIs, see Figure 1.4. This proprietary SI was implemented in the field and showed good results compared to other commercial sulphide SIs.

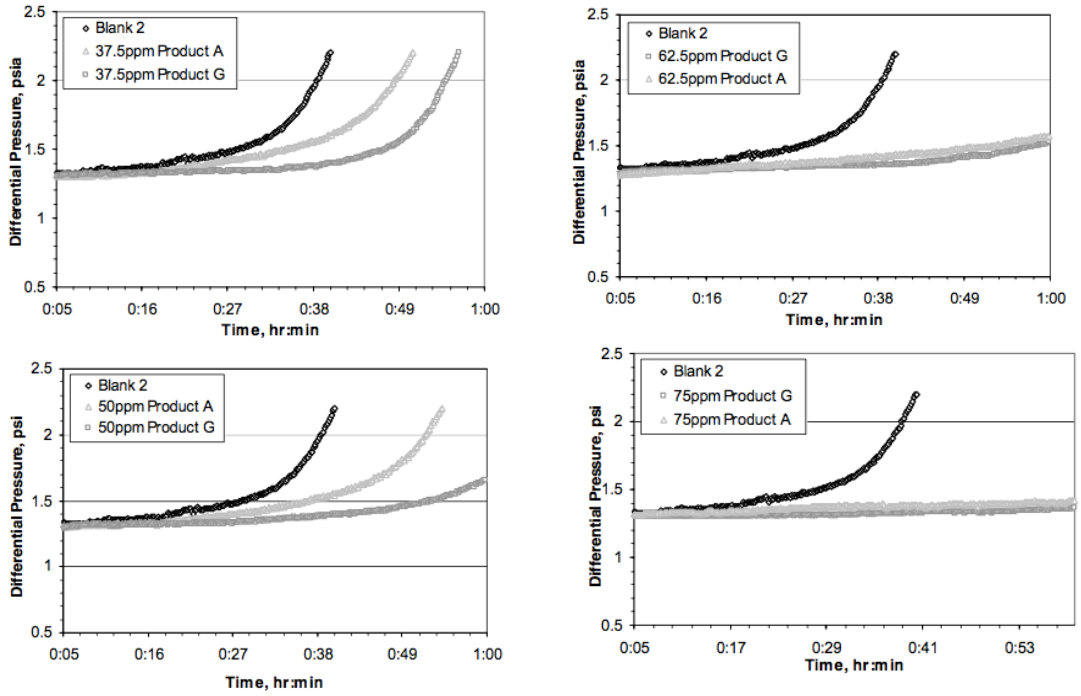

Figure 1.4 Comparison of dynamic tests results in presence of 50 ppm sulphide, 50 ppm Zn and 5 ppm Pb. Product A: commercial sulphide scale inhibitor, product G: proprietary polymer scale inhibitor (after Lopez et al., 2005).

Orski *et al*., (2007) reported the results from sulphide inhibition tests using a dynamic scaling loop. In an effort to replicate scale in the lab, formation water samples containing various concentrations of Pb, Zn and sulphide were used. Although both PbS and ZnS were observed in the field, only PbS formed in the lab even in presence of high Zn concentrations. The final pH and the sulphide concentration were not reported in this paper. So it is not clear whether the absence of ZnS was due to H_2S evolution or ZnS solubility. It is interesting to note that ZnS formed alongside PbS in few samples in the inhibition tests. Results from inhibition experiments revealed that tested scale inhibitors failed to prevent PbS formation but they provided effective inhibition against calcium carbonate in absence of sulphide ions. The scale did not block the coil and, in case of when blockage occurred, the pressure increase versus time behaviour was not repeatable. This was attributed to the laminar flow regime, hence insufficient mixing. In attempt to enhance the scaling kinetics, in-line filter was installed at the outlet of the coil. As a result, the scale increased more rapidly and the results were repeatable; however, the authors noticed that scale as well as other like materials could block the filter.

Savin *et al*., (2014) screened several standard scale inhibitors to assess their ability to prevent zinc sulphide and lead sulphide formation at 20°C, at pH 7 and in presence of

excess sulphide to ensure high scaling tendencies. As shown in Figure 1.5, among the tested SIs in this work, sulphonated/carboxlic acid co-polymer and phosphorus end-capped polymer at high concentrations could provide partial ZnS inhibition. Despite the fact that the sulphonated SI failed to prevent PbS formation, it was able to partially inhibit both ZnS and PbS formation in the mixed system. It was reported that it is easier to prevent mixed sulphide scale (*i.e.* ZnS/PbS) than the single scale (*i.e.* ZnS alone or PbS alone). The inhibition performance of sulphonated SI against ZnS was dramatically affected when it was tested at 95°C, at pH 4.5 and in higher salinity brine (*i.e.* Cl~192060) as complete zinc sulphide precipitation occurred. Novel polymers have been developed and provided acceptable scale inhibition for mixed metals sulphide scales and single zinc sulphide scale.

Table 1.3 Scale inhibitor chemistries used for screening the performance of sulphide scale inhibition (after Savin *et al.*, 2014)

Chemical Name	Chemistry Type
Chemical A	Sulfonated/carboxylic acid co-polymer
Chemical B	Phosphorus end-capped polymer
Chemical C	Phosphate ester/sulfonated co-polymer blend
Chemical D	DETPMP
Chemical E	Sulfonated co-polymer
Chemical F	Phosphate ester
Chemical G	Maleic acid polymer
Chemical H	Sulfonated polymer
Chemical I	Phosphorus functionalized co-polymer
Chemical J	Complex blend
Chemical K	Sulfonated co-polymer
Chemical L	Phosphonate

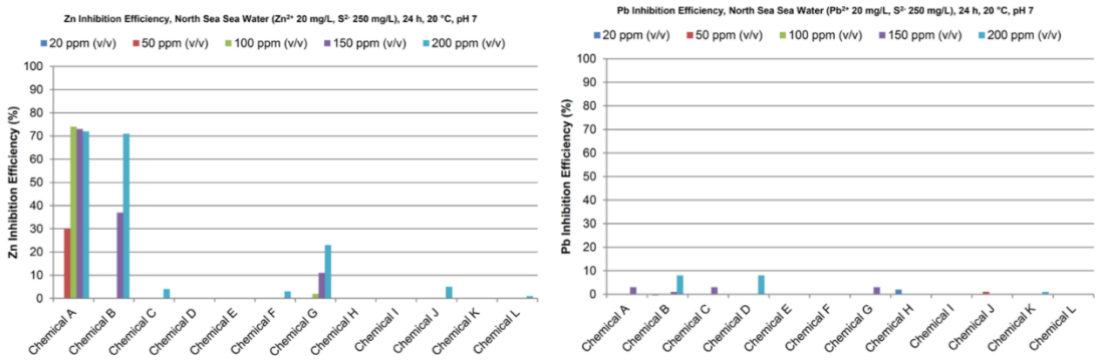

Figure 1.5 ZnS and PbS inhibition efficiency (after Savin *et al.*, 2014).

Dyer *et al.*, 2006 reported scale prediction and experimental results to replicate scale experienced in the field. Static and dynamic scale inhibitor evaluation tests and squeeze

treatments were also discussed. Scale prediction using thermodynamic models showed various scenarios depending on saturation index of PbS and ZnS which was calculated at temperatures of 90, 125 and 190°C and in presence of 0.8 ppm sulphide and various concentrations of Pb and Zn. At the highest tested temperature *i.e.* 190°C, PbS and ZnS had low saturation index *i.e.* $5x10^{-5}$ and $2x10^{-4}$ respectively therefore no sulphide scale formed at this temperature. 190°C aside, there were two cases in terms of the type of sulphide scale. When Pb and Zn mass concentrations were equivalent *i.e.* 300 ppm, PbS was preferentially formed. On the other hand, saturation index of ZnS increased over that of PbS due to the increase in Zn concentration from 300 ppm to 750 ppm and as a result the single ZnS scale formed. In contrast to results obtained from the model, single PbS formed on the filter even at high Zn concentration *i.e.* 750 ppm. Some tested scale inhibitors fulfilled the dynamic test criteria (in this case $\Delta P < 2$ psi in 60 min). However, none of tested scale inhibitors including the high performance SI completely prevented PbS. Besides, one of tested scale inhibitors had negative impact on ZnS as it precipitated alongside PbS.

Okocha *et al.*, 2014 reported the results of scale inhibitors evaluation under severe conditions using static and dynamic tests. Four polymeric scale inhibitors passed the screening tests and therefore were used in more severe scaling conditions. Although H3 (a polymeric SI) prevented sulphide scale completely in NSSW, it did not provide comparable inhibition in a much higher salinity brine. Four scale inhibitors were further tested using a dynamic blocking test, and 2 of these – denoted H3 and POL - were found to be more effective in preventing scale formation even at more severe scaling conditions *i.e.* in the high salinity Glenelg FW at 180°C (Okocha *et al.*, 2014).

Wang *et al.*, 2012 discussed the results of different scale inhibitors for ZnS inhibition using a newly developed stress test method. Based on the results obtained from this study, the tested scale inhibitors were categorized into three types. The inhibition mechanism of the first category was dependent on Zn:S ratio. In the Zn excess region, the inhibition mechanism was nucleation and growth while it was dispersion in the sulphide excess region. The second group showed nucleation and growth effect regardless of Zn:S ratio. The third type of tested scale inhibitors failed to inhibit ZnS.

Williams *et al.*, 2015, further investigated the proposed inhibition mechanisms. While the particle size of ZnS in blank solution was approximately 8 µm, it ranged between 2

µm and 6 µm in inhibited solutions. The decrease in particle size suggests that the inhibition mechanism of ZnS might be dispersion and/or crystal growth. Scale inhibitor, denoted SI-D, had a negative impact rather than inhibition as the particle size in SI-D solution was 11.85 µm compared to 7.69 µm in the blank solution.

Przybylinski (2001) presented FeS inhibition results using several scale inhibitors. Some tested scale inhibitors kept FeS particles suspended for several days, which *might* be considered as being actual inhibition, although this is contested by some. Lehmann and Firouzkouhi (2008) presented results using a new chemical for the prevention of iron sulphide deposition. Their study revealed that the particle size of iron sulphide decreased in the inhibited solution and subsequently deposition could be minimized. Chen *et al.* (2009) further discussed iron sulphide formation and inhibition. In this work, the dispersion effect was proposed as being the major mechanism of iron sulphide inhibition, as the scale inhibitor apparently reduced the agglomeration and kept particles suspended in solution. Wang *et al.*, 2014 evaluated two common scale inhibitors (PPCA and PVS) as well as five chelating agents against iron sulphide using a batch reactor. Chelating agents including citrate and EDTA outperformed PPCA and PVS and provided significant inhibition of FeS nucleation. Polymeric scale inhibitors like 2-ethyl-2-oxazoline (Mw: 5000 g/mol) and polyacrylamide (Mw: 40000-15000 g/mol) were able to disperse the FeS particles on a nano-meter scale and prevent the particles deposition (Li *et al.*, 2018). Also, in this study 100 ppm EDTA prevented FeS precipitation whereas THPS did not show any inhibition for FeS in presence of 30 ppm S and 10 ppm Fe at pH 6.75.

Keogh *et al*, 2018 studied the PbS inhibition and the role of PbS particles on emulsion characteristics. The very low solubility of PbS made it difficult for the polymer scale inhibitor to inhibit PbS nucleation. However, the crystal growth and the deposition was prevented as a result of the adsorption of the inhibitor onto the crystal surface. Both 500 ppm and 5000 ppm scale inhibitors prevented the deposition of PbS. In the blank solution and 500 ppm SI, there was an oil layer, which could prevent the adhesion of the oil in water emulsion on oil-wet surfaces. On the other hand, 5000 ppm stabilized the emulsion and thus it could adhere on the oil-wet downhole coatings.

Baraka-Lokmane *et al.*, 2015 presented extensive study on screening of conventional scale inhibitors and the development of new scale inhibitor for sulphide scale

mitigation. Polymeric scale inhibitors showed better thermal stability compared to the phosphonate scale inhibitors when they were aged at 200 °C. Using dynamic testing, none of the tested conventional scale inhibitors (6 polymeric and 3 phosphonate based SI) prevented PbS while some of the polymeric scale inhibitors showed a good performance against ZnS. It was noted that the pressure increase across the 7 μm filter is quicker than that across the coil.

1.4 Summary, Thesis Content and Structure

In the above review of the literature, particularly the inhibition section which is the focus of this thesis, there are several points which can be addressed. Firstly, there is An apparent contradiction in the reported performance of conventional scale inhibitors (SI) against sulphide scales. There are workers who report that in some cases conventional SIs work against sulphide scales (Jordan et al., 2000; Collins and Jordan, 2001; Lopez et al., 2005), while other researchers concluded that such scale inhibitors cannot be used for sulphide scale inhibition (Orski et al., 2007; Savin et al., 2014). These contradictory conclusions can be attributed to the particular procedures and conditions under which the inhibition tests were performed. The factors such as pH, temperature and salinity were not investigated in details as the majority of sulphide inhibition studies were conducted to evaluate the inhibitors at specific field conditions. All the sulphide inhibition tests were conducted by mixing sulphide solutions with scaling metal solutions concurrently *i.e.* FeS, ZnS and PbS formed by direct reaction as shown in equations 2.1-2.3. However, as discussed above in our literature review, PbS and ZnS can form by different mechanism *i.e.* cation displacement (see equations 2.4-2.6). Analyzing the particle size of sulphide scale is important as it can give an indication of the inhibition mechanism, effectiveness of the scale inhibitor and the interpretation of filter-blocking tests. However, among sulphide scale inhibition studies, few papers discussed the particle size of inhibited FeS. Scale inhibitor consumption in the barium sulphate scaling system has been addressed by some researchers (Shaw and Sorbie 2013), while there are no studies in the literature that investigate scale consumption in sulphide scaling systems; this issue is addressed in this work.

Chapter-2 of this thesis presents and describes the scale inhibitors, the brines and experimental procedure used in this study. Different scale inhibitors were used. However, led by our experimental results, the main focus turned to two of them, namely

high molecular weight sulphonated co-polymeric scale inhibitors (denoted SI-2 and SI-3).

Chapter-3 discusses the results of H_2S evolution, preliminary tests on Pb and Zn compounds solubilites in NSSW, SFNSSW and GFW as well as the FeS, ZnS and PbS formation as a single scale in different brines. These tests were conducted to understand the sulphide scales formation prior to performing the scale inhibition tests which will be discussed in Chapter 4.

Chapter-4 presents experiments investigating the interaction between Fe, Zn and Pb in sulphide solutions. In the first section, different sulphide scales were formed concurrently by mixing Fe/Zn/Pb solution with sulphide solution. Different scaling metal:sulphide ratios were used to test the scaling tendency of FeS, ZnS and PbS. Also, cation displacement experiments were conducted to confirm the affinity of the least soluble scales to form in presence of other more soluble sulphide scales. In these experiments, one scale e.g. ZnS was allowed to form, and then lead acetate solution was added to the pre-formed ZnS to potentially form PbS.

Chapter-5 presents a wide range of inhibition efficiency results for ZnS and PbS as separate single scales and then as combined scales over a range of parameters using different scale inhibitors. Several scale inhibitors were screened but due to their overall poor performance, the focus was on two high molecular weight sulfonated co-polymers *i.e.* SI-2 and SI-3. The initial tests were conducted in sulphate-free North Sea seawater (SFNSSW) at 50 °C in the presence of 100 ppm H_2S and 50 ppm Zn or 50 ppm Pb. SI-2 and SI-3 were evaluated in SFNSSW and Glenelg Formation Water (GFW) at 50 °C and 95 °C at various pH values. Different sampling methods were used including unfiltered samples, 0.45 μm and 5 μm filtered samples in order to give an indication of the particle size of the suspended sulphide scale particles.

Chapter-6 discusses the inhibition efficiency for iron hydroxide and iron sulphide using various scale inhibitors. The ability of the scale inhibitors to prevent the deposition of iron hydroxide was tested over a wide pH range under aerobic conditions. The inhibition efficiency for FeS was first tested under aerobic conditions using commonly used scale inhibitors and the two high molecular weight sulphonated copolymers (SI-2 and SI-3). However, most of the iron sulphide formation and inhibition experiments were conducted under anaerobic conditions. None of the tested scale inhibitors, apart

from SI-2 and SI-3, prevented the deposition of FeS and therefore SI-2 and SI-3 were thoroughly evaluated over a wide range of parameters including pH, salinity, temperature and Fe and sulphide concentrations.

Chapter-7 examines the interaction of Fe, Zn and Pb in sulphide solutions in the presence of scale inhibitors. The procedure was modified to allow a sequence mixing of sulphide scales; for example, PbS was allowed to form followed by ZnS. Also, the impact of the formation mechanism on the inhibition efficiency was studied.

Chapter-8 investigates the inhibition efficiency for ZnS and FeS in the presence of PPCA and DETPMP. The interaction between ZnS and FeS was also studied. For the first time, scale inhibitor consumption experiments in sulphide scale solution was investigated. SI consumption has been studied previously in some detail for barite scale formation and this gives some important information on the mechanism of the scale inhibition process (Shaw and Sorbie 2013), but this has not been reported for sulphide scales.

Chapter-9 discusses ZnS and FeS formation and inhibition using a filter-blocking rig; i.e. a conventional tube blocking rig (TBR) modified by replacing the mixing coil by a filter. The impact of the type and concentration of the scale inhibitor, the filter pore size and the type of scale on the scaling time was studied.

Chapter-10 summarizes the work presented in this thesis and our central conclusions and also presents the recommended future work.

Chapter 2

Experimental Procedures

2.1 Brine preparation

This chapter discusses the experimental procedures of the static formation and inhibition tests used in this work. It also gives the compositions of the synthetic brines used.

Different brines were used in this study including simple sodium chloride solutions, North Sea Seawater (NSSW), sulphate-free North Sea Seawater (SFNSSW), Glenelg formation water (GFW) and Field K formation water (KFW). The cation brine was prepared by dissolving the appropriate salts in distilled water (DW) as listed in Table 2.1**,** Table 2.3 and Table 2.5 without the addition of metal compounds ($FeCl_2.4H_2O$, $Pb(C_2H_3O_2)_2.3H_2O$ or $ZnCl_2$). Similarly, the H_2S brine, see Table 2.2, Table 2.4 and Table 2.6, was prepared initially without $Na_2S.9H_2O$.

Table 2.1 M_{2+} sulphate-free North Sea seawater (SFNSSW)

Ion	ppm	Formula composition	g/L	g/5 L
Na_+	10890	NaCl	27.498	137.49
Ca_{2+}	428	$CaCl_2.6H_2O$	2.34	11.7
Mg_{2+}	2736	$MgCl_2.6H_2O$	22.886	114.43
K_+	460	KCl	0.878	4.39
Ba_{2+}	0	$BaCl_2.2H_2O$	0	0
Sr_{2+}	0	$SrCl_2.6H_2O$	0	0
SO_{42-}	0	Na_2SO_4	0.00	0.00
Cl_-	41,346	-	-	-

Table 2.2 H_2S Sulphate-free North Sea seawater (H2S-SFNSSW)

Ion	ppm	Formula composition	g/L	g/5 L
Na_+	10890	NaCl	27.498	137.49
Ca_{2+}	428	$CaCl_2.6H_2O$	2.34	11.7
Mg_{2+}	0	$MgCl_2.6H_2O$	0	0
K_+	460	KCl	0.878	4.39
Ba_{2+}	0	$BaCl_2.2H_2O$	0	0
Sr_{2+}	0	$SrCl_2.6H_2O$	0	0
SO_{42-}	0	Na_2SO_4	0.00	0.00
Cl_-	29,703	-	-	-

Table 2.3 M_{2+} Glenelg formation water (GFW)

Ion	ppm	Formula Composition	g/L	g/5 L
Na_{+}	80520	NaCl	204.69	1023.45
Ca_{2+}	20000	$CaCl_2.6H_2O$	109.324	546.62
Mg_{2+}	5000	$MgCl_2.6H_2O$	41.823	209.11
K_{+}	8000	KCl	15.254	76.27
Ba_{2+}	3700	$BaCl_2.2H_2O$	6.581	32.91
Sr_{2+}	2000	$SrCl_2.6H_2O$	6.086	30.43
SO_{42-}	0	Na_2SO_4	0.00	0.00
Zn_{2+}	-	$ZnCl_2$	-	-
Pb_{2+}	-	$Pb(C_2H_3O_2)_2.3H_2O$	-	-
Cl_{-}	185,249	-	-	-

Table 2.4 H_2S Glenelg formation water

Ion	ppm	Formula composition	g/L	g/5 L
Na_{+}	80520	NaCl	204.69	1023.45
Ca_{2+}	20000	$CaCl_2.6H_2O$	109.324	546.62
Mg_{2+}	0	$MgCl_2.6H_2O$	0	0
K_{+}	8000	KCl	15.254	76.27
Ba_{2+}	3700	$BaCl_2.2H_2O$	6.581	32.91
Sr_{2+}	2000	$SrCl_2.6H_2O$	6.086	30.43
SO_{42-}	0	Na_2SO_4	0.00	0.00
H_2S	-	$Na_2S.9H_2O$	-	-
Cl_{-}	170,275	-	-	-

Table 2.5 M_{2+} K formation water (KFW)

Ion	ppm	Formula composition	g/l	g/5L
Na	54936.00	NaCl	139.531	**697.66**
Ca	14259.00	$CaCl_2.6H_2O$	77.942	**389.71**
Mg	3048.00	$MgCl_2.6H_2O$	25.495	**127.48**
K	5887.00	KCl	11.225	**56.13**
Ba	0.00	$BaCl_2.2H_2O$	0.000	**0.00**
Sr	1047.00	$SrCl_2.6H_2O$	3.186	**15.93**
SO_4	100.00	Na_2SO_4	0.148	**0.74**
S	0.00	$Na_2S.9H_2O$	0.000	**0.00**
Fe	0.00	$FeCl_2.4H_2O$	0.000	**0.00**
		Actual Cl	12,4948	ppm
HCO_3	0.00			

Table 2.6 H_2S Formation water (H2S-KFW)

Ion	ppm	Formula composition	g/l	g/5L
Na	54936.00	NaCl	139.531	**697.66**
Ca	14259.00	$CaCl_2.6H_2O$	77.942	**389.71**
Mg	0.00	$MgCl_2.6H_2O$	0.000	**0.00**
K	5887.00	KCl	11.225	**56.13**
Ba	0.00	$BaCl_2.2H_2O$	0.000	**0.00**
Sr	1047.00	$SrCl_2.6H_2O$	3.186	**15.93**
SO_4	100.00	Na_2SO_4	0.148	**0.74**
S	0.00	$Na_2S.9H_2O$	0.000	**0.00**
Fe	0.00	$FeCl_2.4H_2O$	0.000	**0.00**
		Actual Cl ppm	11,6056	ppm
HCO_3	0.00			

2.2 ZnS and PbS formation and inhibition

250 ml of each of the Pb or Zn concentrations were made by adding the required amount of $Pb(C_2H_3O_2)_2.3H_2O$ or $ZnCl_2$. Then, two duplicate 100 ml samples were transferred into glass bottles and labelled. Stock solution samples were made up of what was left from the original 250 ml.

Similarly, $Na_2S.9H_2O$ was added according to the desired concentration. The pH value was measured and recorded. Afterwards, samples of 100 ml were transferred to labelled glass bottles.

After heating both brines for 1 hour at the desired temperatures in a water bath, the metal brine samples were added to the corresponding H_2S samples, shaken for 10

seconds, and then placed back into the water bath. Sampling was performed at different times to track the progress of the reaction with samples being diluted 50:50 in DW. The samples, stock solutions, and ICP standards were sent for ICP analysis to measure the concentrations of Zn and Pb ions. After cooling of the original sample, final pH measurements were made and solid particles were collected for particle size analysis.

2.3 ZnS and PbS inhibition

The ZnS and PbS inhibition experiments are similar to those of the formation experiments but, in the inhibitions experiments, a certain amount of the scale inhibitor stock solution (10,000 ppm SI) was added to the Pb and Zn solutions and two duplicate 100 ml samples were transferred into glass bottles and labelled. Different sampling methods were used in the inhibition experiments. Sampling was performed at different times to track the progress of the reaction with collected samples being diluted 50:50 in KCl/PVS as a quenching agent. Some samples were analysed using ICP without filtration while other samples were filtered before the ICP analysis was carried out. Two syringe filters were used to carry out the sample filtration step, namely 0.45 and 5 μm.

2.4 FeS inhibition

The brine was sparged with N_2 for 3 hours and was then transferred to an anaerobic chamber, at which point the appropriate masses of $FeCl_2.4H_2O$ were added to separate solutions. Separately, 250 ml of a 10,000 ppm scale inhibitor stock solution was prepared in 3.5 wt% NaCl and KFW. An aliquot of this scale inhibitor stock solution was then added to the Fe solutions and two duplicate 50 ml samples were transferred into glass bottles and labelled. Stock solution samples were made up from what was left of the original 250 ml sample.

Similarly, $Na_2S.9H_2O$ salt was added according to the required concentration of sulphide in the test solution. The pH value was measured and recorded. Afterwards, samples of 50 ml were transferred to labelled glass bottles.

After heating both brines for 1 hour at the desired temperature in an oven, the H_2S brine samples were added to the corresponding metal samples, shaken for 10 seconds, and then placed back into the oven. Sampling was performed at 2 and 24 hours to track the progress of the reaction, with samples being diluted 50:50 in 3.5% HCl as

quenching/dissolving agent. Some samples were analyzed using ICP without filtration while some samples were filtered through 0.2, 0.45 or 5 μm filters before they were transferred to the quenching solution. The samples, stock solutions, and ICP standards were sent for ICP analysis to measure the concentrations of Fe ions. After cooling of the samples to room temperature, final pH measurements were made and solid particles were collected for particle size analysis.

2.5 Cation displacement experiments

These experiments were conducted under anaerobic conditions. In the cation displacement experiments, 50 ml of Fe solution (with and without SI) were mixed with 50 ml of H_2S solution. Samples were collected and sent for ICP analysis to measure the concentrations of Fe. Then, 100 ml of Zn or Pb solution (with and without SI) were added to the FeS solution. Samples were collected and sent for ICP analysis to measure the final resulting Fe, Zn and Pb concentrations. From these results it was possible to determine whether or not, and to what exact extent, cation displacement had taken place.

2.6 Fe, Zn and Pb interaction in sulphide solutions

These experiments were conducted under anaerobic conditions. An H_2S solution was mixed with a low pH SI-solution to give the desired pH. After that, aliquots of Fe, Zn and Pb solution were added to the mixture to give the desired concentration. The test was repeated with a different order of cation addition.

2.7 Filter-blocking test

In the filter-blocking test, see Figure 2.1, H_2S brine and M^{2+} brine (with and without scale inhibitor) are injected at equal flowrate. The length of pre-heat coils is enough to heat the solutions to the desired temperature. The solutions are mixed before they flow through the in-line filter and the pressure drop cross the filter is measured by dP transducers.

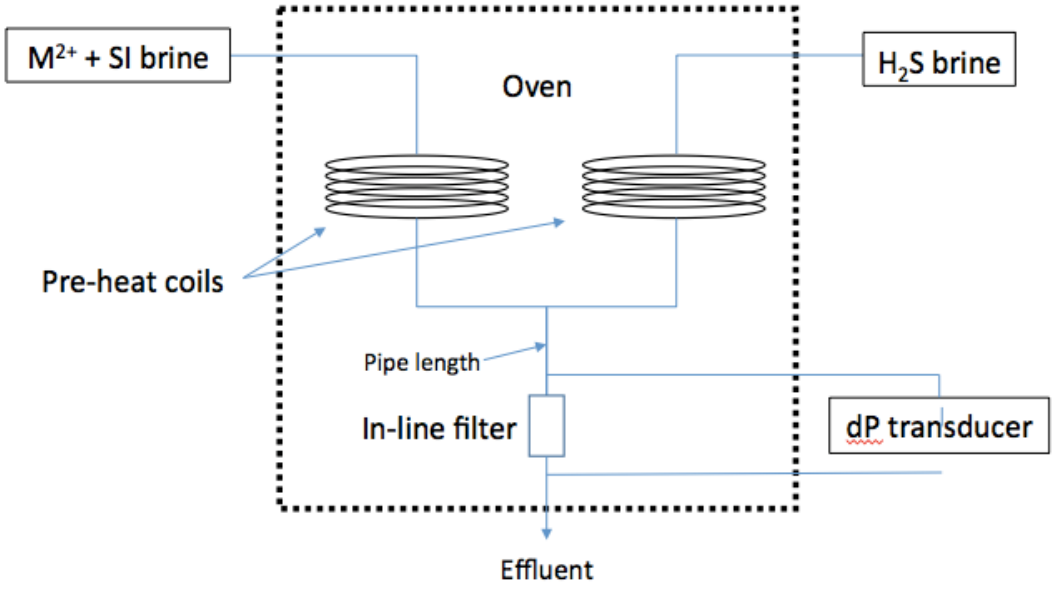

Figure 2.1 Filter-blocking apparatus

2.8 Scale inhibitors used in this study

In this work, various scale inhibitors have been tested to prevent or delay FeS, ZnS and PbS deposition,; these SIs are listed in Table 2.7, which gives the SI structure, chemical name or at least the information we have available about the product.

Table 2.7 Chemical structure and molecular weight of the tested scale inhibitors (SI)

Scale Inhibitor	Chemical Structure	Mw (g/mol)
Phosphinopolycarboxylic acid (PPCA) **SI-1**	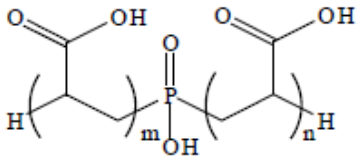	~3800
SI-2 & SI-3	High molecular weight sulphonated co-polymers. The chemical structure has not been disclosed; however, the proposed inhibition mechansim is described below by Savin *et al* (2014).	
Diethlenetriamine penta (methylenephosphonic) acid (DETPMP) **SI-4**	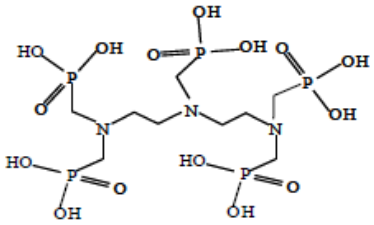	573
Hydroxyethane diphosphonic acid (HEDP) **SI-5**	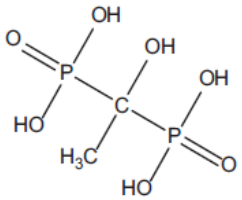	206.03
Vinylsulphonated acrylic acid co-polymer (VS-Co) **SI-6 and SI-7**	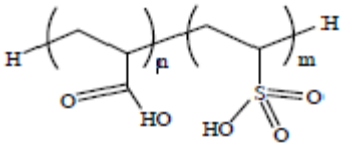	<4000
SI-8	Acrylic sulphonated non-ionic Terpolymer	
SI-9	Aminotris(methylenephosphonic acid) (ATMP)	
SI-10	Maleic acid copolymer	
SI-11	High molecular weight sulphonated co-polymer	

SI-2 and SI-3 are high molecular weight sulphonated co-polymers. The proposed sulphide scale inhibition mechanism of SI-3 has been discussed in the literature (Savin et al., 2014). They propose that these polymers, which have some amide functionality, adsorb on the crystal surfaces and subsequently hinder further growth. Another hypothesis which is discussed is that the resonance forms of the amide bonds can act as nucleation sites and so the sulphide pre-crystals form within the inhibitor. As a result, the colloidal sulphide particles are trapped by the polymer chain and thus their deposition is prevented

2.8 Summary

As described above, different brines were used in this study including North Sea Seawater (NSSW), Glenelg Formation Water (GFW) and Khuff Formation Water (KFW), in addition to various simple sodium chloride brines. ZnS and PbS scales have been observed in several wells in the Glenelg reservoir and thus Glenelg formation water (GFW) was selected as a representative of high salinity brines. FeS, on the other hand, is a major problem in Khuff formation and hence Khuff formation water (KFW) was used for FeS inhibition tests. In addition, other brines such as NSSW and NaCl were used to study the impact of salinity on the inhibition efficiency. As will be shown in the following sections, there was a compatibility issue between sulphate and Pb and therefore sulphate free NSSW (denoted SFNSSW) was used to avoid $PbSO_4$ precipitation.

Conventional static inhibition efficiency scale tests procedures were mainly used in this study. However, some modifications were made to allow mixing the scale in different orders, for example to precipitate PbS then ZnS. Also, similar procedures were used for the cation displacement reactions.

Several scale inhibitors were tested and the focus was on two of them namely the high molecular weight sulphonated co-polymers. SI-2 and SI-3. These 2 products were selected as they showed promising results based on the published work of Okocha et al., 2014. PPCA which is commercially available polymeric scale inhibitor, was used for FeS, ZnS and PbS inhibition and scale consumption tests.

Chapter 3

FeS, ZnS and PbS Formation as single scales

3.1 Introduction

In this chapter, the formation of FeS, ZnS and PbS was studied over a wide range of parameters including pH, salinity, temperature and H_2S, Fe, Zn and Pb concentrations. For the ZnS and PbS systems, the reaction between Zn and sulphide, and Pb and sulphide were both at 1:1 molar ratio at all tested conditions including pH that is encountered in the field *i.e.* ~ 4.5 and above. On the other hand, FeS was very sensitive to pH as it started to form at pH ≥ 4.5. This behaviour was observed when the tests were conducted under aerobic and anaerobic conditions.

The main objective of the following experiments was to validate the experimental procedure prior to performing the inhibition experiments in order to draw accurate conclusions.

3.2 H_2S Evolution

It was essential to determine the composition of the scaling metal and H_2S brines prior to scale formation in order to make an accurate interpretation of the results. This is particularly pertinent for the H_2S brine from which sulphide can be lost due to H_2S gas evolution. In order to monitor the actual amount of aqueous sulphide present in H_2S brines at the time of reaction, quenching experiments were used to determine the total sulphide content. The results of these experiments are plotted in Figure 3.1. The H_2S concentration was calculated by applying equation (3.1):

$$H_2S\ (\text{ppm}) = (\text{M in stock} - \text{M in supernatant}) * \frac{\text{Mw}(H_2S)}{\text{Mw}(\text{M})} \quad \textbf{(3.1)}$$

where M = Zn or Pb

For SFNSSW (Sulphate Free North Sea Water), shown in Figure 3.1 (left) secondary axis, the initial H_2S concentration (time: 0 min) was 15.5 ppm and the H_2S concentration decreased to around 13 ppm after 1 h, hence a loss of 2.5 ppm H_2S was observed over the 60 minute pre-heating period, equating to approximately 16% of the input level. The sulphide content of GFW (Glenelg Formation Water) at different temperatures are plotted in Figure 3.1 (right). Despite a similar mass of sodium sulphide salt being added to the GFW brine, the initial sulphide concentration was lower than that of the SFNSSW. The initial H_2S concentration in GFW was 12 ppm as shown in Figure 3.1 (right) at time 0 min. This was due to the vigorous shaking and increased

time required to dissolve the salt in the high TDS brine, combined with the lower resultant pH (~pH 10) which gives greater time and propensity for H_2S evolution. Unlike the trend in SFNSSW, it was interesting to note that a negligible amount of H_2S evolved from GFW at 50°C over the same 60 minute period as shown in the grey diamonds in Figure 3.1 (right). However, this was not the case at 95°C (Figure 3.1 right: orange triangles) where H_2S evolved continuously from the solution with heating, leading to a loss of 25% of the initial sulphide from the H_2S GFW prior to mixing the brines. These results highlight the importance of tracking the sulphide concentration before and throughout the experiments, both for ZnS and PbS formation experiments and, more significantly, in the sulphide inhibition experiments as will be discussed in this paper and subsequent publications.

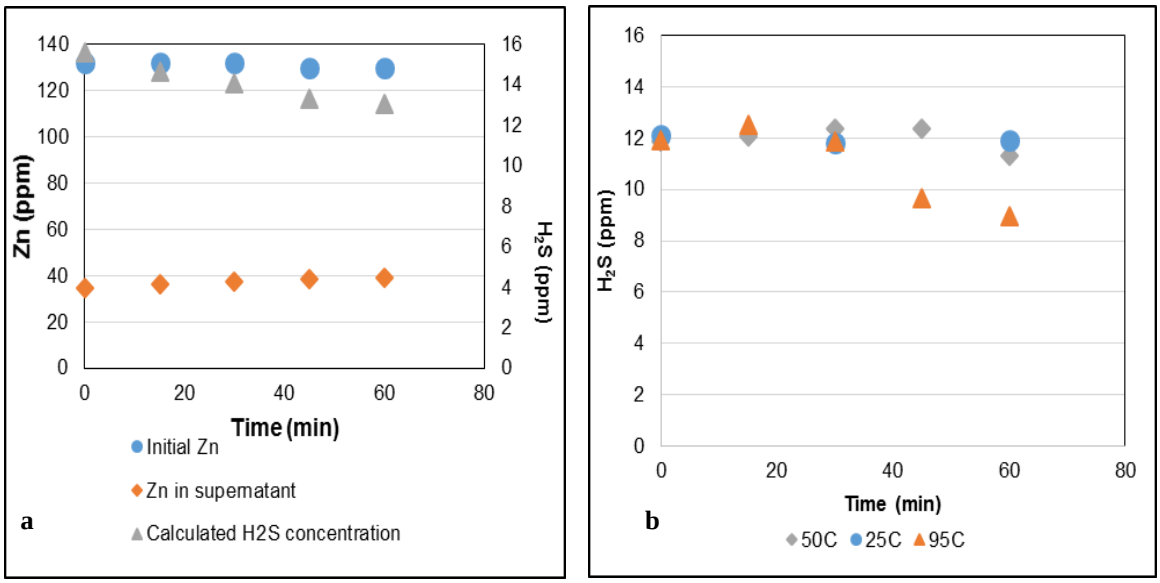

Figure 3.1 Calculated H_2S concentrations in (a) SFNSSW and (b) GFW at 50°C and 95°C as a function of time, pH_0 of M_{2+} SFNSSW was adjusted to 5.

3.3 Solubility of Pb and Zn compounds in different TDS brines

The intention was to use up to 300 ppm Pb and Zn in PbS and ZnS formation experiments *i.e.* 150 ppm Pb and Zn after mixing. The following set of compatibility experiments was conducted to ensure that the tested Pb and Zn concentrations were fully soluble in the brines used in these experiments.

Different masses of lead acetate and zinc chloride were added to DW, SFNSSW, NSSW and GFW such that theoretical Pb and Zn concentrations of 100, 200 and 300 ppm were obtained. As shown in Figure 3.2, ICP analysis revealed that Zn and Pb were completely soluble in the tested brines, except for the Pb in the synthesised NSSW. The

solid formed during these tests was further analysed and found to be lead sulphate, therefore requiring the use of sulphate-free NSSW (SFNSSW) to avoid this loss mechanism.

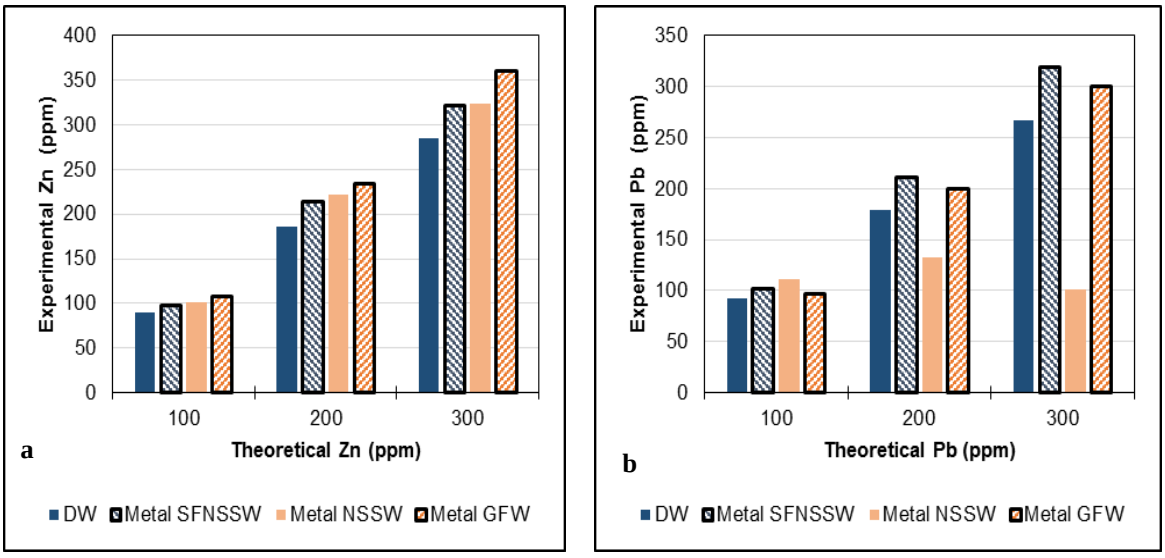

Figure 3.2 Solubility of (a) Zn compounds and (b) Pb compounds in different TDS brines.

3.4 ZnS and PbS formation (as single scales)

3.4.1 Various Zn, Pb and sulphide concentrations and different pH

ZnS and PbS were formed in SFNSSW at 22°C where the metal brine was pH adjusted to different values *i.e.* pH 1.68, 3 and 5.4. All solutions contained approximately 15 ppm H_2S while two concentrations of Zn and Pb were used in order that two regions were covered, namely sulphide excess and scaling metal excess. In addition to ICP data, pH measurements are also presented in Fiure 3.3 and Figure 3.4.

In the sulphide excess samples, a total loss of zinc from solution was observed for pH_0 3 and 5.4, with a white precipitate being observed that was identified as ZnS. These samples had final pH values of 5.7 and 8.7, respectively. Lowering the pH_0 to 1.68 resulted in a final mixed pH of 2.11, with no observed precipitation and a final zinc concentration equal to the original value. The absence of precipitation was caused by the increased solubility of ZnS at very low pH, with pH 2.11 evidently being sufficiently low to solubilize the solid.

In the zinc excess samples, the final pH values of the supernatant were 3.6 and 5.9 for pH_0 3 and 5.4, respectively. The final zinc concentration was found to be 23.6 and 20.7 ppm, respectively, with the difference in zinc dropout being attributed to the slight

evolution of H_2S gas during the mixing stage; this effect is more pronounced with decreasing pH of the metal brine.

Figure 3.4 shows the pH measurements and ICP data when Pb was reacted with H_2S. PbS has extremely low solubility ($K_{sp} \approx 2.5 \times 10^{-29}$) and, as a result, the limiting reactants whether Pb or sulphide were completely consumed regardless of the final pH. Of particular interest is that the difference between Pb concentration in the stock solution and the supernatant solution is consistent over this pH range. Therefore, the H_2S concentrations in low and high pH solutions are equivalent. So, based on the previous results, it appears that the PbS formation is faster than the H_2S evolution.

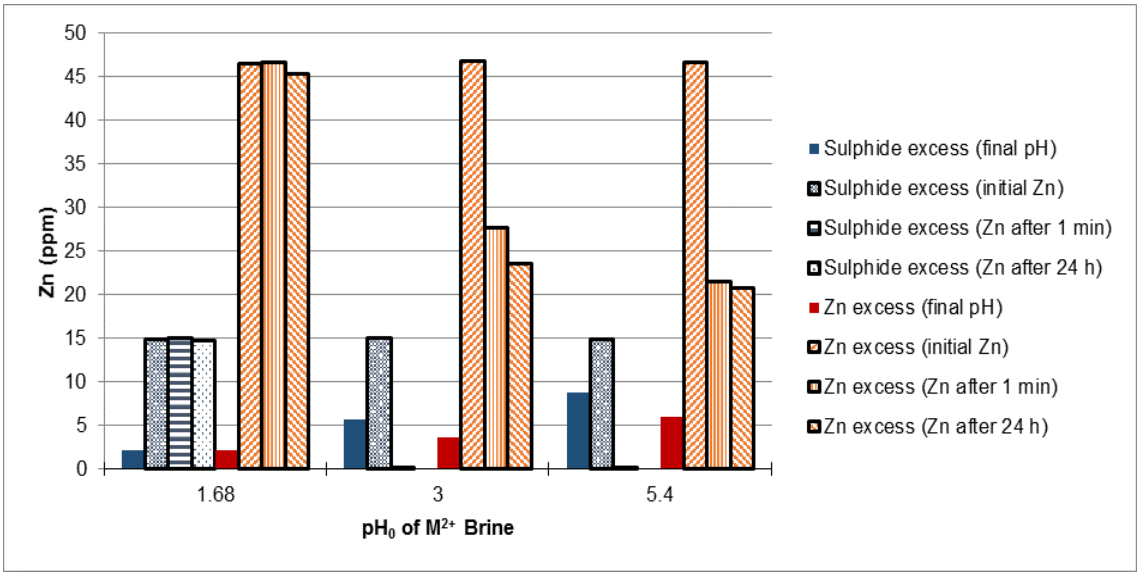

Fiure 3.3 ZnS formation in SFNSSW at 22°C and different pH_0 values.

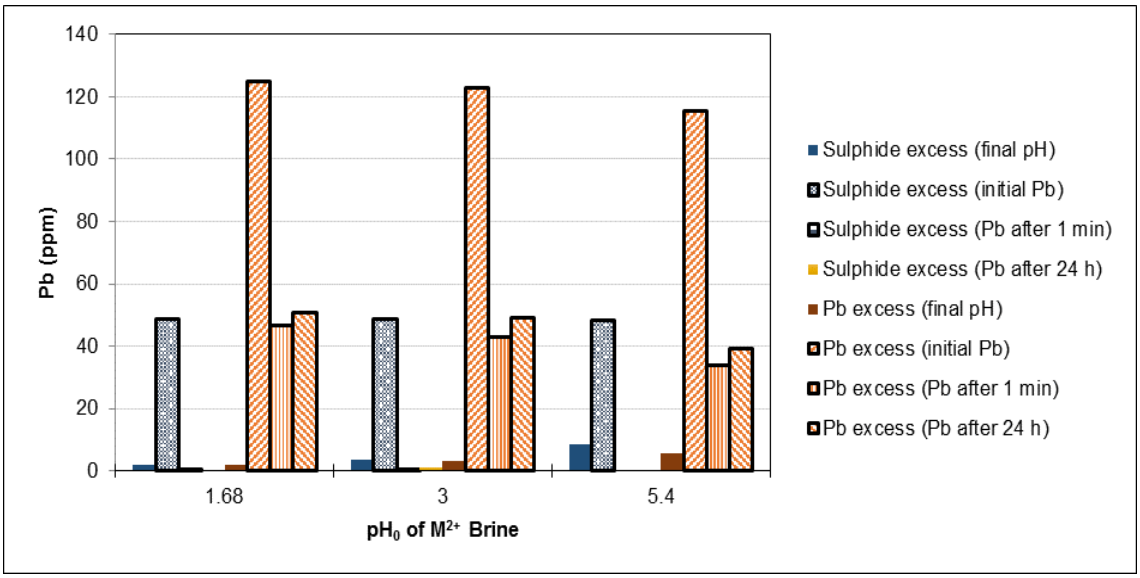

Figure 3.4 PbS formation in SFNSSW at 22°C and different pH_0 values

The experimental pH measurements and particle size distribution for these single scale experiments are shown in Table 3.1 and Table 3.2. When Zn SFNSSW, at an adjusted pH of 1.65, was mixed with H_2S SFNSSW, the final pH of the supernatant solutions was 1.95, and all Zn ions remained in solution. To determine whether Zn ions remained unreacted because of high ZnS solubility or complete H_2S evolution, the H_2S concentration was monitored at two temperatures, with the pH of SFNSSW adjusted to 1.67. As clearly shown in Figure 3.5, even although the final pH was 2.08, the amount of H_2S remaining in the solution was sufficient to react with nearly 12 ppm Zn. Thus, Zn ions were held in the solution because the high solubility of ZnS at pH of 1.95 rather than complete H_2S evolution prior to Zn and sulphide reaction.

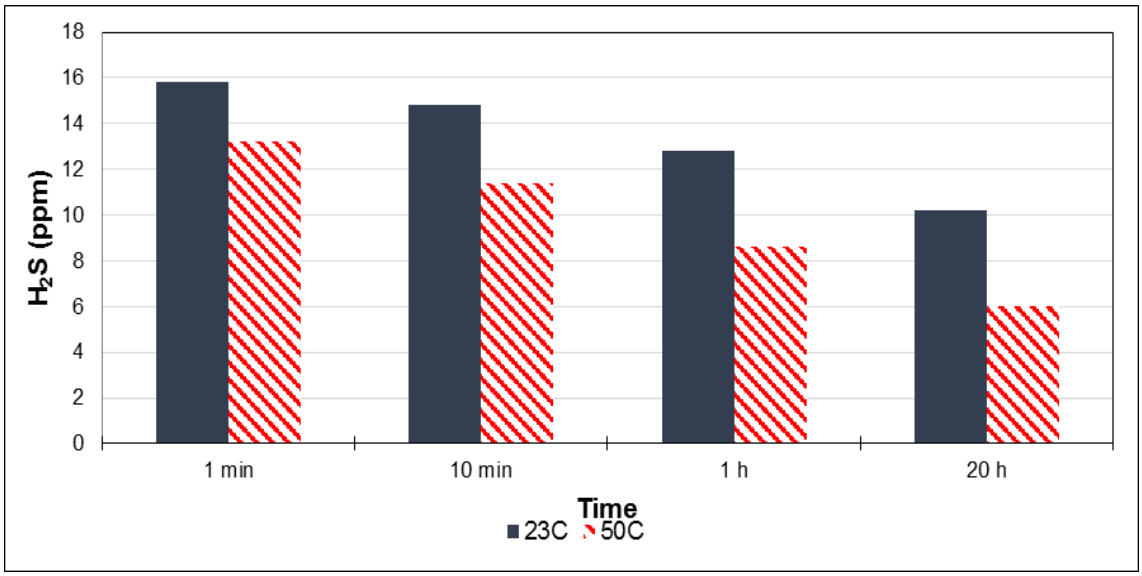

Figure 3.5 Calculated H_2S concentrations in SFNSSW at different temperature values and as a function of time. pH_0 of SFNSSW was adjusted to 1.67

By contrast, ZnS completely precipitated in the other 2 solutions where the final pH values were pH 6.5 and 8.9. Similarly, when Zn and H_2S concentrations were raised to 50 and 100 respectively, all solutions were stripped of Zn as a result of complete ZnS formation at the tested pH values between pH 2.4 and 8.8. This discrepancy in reactivity can be attributed to the higher final pH value as well as to the higher H_2S concentration.

As presented in Table 3.1, the particle size of PbS was greater than that of the ZnS at the corresponding test pH value and, moreover, the particle size of the single scale *i.e.* ZnS and PbS did not change at different pH values. However, the particle size of mixed scale decreased from nearly 20 to 7 µm when the pH decreased from pH 8.5 to 3.8. As

pH was further reduced, the particle size increased to 20 µm as a result of single PbS formation rather than mixed scale at pH of 1.95. A similar trend was observed when H_2S and scaling metals were raised to 100 ppm and 50 ppm respectively, see Table 3.2. The particle size of PbS remained constant at all tested pH values while ZnS and mixed scale showed a downward trend. The increase in the particle size at higher pH values might be attributed to the formation of other scales such as zinc hydroxide alongside ZnS. The particle size analysis of different sulphide scales formed at different conditions should lead to a better understanding of the sulphide inhibition results in future work.

Table 3.1 ZnS and PbS formation in SFNSSW at 50°C in presence of 20 ppm H_2S after 20 hours

Zn (ppm)	Pb (ppm)	Adjusted pH	Final pH	D_{10} (µm)	D_{50} (µm)	D_{90} (µm)
15	0	5	8.89	6.25	12.58	24.06
15	0	3	6.48	6.34	13.16	24.53
15	0	1.67	1.93	-	-	-
0	15	5	9.24	7.11	20.15	73.82
0	15	3	7.08	9.36	20.56	35.57
0	15	1.67	1.94	10.89	20.61	33.76
15	15	5	8.52	9.72	20.57	40.17
15	15	3	3.78	3.64	7.32	15.69
15	15	1.67	1.95	10	19.76	33.07

Table 3.2 ZnS and PbS formation in SFNSSW at 50°C in presence of 100 ppm H_2S after 20 hours

Zn (ppm)	Pb (ppm)	Adjusted pH	Final pH	D_{10} (µm)	D_{50} (µm)	D_{90} (µm)
50	0	5	8.78	5.8	14.77	30.61
50	0	2	7.01	3.99	8.67	23.29
50	0	1.67	2.42	1.2	2.47	5.03
0	50	5	8.97	5.35	19.15	62.78
0	50	2	6.77	12.86	24.81	46.82
0	50	1.67	2.68	11.77	23.33	41.77
50	50	5	8.86	8.59	19.4	35.27
50	50	2	6.05	5.18	12.54	27.12
50	50	1.67	2.36	0.88	2.04	3.71

3.4.2 PbS formation in different TDS brines

Lead acetate trihydrate was added to distilled water to give a wide range of Pb concentrations (140 - 3,600 ppm Pb). Pb concentration in the supernatant solutions after 24 hours and the resulting pH values are shown in Figure 3.6 (a). Up to a Pb:S molar ratio of 1, all solutions were stripped of Pb, as expected from the extremely low solubility of PbS. As sulphide became the limiting species, lead started to be detected in solutions with a consistent difference in concentration between stock solutions and

Pb detected in the supernatant solutions equivalent to the quantitative molar loss of Pb consumed by the initial sulphide concentration.

Initial pH values of H_2S DW and Pb DW were pH 12 and 5, respectively. After mixing, the pH was controlled by sulphide, lead and to a lesser extent acetate. As shown in Figure 3.6-a (secondary axis), at the lowest Pb:S molar ratio, *i.e.* Pb:S = 0.15, the pH was 11.2. At this ratio, the solution contained excess sulphide and, consequently, all Pb precipitated as PbS and hence pH was mainly governed by aqueous sulphide species. The pH value declined between Pb:S molar ratios 0.15 to 0.5, from 11.2 to 9.93. In this region, pH was mainly controlled by sulphide content; yet, the effect of acetate on pH was distinct. There was a sharp drop in pH when Pb:S molar ratio increased from 0.5 to 0.6. At Pb:S molar ratio of 1, the pH value was 5.46 and remained constant afterwards. In the region of excess Pb, all sulphide reacted with lead and precipitated, and mainly the remaining lead and acetate in solution controlled the pH.

The correlation between particle size and Pb:S molar ratio was not conclusive. Nonetheless, a broad overall trend can be observed in Figure 3.6 (b). The mean particle size increased as Pb:S ratio increased until it reached a plateau at a 1:1 Pb:S molar ratio, which then fluctuated around 25 μm at higher molar ratios.

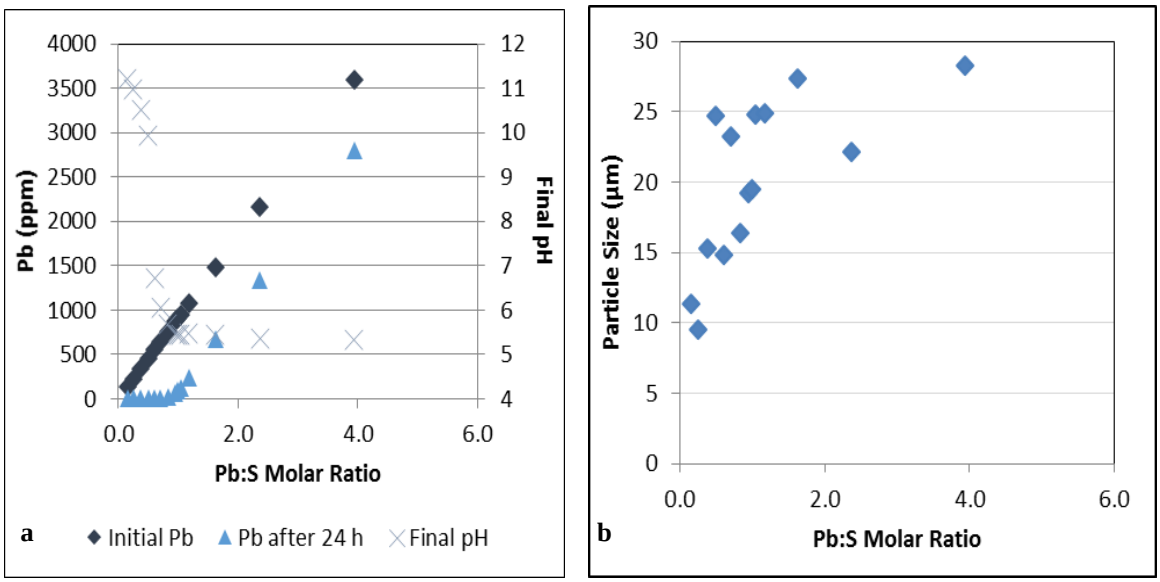

Figure 3.6 (a) Pb concentrations detected in stock solutions and supernatants after 24 h and final pH values, (b) Particle size distribution of PbS DW solutions.

In the next set of experiments, 15 – 142 ppm Pb was used instead of 140 – 3600 ppm Pb, which is more representative of field Pb levels. Figure 3.7 (a and b) show Pb concentrations in ppm versus Pb:S molar ratio before and after sulphide concentration correction, respectively. Different masses of lead acetate were added to SFNSSW to give various Pb concentrations and the resulting Pb:S molar ratios varied from Pb:S = 0.2 to 2. Up to approximately Pb:S molar ratio of 1, the supernatant solutions were stripped of Pb indicating complete precipitation of Pb as PbS. As the molar ratio increased above 1:1, Pb was detected in solution and increased gradually. The difference between the stock Pb concentrations and supernatant solutions is constant in the Pb excess region, regardless of Pb:S ratio. Since the Pb:S molar ratio was calculated based on the theoretical concentration of sulphide, a slight shift was observed when the sulphide concentration was corrected for H_2S gas evolution. When sulphide SFNSSW and Pb SFNSSW were mixed, the pH dropped to different values depending on initial Pb concentration. For example, at the minimum Pb:S molar ratio, the pH was 9 while at maximum Pb:S molar ratio pH was 5. Additionally, pH decreased gradually at Pb:S molar ratios less than 1 where the pH is predominantly controlled by sulphide contents. When sulphide was completely consumed *i.e.* Pb:S greater than 1, pH remained almost constant.

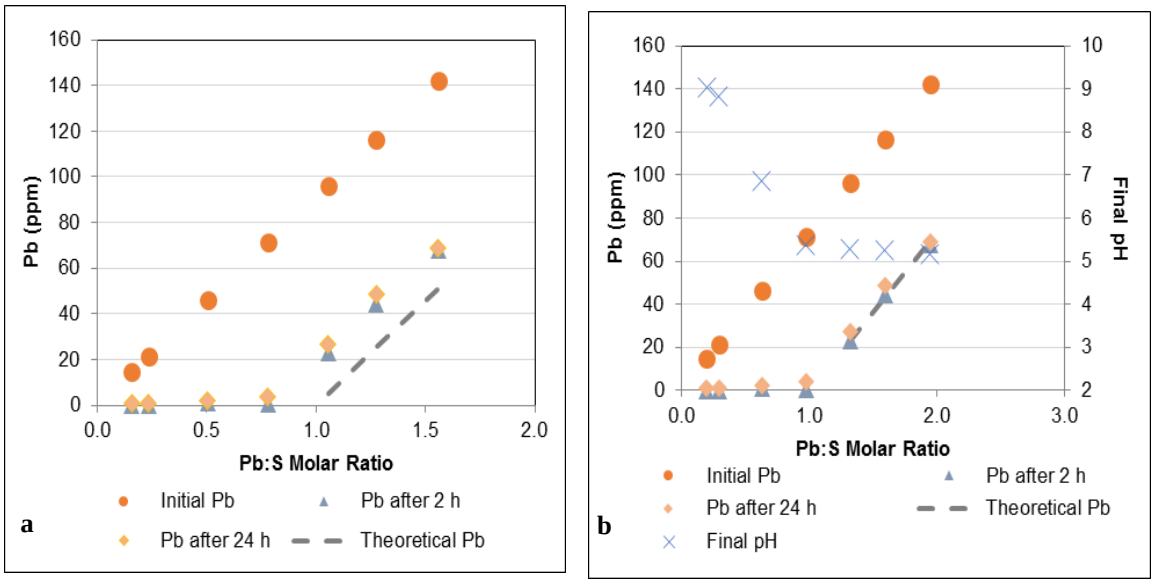

Figure 3.7 PbS formation in SFNSSW at 50°C, pH_0 of M_{2+} brine = 5 (a) sulphide concentration was not corrected, and (b) sulphide concentration was corrected.

3.4.3 The impact of pH on PbS formation

In an attempt to study the effect of pH on PbS formation, the initial pH of Pb SFNSSW was adjusted to 1.67. In addition to pH measurements, the Pb concentration in stock solutions and supernatant solutions at different Pb:S molar ratios are presented in Figure 3.8. In the excess Pb region, all solutions were deficient in Pb ions indicating complete precipitation of PbS. In the sulphide excess region, Pb started to be detected in supernatant solutions and increased gradually. It is interesting to note that the amount of Pb ions that reacted with sulphide at pH of 1.95 is equivalent to that reacted at pH of 5.5. Therefore, PbS formed before the H_2S was liberated from solution. This is in complete agreement with the results discussed above. Unlike PbS formation at pH 5, when the initial pH was adjusted to 1.65 the final pH was 1.95, regardless of the Pb:S molar ratio. This indicates that the final pH was primarily controlled by initial pH of solution and sulphide no longer has an effect on pH even in the sulphide excess region.

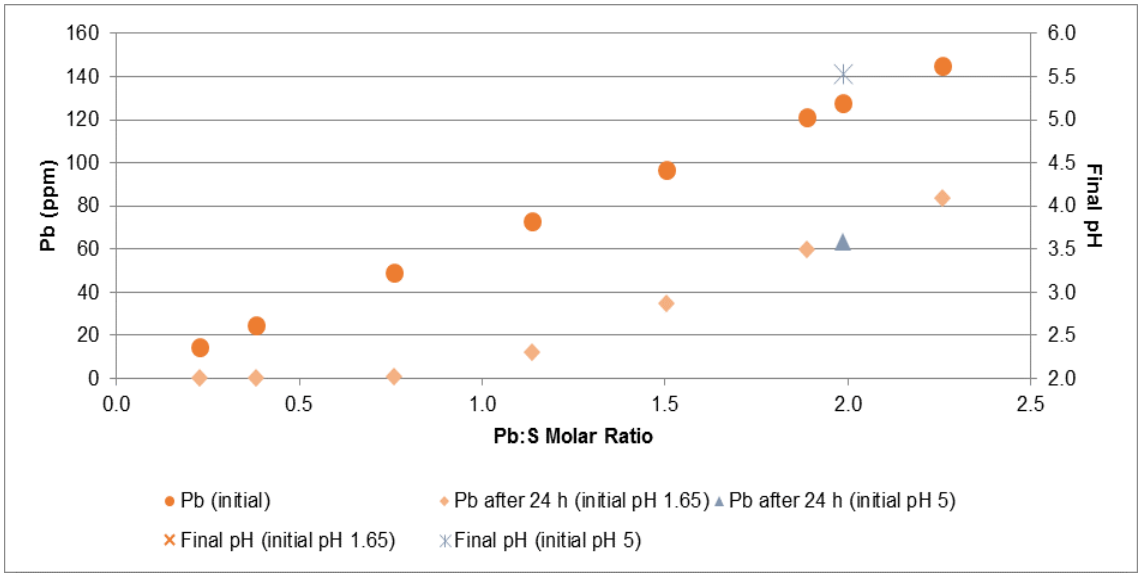

Figure 3.8 PbS formation in SFNSSW at 50°C and pH_0 1.65 and 5

In order to study the effect of salinity on PbS formation, PbS formation experiments were repeated under the same conditions, except for brine composition; the very high salinity GFW was used instead of SFNSSW. Figure 3.9 shows the Pb concentrations versus Pb:S molar ratio when PbS was formed in GFW. Although sulphide based scale solubility increases with increasing salinity, there was no apparent difference in Pb levels at Pb:S molar ratios less than unity when PbS formed in very saline brine. At Pb:S molar ratios greater than 1:1, the increase in Pb concentrations in high salinity brine resulted from the total consumption of sulphide species, rather than any increase in solubility.

As shown in Figure 3.9, the pH behaviour when PbS formed in GFW is quite similar to that observed in SFNSSW with some minor differences. At the minimum Pb:S molar ratio (Pb:S ~0.19), the pH was 8, while it was 9 in SFNSSW. This is attributed to the difference in natural pH of H_2S SFNSSW (pH of 11) and H_2S GFW (pH of 10).

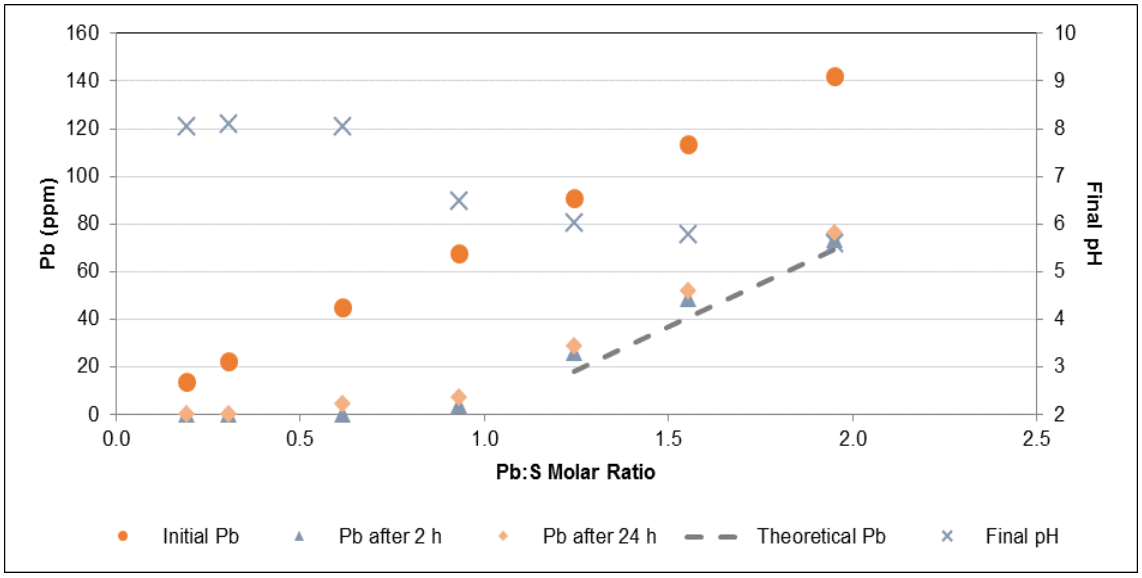

Figure 3.9 PbS formation in GFW at 50°C and pH_0 of M^{2+} brine = 5

3.4.4 ZnS formation in GFW

Like PbS, the solubility of ZnS is very low and hence it was expected that both PbS and ZnS would show very similar behaviour in terms of pH and reactivity. This is indeed shown in the results in Figure 3.10. When sulphide was in excess to Zn, all solutions were deficient in Zn. However, when the Zn:S ratio exceeded unity (*i.e.* zinc was in excess), Zn was detected in the supernatant solutions. In this region, sulphide was completely consumed and whatever amount of Zn was added to solution remained unreacted. It is worth noting that the ZnS reactivity and pH behaviour are in good agreement with the results reported by Graham *et al.*, 2016 in spite of the significant difference in initial Zn and H_2S concentrations.

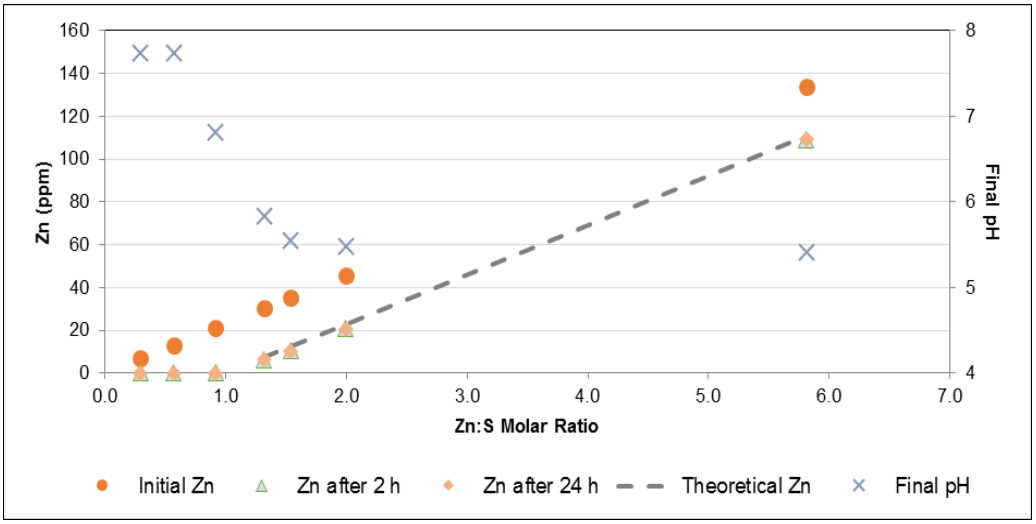

Figure 3.10 ZnS formation in GFW at 50°C and pH$_0$ of M^{2+} brine = 5

3.5 FeS Formation in 3.5 wt% NaCl

A series of aerobic FeS formation experiments were carried out over a range of pH values (see results in Figure 3.11). Up to and including pH 3.54, no loss of iron was noted by ICP analysis, however at pH values 4.55 and 4.98, it was seen that 10 and 40 ppm Fe precipitated, respectively. Complete FeS precipitation occurred as a consequence of increasing the pH to 6.72 and above. It can be clearly seen from Photo 3.1 at pH 3.54, the colour changed to orange due to $Fe(OH)_3$ formation then it turned black as a result of FeS formation. Minutes later, the solution became clear indicating that FeS re-dissolved and this observation was confirmed by ICP analysis. The cloudiness resulted from sulphide oxidation as the experiments were performed in presence of oxygen and Fe^{3+}.

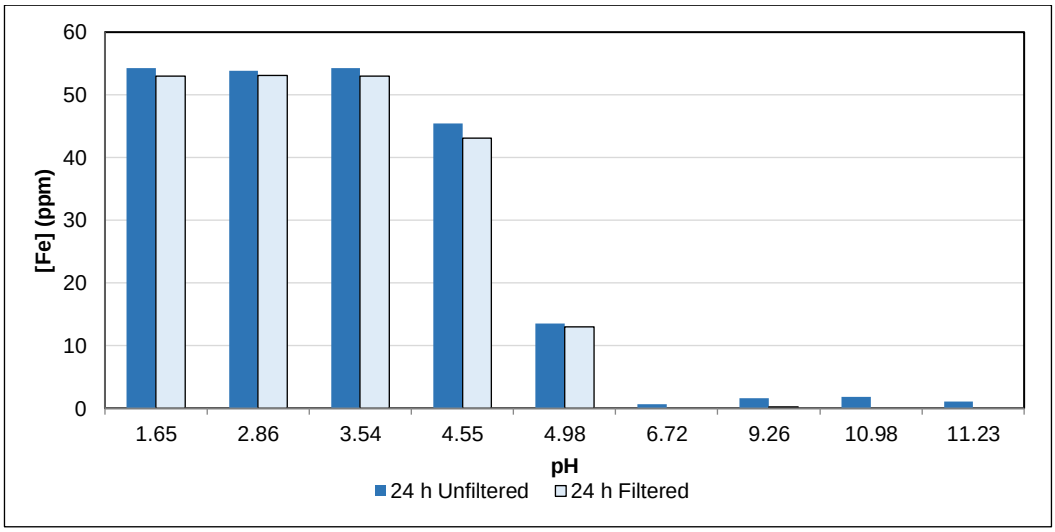

Figure 3.11 Iron concentrations in FeS solutions under aerobic conditions at different pH in 3.5% NaCl. The initial iron concentration was 54 ppm.

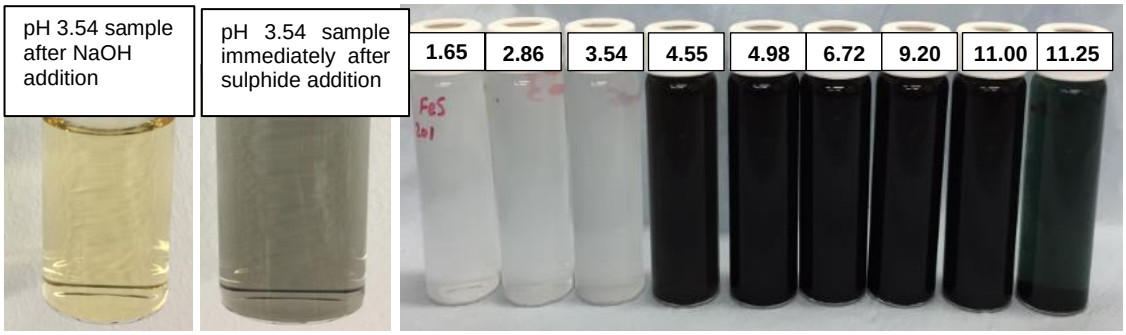

Photo 3.1 FeS formation under aerobic conditions at different pH values in presence of 100 ppm H_2S and 54 ppm Fe.

The FeS formation tests described above were repeated under anaerobic conditions. Similar behaviour was observed as FeS started to precipitate at pH 4.59, as shown in Figure 3.12. Note the discernible decline in the Fe concentrations when pH was raised from 4.6 to 5 and then to pH 5.7. Thus, in FeS inhibition experiments performed within this pH range, Fe detected in an inhibited solution will be a combination of dissolved Fe ions (based on pH) and suspended FeS particles as ICP measures the total Fe concentration. Therefore, it is critical to consider the solubility of FeS, *i.e.* dissolved Fe, in order to accurately analyze FeS inhibition results otherwise the inhibition efficiency might be overestimated, as will be discussed in the following sections.

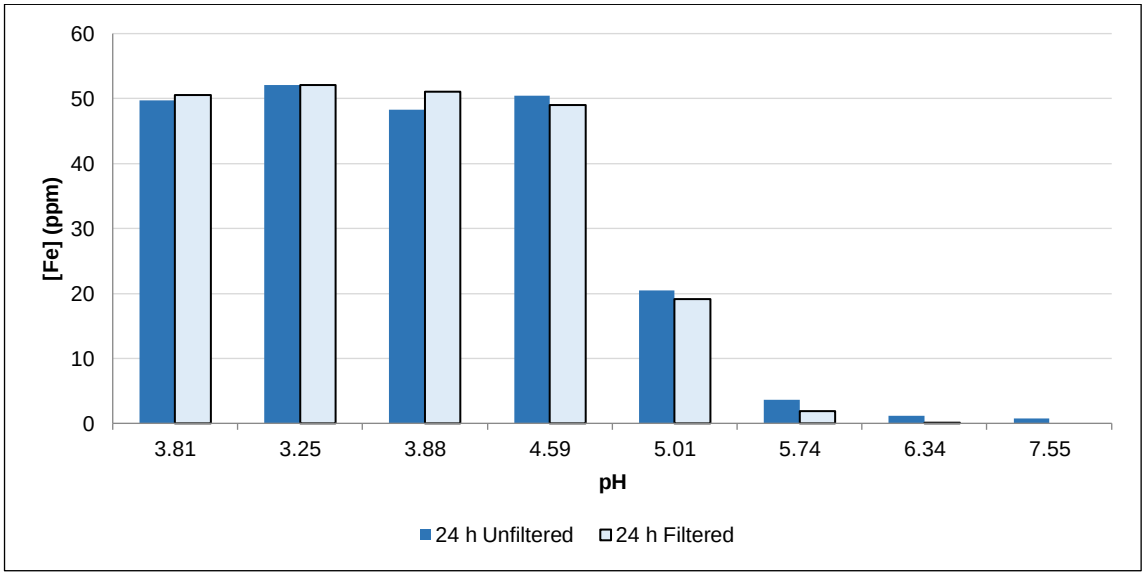

Figure 3.12 Iron concentrations in FeS solutions under anaerobic conditions at different pH in 3.5% NaCl. $[Fe]_0$ = 52 ppm.

3.6 Conclusions

In this work, FeS, ZnS and PbS were precipitated using iron chloride, zinc chloride and lead acetate respectively in sodium sulphide brines. Due to solubility effects in the

presence of sulphate ions at high concentrations, PbS was precipitated in sulphate-free NSSW to avoid lead sulphate ($PbSO_4$) precipitation. In absence of sulphide, Fe, Zn and Pb compounds were soluble regardless of the presence of other cations including Na, Ca and Mg. The precipitation of $PbSO_4$ was observed only in NSSW rich in sulphate. Similarly, none of the cations including Na, Ca and Mg have an impact on the solubility of ZnS, PbS and FeS due to the very low solubility of these scales. Unlike the salinity, temperature and pH had an impact on the solubility of sulphide scales. Under conditions tested in this study, PbS was insoluble regardless of the tested conditions while ZnS was soluble in low pH values. The impact of pH and temperature were clearer in FeS solutions as the higher pH and temperature, the lower solubility of FeS. The main conclusions from this study are as follows:

- Temperature, pH and salinity played a significant role in the amount of H_2S evolution (loss) in the experiments using sodium sulphide.
- The final pH was found to be dependent on the initial pH of metal brine and the H_2S concentration. Furthermore, the pH of solutions might decrease as a consequence of sulphide concentration reduction due to continuous H_2S evolution and spontaneous sulphide consumption in precipitating ZnS and PbS. This should be considered while performing inhibition experiments as the performance of some scale inhibitors are affected by pH.
- The reactions between Zn^{2+} and S^{2-}, and Pb^{2+} and S^{2-} were both 1:1 molar ratio according to the zinc and lead concentrations detected by the ICP. Both PbS and ZnS formation reactions are spontaneous as Pb and Zn ions were completely consumed within 1 min.
- In the sulphide excess region, all added zinc or lead ions were precipitated as ZnS or PbS, respectively. As soon as Zn or Pb are in excess, this is directly detected by ICP.
- The particle size of ZnS and mixed sulphide scales decreased as pH decreased. This effect should be considered when analysing sulphide inhibition results where the inhibitor chemical is acting via a dispersal mechanism.
- The well-documented sensitivity of FeS solubility to pH was observed, with solids only formed at pH $\geq$ 4.5 at the conditions tested. Therefore, the test pH is important when studying FeS inhibition both for this reason, and also because the pH can affect the SI efficiency.

Many previous scale inhibition efficiency studies have evaluated the performance of the scale inhibitors based on the amount of Fe, Zn and Pb detected in the supernatant solutions in comparison to blank solutions. This may not be always an accurate way to assess inhibition efficiency for sulphides. This is the case in particular when sulphide is the limiting reactant since significant H_2S evolution can occur and thus the theoretical concentration of reacted scaling metal would be different to the experimentally designed value. Also, in FeS systems, small change in the pH can result in significant difference in the solubility of FeS and therefore it is crucial to find a way to differentiate between the dissolved Fe and the suspended FeS to avoid misinterpretation of the scale inhibitor results. This matter has been studied further based on the findings of this chapter. As discussed later in this thesis in Chapter 6, certain filter sizes can retain the suspended scale particles.

Chapter 4

Fe, Zn and Pb Interactions in Sulphide Solutions

4.1 Introduction

The objective of this work is to study the interaction between Zn and Pb in solutions containing sulphide species. Two types of experiments were performed in this study. Firstly, ZnS and PbS were formed by mixing Zn/Pb solutions with sulphide solutions over a wide range of Zn:S and Pb:S ratios. Also, Fe, Zn and Pb solutions were mixed with different concentrations of sulphide. These experiments provide an insight into the effect of the detailed *sequence* of FeS, ZnS and Pb precipitation. The second set of experiments (*i.e.* cation displacement experiments) was conducted to investigate the ability of the least soluble scale to form by extracting sulphide from the other pre-formed scales e.g. the ability of Pb to extract sulphide from ZnS. As long as there is dissolved Pb in the solutions, we find that there would be no ZnS and FeS precipitation. Similarly, if there are Zn ions in the solutions, no FeS would precipitate. Furthermore, Pb extracted the sulphide from ZnS and FeS to precipitate PbS, and Zn extracted the sulphide from FeS to precipitate ZnS. It is found that when we attempt to inhibit a given system, the sequence of scale formation matters.

4.2 Zn and Pb interaction in sulphide solutions

4.2.1 Constant Zn and variable Pb concentrations

Figure 4.1 (a) shows the initial Zn and Pb concentrations and the Zn and Pb levels detected in the supernatant solutions 24 h after mixing with sulphide solutions. As shown in Figure 4.1, the initial Zn concentration was constant at 44 ppm in all experiments while Pb varied from 16 ppm up to 138 ppm. Therefore, based on the initial H_2S concentration, Zn:S molar ratio was 2 whereas the Pb:S molar ratio varied from 0.2 to 1.9. At Pb:S less than unity, all solutions were stripped of Pb whereas Zn precipitated partially. As Pb concentration approached approximately 75 ppm which corresponded to Pb:S = 1, the mass of ZnS precipitate decreased. For Pb:S > 1, only Pb precipitated despite the fact that both Pb and Zn existed in excess to sulphide. This was primarily due to the lower solubility of PbS compared with ZnS. The pH values of the supernatant ranged between 5 and 6.5, as seen in Figure 4.1. The increase in pH was associated with the decrease in ZnS. At Pb:S = 0.66, the pH started to decrease as an effect of the increase in acetate concentration in solution.

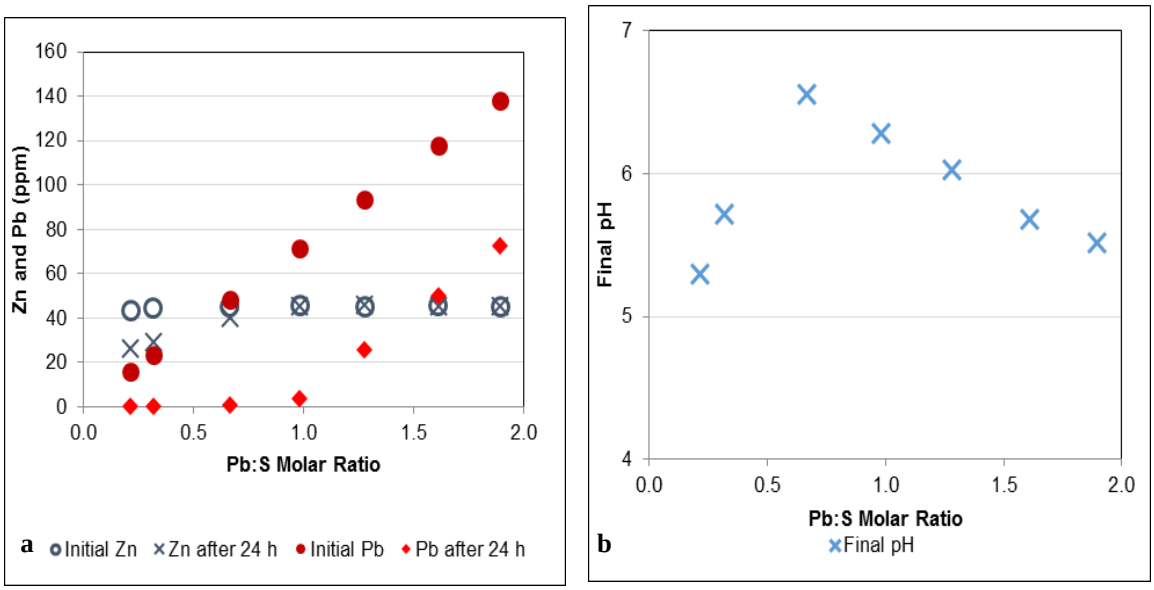

Figure 4.1 ZnS and PbS formation in GFW at 50°C. Zn:S molar ratio was constant at 2 while Pb:S molar ratio was variable

4.2.2 Constant Pb and variable Zn concentrations

To confirm that ZnS did not precipitate in cases where Pb was present in excess to sulphide, another set of experiments was performed. In this set, the Pb:S ratio was kept constant at 1.9 while Zn:S was altered from, Zn:S = 0.34 to 5.5. It is clearly shown in Figure 4.2 that the difference between initial Pb concentration and Pb in supernatant solutions was constant and consistent with a quantitative reaction. Furthermore, the initial Zn and Zn in supernatant solutions are very similar. Therefore, all sulphide ions were consumed by the Pb and hence there was no dissolved sulphide in solutions to react with Zn. This behaviour clearly indicated higher affinity of sulphide towards Pb than that to Zn even at high Zn/Pb molar ratios. The tendency of PbS to precipitate in the presence of Zn while sulphide is the limiting reactant was observed by Dyer *et al.*, 2006 and Orski *et al.*, 2007. The pH measurements of supernatant solutions indicate that acetate was influencing the pH value, while $ZnCl_2$ has an insignificant effect, as seen in Figure 4.2.

The difference between the solubility of ZnS and PbS decreases with increasing temperature (Barret and Anderson, 1988). Therefore, the chance to form mixture of PbS and ZnS increases at higher temperatures. In an attempt to investigate scale formation at higher temperature in presence of Pb, Zn and sulphide, these tests were repeated at 95°C. Increasing the temperature from 50°C (Figure 4.2) to 95°C (Figure 4.3) had no impact on the type of scale, with PbS precipitating while Zn ions were completely held in solution. The difference between Pb concentrations in stock

solutions and supernatant solutions at 50 and 95°C was equivalent to almost 12 ppm and 9 ppm of H_2S, respectively, which was in line with the results from the quenching experiments.

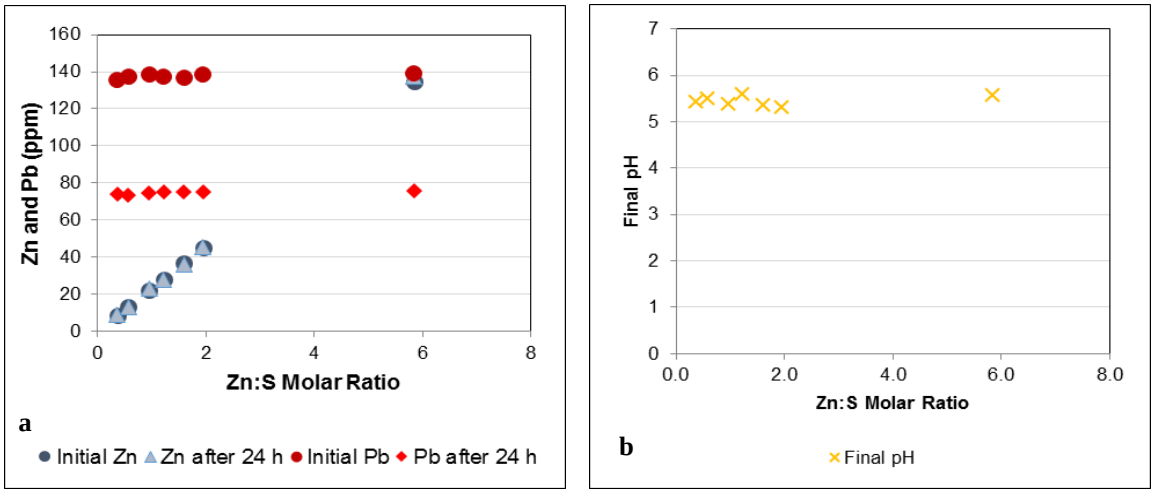

Figure 4.2 ZnS and PbS formation in GFW at 50°C. Pb:S molar ratio was constant at 1.9 while Zn:S molar ratio was variable

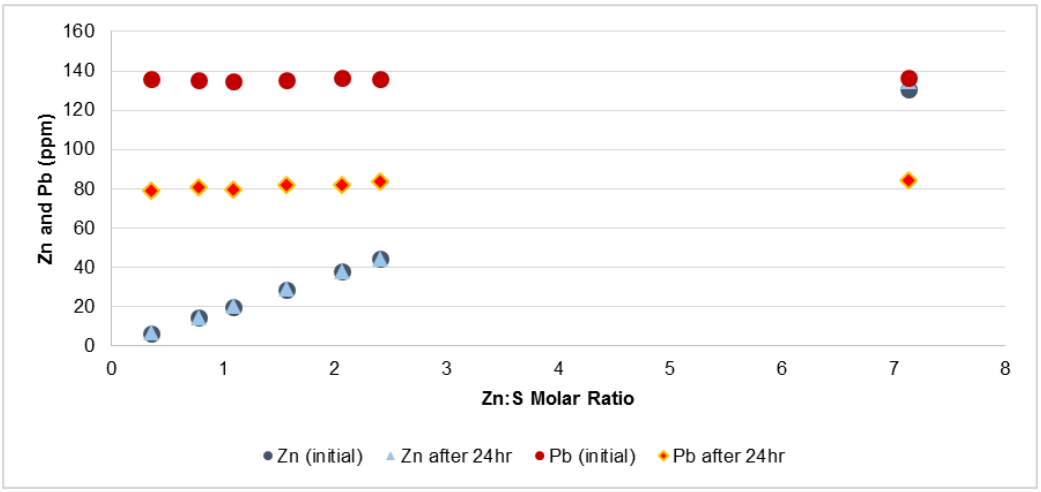

Figure 4.3 ZnS and PbS formation in GFW at 95°C. Pb:S molar ratio was constant at 1.9 while Zn:S molar ratio was variable

4.3 Fe, Zn and Pb interaction in sulphide solutions

Figure 4.4 shows the concentrations of Fe, Zn and Pb in the presence of various sulphide concentrations. For the 5 ppm sulphide solution, single PbS precipitated as can be clearly seen from the drop in Pb concentration, while Fe and Zn remained at input concentration. Increasing the sulphide concentration to 50 ppm resulted in precipitating both PbS and ZnS. Note that FeS started to precipitate *only* when Pb and Zn ions were completely consumed. The EDX analysis results are listed in Table 4.1 and are in good agreement with ICP results *i.e.* PbS was detected at 5 ppm sulphide, PbS and ZnS were

detected in 50 ppm sulphide solutions, and all three sulphide scales formed when the sulphide was in excess to the scaling metals.

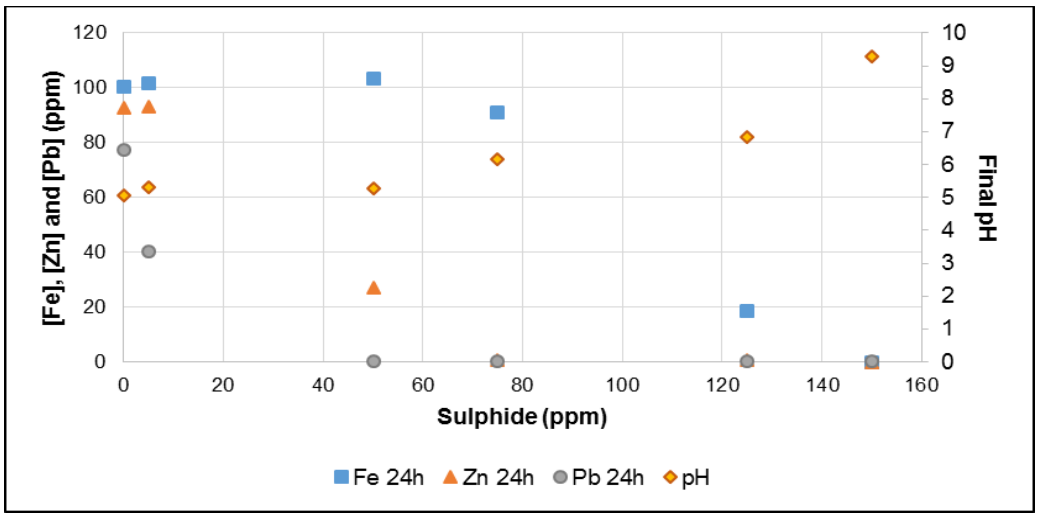

Figure 4.4 Fe, Zn and Pb interaction in sulphide solutions in 3.5 wt% NaCl at 90°C. Initial Fe, Zn and Pb concentrations were 100, 93 and 77 ppm, respectively. Sulphide concentrations were calculated based on Na_2S addition.

Table 4.1 EDX analysis. Samples were collected after 72 h.

Sulphide concentration	5 ppm	50 ppm	125 ppm
Element	**Weight**	**Weight**	**Weight**
S	11.55	18.32	31.58
Pb	76.5	32.72	23.29
Zn	0	30.81	30.05

4.4 Cation Exchange in Sulphide Solutions

The following experiments were conducted to examine the ability of Zn and Pb to extract sulphide from pre-formed FeS. Figure 4.5 (a) shows the Fe concentrations in supernatant solutions 2 h after mixing sulphide solutions with Fe solutions and (b) 22 h after mixing with Zn solutions.

25 ml of 200 ppm Fe were mixed with 25 ml of:

(1) blank *i.e.* no sulphide

(2) 40 ppm H_2S, and

(3) 80 ppm H_2S solution.

After mixing the Fe solution with the sulphide solution, the Fe concentration decreased from 100 ppm to 71 ppm in sample # 2 and to 39 ppm in sample # 3 as a result of FeS precipitation. Note that sulphide was the limiting reactant in these tests, therefore the only source of sulphide in these solutions was FeS scale i.e. mackinawite. After collecting the samples (5 ml) for Fe analysis, 50 ml of 100 ppm Zn solution were added

to the FeS-containing solution. Therefore, after mixing, the zinc and iron concentrations would be 50 and 46 ppm, respectively if no precipitation had taken place. (Figure 4.5 (b)). 24 h later, the Zn concentration had declined from 50 ppm to 36 ppm (# 2) and 21 ppm (# 3) indicating that Zn had reacted with the pre-formed FeS to form ZnS with the simultaneous release of Fe^{2+} into solution up to nearly 45 ppm. Similar results were obtained when Pb solution was mixed with FeS solution, see Figure 4.6. When a Pb solution was added to an identical FeS solution the Pb level dropped from 126 ppm to 73 ppm and 13 ppm in samples 2 and 3 respectively, while the Fe concentration increased to 49 ppm.

Based on these results, the cation which has higher affinity towards sulphide, in this case Pb and Zn, would extract sulphide from the preformed scale *i.e.* FeS. The displacement reaction is spontaneous when static tests were performed. But, in the production system the displacement reaction might become slow due to the significant decrease in the reactive surface area and the exposure time between Pb and Zn ions and FeS. In other words, the suspended FeS scale has a much larger reactive surface area than the deposited scale. In spite of that, continuous exposure to Pb and Zn ions can result in partial displacement and a consequential insoluble layer of PbS and/or ZnS may be produced on the deposited FeS, which would make it significantly harder to dissolve by chemical means. This is somewhat analogous to the formation of less soluble FeS_2 from deposited FeS as a result of extended exposure to H_2S (Nasr-El-Din and Al-Humaidan, 2001). The difference in solubility between the scales should be considered when designing removal treatments because the outer layer could act as a barrier that prevents the dissolution of the other scales.

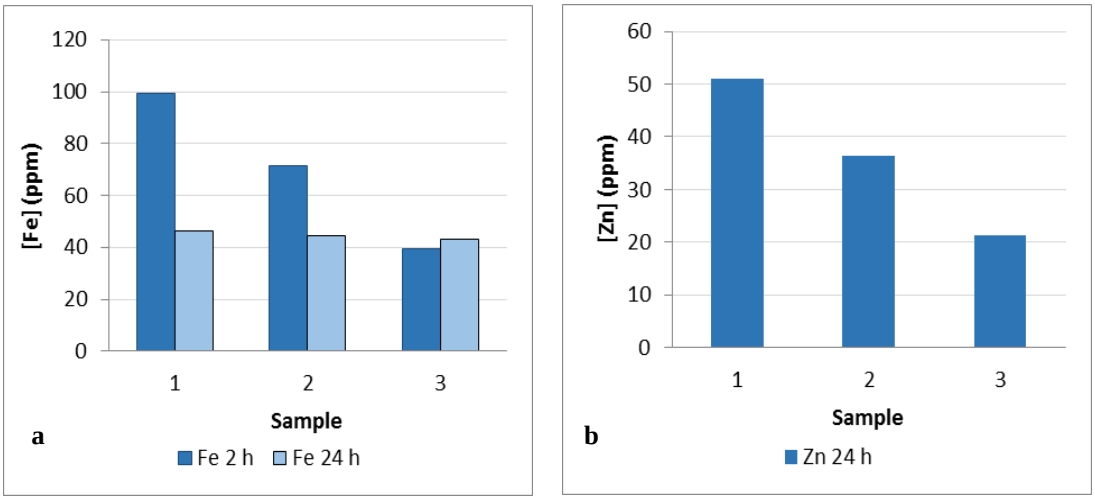

Figure 4.5 Cation exchange in sulphide solutions in 3.5 wt% NaCl at 90°C in presence of (a) Fe before and after Zn addition, and (b) Zn after 24 hours.

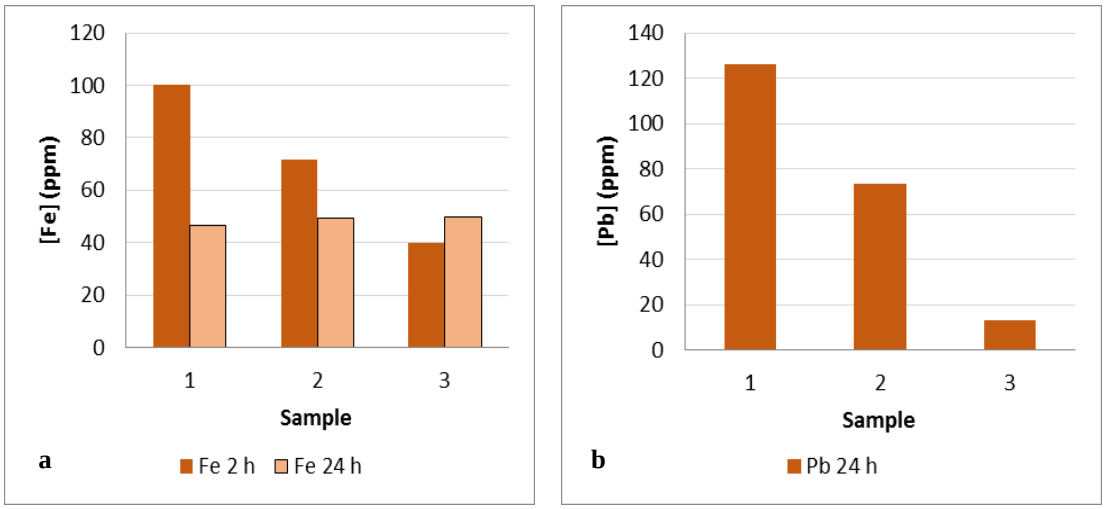

Figure 4.6 Cation exchange in sulphide solutions in 3.5 wt% NaCl at 90°C in presence of (a) Fe before and after the Pb addition, and (b) Pb after 24 hours.

The tests described above were repeated at 23°C to examine the cation displacement reactions between Zn and FeS at different pH values. The ICP results are shown in Figure 4.7. Fe solutions were adjusted to 3 different initial pH values before mixing with sulphide solutions. When 155 ppm Fe was mixed with nearly 20 ppm and 40 ppm H_2S, a larger mass of FeS deposited at high pH values *i.e.* the Fe concentration decreased from 155 ppm to 130 ppm at pH 5.3 while Fe levels dropped from 157 ppm to 123 ppm at pH 7. This is clearly due to the difference in the FeS solubility at different pH levels.

Zn solutions were added to the duplicate of FeS solutions 2 hours after FeS formation and the resulting Fe concentration was around 100 ppm, which is equivalent to the input Fe concentration. The Zn concentration, on the other hand, decreased to different levels due to Zn exchanging with FeS. Note that in sample # 2, 4 ppm Fe precipitated; however, after adding Zn, 10 ppm Zn precipitated. Therefore, there was another source of sulphide *i.e.* dissolved sulphide and Zn reacted with FeS and dissolved sulphide. In addition, note the change in the pH measurement before and after Zn addition. For example, in sample # 1 and # 3 the pH increased from 3.31 to 5.30 as Fe ions partially consumed, see Table 4.2 Then, after Zn addition (sample # 3) the pH decreased to 3.75 as FeS was dissolved, see Table 4.3.

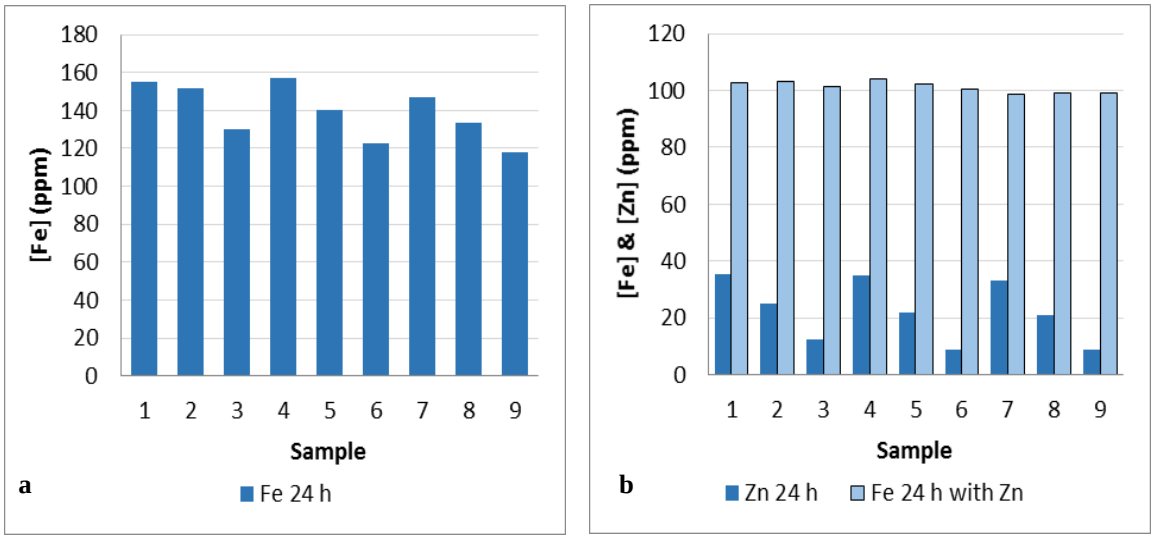

Figure 4.7 Cation exchange in sulphide solutions in 3.5 wt% NaCl at 23°C in presence of (a) Fe, and (b) Fe and Zn

Table 4.2 pH measurements of FeS supernatant solutions after 24 h at 23°C.

Sample	H_2S (ppm)	Final pH
1	0	3.31
2	20	5.53
3	40	5.30
4	0	4.64
5	20	6.84
6	40	7.10
7	0	6.63
8	20	7.13
9	40	7.21

Table 4.3 pH measurements of Fe/ZnS solutions after 24 h at 23°C.

Sample	H_2S	Final pH
1	0	3.48
2	20	3.66
3	40	3.75
4	0	5.05
5	20	5.39
6	40	5.30
7	0	6.75
8	20	6.60
9	40	6.33

As previously mentioned in the literature review, ZnS can be dissolved by adding a lead compound under the appropriate conditions (Chenglong *et al.*, 2008). According to these authors, ZnS cannot be dissolved at neutral pH (*i.e.* no NaOH) in the presence of lead compounds. To examine the ability of lead acetate to extract sulphide from ZnS the following set of experiments was performed. ZnS was allowed to form in the absence of Pb ions by mixing Zn GFW (95 ppm Zn) and H_2S GFW (30 ppm H_2S). After 1 hour aging, Photo 4.1 was taken and samples were collected and analysed for Zn and Pb.

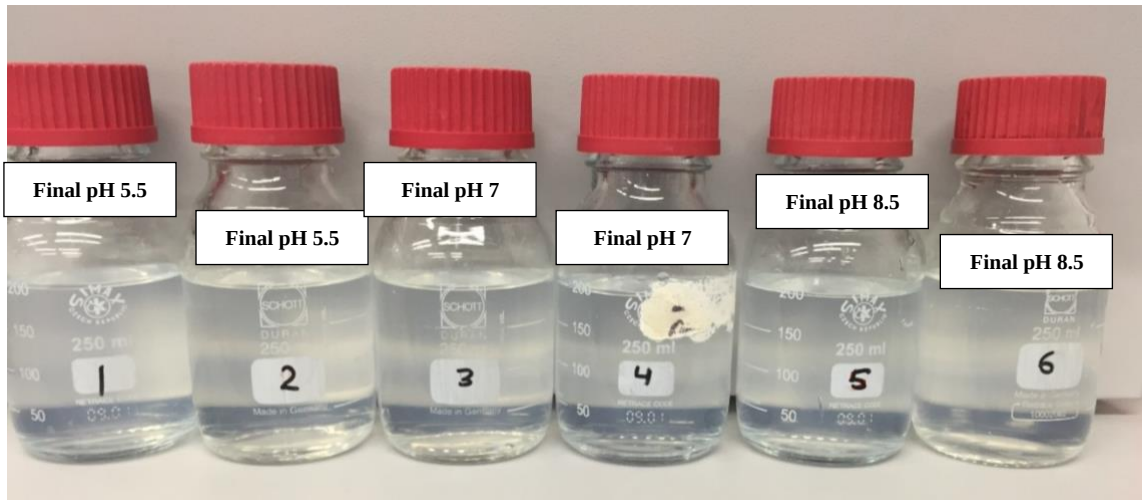

Photo 4.1 ZnS formation in GFW (photo taken 1 hour after mixing)

Lead acetate was then added to give approximately 300 ppm *i.e.* Pb/S molar ratio of 3. Two samples were then taken after 1 hour and 20 hours and analysed for Zn and Pb. As shown in Figure 4.8, the Zn concentration dropped from 42 to 22 ppm when the two brines were mixed. Therefore, 47% of the initial Zn concentration precipitated as ZnS within 1 hour. Photo 4.1 shows the solutions that contain ZnS precipitate in the absence of Pb.

When 300 ppm Pb was added to the solution, the zinc concentration noticeably increased to 40.7 ppm and 42 ppm after 1 and 20 h, respectively, indicating complete dissolution of ZnS. **Photo 4.2** shows solutions containing PbS scale in presence of Zn. It should be noted that the solution colour turned to brown and then black after 2 and 5 min, respectively (Photo 4.3) suggesting that PbS formation, resulting from extracting sulphide, is a spontaneous reaction despite the low solubility of ZnS.

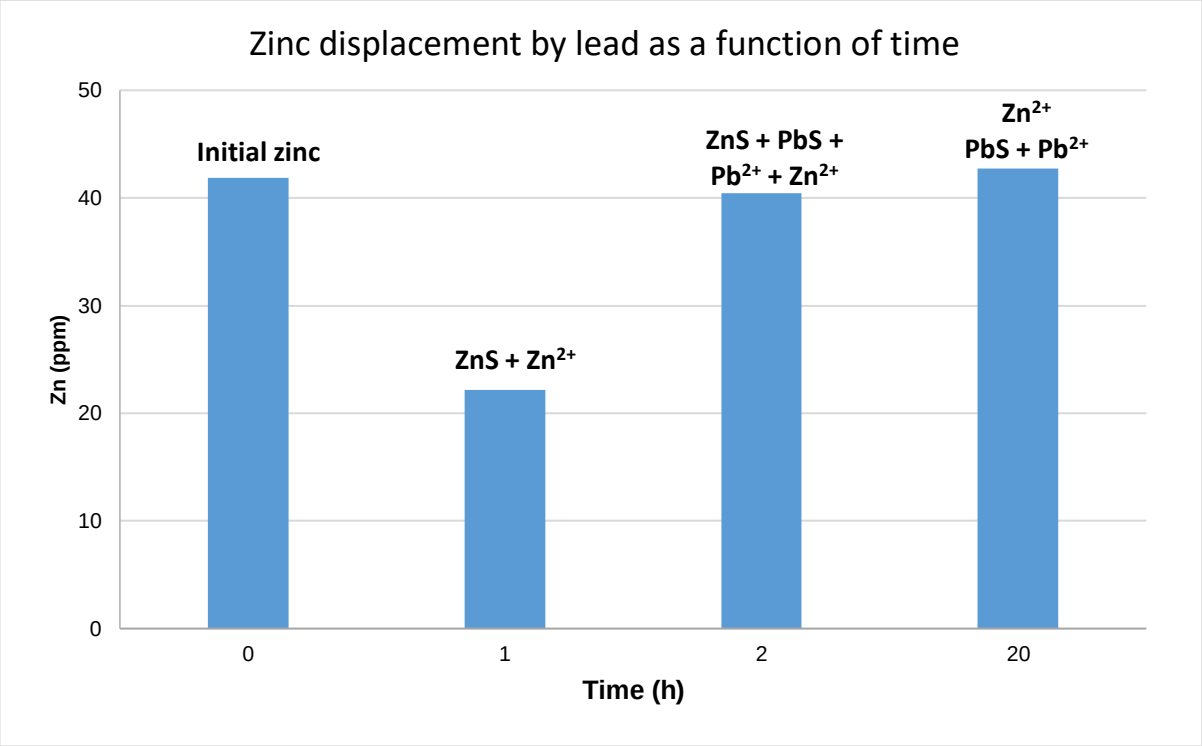

Figure 4.8 ZnS extraction by adding lead acetate at 25°C

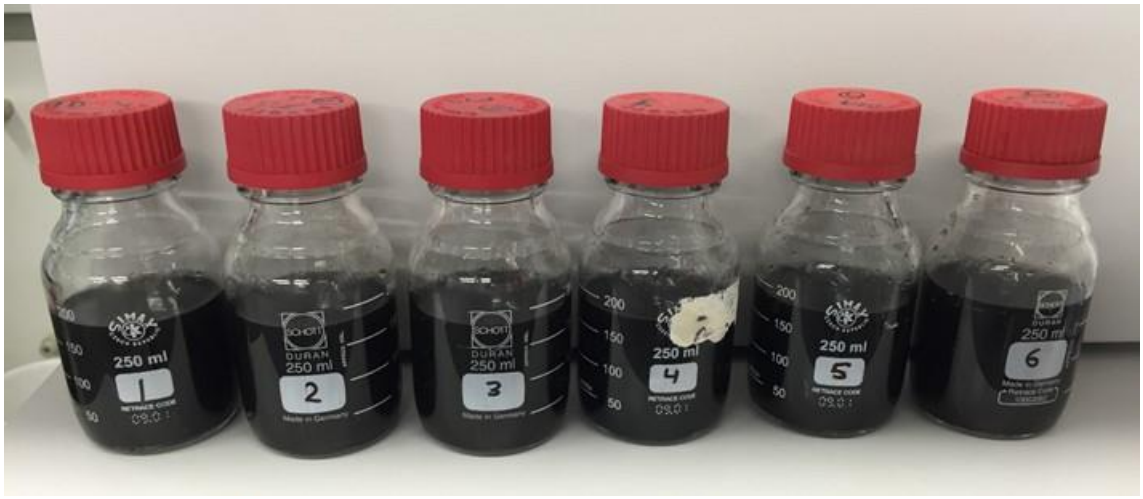

Photo 4.2 PbS/ZnS formation in GFW (photo taken 20 hours after adding lead acetate)

Photo 4.3 PbS/ZnS mixed scale formed by subsequent addition of Pb to pre-formed ZnS. Photos taken after 2 min (left) and 5 min (right)

4.5 Conclusions

In this chapter, different concentrations of Zn and Pb were mixed with a given sulphide concentration such that sulphide was limiting to Zn but in excess to Pb while in some cases it was limiting to Pb. In addition, the constant concentrations of Fe, Zn and Pb were mixed with different sulphide concentrations and hence sulphide ranged from being limiting to Pb to excess to all sulphide scaling metals. Also, cation displacement experiments were conducted by allowing the higher soluble sulphide scale e.g. ZnS to form first then adding Pb acetate to extract sulphide from ZnS. This was also performed with PbS/FeS and ZnS/FeS systems.

In mixed scale, *i.e.* ZnS and PbS, ZnS, precipitation continued to occur until Pb to sulphide ratio becomes 1, and then ZnS diminishes at higher molar ratios. This observation was supported by precipitation of only PbS when Pb:S molar ratio was 1.9. Therefore, provided that sulphide exists in excess to Pb, ZnS will start to precipitate only when all Pb ions have been consumed.

In Pb, Zn, Fe and H_2S solutions, as long as there is Pb in solution, there would be no ZnS and FeS precipitation. Similarly, if there are free Zn^{2+} ions in the solution, no FeS would form.

Solid ZnS was completely redissolved in a Pb acetate solution by exchange of Pb for Zn to form PbS, thus confirming the much higher affinity of Pb towards sulphide and the higher tendency of PbS to form. Similarly, FeS was redissolved in a Pb acetate and $ZnCl_2$ solutions.Similarly, solid FeS was completely redissolved in Pb acetate and Zn chloride solutions.

Finally, we consider some of the field implications of the findings in this chapter. It is known that PbS is preferentially formed even in presence of high Zn concentrations; however, the PbS formation by cation exchange can occur when ZnS pre-exists in the system. Pb ions can react with the un-dissolved ZnS after an unsuccessful sulphide dissolution treatment. Pb can react with the dissolved sulphide and extract sulphide from preformed ZnS. Another scenario is that when produced sulphide is in excess to Pb both ZnS and PbS would precipitate. If there is a decrease in sulphide concentration due to dilution for example, sulphide would react preferentially with Pb to precipitate PbS and the excess Pb would react with the preformed ZnS to precipitate PbS. Continuous exposure to Pb ions can result in partial displacement and in consequence the formation of an insoluble layer of PbS can be produced on the deposited ZnS and FeS, which could make it harder to dissolve by chemical means. The difference in solubility between the scales should be considered when designing removal treatments because the outer layer would probably act as a barrier that prevents the dissolution of the other scales. More significantly, the difference in formation mechanism can have a significant impact on the inhibition efficiency as will be discussed later. Therefore, before implementing the scale treatment, any suspended or deposited sulphide scale should be efficiently removed from the production system.

Chapter 5

ZnS and PbS Inhibition

5.1 Introduction

In this section, we now turn to the **inhibition** of the sulphide scales using a range of scale inhibitors (SI). Note that we refer to all the chemicals used as SIs whether they work by threshold inhibition or through a dispersant mechanism. The results of inhibition efficiency experiments for ZnS and PbS using a range of scale inhibitors are discussed. In the first set of experiments, 5 scale inhibitors were tested against each of ZnS and PbS as a single scale in the presence of 100 ppm H_2S, and 50 ppm Zn or Pb. The inhibition efficiency results of the 2 most successful inhibitors, SI-2 and SI-3, will be discussed in more details in the following sections. The information which we have on these products SI-2 and SI-3 (Table 2.7) is limited but they are described as high molecular weight sulphonates co-polymers and the proposed mechanism they operate by is described by Savins et al (2014). Among the tested scale inhibitors, only two scale inhibitors namely SI-2 and SI-3 showed a high inhibition efficiency for ZnS and PbS and therefore they were further tested at various conditions. SI-2 was effective for ZnS and PbS over wide range of parameters while SI-3 was less effective at high salinity and high pH. The particle size of inhibited ZnS and PbS was found to decrease as a function of increasing the scale inhibitor concentrations and this fact has some relevance in what we may interpret as "inhibition efficiency" for sulphide scales; this will become evident in Chapter 9 when we discuss filter blocking assessment of sulphide inhibitor efficiency.

5.2 ZnS and PbS inhibition using conventional SIs

Several laboratory experiments incorporated with modelling and filed data showed that the scale inhibitor concentration in the flowback decreased significantly to levels below 100 ppm depending on several factors including the type of rock formation and scale inhibitor, the intial concentration of the scale inhibitor (Chen et al., 2013; Kan et al., 2005; Gdanski, 2008; Baraka-Lokmane et al., 2016). Chen et al (2013) showed the core flood scale inhibitor (acrylate polymer) return profile where the scale inhibitor concentration dropped sharply below 100 ppm after around 25 pore volume (PV) and followed by a gradual decrease. After 3 PVs were injected, around 86 % of the intial PPCA was returned and then the PPCA concentration gradually declined to 1 ppm after 100 PV (Kan et al., 2005). Therefore, for screening purposes, 100 ppm of several scale inhibitors was evaluated for ZnS and PbS inhibition. **Figure 5.1** (a and b) show the Zn and Pb concentrations in the supernatant solutions after 24 h in SFNSSW in presence of 100 ppm SI. 200 ppm H_2S was mixed with 100 ppm Zn or 100 ppm Pb separately and therefore sulphide was in excess to Zn and Pb. Note that, if there was no ZnS and PbS precipitation, the Zn and Pb concentration would be 50 ppm. It is evident from Figure **5.1** (a) that none of the tested scale inhibitor was effective in preventing the deposition of ZnS. It is known that many scale inhibitors perform better at lower pH values. So, the pH_0 of Zn SFNSSW was adjusted to 1.8 instead of 2 to examine the ability of these scale inhibitors to prevent the ZnS deposition at lower pH values. As shown in Figure **5.1** (b), despite the decrease in the final pH, the tested SIs did not prevent ZnS formation and deposition. The particle size of ZnS in SFNSSW blank solutions was found to be 8.7 µm and 2.5 µm at pH 7 and 2.4 respectively (Chapter 3). Although the tested scale inhibitor did not prevent the deposition of ZnS, some of them caused the particle size to decrease *e.g.* 100 ppm SI-4 reduced the particle size from 8.7 µm to 4.8 µm. By contrast, 100 ppm SI-1 *increased* the average particle size to 22 µm.

It has been reported that many scale inhibitors failed to inhibit PbS, while they have been shown to effectively or partially inhibit ZnS. Therefore, the failure of these tested SIs to inhibit PbS was likely. Indeed, as expected, the tested scale inhibitors did not show any inhibition against PbS as shown in Figure 5.2 (a and b). The inhibition efficiency results using these conventional polymeric and phosphonate scale inhibitors will be compared with the inhibition efficiency using proprietary scale inhibitors shown in Figure 5.4.

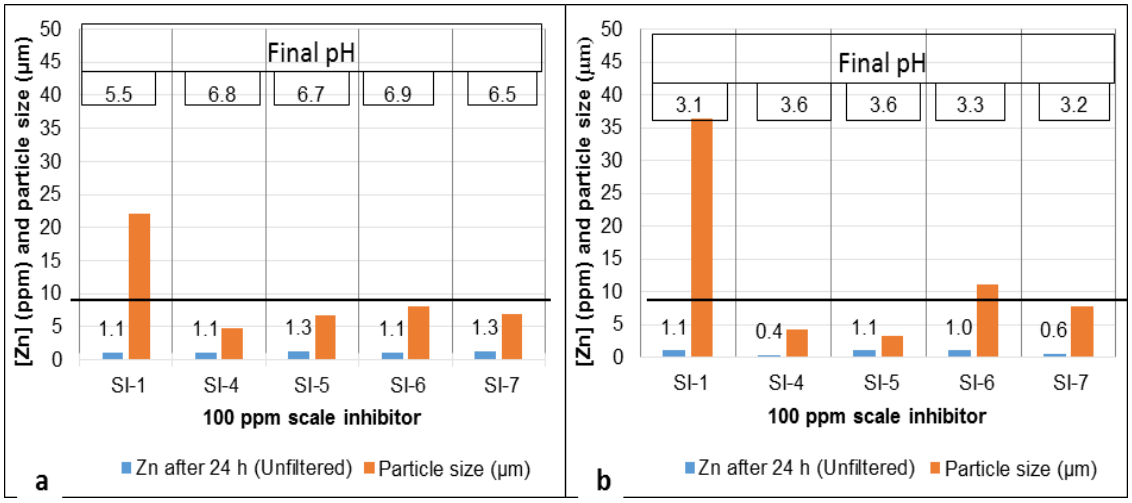

Figure 5.1 ZnS inhibition using different scale inhibitors (100 ppm) in SFNSSW at 23°C. Samples were not filtered. The solid black line represents the particle size of ZnS in blank solution i.e. 8 µm.

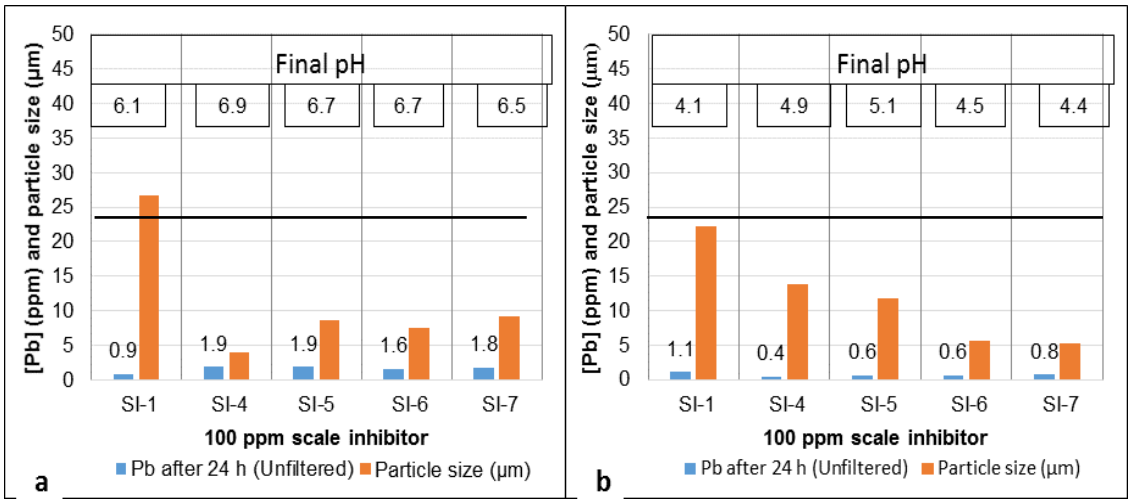

Figure 5.2 PbS inhibition using different scale inhibitors (100 ppm) in SFNSSW at 23°C. Samples were not filtered. The solid black line represents the particle size of PbS in blank solution i.e. 25µm.

5.3 ZnS and PbS inhibition using proprietary SIs

5.3.1 ZnS and PbS inhibition in SFNSSW

Figure 5.3 (a and b) show the inhibition efficiency (%) for ZnS and PbS when they formed as a single scale or combined scales using SI-2 and SI-3 respectively. The inhibition efficiency was calculated by dividing the detected Zn and Pb concentration over the initial concentrations *i.e.*15. As shown in Figure 5.3 (a), 10 ppm SI-2 could provide 60-80% inhibition efficiency against ZnS and PbS when they formed as a single scale or combined scales in the presence of 30 ppm H_2S, 15 ppm Zn and/or Pb. When the SI-2 concentration was raised to 100 ppm, the inhibition efficiency significantly improved to around 95%, regardless of the type of scale. It is evident that 10 ppm SI-3

is not sufficient to inhibit any sulphide scale, as shown in Figure 5.3 (b). When SI-3 concentration was increased to 100 ppm, the inhibition efficiency rose to 70-80%.

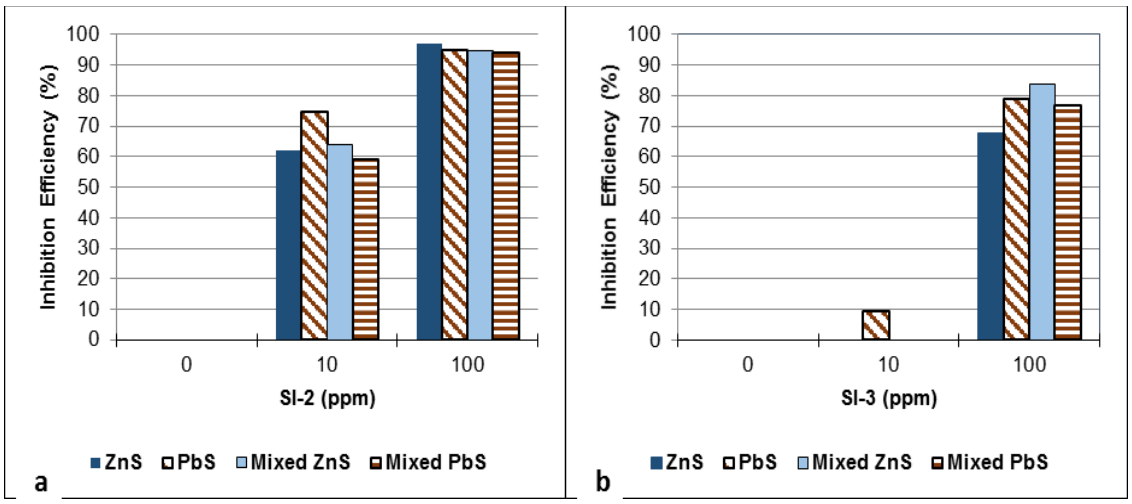

Figure 5.3 Inhibition efficiency after 24 h in presence of 30 ppm H_2S and 15 ppm Zn and/or Pb. (a) using SI-2, (b) using SI-3

To study the impact of increasing sulphide scale loading on the performance of the tested SIs, the H_2S concentration and Zn/Pb ions concentrations were increased to 100 ppm and 50 ppm, respectively, in the final solution mix. This ensured a much higher sulphide scaling tendency. The ICP analysis and pH measurements for these samples are shown in Table 5.1 and Figure 5.4. Under the same conditions, *i.e.* 50 °C, SFNSSW and pH_0 5, SI-2 managed to keep the scale particles suspended. By contrast, SI-3 failed to prevent scale particles deposition.

Different levels of pH can be encountered in oilfield production systems. Flowback samples form Piceance Basin and Northest Texas had pH values of 8 and 5.5, respectively (Rimassa et al., 2009). In acid pickling and stimulation treatment, different chemicals with various acidity can be used to clean the wellbore and stimulate the reservoir respectively which would result in wide range of pH values (Al-Dahlan and Nasr-El-Din, 2000; Taylor and Nasr-El-Din, 2000; Frenier et al., 2004)

To further investigate the role of pH on the sulphide inhibition efficiency, SI-2 and SI-3 were evaluated at different pH values varying from 2.3 to 10. Figure 5.4 (a and b) show the inhibition efficiency for single ZnS, PbS and combined ZnS/PbS sulphide scales at different pH_0 values. pH measurements were taken and these are presented in Table 5.1. Note that, at every pH_0 there are four values namely inhibition efficiency for single ZnS, single PbS, ZnS and PbS when they formed concurrently. It can be observed from

Figure 5.4 (a), 100 ppm SI-2 was very effective in inhibiting all types of sulphide scales over a wide range of pH values *i.e.* 2.3-9. By contrast, the performance of SI-3 showed a distinct dependency on the pH of the test solution, as shown in Figure 5.4 (b). At low pH values *i.e.* pH ~ 2.3-2.7, 100 ppm SI-3 was able keep the ZnS and PbS particles suspended in inhibited solutions. In particular, note that the inhibition efficiency for ZnS gradually decreased as pH increased. The inhibition effciency for mixed sulphide scale was comparable to that for PbS and greater than for the the single ZnS scale. This difference in inhibition efficiency can be explained when the final pH is considered. SI-3 was found to be more effective at low pH values. The final pH values of single PbS, single ZnS and mixed sulphide were pH ~ 6.6, 6.5 and 4.5 respectively. Hence, SI-3 provided better inhibition efficiency against combined sulphide scale because of the lower solution pH. The detrimental impact of pH on the performance of SI-3 must be considered when designing scale inhibition treatments. SI-3 might be effective at low pH values but as pH increases (e.g. due to carbon dioxide liberation from produced water), the ability of SI-3 to inhibit scale deposition is negatively affected.

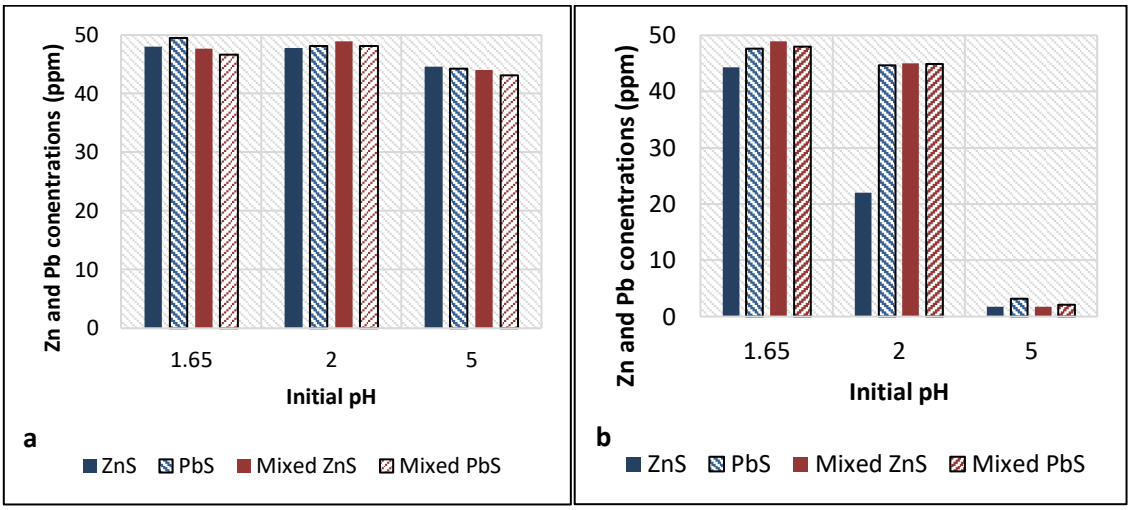

Figure 5.4 Inhibition efficiency for sulphide scales after 24 h in SFNSSW at 50 °C and different pH values. (a) using SI-2, (b) using SI-3.

Table 5.1 Experimental pH measurements of supernatant solutions in SFNSSW

Zn (ppm)	Pb (ppm)	SI-2 (ppm)	SI-3	Adjusted pH	Final pH
50	0	100	0	1.67	2.29
0	50	100	0	1.68	2.62
50	50	100	0	1.67	2.32
50	0	0	100	1.67	2.3
0	50	0	100	1.67	2.57
50	50	0	100	1.69	2.33
50	0	100	0	2.02	7.03
0	50	100	0	2.03	7.01
50	50	100	0	2.04	5.03
50	0	0	100	2.03	6.06
0	50	0	100	2.02	6.36
50	50	0	100	2.02	4.52
50	0	100	0	5	8.9
0	50	100	0	5	9.15
50	50	100	0	5	8.97
50	0	0	100	5	10.07
0	50	0	100	5	10.1
50	50	0	100	5	10

The following set of experiments was conducted in order to study the inhibition efficiency over time using different sampling methods. Different samples were collected from the same solution and analysed for Zn and Pb. Some samples were analysed using ICP without filtration while some samples had been filtered through 0.45 μm and 5 μm before ICP analysis. Figure 5.5 (a) shows Zn levels in the blank solution and inhibited solutions at different times and for the various sampling methods. Initially, ~47 ppm Zn existed in all solutions. Within 1 min, a significant amount of Zn was consumed as ZnS precipitates. At the end of the reaction, the solution was stripped of Zn as expected. In the presence of 100 ppm SI-2, the Zn concentration in the supernatant solution was comparable to the initial Zn concentration. The minor difference could be attributed to a marginal error in the ICP measurement. After 24 hours reaction time, nearly 46 ppm Zn was detected in solution even after filtration through a 5 μm filter. When the sample was filtered with a 0.45 μm filter, Zn concentration decreased from 46 ppm to 39 ppm indicating that small portion of scale particles were in the size range between 0.45 μm and 5 μm, but that most were smaller than 0.45 μm. The ICP analysis of the PbS inhibition samples is shown in Figure 5.5 (b). PbS completely precipitated within the first minute which confirms the spontaneity of the PbS formation reaction. The Pb levels detected in inhibited solutions clearly show that both tested scale inhibitors effectively hindered PbS deposition.

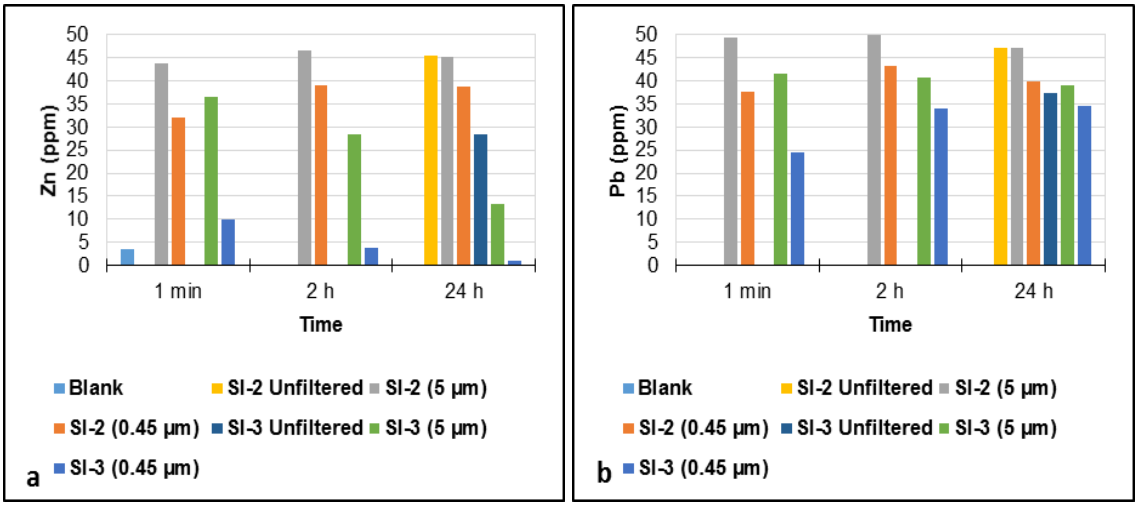

Figure 5.5 Inhibition efficiency for single ZnS in SFNSSW at 50°C using 100 ppm SI-2 and 100 ppm SI-3 in presence of 100 ppm H_2S and 47 ppm Zn or 50 ppm Pb. (left) single ZnS, (right) single PbS.

It is evident from Figure 5.6 (a and b) only SI-2 could prevent sulphide scale deposition when ZnS and PbS formed together. It is noteworthy that SI-3 failed to prevent PbS deposition in mixed sulphide scale although it was effective against the single PbS scale.

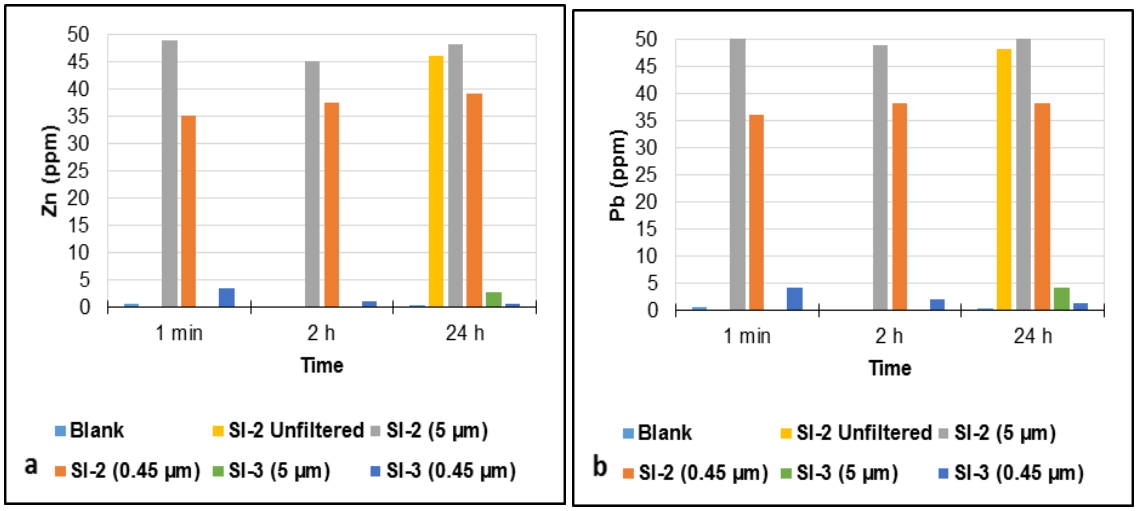

Figure 5.6 Inhibition efficiency for single PbS in SFNSSW at 50°C using 100 ppm SI-2 and 100 ppm SI-3 in presence of 100 ppm H_2S, 50 ppm Zn and 50 ppm Pb . (left) ZnS, (right) PbS (combined scale).

The performance of SI-2 for inhibiting sulphide scale was evaluated further by testing it over a range of SI concentrations. The experimental pH measurements of the supernatant solutions were taken at the end of the experiment, and these pH results are shown in Table 5.2. The final pH of ZnS and PbS solutions were pH ~6.79 and pH ~6.27, respectively. When ZnS formed alongside PbS, there was a sharp decline in pH values despite the fact that the pH of the initial cation solution was adjusted to a higher

pH value *i.e.* pH 2.1. The drop in the pH resulted from the further decrease in sulphide contents in solution due to reaction with both Zn and Pb ions.

Table 5.2 Experimental pH measurements of supernatant solutions

Zn (ppm)	Pb (ppm)	SI-2 (ppm)	Adjusted pH	Final pH
46	0	10	1.95	6.79
0	50	10	1.95	6.27
46	50	10	2.09	5.69
46	0	25	1.95	6.79
0	50	25	1.96	6.32
46	50	25	2.11	5.71
46	0	50	1.97	6.89
0	50	50	1.93	5.96
46	50	50	2.1	5.55

Figure 5.7 shows the Zn concentrations detected in the supernatant solutions containing 100 ppm H_2S and three concentrations of SI-2 namely 10, 25 and 50 ppm. In the presence of 10 ppm SI-2, a small portion of ZnS *i.e.* ~6 ppm was detected in the filtrate; after 1 minute 10 ppm of SI-2 managed to hold nearly 24 ppm Zn in the inhibited solution. In spite of that, no Zn was detected by ICP in the filtered samples indicating that all ZnS particles are greater than 0.45 µm. The Zn contents plateaued out at 25 ppm SI-2. Of particular note is the difference in the amount of scale particles that are less than 0.45 µm. Although 25 ppm and 50 ppm SI-2 provided comparable inhibition efficiency, more particles were smaller than 0.45 µm for the higher SI-2 concentration (50 ppm). It can be observed from the results in Figure 5.8 that SI-2 was effective against PbS at all tested concentrations and that the majority of PbS particles were smaller than 0.45 µm. It is also worth noting that the PbS particle size decreased with time. For example, 22 ppm Pb was detected in the filtrate; after 1 minute reaction time and when the reaction time was extended to 24 hours, the Pb concentration increased to 38 ppm. As shown in Figure 5.9, the inhibition efficiency for ZnS in combined sulphide scales was not affected by the presence of PbS, the 10 ppm, except for the SI-2 case. Similarly, the inhibition efficiency for PbS dropped sharply in the presence of ZnS when 10 ppm SI-2 was tested, as shown in Figure 5.10. However, at higher SI-2 concentrations, the drop in the Pb concentration, in the single PbS solutions in comparison to combined sulphide solutions, was negligible. Interestingly, when samples were filtered through a 0.45 µm filter, the Pb concentration dropped to different levels.

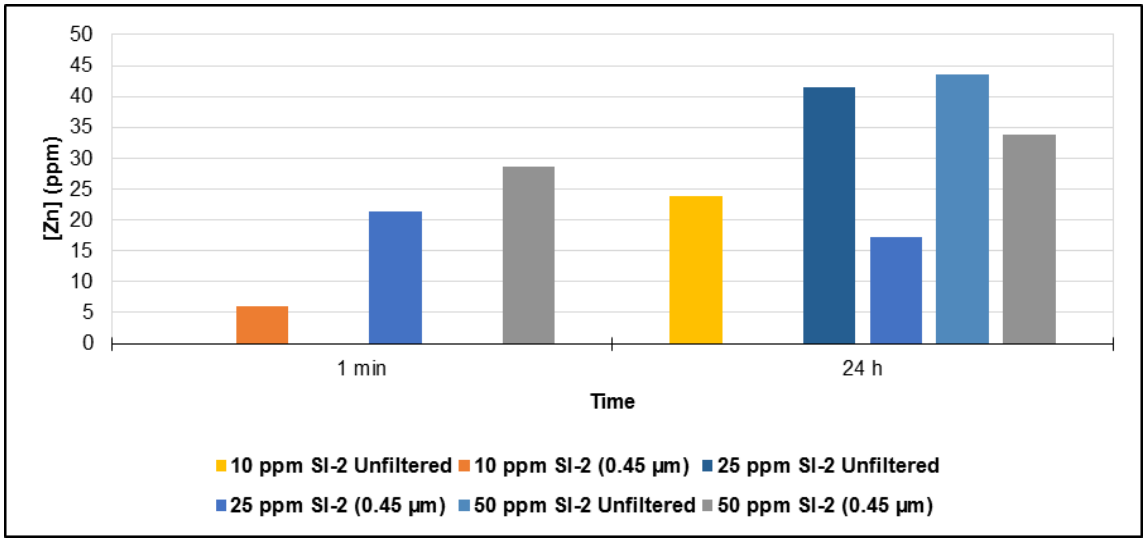

Figure 5.7 Inhibition efficiency for single ZnS in SFNSSW at 50°C using SI-2 in presence of 100 H_2S and 46 ppm Zn.

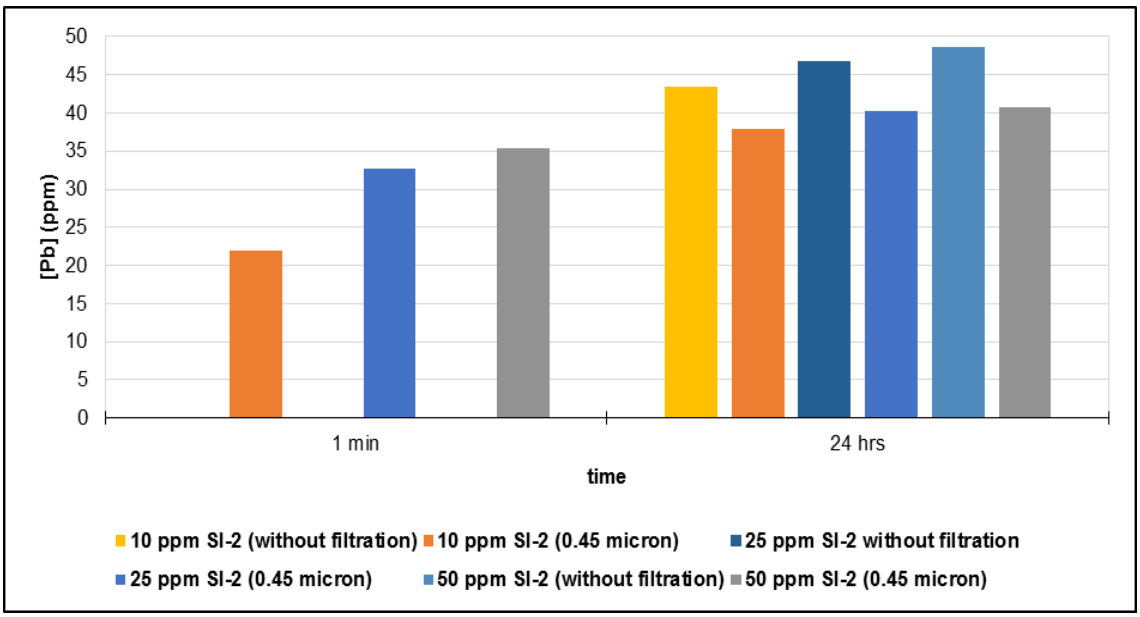

Figure 5.8 Inhibition efficiency for single PbS in SFNSSW at 50°C using SI-2 in presence of 100 ppm H_2S and 50 ppm Pb.

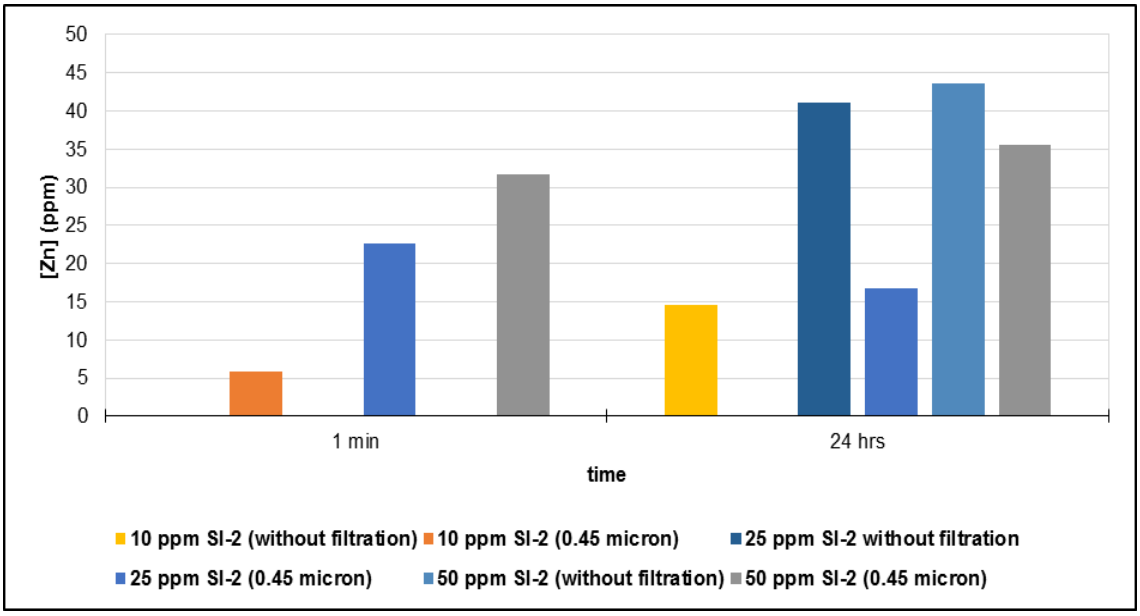

Figure 5.9 Inhibition efficiency for ZnS (combined scale) in SFNSSW at 50°C using SI-2 in presence of 100 ppm H_2S, 46 ppm Zn and 50 ppm Pb.

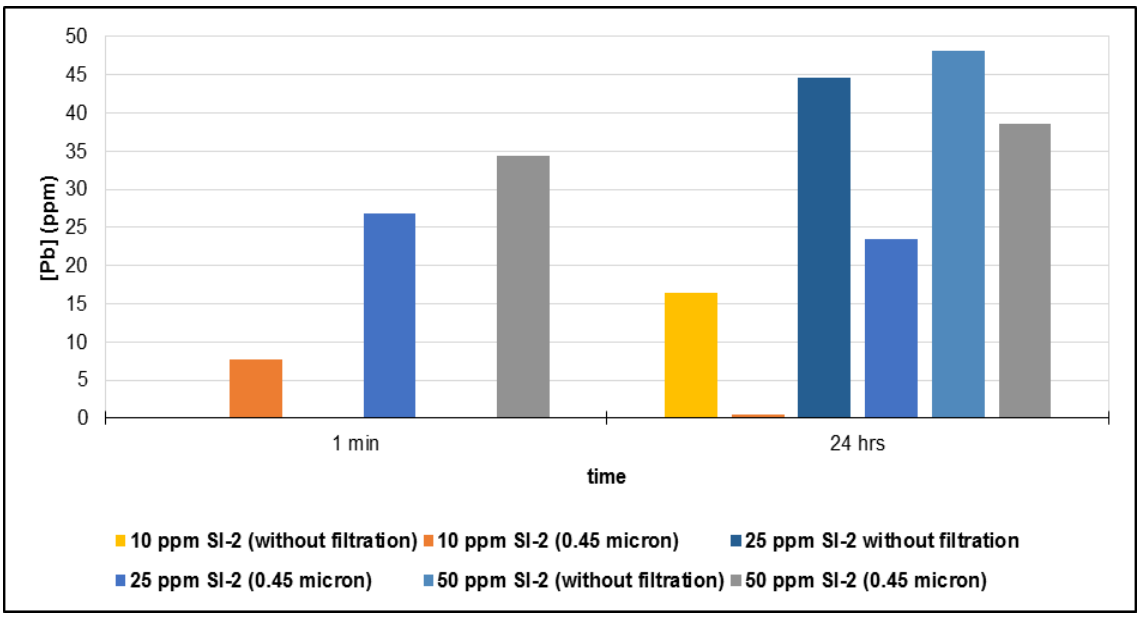

Figure 5.10 Inhibition efficiency for PbS (combined scale) in SFNSSW at 50°C using SI-2 in presence of 100 ppm H_2S, 46 ppm Zn and 50 ppm Pb.

As shown in Photo 5.1, different degrees of cloudiness were generated in ZnS solutions containing 10 ppm, 25 ppm and 50 ppm of SI-2. More Zn ions were detected in the supernatant solution when 50 ppm SI-2 was tested. Nonetheless, the 10 ppm SI-2 solution was cloudy whereas the 50 ppm SI-2 solution was clear. Hence, the difference in cloudiness can be attributed to the particle size of ZnS in the inhibited solutions. Another interesting observation, as shown in Photo 5.2, is that the 50 ppm SI-2 solution turned cloudy after 7 days reaction time. As shown in Photo 5.3 and Photo 5.4, even low concentration (*i.e.* 10 ppm) managed to keep PbS particles suspended in

supernatant solutions for 7 days. On the other hand, a high proportion of the combined scales settled after 7 days, when ZnS and PbS formed in the same solution, as shown in Photo 5.5 and Photo 5.6. From the ICP data described earlier, the particle size of the single PbS is smaller than that of single ZnS and mixed sulphide scales. Therefore, the deposition rate is dependent on both scale inhibitor concentration and the particle size of the resulting scale that is formed.

Photo 5.1 ZnS supernatant solutions after 24 h from left to right (10, 25 and 50 ppm SI-2)

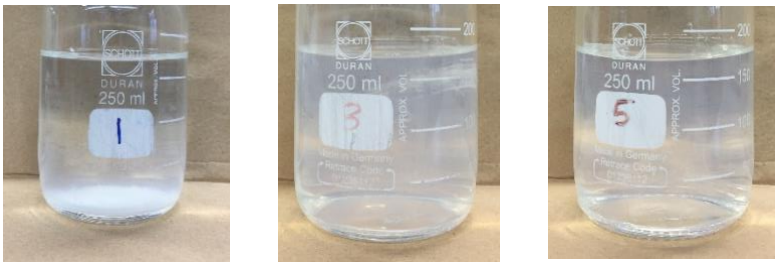

Photo 5.2 ZnS supernatant solutions after 7 days from left to right (10, 25 and 50 ppm SI-2)

Photo 5.3 PbS supernatant solutions after 24 h from left to right (10 and 50 ppm SI-2)

Photo 5.4 PbS supernatant solutions after 7 days from left to right (10 and 50 ppm SI-2)

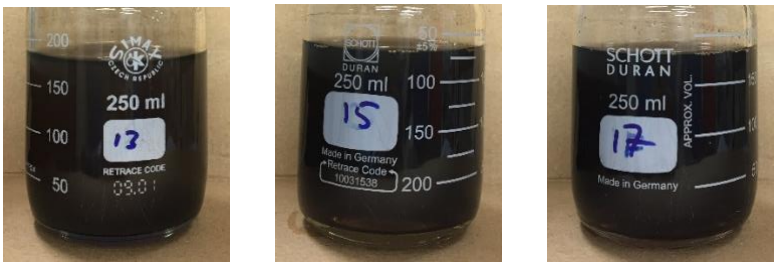

Photo 5.5 Mixed ZnS and PbS supernatant solutions after 24 h from left to right (10, 25 and 50 ppm SI-2)

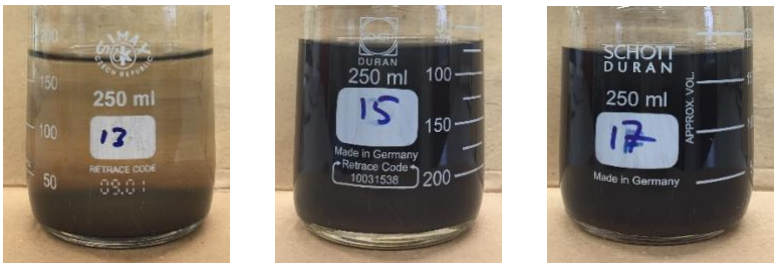

Photo 5.6 Mixed ZnS and PbS supernatant solutions after 7 days from left to right (10, 25 and 50 ppm SI-2)

5.3.2 ZnS and PbS inhibition in GFW

To study the role of salinity on the performance of scale inhibitors, GFW (Glenelg formation water), a high salinity brine, was used instead of SFNSSW. The ICP analysis of ZnS inhibition at different times using SI-2 and SI-3 is plotted in Figure 5.11 (a). In addition to ICP analysis, pH measurements were also taken, see Table **5.3**. After 24 hours reaction time, SI-2 managed to retain 41 ppm of Zn in solution out of the expected 45 ppm. In terms of inhibition efficiency using a 0.45 μm filter, the amount of Zn detected in solution increased in the first 2 hours and reached a plateau at 16 ppm. The resultant inhibition suggests that the particle size of ZnS decreases with time in inhibited solution. When SI-2 and SI-3 were tested against the single scale PbS, high inhibition efficiency was obtained but SI-2 outperformed SI-3. Hence, it is easier to prevent PbS deposition than ZnS at comparable cation concentration *i.e.* 50 ppm Zn and 50 ppm Pb. It can be observed from Figure 5.11 (b), the Pb contents sharply decreased after filtration indicating that the particle size of formed scale is greater than 0.45 μm.

Table 5.3 pH measurements of supernatant solutions in GFW

Zn (ppm)	Pb (ppm)	SI-2 (ppm)	SI-3	Adjusted pH	Final pH
45	0	0	0	0.91	6.99
45	0	0	0	0.76	5.24
45	0	100	0	0.92	6.55
45	0	100	0	0.78	2.72
45	0	0	100	0.93	6.07
45	0	0	100	0.78	2.62
0	48	0	0	0.91	7.02
0	48	0	0	0.77	6.05
0	48	100	0	0.9	6.49
0	48	100	0	0.76	4.24
0	48	0	100	0.86	5.39
0	48	0	100	0.8	3.81
45	48	0	0	0.87	3.44
45	48	0	0	0.79	2.52
45	48	100	0	0.94	3.84
45	48	100	0	0.79	2.37
45	48	0	100	0.95	3.46
45	48	0	100	0.79	2.3

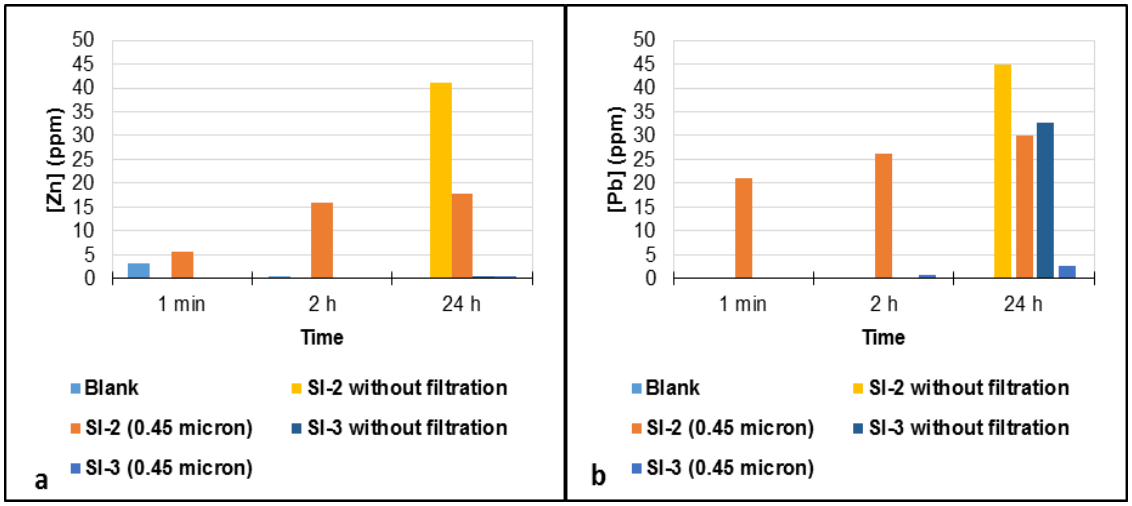

Figure 5.11 Inhibition efficiency for (a) single ZnS and (b) single PbS in GFW at 50°C using 100 ppm SI-2 and 100 ppm SI-3 in presence of 100 ppm H_2S, 45 ppm Zn or 48 ppm Pb.

In mixed ZnS/PbS solutions, inhibitor SI-3 failed to perform at all, as shown in Figure 5.12 (a and b). On the other hand, SI-2 was effective in hindering the deposition of both ZnS and PbS.

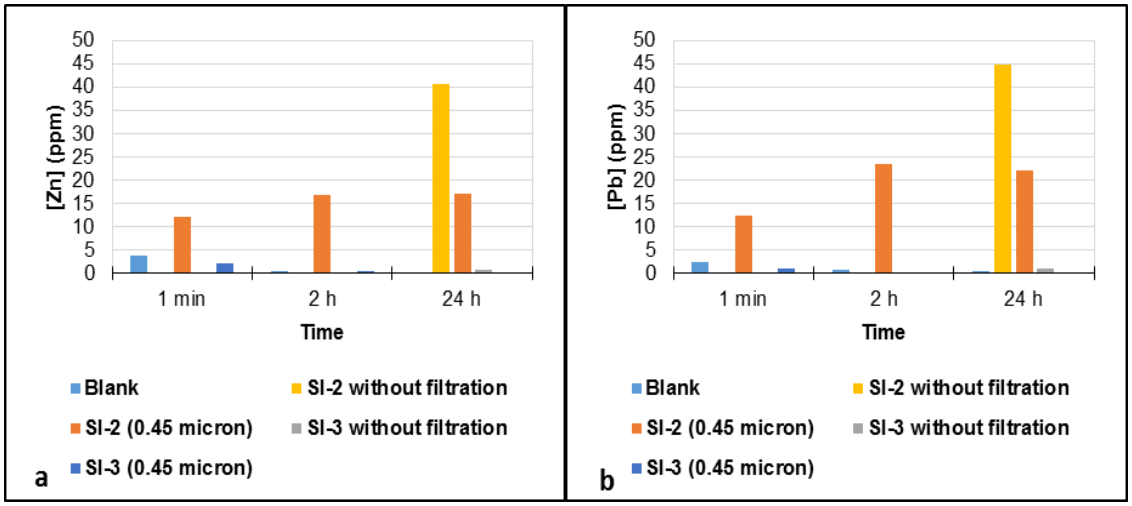

Figure 5.12 Inhibition efficiency for (a) ZnS and (b) PbS (combined scale) in GFW at 50°C using SI-2 and SI-3 in presence of 100 ppm H_2S, 45 ppm Zn and 48 ppm Pb.

When the initial pH of the Zn/Pb brine was adjusted to pH ~ 0.75 rather than pH ~ 0.95, the final pH noticeably declined, see Table **5.3**. The sharp drop in final pH had a beneficial influence on inhibition efficiency. For instance, at pH of 6.07 the performance of SI-3 was very poor, whereas at low pH *i.e.* 2.62, SI-3 managed to keep significant amount of Zn suspended in solution, see Figure 5.13 (a). Similarly, SI-3 prevented ZnS and PbS deposition in mixed solution as observed in Figure 5.14 (a and b) as well as single PbS as shown in Figure 5.13 (b).

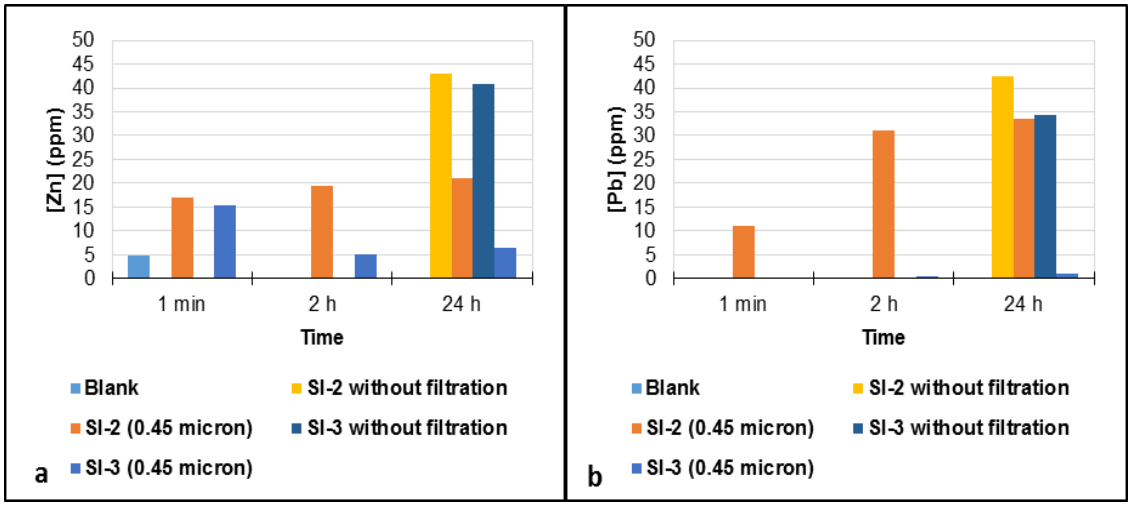

Figure 5.13 Inhibition efficiency for (a) ZnS and (b) PbS in GFW at 50°C using SI-2 and SI-3 in presence of 100 ppm H_2S, 45 ppm Zn or 48 ppm Pb.

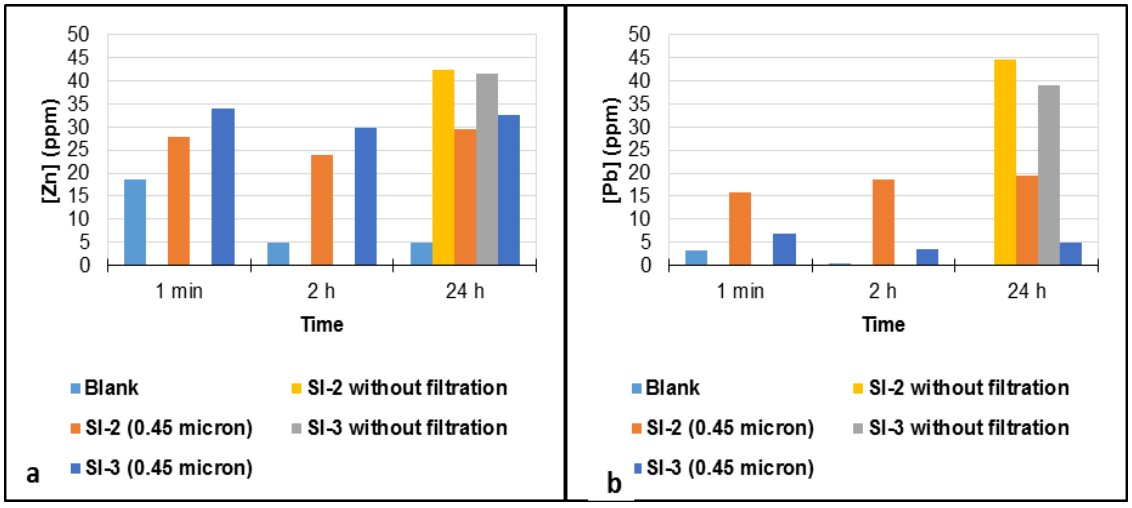

Figure 5.14 Inhibition efficiency for (a) ZnS and (b) PbS (combined scale) in GFW at 50°C using SI-2 and SI-3 in presence of 100 ppm H_2S, 45 ppm Zn and 48 ppm Pb.

5.4 The impact of temperature on ZnS and PbS inhibition

To study the impact of temperature on the inhibition of ZnS and PbS, 10, 50 and 100 ppm SI-2 and 100 ppm SI-3 were tested against ZnS and PbS in SFNSSW at 95°C. In addition, 100 ppm SI-2 and SI-3 were evaluated in GFW at 95°C at two pH values.

Based on $Na_2S.9H_2O$ addition, the H_2S concentration in SFNSSW was 100 ppm while the measured Zn and Pb concentrations in stock solutions were approximately 45 ppm and thus, at initial conditions, sulphide was in excess to both Zn and Pb. The natural pH of 200 ppm H_2S SFNSSW was around pH ~ 12 and it was used without pH adjustment. The pH_0 of Zn SFNSSW and Pb SFNSSW was adjusted to 2, such that the final pH of the supernatant solutions was pH ~ 7. Figure 5.15 (a and b) show the Zn concentrations in the supernatant solutions after 2 and 24 hours for filtered and unfiltered samples when ZnS formed in SFNSSW at 95°C. It has been reported that a significant portion of H_2S can evolve from solution during the preheating stage (Graham *et al.*, 2017). Blank solutions (*i.e.* with no scale inhibitor), were tested under the same conditions to ensure that sulphide was in excess to Zn and Pb and thus complete ZnS and PbS precipitation had occurred.

It is clear from Figure 5.15 that the ZnS formation reaction reached completion within 2 hours and a very small amount of Zn *i.e.* [Zn] ~ 2.2 ppm, remained suspended in the supernatant solution. All tested scale inhibitors managed to delay the deposition of ZnS to different extents. 10 ppm SI-2 held 25 ppm Zn for two hours; however, when the reaction time was extended to 24 hours, the Zn concentration dropped to 2.6 ppm.

Similar behaviour was observed when 100 ppm SI-3 was used, *i.e.* the Zn concentration in the supernatant solution containing 100 ppm SI-3 decreased from 30 ppm to 5 ppm at 2 and 24 hours reaction time, respectively. It is worth noting that the filtered samples of these two solutions, namely 10 ppm SI-2 and 100 ppm SI-3, were deficient in Zn. This indicated that the ZnS particles were larger than 0.45 μm in diameter. The inhibition efficiency for ZnS significantly improved when the concentration of SI-2 was raised from 10 ppm to 50 and further to 100 ppm. It is interesting to note that the ZnS particle size was less than 0.45 μm, as indicated by the comparable Zn concentration in the filtered and unfiltered samples. It is also worth pointing out the slight, unexpected, drop in Zn concentration in the unfiltered samples compared to the filtered ones. At 95°C, although the 2 ml sample was immediately added to the 8 ml quenching solution, a small amount of the solution dropped from the pipette while transferring the solution from the glass bottle to the test tube.

The inhibition efficiency for ZnS in SFNSSW at 50°C and pH 6 using 100 ppm SI-2 and 100 ppm SI-3 was 96% and 44%, respectively. In comparison, when the temperature was raised from 50 to 95°C, the inhibition efficiency of 100 ppm SI-2 slightly decreased to 90% while that of 100 ppm SI-3 dropped drastically to 10%.

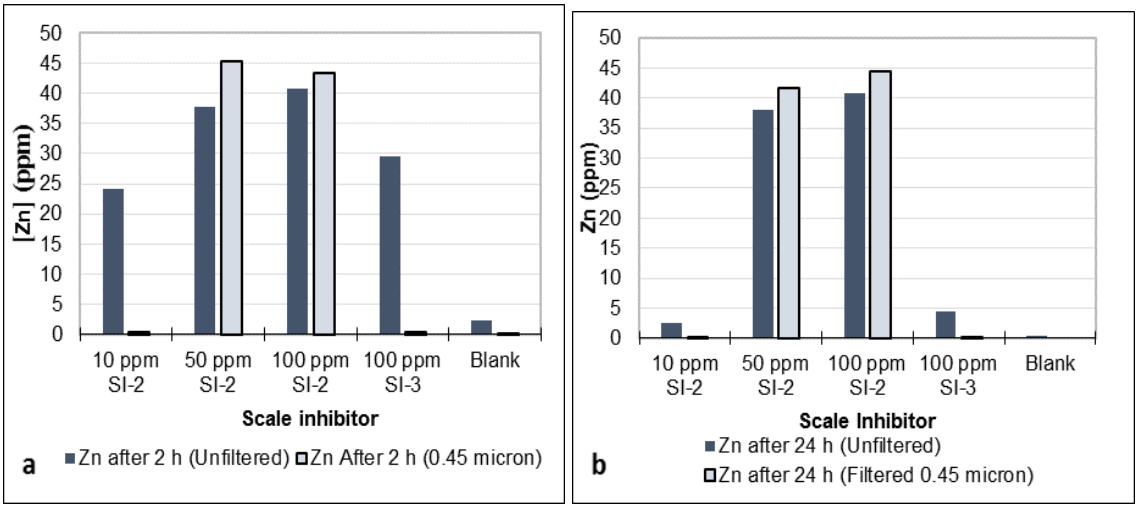

Figure 5.15 ZnS inhibition in SFNSSW at 95°C after (a) 2 h and (b) 24 h, using 10, 50, 100 ppm SI-2 and 100 ppm SI-3. 100 ppm H_2S and 50 ppm Zn so sulphide is in excess to Zn.

Figure 5.16 (a and b) show the ICP results for the supernatant solutions when PbS formed in SFNSSW at 95°C. Pb completely precipitated as PbS within 2 hours in the blank solution, as expected. An insignificant amount of PbS remained suspended in the blank solution reflected by the small Pb concentration detected by ICP. In comparison, all inhibited solutions were able to hold significant amounts of PbS in the solutions for

24 hours. Unlike the performance against ZnS, 10 ppm SI-2 and 100 ppm SI-3 were effective in preventing PbS deposition, which appears to go against the relative solubility products and expected ease of inhibition. In addition to the ability of SI-2 and SI-3 to keep PbS particles suspended in the solution, they caused the particle sizes of the solids to drop significantly from 25 µm in the blank solution (measured by particle size analyser) to <0.45 µm indicated by the comparable Pb concentration in the filtered and the unfiltered samples.

At 50°C and a final pH of 7, the inhibition efficiency for PbS was determined to be 96% in presence of 100 ppm SI-2. Increasing the temperature from 50°C to 95°C resulted in a slight decrease in the inhibition efficiency. At 50°C (final pH of 6.4), 100 ppm SI-3 provided approximately 90% inhibition efficiency for PbS. SI-3 was previously found to be more effective at lower pH values. Nonetheless, when 100 ppm SI-3 was tested at 95°C and final pH of 4.6, the inhibition efficiency decreased to 72% due to the increase of the temperature despite the decline in the pH (from pH ~ 6.4 to pH ~ 4.6).

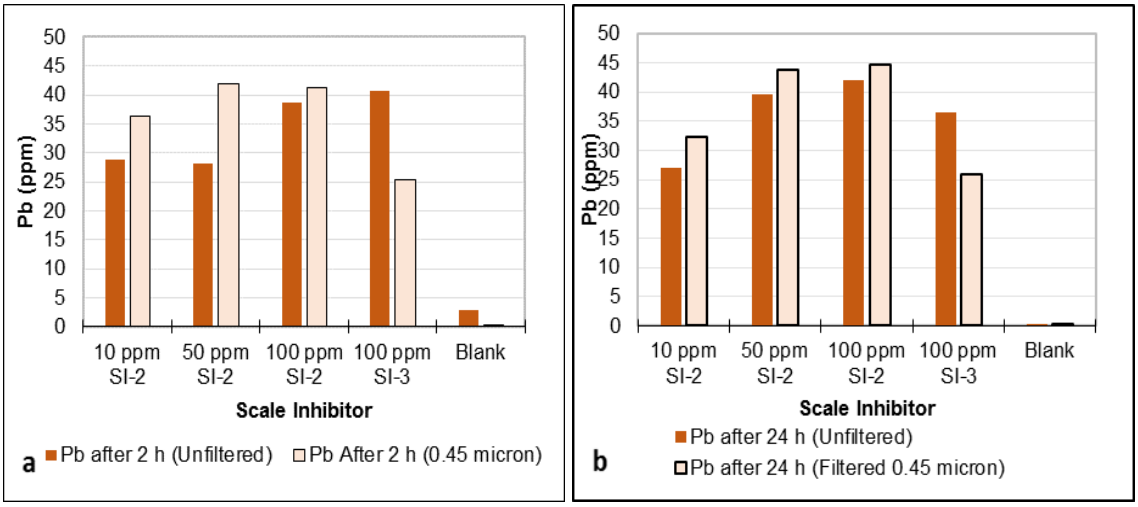

Figure 5.16 PbS inhibition in SFNSSW at 95°C after (a) 2 h and (b) 24 h, using 10, 50, 100 ppm SI-2 and 100 ppm SI-3. 100 ppm H_2S and 50 ppm Pb so sulphide is in excess to Pb.

In order to study the impact of salinity and temperature on the performance of SI-2 and SI-3, these inhibitors were tested against ZnS and PbS in GFW at 95°C. The Zn containing brine solutions were pH adjusted to pH ~0.95 and pH ~ 0.82 and consequently different final pH values were obtained as shown in Figure 5.17. It is evident from Figure 5.17 that a small amount of ZnS remained suspended in the blank solution and 100 ppm SI-3 where the final pH was 6.5 after 2 hours. SI-3 was previously found to be more effective at low pH values. Hence, the performance of SI-3 was expected to improve when it was tested at pH of 3.4.

Results in Figure 5.17 show that 100 ppm SI-3 delayed the deposition of ZnS for at least 2 h compared to the blank solution and 100 ppm SI-3 where the pH_{final} was 6.5. But, when the reaction time was extended to 24 h, the inhibition efficiency for ZnS dropped significantly as 7 ppm Zn was detected by ICP. 100 ppm SI-2, on the other hand, was very effective in controlling ZnS deposition, as shown in Figure 5.17. Of particular interest is that the particle size of inhibited ZnS in GFW ranged between 0.45 and 5 µm while it was less than 0.45 µm in SFNSSW. Photo 5.7 shows that the turbidity was different when ZnS was inhibited in SFNSSW and GFW although comparable Zn contents existed in these solutions.

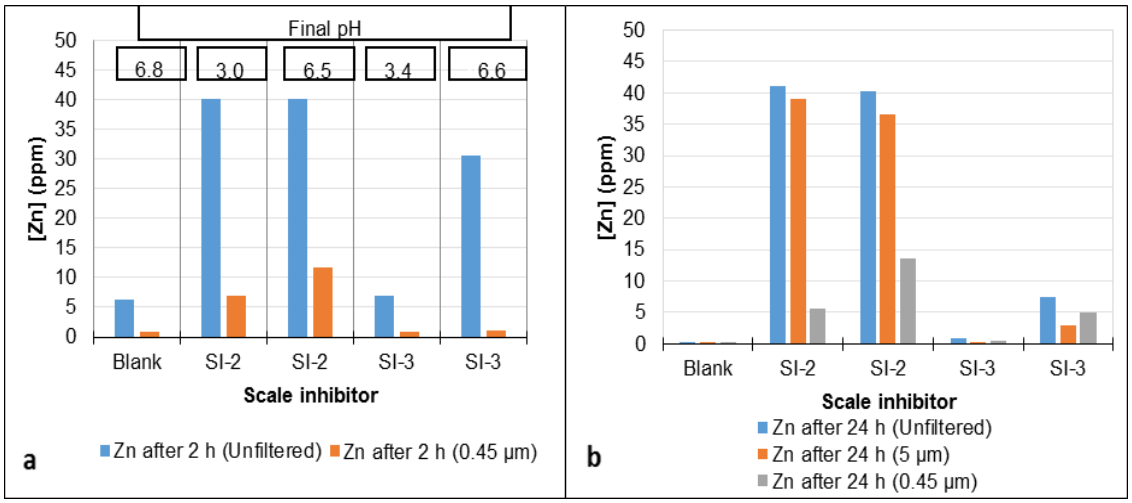

Figure 5.17 ZnS inhibition in GFW at 95°C after (a) 2 h, (b) 24 h using 100 ppm SI-2 and 100 ppm SI-3. 100 ppm H_2S and 45 ppm Zn so sulphide is in excess to Zn. Final pH measured after 24

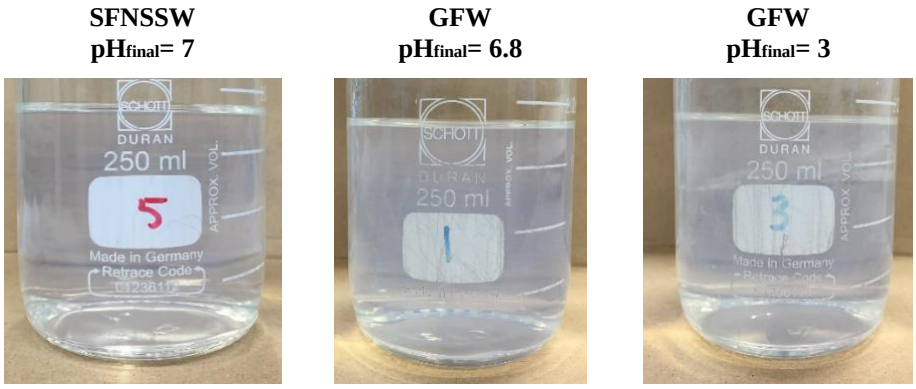

Photo 5.7 Supernatant solutions after 24 h using 100 ppm SI-2 at 95°C in the brines SFNSSW and GFW; GFW had initial pH = 6.8 AND 3.

The ability of SI-2 and SI-3 to control PbS scale has also been studied. The ICP results and pH measurements, including initial pH of Pb GFW and final pH, are shown in Figure 5.18. Despite the fact that PbS has lower solubility than ZnS, it was easier to inhibit the PbS. After 24 h, 100 ppm SI-2 and 100 ppm SI-3 were able to hold 40 ppm

and 20 ppm Pb in the supernatant solutions, respectively. Like ZnS, the particle size of PbS formed in GFW increased from (<0.45 μm) to (0.45-5 μm).

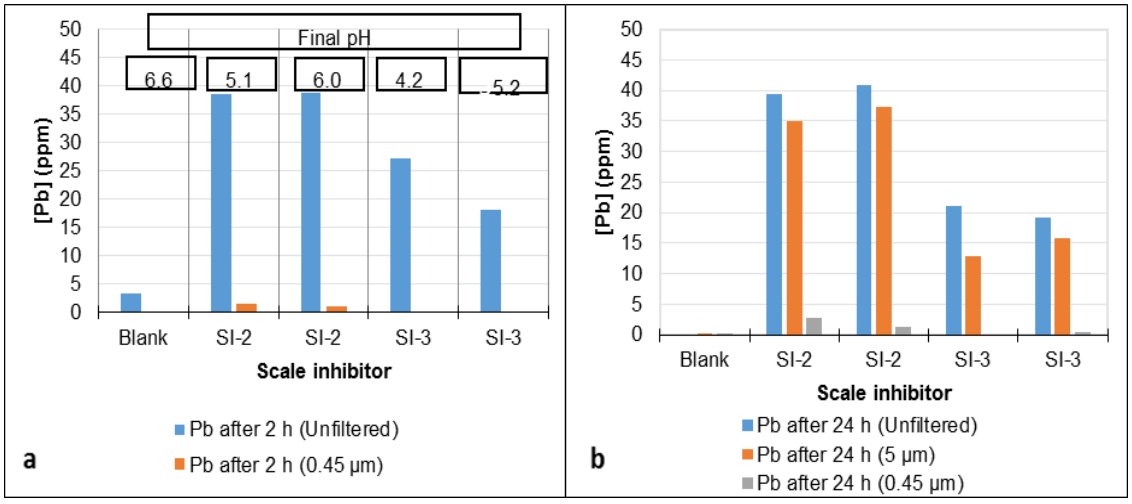

Figure 5.18 PbS inhibition in GFW at 95°C after 2 h using 100 ppm SI-2 and 100 ppm SI-3. 100 ppm H_2S and 45 ppm Pb so sulphide is in excess to Pb.

In the next set of experiments (results in Figure 5.19) using SI-2, sulphide was the limiting reactant and therefore equivalent moles of Zn and Pb would react with sulphide to preciptate ZnS and PbS, respectively. As shown in Figure 5.19 (a), in the ZnS blank solution, the Zn concentration decreased from 100 ppm to 74 ppm and thus 26 ppm Zn was consumed in precipitating ZnS. 10 ppm of SI-2 was not sufficient to prevent ZnS deposition as 20 ppm Zn precipiated as ZnS. 50 ppm and 100 ppm of SI-2, on the other hand, were very effective in hindering the deposition of ZnS. Figure 5.19 (b) shows the initial Pb concentrations and the supernatant solutions after 24 h reaction time. Approximately 75 ppm Pb reacted with the sulphide to precipitate PbS in the blank solution and 10 ppm SI-2 solution. Increasing the SI concentration to 50 ppm resulted in a slight improvement in the inhibition efficiency. 100 ppm SI-2 was able to hold 87 ppm in the solution. After filtration with 5 μm and 0.45 μm filters, the Pb levels dropped to 50 ppm and 25 ppm, respectivley.

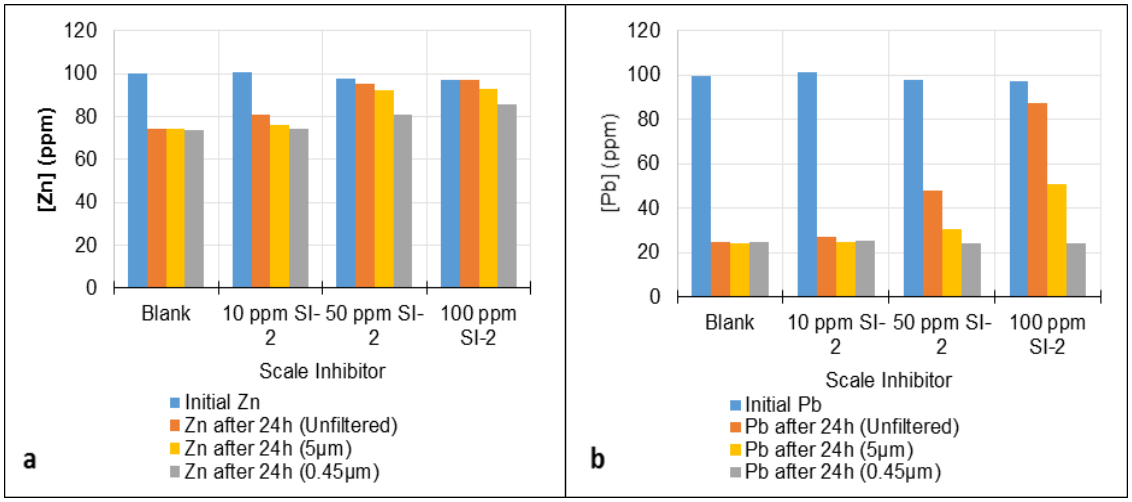

Figure 5.19 ZnS and PbS inhibition in GFW at 50°C after 24 h using SI-2. 15 ppm H_2S (calculated based on $Na_2S.9H_2O$ addition) and 100 ppm Zn or 100 ppm Pb so sulphide is the limiting reactant.

As discussed previously, PbS can form by direct reaction between sulphide and Pb^{2+} or by extracting sulphide from ZnS, *i.e.* by cation displacement/exchange. Figure 5.20 (a and b) show the Zn and Pb concentrations, respectively, when a single sulphide scale namely ZnS and PbS formed in SFNSSW at 50°C prior to scale inhibitor addition. The dark blue column and the orange column show the Zn and Pb concentrations respectively prior to scale inhibitor addition. The initial Zn and Pb concentrations were ~48 ppm and ~50 ppm respectively. One minute after the scale formed, 100 ppm SI-2 and 100 ppm SI-3 were added to separate ZnS and PbS solutions. As shown in Figure 5.20 (light blue column for Zn and red column for Pb), all solutions were stripped of Zn and Pb. Based on these results, it can be concluded that once sulphide scale has formed, its deposition is inevitable even when a very effective scale inhibitor, *e.g.* SI-2, is subsequently used.

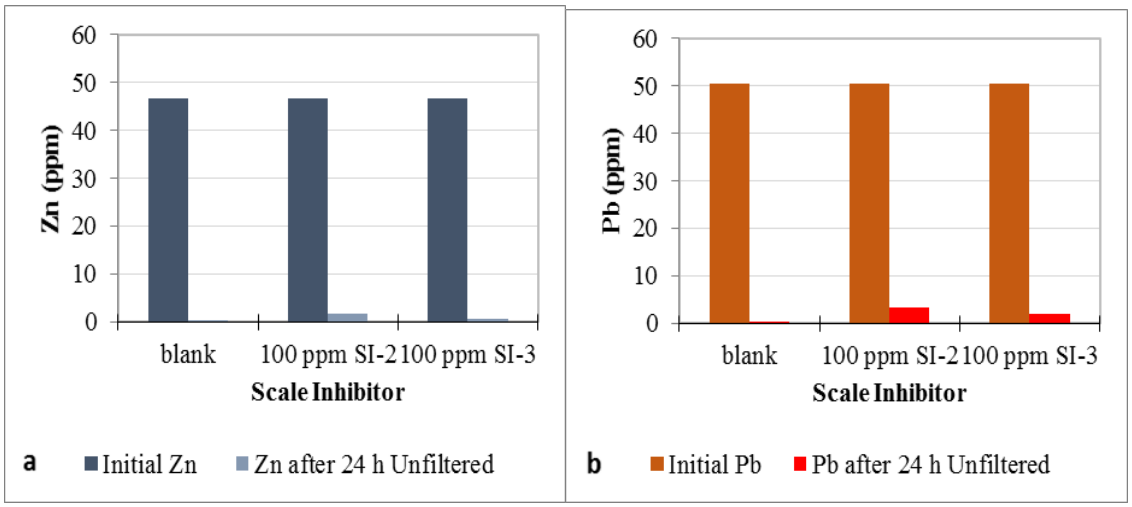

Figure 5.20 ZnS and PbS inhibition in SFNSSW at 50°C when scale inhibitors were added 1 min after scale formation.

Figure 5.21 (a and b) show the Zn and Pb concentrations in the supernatant solutions when ~7.5 ppm H_2S SFNSSW (calculated based on $Na_2S.9H_2O$ addition) was mixed with 50 ppm Zn and 50 ppm Pb SFNSSW containing 0, 5, 25 and 50 ppm SI-2. In these solutions, Pb is present in excess to sulphide and consequently single PbS is expected to form because PbS has higher tendency to precipitate, even in presence of higher concentrations of Zn (Chapter 4). No drop was observed in the Zn concentration in the supernatant solutions compared to the stock solutions. In the blank solution and 5 ppm SI-2, Pb completely precipitated as PbS. When SI-2 was increased to 25 and 50 ppm, the Pb concentration rose to nearly 48 ppm. After filtration, Pb concentration decreased by ~5 ppm.

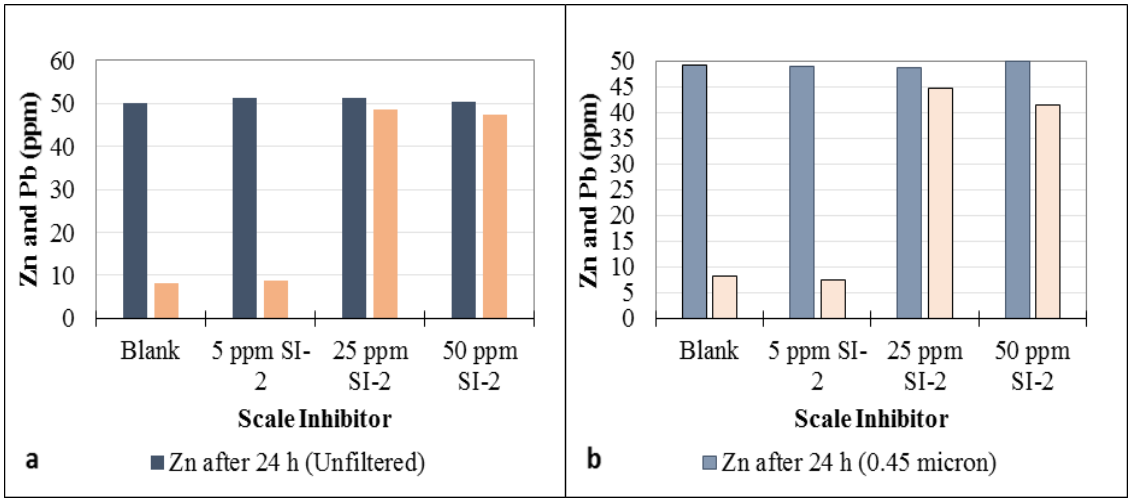

Figure 5.21 ZnS and PbS inhibition after 24 h in SFNSSW at 50°C using SI-2.

5.5 Conclusions

In this work, ZnS and PbS formation and inhibition tests were performed over a wide range of parameters. Different scale inhibitors were evaluated for their ability to inhibit ZnS and PbS, and the effect of adding the scale inhibitor on the particle size of formed scales. Two polymeric products (see Table 2.7, SI-2 and SI-3 clearly outperformed all of the other scale inhibitors and these were thoroughly evaluated in the presence of different Zn, Pb and H_2S concentrations. The impact of brine salinity on the inhibition efficiency was also examined. Also, different sampling methods, *i.e.* filtered and unfiltered, were tested to investigate the inhibition efficiency in addition to measuring the particle size distribution (PSD) of ZnS and PbS. The main conclusions from this study are as follows:

1. At a dosage level of 100 ppm active, none of the tested scale inhibitors, except SI-2 and SI-3, managed to prevent the deposition of ZnS and PbS scales

regardless of the final pH of the supernatant solutions. However, some other scale inhibitors did manage to reduce the particle size of the deposited ZnS scale to some degree. SI-2 and SI-3 are high molecular weight sulphonated co-polymers and this may give some information as to which direction might be followed by a SI manufacturer trying to develop new products for this application (i.e. ZnS/PbS inhibition).

2. SI-2 was remarkably effective at hindering ZnS and PbS deposition at all tested condition *i.e.* 95°C, SFNSSW, GFW and pH range 3-7. It outperformed all of the other tested scale inhibitors. By contrast, increasing the temperature and salinity had a detrimental impact on the performance of SI-3, although a slight improvement was observed at low pH values.

3. The information in conclusion 2 above is important to consider when designing scale inhibitor treatments. For example, if carbon dioxide is liberated from produced water due to pressure decline, pH increases which might cause drop in the inhibition efficiency of SI-3. Also, in dynamic tests at the time of mixing the two brines namely Zn/Pb/Fe brine and H_2S brine (particularly if the mixing is not efficient) the pH of the mixture might be too high and thus the performance of some scale inhibitors may be negatively affected. So, to avoid the exposure to high pH, it is recommended that the H_2S should be injected and mixed with low pH brine prior to mixing with the Zn/Pb/Fe brine.

4. A minimum recommendation from these studies is that pH be carefully measured for both the initial fluids and the final fluid in order to ensure that a realistic pH in the final solution mix is achieved. Otherwise, some SI products which have some efficacy against ZnS/PbS scales may be incorrectly rejected.

.

Chapter 6

$Fe(OH)_3$ and FeS Inhibition

6.1 Introduction

In this chapter, the inhibition of iron hydroxide and iron sulphide is discussed using different scale inhibitors which have been tested over a wide range of parameters. Some scale inhibitors including the conventional ones prevented the deposition of $Fe(OH)_3$ while only SI-2 and SI-3 prevented the deposition of FeS.

6.2 Iron hydroxide inhibition

The first set of experiments was conducted to investigate the ability of the tested scale inhibitors to prevent $Fe(OH)_3$ precipitation at different pH values under aerobic conditions and to study the compatibility of the scale inhibitors with the iron solutions. HCl was added to DW, 3.5 and 20 wt% NaCl prior to $FeCl_2$ addition. The initial pH of Fe solutions was around pH ~1. In this pH range, no $Fe(OH)_3$ deposition would be expected and thus if there were any Fe deposition, it would be a compatibility issue. After NaOH addition to the prepared Fe-NaCl solution, $Fe(OH)_3$ formed in all samples including the blank and inhibited solutions, indicated by the colour change (Photo 6.1) and confirmed by ICP analysis (Figure 6.1). For the blank samples, iron remained in solution or suspension up to pH of ~2.48. A colour change was noted for the samples at pH 2.18 and 2.48 but a loss of Fe was not observed by ICP analysis, suggesting that the particles formed were colloidal suspensions. Nearly 50 ppm (~50%) Fe was lost from solution at pH 4 and complete precipitation was observed at pH 10. It is interesting to note that a distinctly different colour of precipitate was formed between pH 4.04 and pH 10.34, which we believe to be indicative of a different phase of iron hydroxide. Of interest is that, in the 100 ppm SI-1 solutions Fe precipitated at pH 2-2.5 and then remained suspended at higher pH values *i.e.* pH 4.5 and pH 7.7 which suggests that SI-1 performs better at higher pH values. SI-2, on the other hand, maintained Fe ions in solutions over a wide range of pH values.

Neither SI-3 nor SI-4 exhibited any ability to prevent $Fe(OH)_3$ deposition, regardless of pH values. Also, it is worth mentioning that SI-4 solutions turned cloudy after $FeCl_2.4H_2O$ addition suggesting that there may be a compatibility issue; e.g. a possible Fe-SI complex forming which is sparingly soluble.

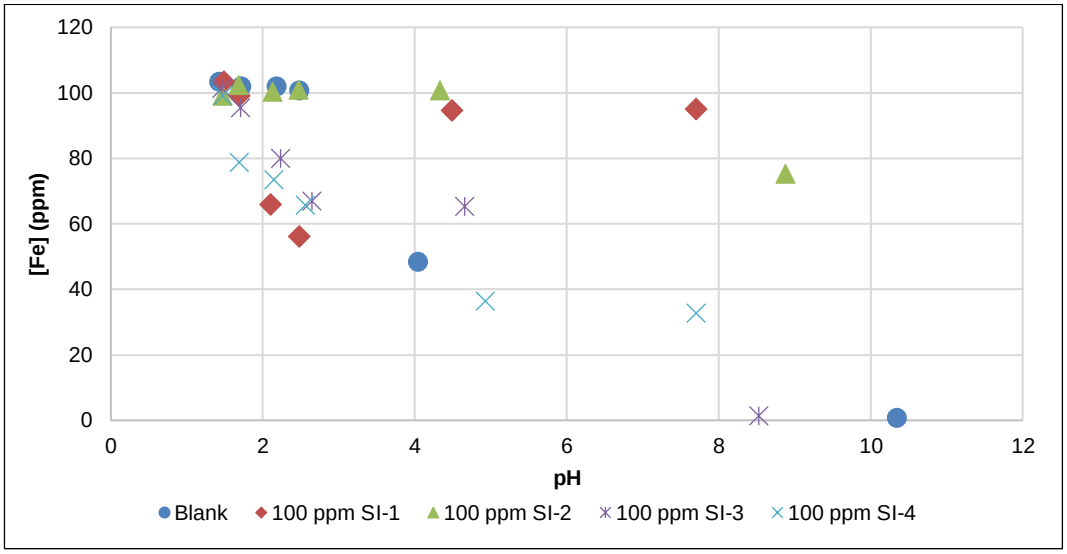

Figure 6.1 Iron concentrations in blank and inhibited solutions at different pH values in DW

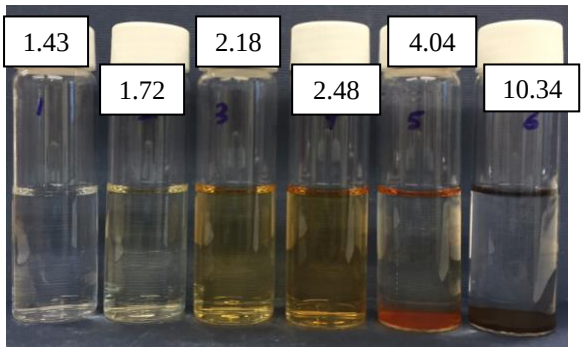

Photo 6.1 Blank solutions after 24 h from adding NaOH 100 ppm Fe-distilled water

It is clear from Figure 6.2, at scale inhibitor concentrations of [SI] = 100 ppm, none of the tested inhibitors completely prevented $Fe(OH)_3$ deposition in 3.5 wt% NaCl solutions at 23°C. Increasing SI concentrations to 200 ppm resulted in a significant improvement in the performance of the tested scale inhibitors, particularly SI-1, SI-2 and SI-3 (Figure 6.3). Note that the Fe concentrations used in these experiments are much less than those detected in flow back samples after acid treatments in the field (reviewed in chapter 2).

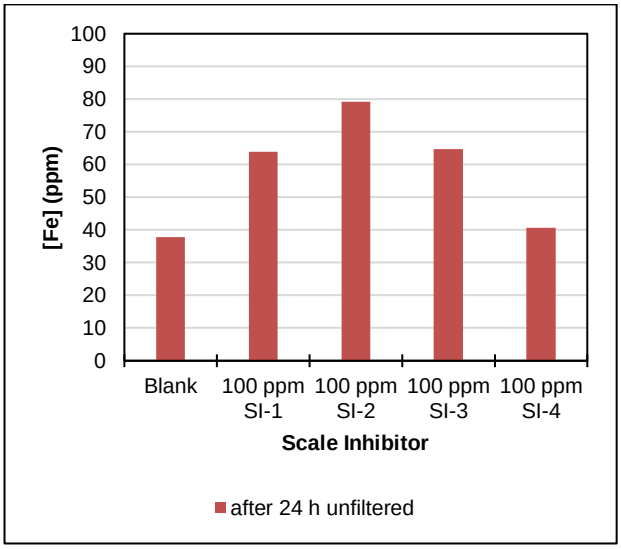

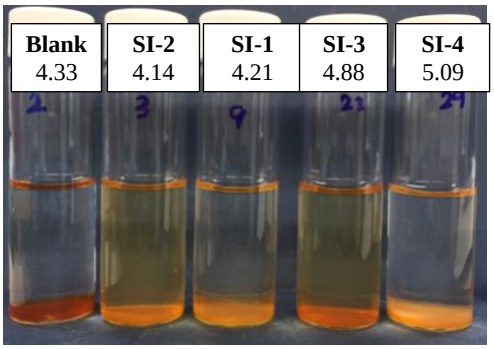

Figure 6.2 Iron concentrations in blank and inhibited solutions at pH 4-5 in 3.5% NaCl. The initial Fe concentration was 100 ppm

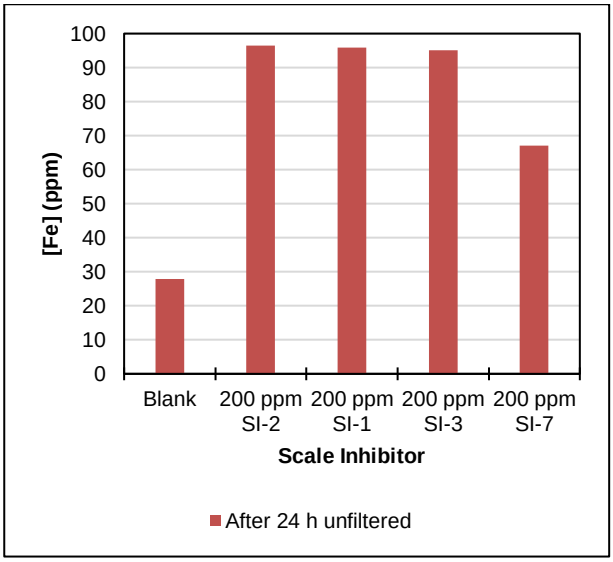

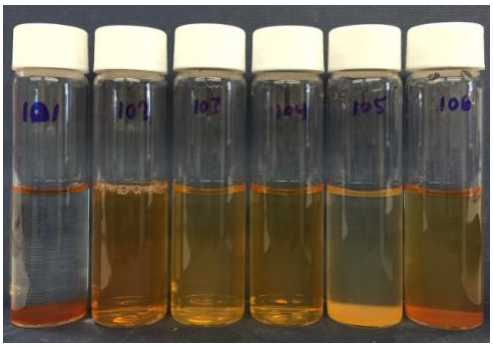

Figure 6.3 Iron concentrations in blank and inhibited solutions at pH 4-5 in 3.5% NaCl. The initial Fe concentration was 100 ppm

Three scale inhibitors, which showed a high inhibition efficiency for iron compounds (in absence of sulphide), were further tested in presence of higher iron concentrations at T = 50°C and 90°C. The performance of these scale inhibitors [SI] = 10,000 ppm was tested against 1000 ppm Fe in 3.5 and 20 wt% NaCl.

As shown in Photo 6.2, $Fe(OH)_3$ deposited in the blank solution and 5000 ppm SI-1 while the rest of scale inhibitors managed to hold $Fe(OH)_3$ in solution. The test was repeated at higher salinity *i.e.* 20 wt% NaCl and there was no $Fe(OH)_3$ deposition in scale inhibitor solutions as shown in Photo 6.3. By contrast, when the temperature was increased from 50°C to 90°C, SI-1 did not prevent the deposition of $Fe(OH)_3$ even in

presence of 10,000 ppm SI-1 which provided high inhibition efficiency at 50°C, see Photo 6.4 and Photo 6.5.

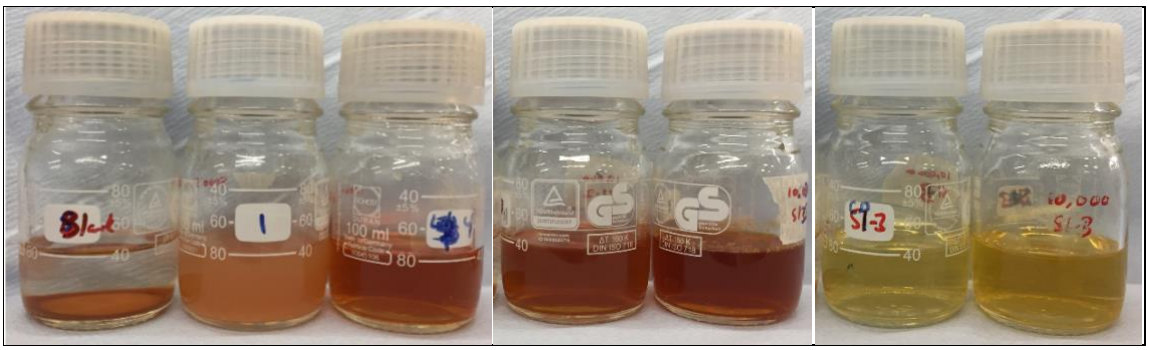

Photo 6.2 From left to right, blank (pH 3.12), 5000 ppm SI-1 (pH 3.65), 10,000 ppm SI-1 (pH 3.67), 10,000 ppm SI-2 (pH 3.67 and pH 3.78) and 10,000 ppm SI-3 (pH 2.95 and 3.23) in presence of 1000 ppm Fe at 50°C in 3.5 wt% NaCl.

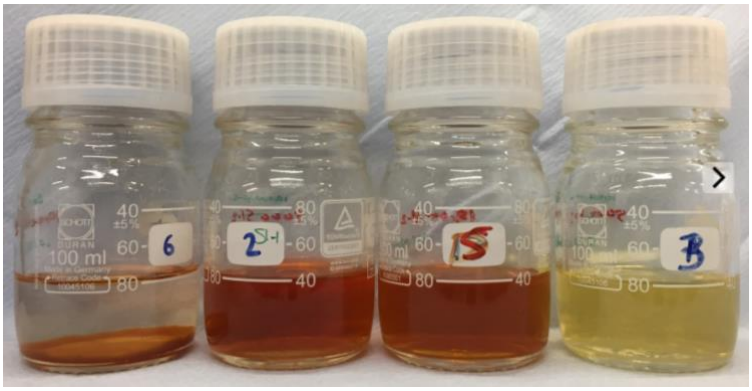

Photo 6.3 From left to right, blank (pH 2.66), 10,000 ppm SI-1 (pH 3.64), 10,000 ppm SI-2 (pH 3.61) and 10,000 ppm SI-3 (pH 3.02) in presence of 1000 ppm Fe at 50°C in 20 wt% NaCl.

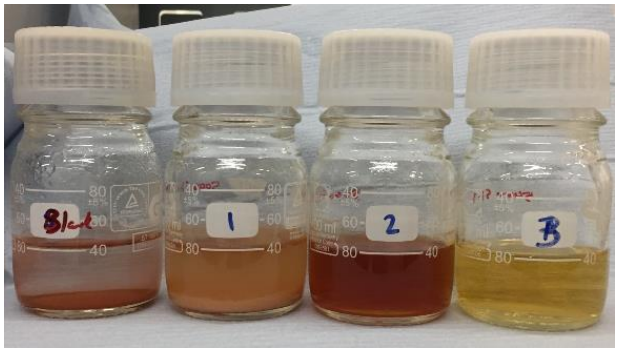

Photo 6.4 From left to right, blank (pH 2.46), 5000 ppm SI-1 (pH 3.3), 5000 ppm SI-2 (pH 2.62) and 5000 ppm SI-3 (pH 2.65) in presence of 1000 ppm Fe at 90°C in 3.5 wt% NaCl.

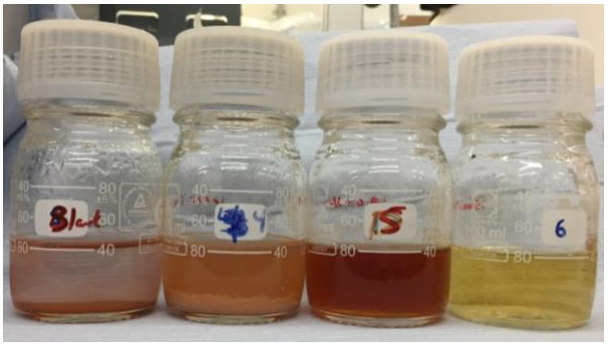

Photo 6.5 From left to right, blank (pH 2.46), 10,000 ppm SI-1 (pH 3.5), 10,000 ppm SI-2 (pH 2.8) and 10,000 ppm SI-3 (pH 2.65) in presence of 1000 ppm Fe at 90°C in 3.5 wt% NaCl.

6.3 Iron sulphide inhibition

6.3.1 FeS inhibition under aerobic conditions

As shown in Figure 6.4, at pH ~5 a small amount of Fe remained in the blank solution and the solutions containing 50 ppm SI-1, SI-3 and SI-4. The presence of iron in these inhibited solutions was attributed to the solubility of FeS at low pH rather than FeS "inhibition". At higher pH values, complete deposition of FeS occurred in the presence of all tested scale inhibitors, except SI-2. Of the various scale inhibitors tested, only 50 ppm SI-2 was effective against FeS even when the pH was as high as 7 *i.e.* at a higher scaling tendency.

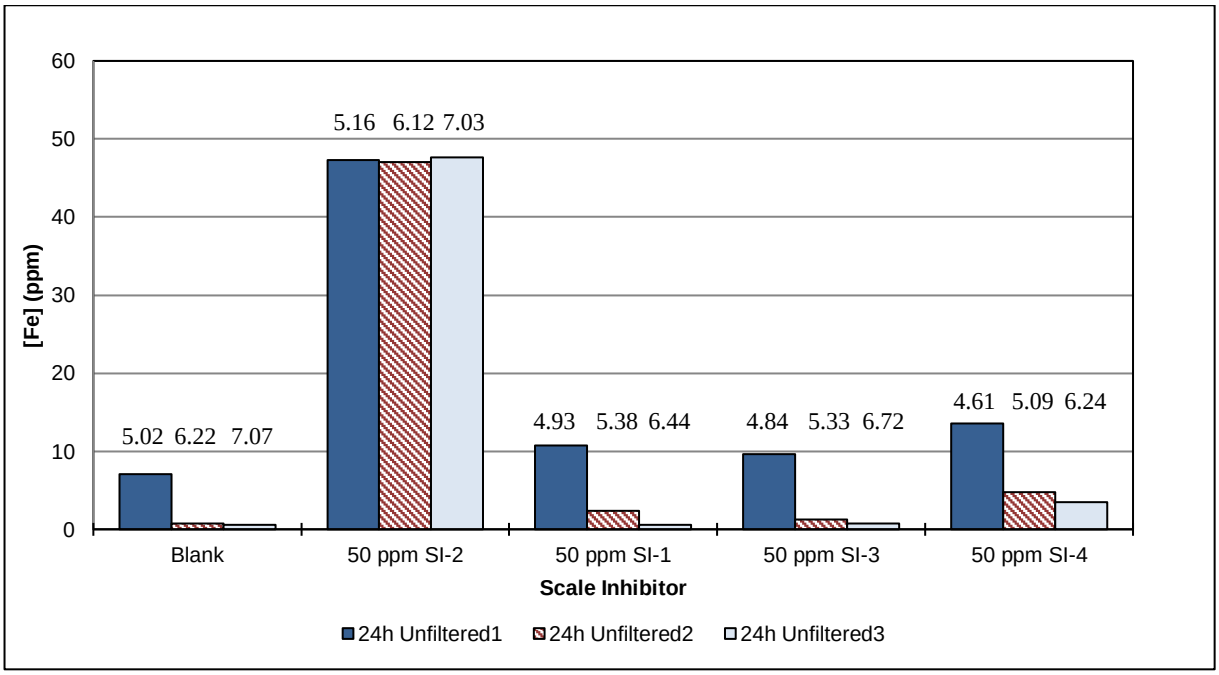

Figure 6.4 Fe concentration in blank and inhibited solutions (unfiltered samples) under aerobic conditions after 24 h and 23°C in presence of 100 ppm H_2S and 50 ppm Fe. The impact of pH on FeS inhibition.

As SI-2 was the only inhibitor that showed efficacy against FeS at 50 ppm, all scale inhibitors were tested under the same conditions, with the SI concentration increased to 100 ppm. All solutions, apart from SI-2, were deficient in Fe because of the complete precipitation and deposition of FeS as shown in Figure 6.5. The small amount of Fe detected in the 100 ppm SI-4 sample was attributed to the solubility of FeS rather than inhibition.

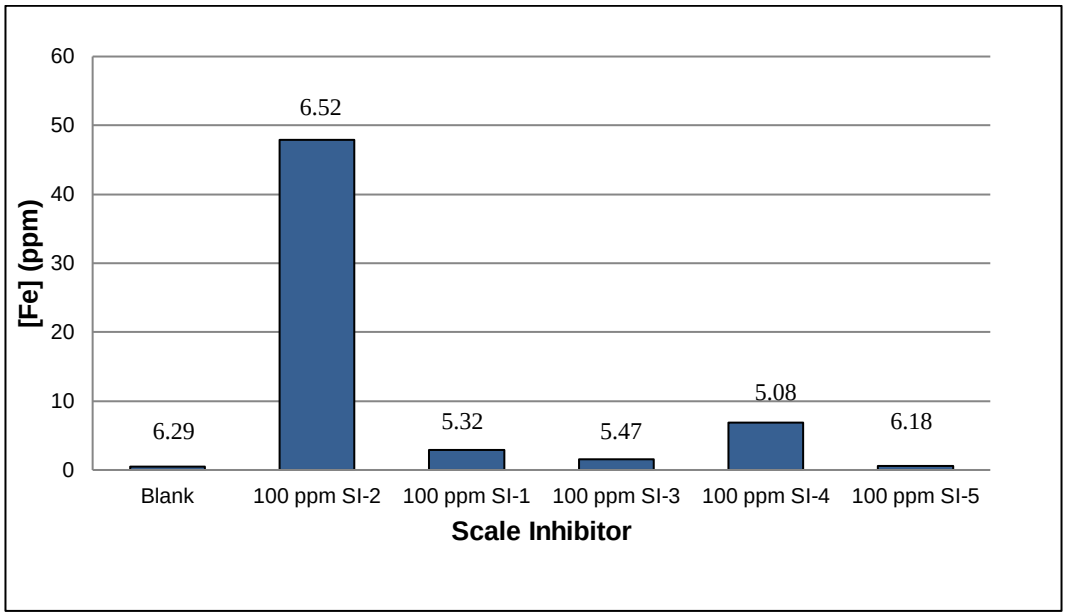

Figure 6.5 Fe concentration in blank and inhibited solutions (unfiltered samples) under aerobic conditions after 24 h and 23°C in presence of 100 ppm H_2S and 50 ppm Fe.

6.3.2 FeS inhibition under anaerobic conditions

Different concentrations of SI-2 and SI-3 were tested against FeS at 23°C under ***anaerobic*** conditions and the results are shown in Figure 6.6 and Figure 6.7. At pH 4.8, 30 ppm (~60%) Fe remained in the blank solution and the Fe concentration dropped to 3 ppm at pH 5.7. At low pH values (pH ~ 4.8 - 5.3), all tested concentrations of SI-2 were effective against FeS, however when the pH was higher (pH 5.9), 10 ppm SI-2 was no longer able to prevent FeS deposition.

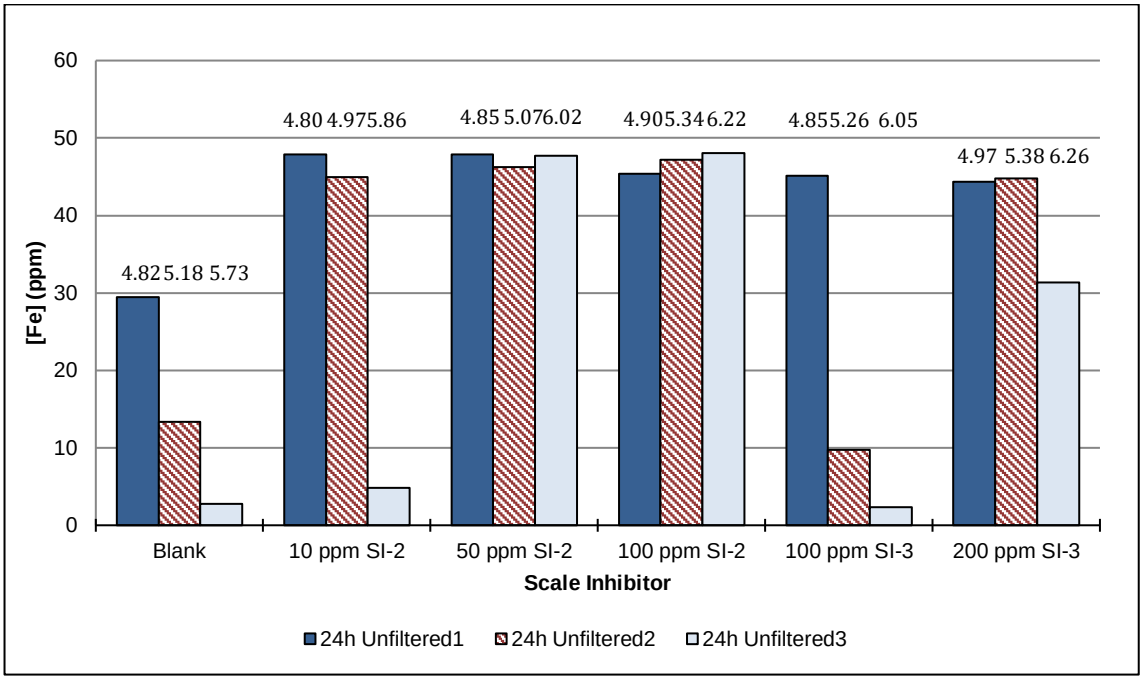

Figure 6.6 Fe concentrations in blank and inhibited solutions (unfiltered samples) under anaerobic conditions after 24 h and 23°C in presence of 100 ppm H_2S and 50 ppm Fe. The impact of pH on FeS inhibition.

Figure 6.7 shows a sharp decline in the apparent inhibition efficiency in the 10 ppm SI-2 solution as a result of increasing the amount of FeS scale. Similar behaviour was observed with SI-3 as increasing the pH caused more FeS to deposit. So, the inhibition efficiency for FeS using 10 ppm SI-2 and 100 ppm SI-3 would be overestimated if the FeS solubility were not considered. In addition to the impact of pH on the solubility, SI-3 was found to perform well at lower pH values (Chapter 5). It is of interest to note the similarity between inhibition efficiency of 50 ppm and 100 ppm SI-2 and 100 ppm SI-3 under aerobic and anaerobic conditions. The reason for the comparable results is that sulphide solutions were mixed with low pH Fe solutions (Fe^{2+} or Fe^{3+}), hence no preformed $Fe(OH)_3$ deposition occurred. But, when sulphide is the limiting reactant, the inhibition results would be different as two scales would form namely FeS and $Fe(OH)_3$ under aerobic conditions.

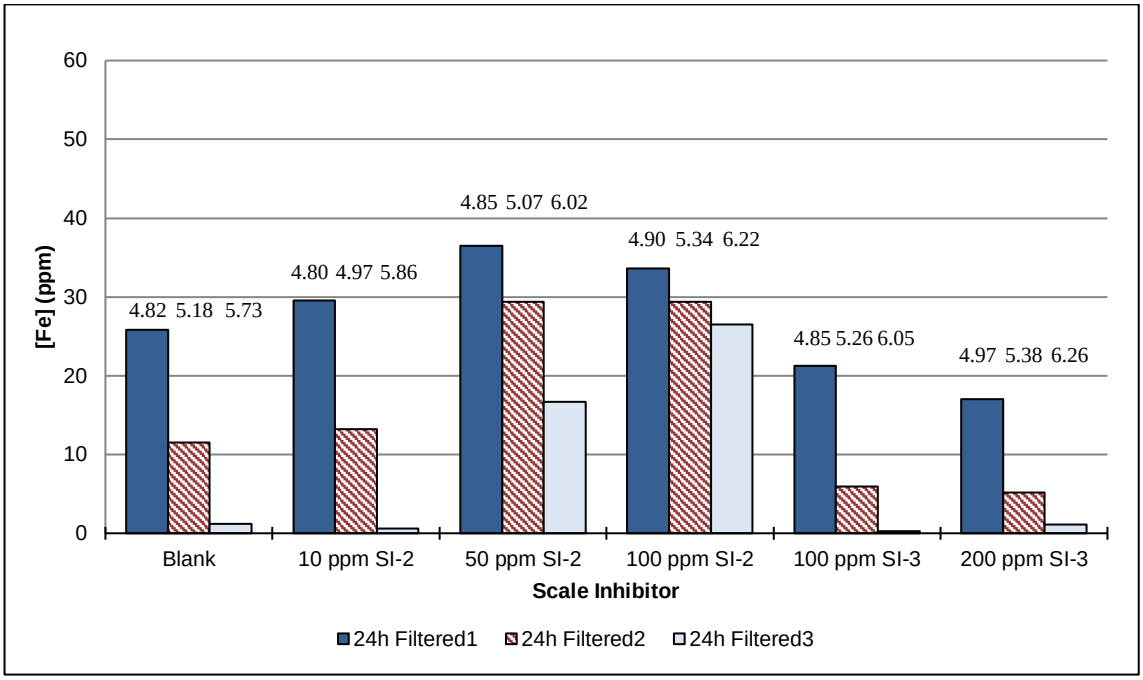

Figure 6.7 Fe concentrations in blank and inhibited solutions (filtered samples with 0.45 µm) under anaerobic conditions after 24 h and 23°C in presence of 100 ppm H_2S and 50 ppm Fe. The impact of pH on FeS inhibition.

6.4 FeS inhibition using different scale inhibitor chemistries in 3.5 wt% NaCl

Eight scale inhibitors (SI) were tested against iron sulphide to examine the inhibition efficiency and the impact of the SI on FeS particle size. The 8 SIs tested were SI-1 to SI-8 as listed and described in **Table 1.3**. The tests were conducted at 23°C in 3.5% NaCl in presence of 100 ppm Fe and nearly 20 ppm H_2S. The ICP results and particle size analysis are shown in Figure **6.8** and Table **6.1**, respectively. **Figure 6.8** showed that based on the unfiltered samples, 22 – 30 ppm Fe precipitated in blank solution and all tested scale inhibitors, except SI-2. The 0.2 µ filter would retain any suspended FeS including inhibited FeS. So, when the solutions were filtered with 0.2 µ filter, the Fe level in SI-2 solution dropped significantly. Despite the fact that the tested scale inhibitors, apart from SI-2, did not prevent FeS deposition, some scale inhibitors caused the particle size to decrease noticeably, see **Table 6.1**. In general, the FeS scale particle size decreased when the impeller speed was increased suggesting the formation of agglomerated particles, which are broken up by the impeller. At high impeller speed, the FeS particle size in blank solution was 16.8 µm. The particle size was 2 and 3.4 µm in SI-4 and SI-6 solutions, which are phosphonate scale inhibitors. It is interesting to note the significant decrease in the particle size in polymer scale inhibitor solutions including SI-1, SI-3, SI-7 and SI-8.

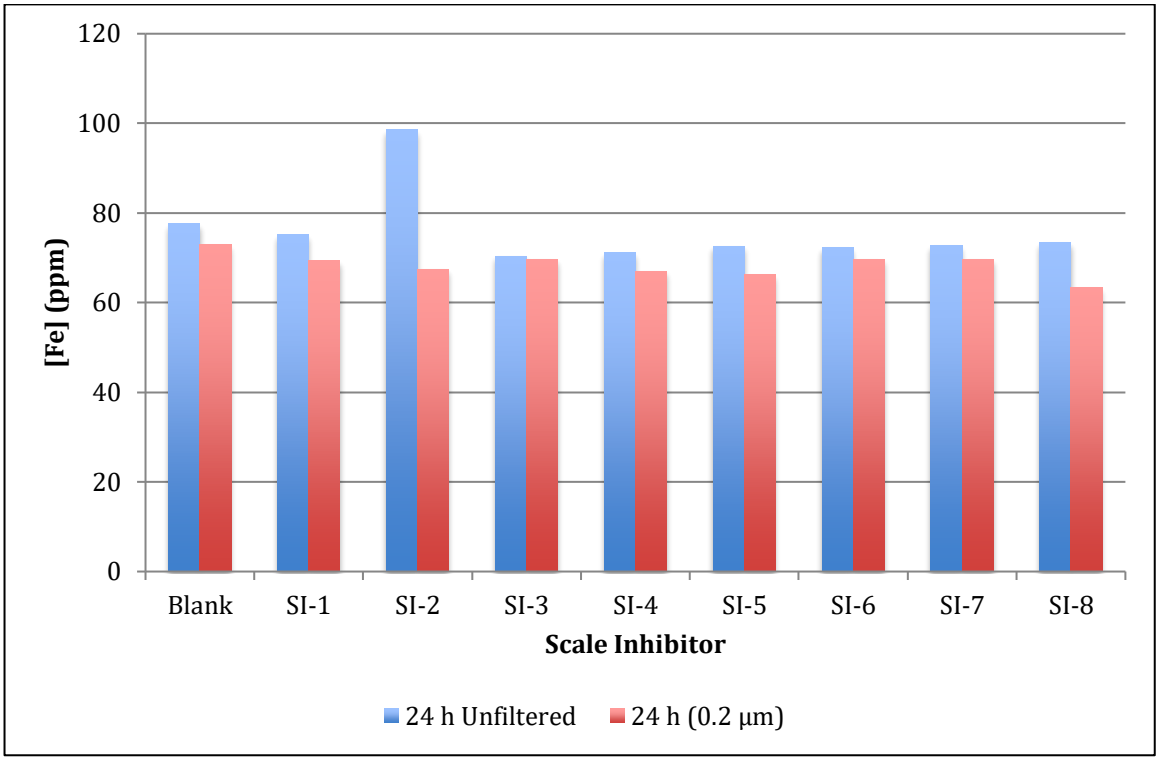

Figure 6.8 FeS inhibition at pH 6.5-7, 23°C in 3.5%NaCl in presence of 100 ppm Fe and 20 ppm H_2S. Scale inhibitor concentration is 100 ppm

Table 6.1 Particle size distribution of FeS supernatant solutions in presence of 100 ppm Fe and 20 ppm H_2S. Scale inhibitor concentration is 100 ppm.

	PSD					
	⅓ rpm			⅔ rpm		
SI	**D10**	**D50**	**D90**	**D10**	**D50**	**D90**
Blank	44.36	84.26	144.39	5.33	16.79	30.3
SI-1	0.49	1.39	6.1	0.37	0.57	0.95
SI-2	No data			No data		
SI-3	1.16	2.52	4.25	0.35	0.54	0.8
SI-4	7.26	15.33	25.5	1.06	2.26	3.85
SI-5	18.81	27.94	47.1	4.06	8.06	17.01
SI-6	14.25	22.83	38.3	1.99	3.45	5.4
SI-7	0.4	0.53	1.09	0.3	0.47	0.66
SI-8	0.74	2.32	5.01	0.36	0.56	0.89

6.5 The effect of salinity and pH on FeS inhibition

SI-2 and SI-3 were tested at 90°C in 3.5 and 20 wt% NaCl, and SI-2 was additionally tested at 30 wt% NaCl. Figure 6.9 and Figure 6.10 show the iron concentrations in 3.5 wt% NaCl after 2 and 24 hours, respectively. In addition, pH measurements were taken at the end of the experiment, and these pH values are presented in Table 6.2. After 2 hours, approximately 17 ppm (34%) Fe remained in the blank solution and in the 100 ppm SI-3 solution, while the other tested inhibitor concentrations successfully delayed FeS deposition. At 24 hours, complete FeS deposition had occurred in the blank, 10

ppm SI-2 and 100 ppm SI-3 solutions, while significant amounts of Fe were detected in the other solutions. The particle size varied with the type of scale inhibitor and concentration, as indicated by the difference in Fe concentrations in the unfiltered and filtered samples. This has important consequences for the definition of the apparent inhibition efficiency observed as operational needs and/or limitations may influence the maximum size of the dispersed FeS-SI particles that are acceptable.

Table 6.2 pH measurements, 3.5 wt% NaCl, in presence of 100 ppm H_2S and 50 ppm Fe.

SI	Blank	SI-2 **10 ppm**	SI-2 **25 ppm**	SI-2 **50 ppm**	SI-2 **100 ppm**	SI-3 **100 ppm**	SI-3 **150 ppm**	SI-3 **200 ppm**
Final pH	7.9	7.9	8.05	8.52	8.55	7.97	7.74	7.72

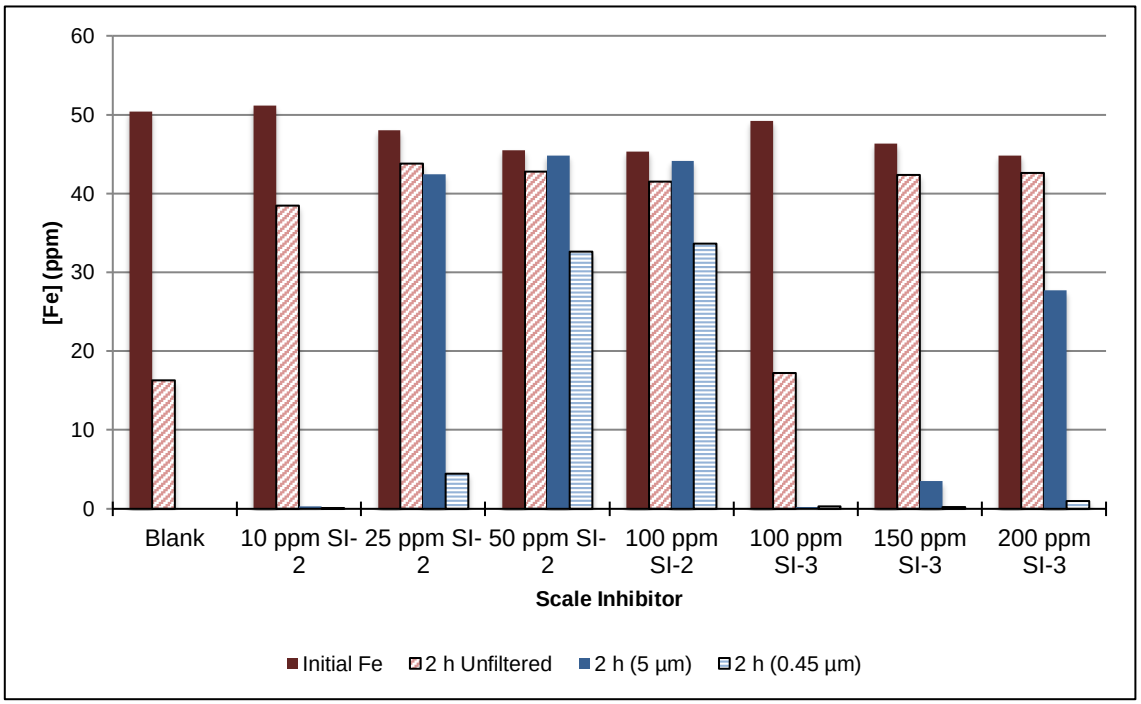

Figure 6.9 Fe concentrations in blank and inhibited solutions under anaerobic conditions after 2 h and 90°C in 3.5 wt% NaCl, in presence of 100 ppm H_2S and 50 ppm Fe.

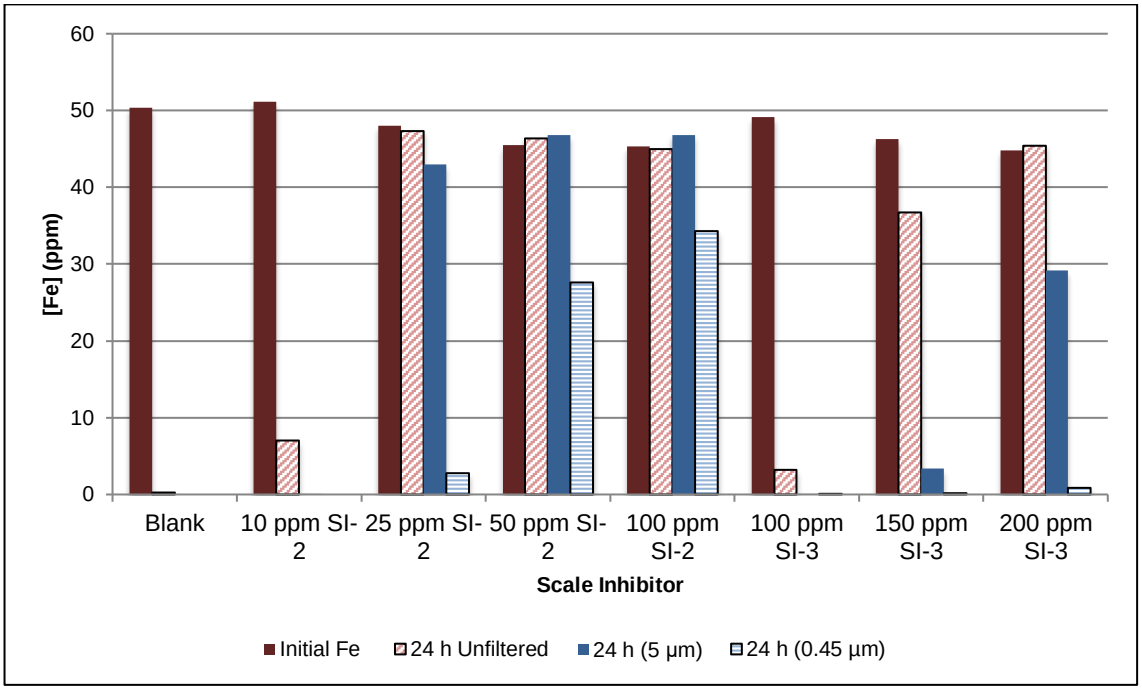

Figure 6.10 Fe concentrations in blank and inhibited solutions under anaerobic conditions after 24 h and 90°C in 3.5 wt% NaCl, in presence of 100 ppm H_2S and 50 ppm Fe.

The tests described above were repeated under the same conditions, with the salinity increased from 3.5 to 20 wt% NaCl, and the results are shown in Figure 6.11 and Table 6.3. At this higher salinity, the MIC for SI-2 increased from ≈ 10 - 25 ppm to ≈25 - 50 ppm. SI-3, in contrast, did not prevent the deposition of FeS even at a dosage of 200 ppm. SI-3 was found to perform better against PbS and ZnS at lower pH values (Chapter 5), and thus it was re-tested at potentially more favourable pH values *i.e.* 5.5 - 6 instead of 7, (Table 6.4). In this pH range, the solubility of FeS is relatively high and therefore the Fe concentrations detected by ICP may be a combination of dissolved Fe and suspended FeS. In order to differentiate between the two, a 0.2 µm filter was used to remove any suspended FeS particles from samples before being added to the quenching solution, therefore any Fe detected in the filtrate could be confirmed as aqueous Fe.

Table 6.3 pH measurements, 20 wt% NaCl, in presence of 100 ppm H_2S and 50 ppm Fe.

SI	**Blank**	**SI-2** 25 ppm	**SI-2** 50 ppm	**SI-2** 100 ppm	**SI-3** 150 ppm	**SI-3** 200 ppm
Final pH	6.99	7.1	7.16	7.5	6.9	6.9

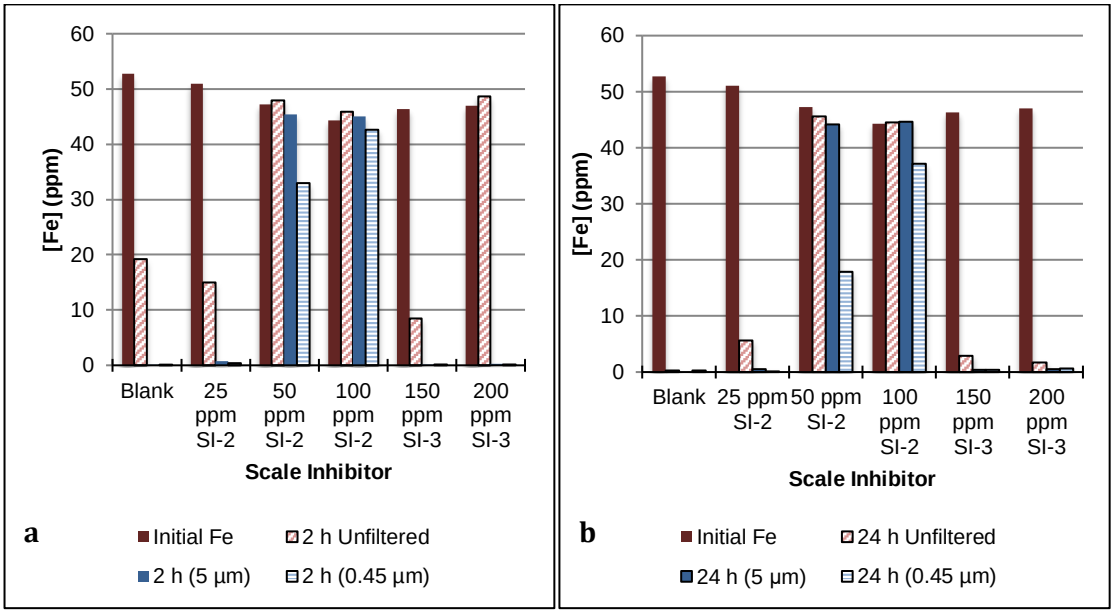

Figure 6.11 Fe concentrations in blank and inhibited solutions under anaerobic conditions after 2 and 24 h, at 90°C in 20 wt% NaCl, in presence of 100 ppm H_2S and 50 ppm Fe.

As shown in Figure 6.12 a) and b), the performance of SI-2 improved when the test was conducted at lower pH values; the inhibition efficiency for FeS using SI-3 was insignificant. When the pH was reduced to pH~4.5 (see Table 6.5), the Fe levels measured in the blank and inhibited solutions slightly increased, see Figure 6.13. This increase was a result of the increase in FeS solubility and the improvement of SI performance at lower pH values. Note the dramatic decline in Fe concentration as a result of increasing the temperature from 23 to 90°C at corresponding pH values. This is in a good agreement with field observation and predictions where FeS scale was seen in the lower part of the production system in Khuff wells (Verri *et al.*, 2017).

Table 6.4 pH measurements, 20 wt% NaCl, in presence of 100 ppm H_2S and 50 ppm Fe.

SI	**Blank**	**SI-2** 25 ppm	**SI-2** 37.5 ppm	**SI-2** 50 ppm	**SI-2** 100 ppm	**SI-3** 150 ppm	**SI-3** 200 ppm
Final pH	5.49	5.61	5.83	5.96	6.28	5.44	5.43

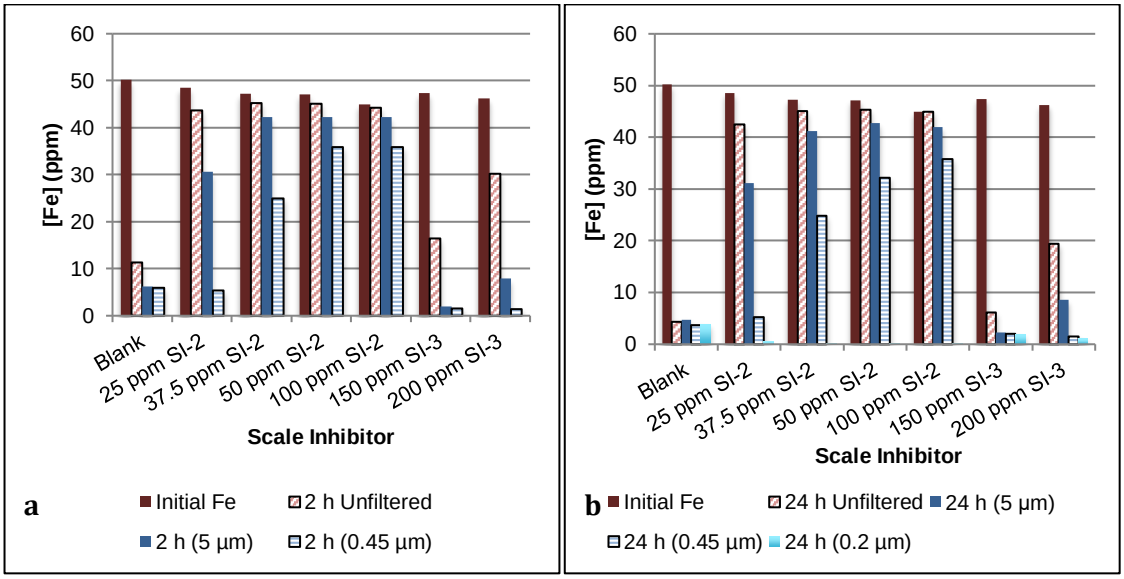

Figure 6.12 Fe concentrations in blank and inhibited solutions under anaerobic conditions after 2 and 24 h, at 90°C in 20 wt% NaCl, in presence of 100 ppm H_2S and 50 ppm Fe.

Table 6.5 pH measurements, 20 wt% NaCl, in presence of 100 ppm H_2S and 50 ppm Fe.

SI	**Blank**	**SI-2** 25 ppm	**SI-2** 50 ppm	**SI-2** 100 ppm	**SI-3** 150 ppm	**SI-3** 200 ppm
Final pH	4.4	-	4	4.7	4.6	4.5

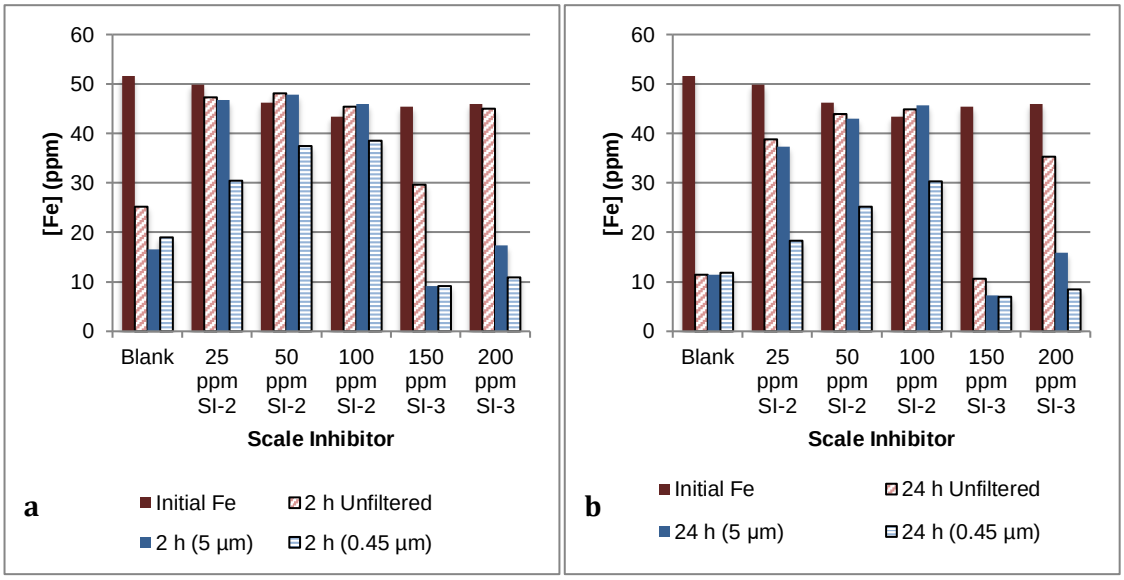

Figure 6.13 Fe concentrations in blank and inhibited solutions under anaerobic conditions after 2h and 24 h, at 90°C in 20 wt% NaCl, in presence of 100 ppm H_2S and 50 ppm Fe.

Only SI-2 showed a high inhibition efficiency for FeS in the 20 wt% NaCl solution and consequently it was the only inhibitor tested at 30 wt% NaCl (Table 6.6 and Figure 6.14). At this salinity, despite the fact that 50 ppm SI-2 and above managed to hold FeS in the solutions, the particle size of FeS varied considerably. In the 50 ppm SI-2 solution, a portion of the FeS ranged between 0.45 and 5 µm and a portion had a particle

size greater than 5 µm. Whereas, in the 75 and 100 ppm SI-2 cases, all particle sizes ranged between 0.45 and 5 µm. It was concluded from these results that the type of scale inhibitor, the SI concentration, the solution salinity and pH can all play a significant role on the inhibition efficiency and the resulting particle size of the FeS formed. Moreover, the particle size might be different even if the inhibition efficiency is comparable, and this should be considered in filter blocking tests. That is, a filter blocking test might erroneously be responding mainly to the FeS particle size and not to the formation/inhibition of the FeS.

Table 6.6 pH measurements, 30 wt% NaCl, in presence of 100 ppm H_2S and 50 ppm Fe.

SI	Blank	25	37.5	50	75	100
Final pH	6.3	6.32	6.2	6.45	6.27	6.57

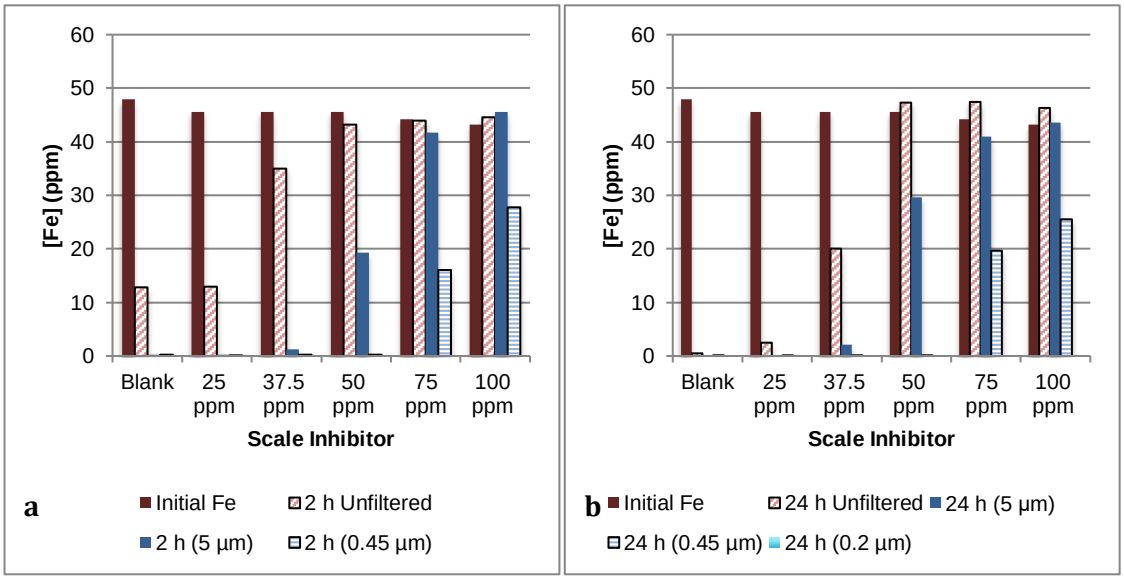

Figure 6.14 Fe concentrations for blank and inhibited solutions under anaerobic conditions after 2 and 24 h, at 90°C in 30 wt% NaCl, in presence of 100 ppm H_2S and 50 ppm Fe.

From previous work on FeS, ZnS and PbS inhibition, one scale inhibitor (SI-2) provided high inhibition efficiency when the tests were performed in high saline brine *i.e.* 30 wt% NaCl and Glenelg formation water (GFW). Therefore, this high molecular weight scale inhibitor was selected for FeS inhibition in Khuff formation water with high salinity.

Figure 6.15 shows the Fe concentration after 2 hours when Fe solutions, containing different SI-2 concentrations, were mixed with H_2S solutions. In this case, sulphide is in excess to Fe and the final pH was around 6 so complete Fe precipitation is expected. It is clear from Figure 6.15 the addition of 10 ppm and 25 ppm SI-2 resulted in slight delay in the FeS deposition compared to the blank solution. 37.5 ppm and above

effectively prevented the deposition of FeS even when the time was extended to 24 hours as shown in Figure 6.16. Another interesting observation is the correlation of particle size and scale inhibitor concentration. Increasing the scale inhibitor concentration caused the particle size to decrease. Accordingly, to reduce the particle size of inhibited FeS below 0.45 µm, higher SI concentration should be used.

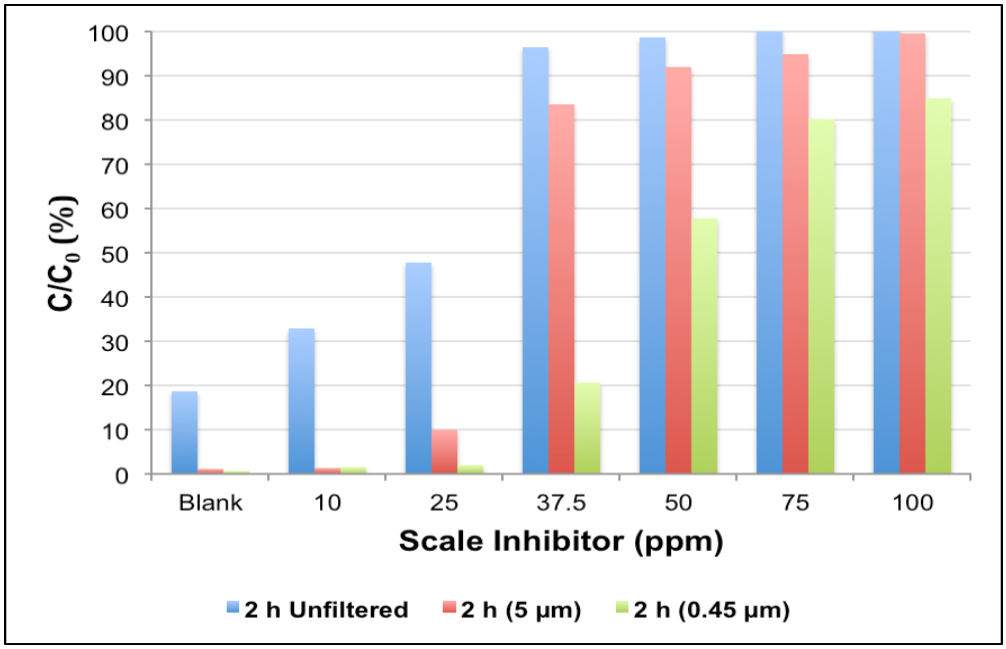

Figure 6.15 Fe in supernatant solution after 2 h, in Khuff formation water at 90°C. Initial Fe concentration was 50 ppm

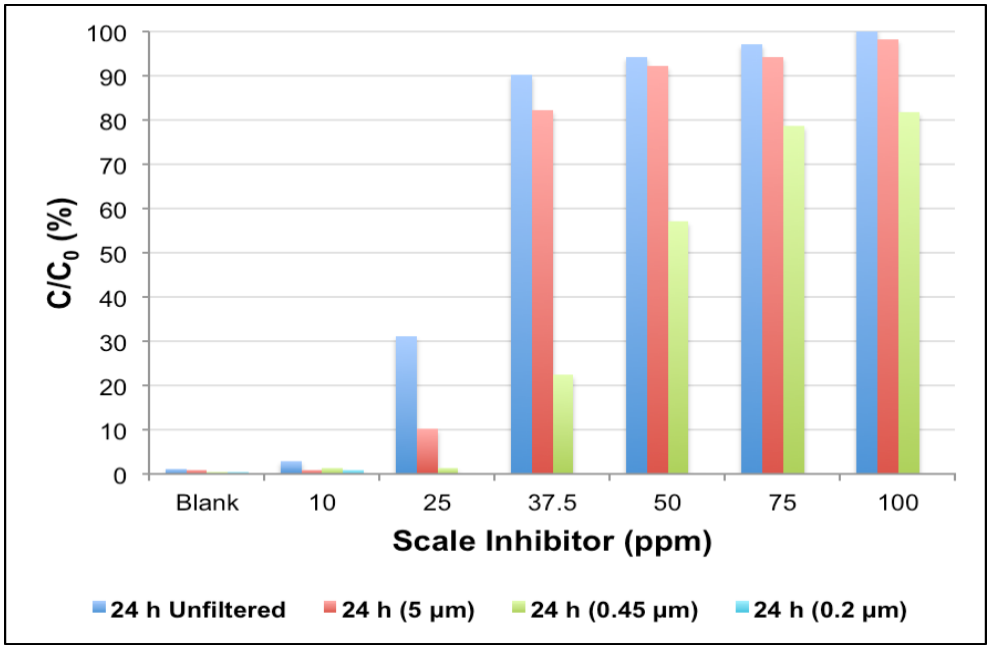

Figure 6.16 Fe in supernatant solutions after 24 h, in Khuff formation water at 90°C. Initial Fe concentration was 50 ppm.

Chapter 6: $Fe(OH)_3$ and FeS inhibition

To study the impact of increasing the Fe and sulphide concentrations on the inhibition efficiency of SI-2, the tests were repeated under the same conditions except that Fe and H_2S concentrations were raised to 100 ppm and 130 ppm, respectively. The increase in Fe and sulphide concentrations, hence scaling tendency, required the use of significantly higher concentration of SI-2 to prevent FeS scale deposition, as shown in Figure 6.17 and Figure 6.18. In presence of 50 ppm Fe, 37.5 ppm was sufficient to provide around 90% inhibition efficiency. Whereas in presence of 100 ppm Fe, the inhibition efficiency was 70% and 92% in 75 ppm and 100 ppm SI-2 solutions, respectively.

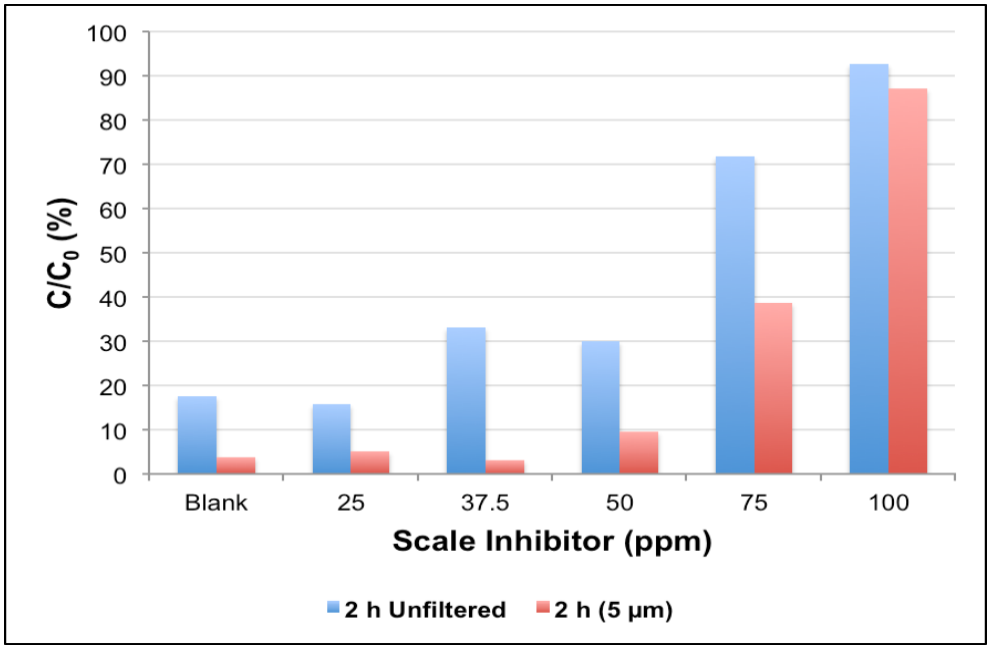

Figure 6.17 Fe in supernatant solution after 2 h, in Khuff formation water at 90°C. Initial Fe concentration was 100 ppm

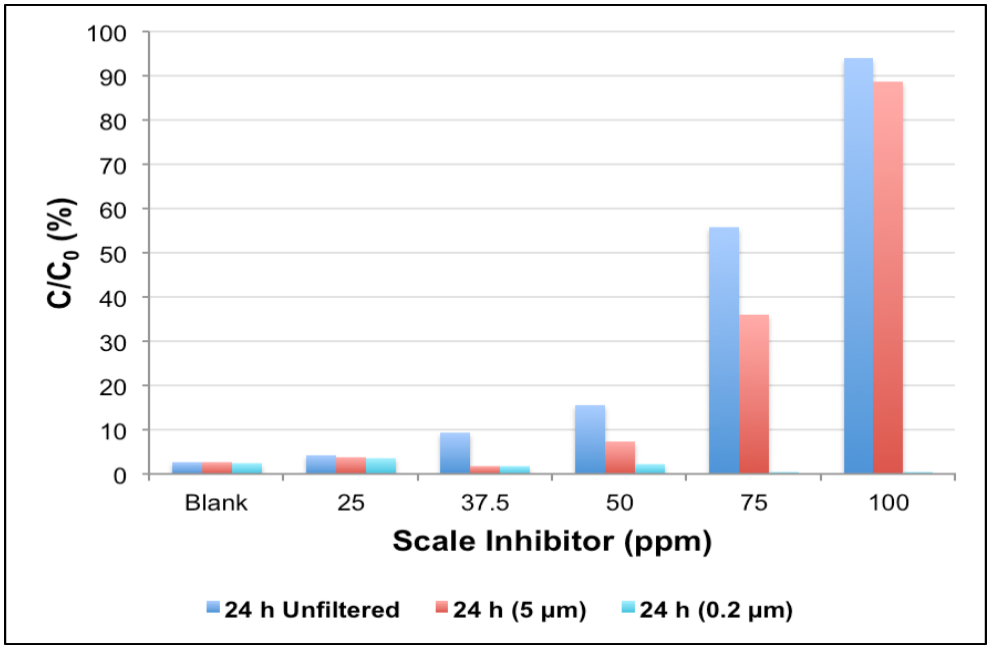

Figure 6.18 Fe in supernatant solutions after 24 h, in Khuff formation water at 90°C. Initial Fe concentration was 100 ppm.

To further investigate the impact of scaling tendency on inhibition efficiency, 450 ppm Fe containing 100 ppm SI-2 was mixed with different concentrations of sulphide. The ICP results are plotted in Figure 6.19. Unfiltered samples were collected after 2 hours which show the total Fe concentration including dissolved Fe and colloidal FeS. Up to 150 ppm sulphide, no decline in total Fe concentration was noted indicating that 100 ppm effectively held FeS suspended in the solutions. Increasing the sulphide concentration to 200 ppm and 250 ppm resulted in discernible decrease in Fe concentration and hence in the SI-2 efficiency. After 24 h, in addition to the unfiltered samples, filtered samples with 0.2 µm filter were collected to differentiate between the dissolved Fe and FeS. Extending the reaction time to 24 hours had no impact on the inhibition efficiency for 0 - 100 ppm sulphide solutions. On the other hand, significant amount of FeS deposited at extended reaction time *i.e.* 24 hours.

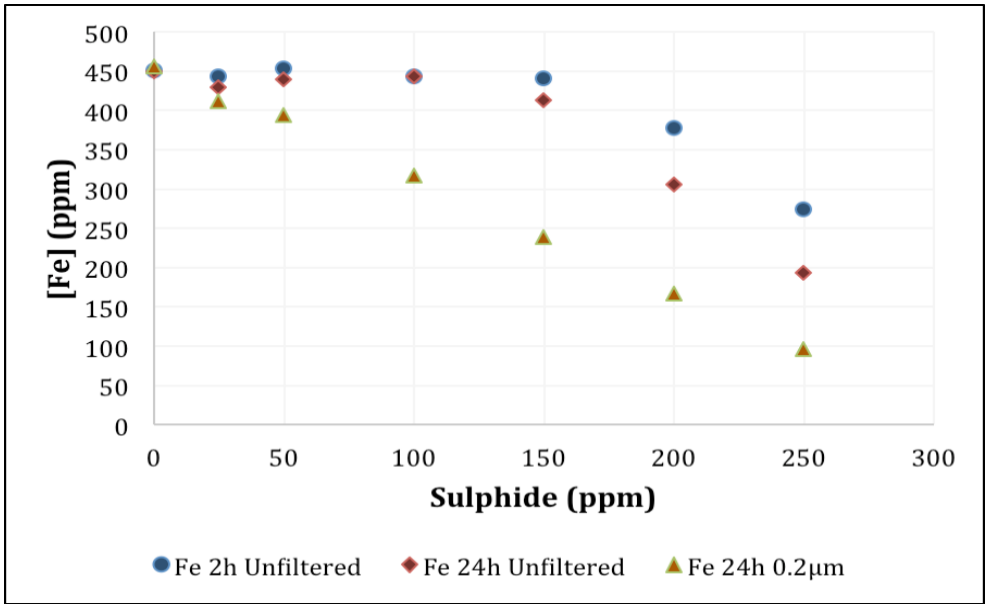

Figure 6.19 Fe in supernatant solutions after 2 and 24 h, in 3.5 wt% NaCl at 90°C. Initial Fe concentration was 450 ppm. Sulphide concentrations were calculated based on $Na_2S.9H_2O$ addition

Different sulphide concentrations were mixed with 250 ppm Fe in Khuff formation water at 90°C in the presence of 50, 100 and 200 ppm SI-2. The sulphide is the limiting reactant to Fe and thus Fe concentrations detected by ICP could be dissolved Fe in addition to suspended FeS. As shown in Figure 6.20, in the presence of 32 ppm sulphide, the Fe concentrations detected in the inhibited solutions are higher than that in the blank solution, thus indicating that all tested concentrations were effective in hindering the deposition of FeS. However, when sulphide concentration was raised to 65 ppm, hence increasing the scaling tendency, only 100 ppm and 200 ppm SI-2 delayed the FeS deposition. When sulphide concentration was further increased to 130 ppm, 200 ppm of SI-2 managed to hold FeS in solution. When the time was extended to 24 hours, see Figure 6.21 and Figure 6.22, 50 ppm SI-2 was effective in presence of 32 ppm sulphide. 100 ppm and 200 ppm SI-2 held FeS suspended in 32 ppm and 65 ppm sulphide solutions. There was a significant decrease in Fe concentrations in presence of 200 ppm SI-2.

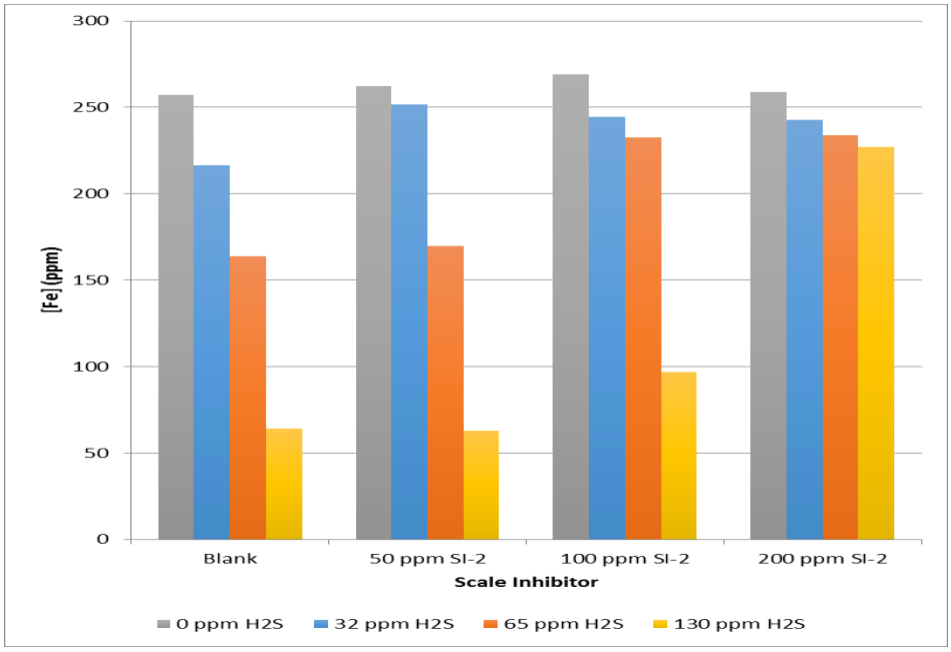

Figure 6.20 FeS inhibition after 2 h (unfiltered) in Khuff formation water at 90°C in presence of different sulphide concentrations. Final pH values are 4.5, 6.2, 6.3 and 6.5 in presence of 0, 32, 65 and 130 ppm H_2S, respectively.

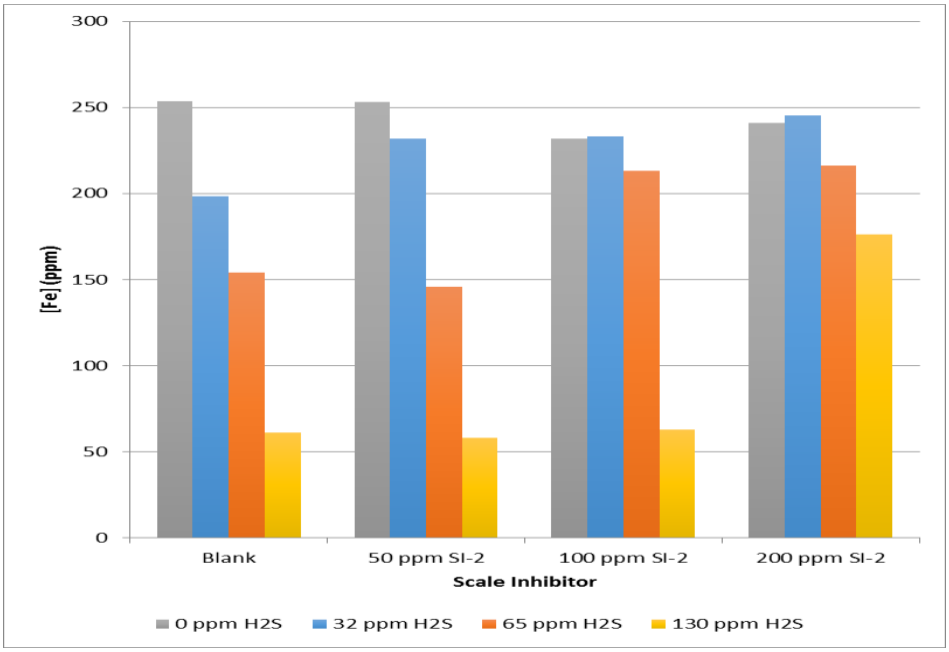

Figure 6.21 FeS inhibition after 24 h (unfiltered) in Khuff formation water at 90°C in presence of different sulphide concentrations. Final pH values are 4.5, 6.2, 6.3 and 6.5 in presence of 0, 32, 65 and 130 ppm H_2S, respectively.

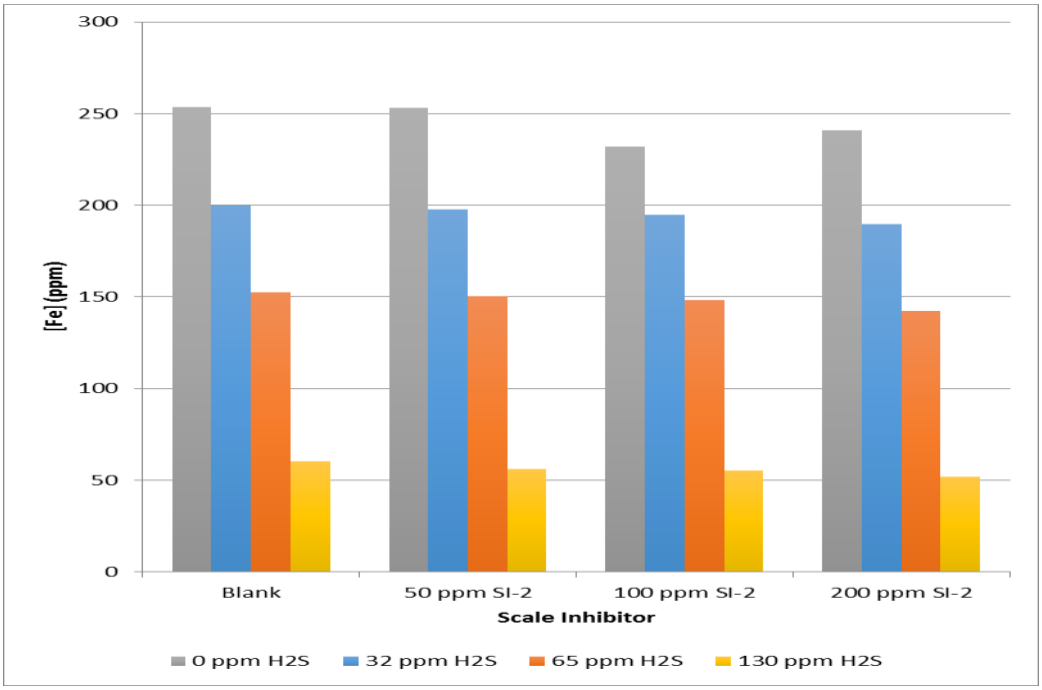

Figure 6.22 FeS inhibition after 24 h (filtered with 0.2 µm) in Khuff formation water at 90°C in presence of different sulphide concentrations. Final pH values are 4.5, 6.2, 6.3 and 6.5 in presence of 0, 32, 65 and 130 ppm H_2S respectively.

6.6 Conclusions

Several scale inhibitors were tested for iron hydroxide inhibition at different pH values in distilled water and in sodium chloride brines. The ones that showed some effect were further evaluated in higher TDS brines and at higher temperatures. In addition, different scale inhibitors were tested for FeS inhibition under aerobic and anaerobic conditions. SI-2 and SI-3, which both outperformed the other scale inhibitors, were further examined at higher temperature *i.e.* 90 °C and KFW (TDS = 200,000 ppm). Also, the impact of the mass of FeS on the inhibition efficiency of SI-2 was investigated by increasing the concentration of H_2S in the presence of 450 ppm Fe for various SI-2 concentrations. The main conclusions from this study are as follows:

1. Some scale inhibitors prevented the deposition of iron hydroxide even in the presence of high Fe concentrations i.e. 1000 ppm, and therefore they might be used as additives to acidisation fluids to prevent the iron hydroxide deposition when the acid is spent. Further work is required to examine the inhibition ability in presence of higher Fe concentrations and other iron control additives such as EDTA and citric acid as some published work showed that the presence of chelating agents might affect the performance of scale inhibitors (Barthorpe, 1993).

2. For the first time, SI-2 was extensively tested against FeS. Overall, the best inhibitor for FeS tested in this work was SI-2 (the high molecular weight sulphonated co-polymer; see Table 2.7), with an MIC of 25-50 ppm over a broad range of test conditions *i.e.* anaerobic, 90°C, 3.5% to 30% NaCl, maximum Fe ~50 ppm.

3. SI-2 decreased the size of the resultant precipitate particles, believed to be a SI-FeS complex, to below the size of the uninhibited FeS. This effect was magnified by increasing the scale inhibitor concentration. Therefore, if operational need requires the reduction of FeS particles below certain sizes, *e.g.* 0.45 or 0.2 µm, then higher concentrations of SI-2 will be required for the smaller particle sizes. In this work, inhibited test solutions passed the 0.45 µm size criterion, but none passed through the 0.2 µm filter.

4. Increasing the pH and salinity had a negative impact on the performance of SI-3, which is consistent with previous data on ZnS and PbS inhibition (Chapter 6).

5. As noted above, no inhibited sulphide solution passed through the 0.2 µm filter test. This filter size retained inhibited FeS, ZnS and PbS particles and so can be used to remove sulphide scales to differentiate between the truly dissolved metal ions and colloidal sulphide scale, to obtain accurate SI measurements using Hyamine and sulphide measurements using UV-Vis spectrophotometric analytical methods.

Chapter 7

Inhibition of Mixed Sulphide Scales

7.1 Introduction

In this chapter, we present our results on the inhibition of mixed ZnS/PbS/FeS sulphide scales. In particular, the impact of cation displacement and the sequence of sulphide scales deposition on the inhibition efficiency is investigated. In the cation displacement experiments, PbS deposition was prevented when the scale inhibitor was added to Zn solution *i.e.* ZnS was inhibited. Similar behaviour was observed when PbS and ZnS formed by extracting sulphide from FeS. Therefore, the deposition of sulphide scale forming by cation displacement can be prevented provided that the preformed sulphide scale is inhibited. When PbS was allowed to form before ZnS, the MIC was found to be higher compared to that when PbS and ZnS formed together despite the Pb and Zn concentrations being the same regardless of the mixing method.

7.2 Cation displacement in presence of scale inhibitors (Zn, Pb and sulphide)

To examine the ability of SI-2 to prevent PbS deposition when it forms by a cation displacement mechanism, the following tests were conducted. In the first set of experiments, ZnS was allowed to form in presence of SI-2 followed by lead acetate addition such that the final Pb, Zn and SI-2 concentrations are comparable to the concentrations used in the previous test. For illustration, 50 ml of 200 ppm Zn SFNSSW was mixed with 50 ml of 15 ppm H_2S SFNSSW in presence of 0, 10, 20, 50 and 100 ppm SI-2 after that 100 ml of 100 ppm Pb SFNSSW was added to these solutions. Assuming no scale precipitation, the final concentrations would be 50 ppm Zn, 50 ppm Pb, 0, 5, 10, 25 and 50 ppm SI-2. As shown in Figure 7.1, the Zn concentration in the blank solution dropped from 100 ppm to 73 ppm due to ZnS formation.

Similar results were obtained in presence of 10 ppm SI-2; see Figure 7.2. As the samples were filtered through a 0.45 μm filter, the drop in Zn concentration in the presence of 10 ppm SI-2 indicated that the particle size of ZnS is greater than 0.45 μm, rather than being due to the failure of SI-2 to inhibit ZnS. 20, 50 and 100 ppm SI-2 cases, on the other hand, managed to considerably reduce the particle size of ZnS and subsequently prevent its deposition. 2 hours after the ZnS scale formation, Pb containing brine was added to ZnS solutions. The ICP data and pH measurements are shown in Figure 7.2. In all solutions, ZnS redissolved and subsequently Zn

concentrations increased to the initial value *i.e.* 50 ppm. Two distinct types of behaviour were noticed in terms of PbS inhibition. PbS deposited in the blank solution and 5 ppm SI-2 whereas it remained suspended in the higher tested SI-2 concentrations. As shown in Photo 7.1, the inhibited ZnS solution was crystal clear. After Pb solution was added to this solution, the colour started to change and within minutes the solution turned black. In addition, two samples, namely ZnS in presence of 10 ppm SI-2 before and after Pb addition, were analyzed using SEM. As shown in Table 7.1 after 2 hours, ZnS was detected on the 0.45 µm filter. 1 hour after Pb addition, only PbS was detected on the filter.

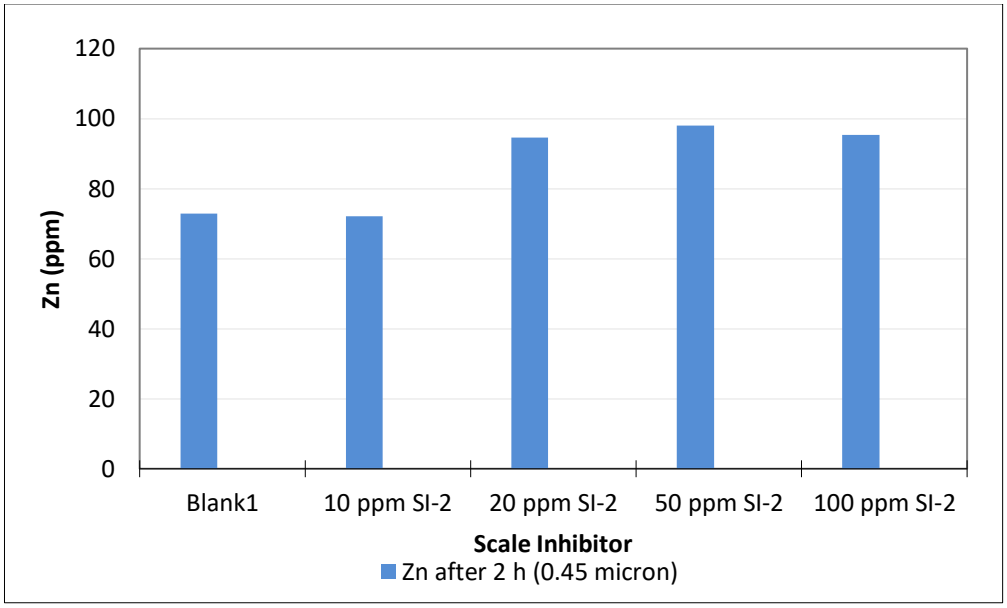

Figure 7.1 ZnS inhibition after 2 h in SFNSSW at 50°C using SI-2.

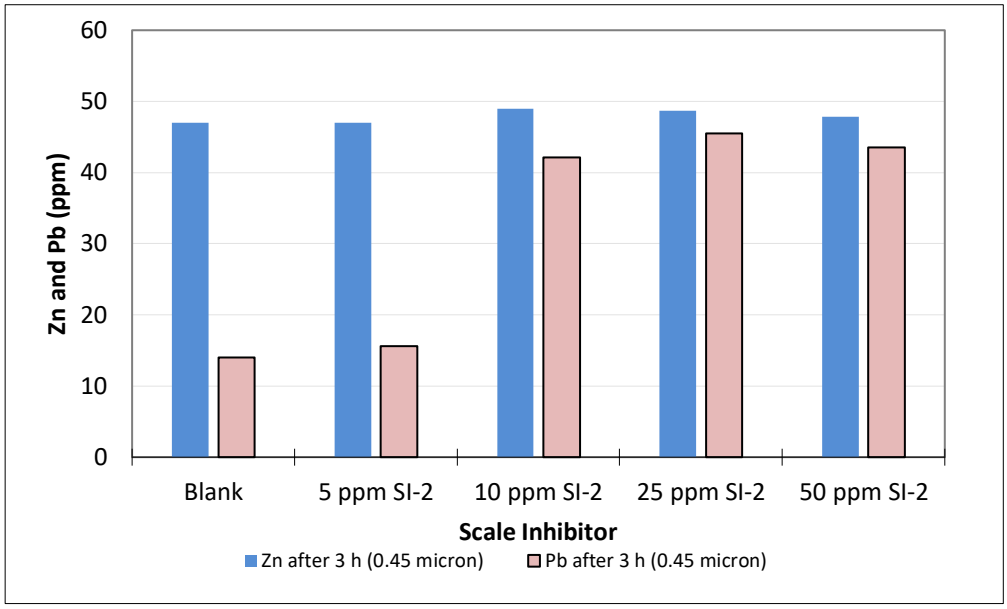

Figure 7.2 ZnS and PbS inhibition after 3 h (1 h after ZnS formation) in SFNSSW at 50°C using SI-2.

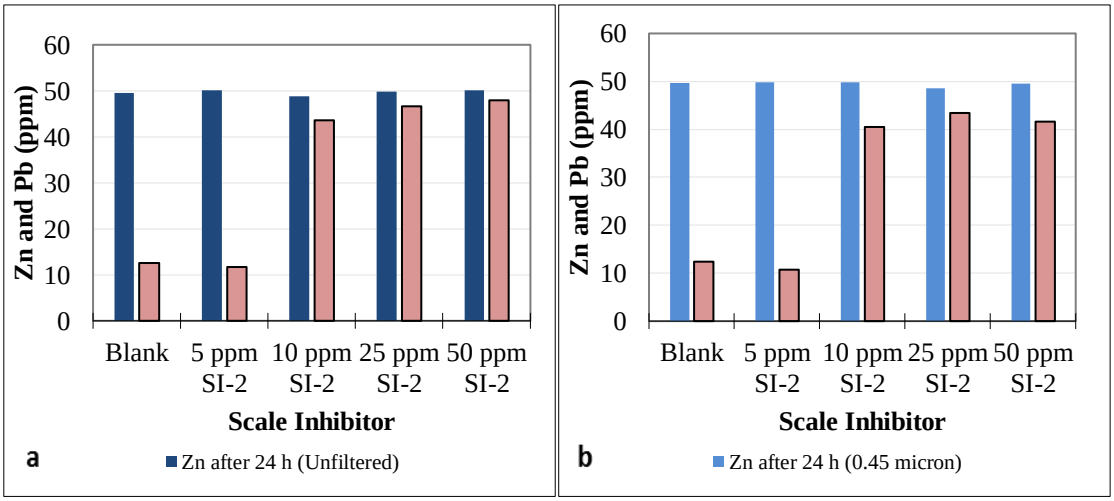

Figure 7.3 ZnS and PbS inhibition after 24 h (22 h after ZnS formation) in SFNSSW at 50°C using SI-2.

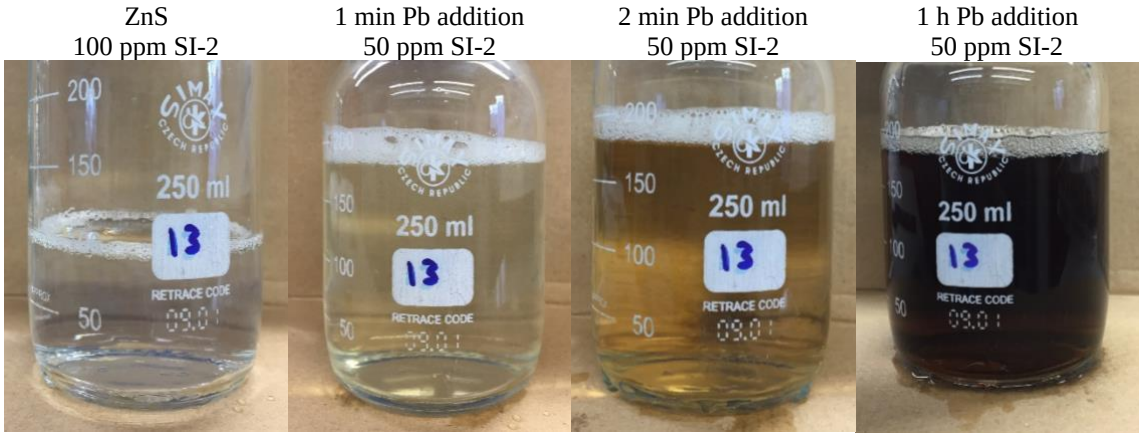

Photo 7.1 Visual evidence of cation displacement reaction.

Table 7.1 ZnS and PbS in presence of 10 ppm SI-2

	Weight %	
Element	**2 h**	**3 h**
C	31.58	51.37
O	37.78	36.53
Cl	0	0.66
S	8.72	1.39
Zn	21.92	0
Pb	0	10.05

The cation displacement test was repeated under the same conditions, except that 1000 ppm SI-2 was added to the Pb SFNSSW solution rather than to the Zn SFNSSW brine. Zn concentrations decreased from 100 ppm to 72 ppm (Figure 7.4). After that, Pb SFNSSW with and without SI-2 was added to the ZnS solutions and consequently Zn concentration increased to 48 ppm while Pb concentration decreased to 16 ppm after 24 hours in both filtered and unfiltered samples, as shown in Figure 7.5.

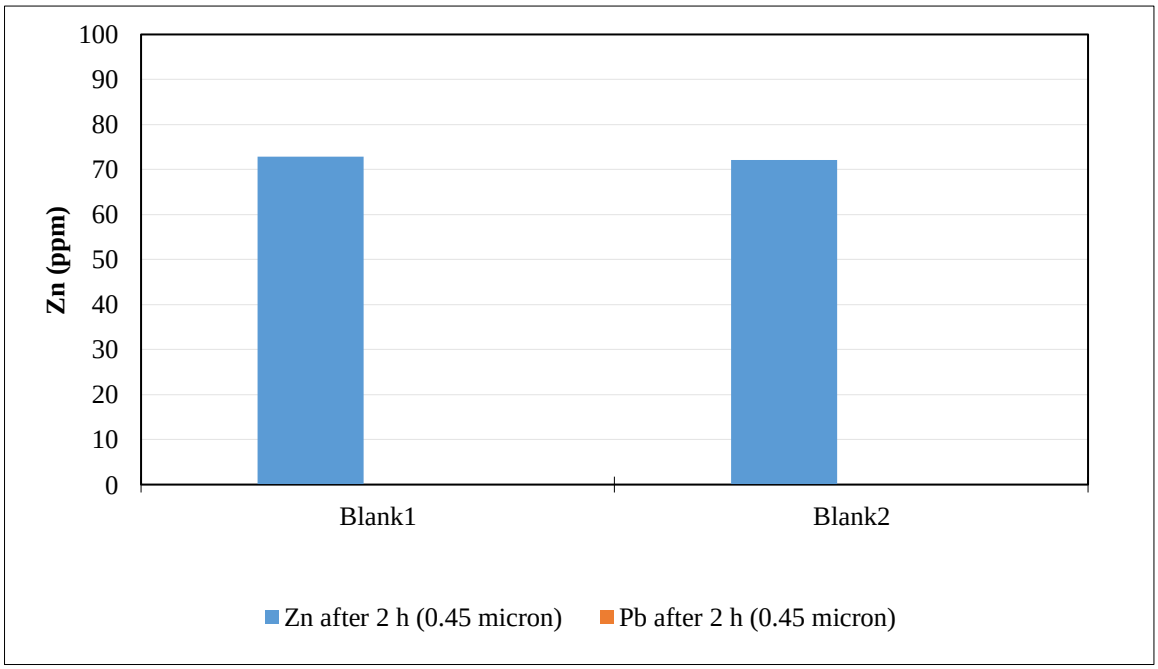

Figure 7.4 ZnS formation after 2 h in SFNSSW at 50°C.

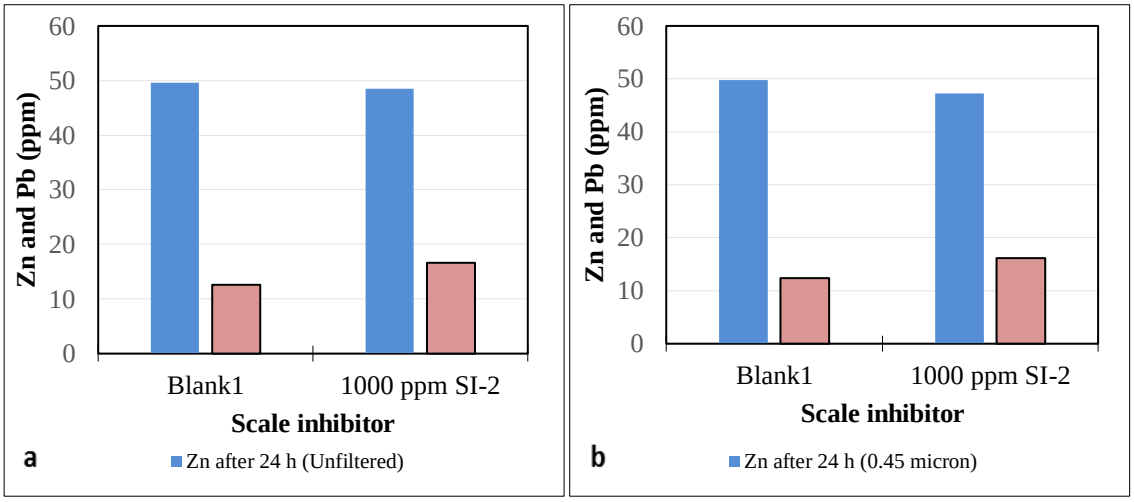

Figure 7.5 ZnS and PbS inhibition after 24 h (22 h after ZnS formation) in SFNSSW at 50°C using SI-2.

The next test was conducted to study the impact of preformed PbS on ZnS inhibition and ICP results are presented in Table 7.2. Different mixing steps were involved in this procedure (as described in Table 7.2); however, the final SI concentration and the final Zn and Pb concentrations, if there was no precipitation, would be the same. Blank (sample 1) and 100 ppm SI-2 (sample 2) were mixed using the conventional method. Sulphide was in excess to both Zn and Pb and thus complete precipitation occurred in the blank solution. 100 ppm SI-2 managed to hold Zn and Pb in solution for 24 hours. Blank (sample 3) was mixed using a two step procedure. First, 100 ml H_2S brine was mixed with 50 ml Pb brine and 10 min later 50 ml Zn brine was added to the PbS solution. Like the blank (sample 1), complete Zn and Pb precipitation occurred after 24 hours. In sample 4, 100 ml H_2S brine was mixed with 50 ml Pb brine (with SI) and then 10 min later 50 ml Zn brine (without SI) was added to the solution. Both PbS and ZnS were effectively inhibited as the scale inhibitor coexisted with Pb ions and pre-existing Zn ions. In sample 5, PbS preformed in absence of scale inhibitor then Zn brine (with SI) was added to PbS solution. ZnS was effectively inhibited despite the presence of uninhibited PbS in solution.

Table 7.2 PbS and ZnS inhibition in 3.5 wt% NaCl at 50 °C and final pH 6 in presence of 100 ppm H_2S, 50 ppm Zn and Pb

#	Solution	Zn (ppm) 24 h	Pb (ppm) 24 h	Description
1	Blank	0.4	0.4	100 ml H_2S brine was mixed with 100 ml Zn/Pb brine
2	100 ppm SI-2	48.6	49.1	
3	Blank	0.6	0	100 ml H_2S brine was mixed with 50 ml Pb brine. 10 min later 50 ml Zn brine was added to the solution.
4	100 ppm SI-2	46.4	43.1	100 ml H_2S brine was mixed with 50 ml Pb brine (with SI). 10 min later 50 ml Zn brine (without SI) was added to the solution.
5	100 ppm SI-2	45.5	3	100 ml H_2S brine was mixed with 50 ml Pb brine (without SI). 10 min later 50 ml Zn brine (with SI) was added to the solution.

In previous work, the interaction between Fe, Zn and Pb with and without scale inhibitors (high molecular weight sulphonated co-polymer) was investigated (Chapters 4-7). The inhibition efficiency for ZnS and PbS using SI-1 (PPCA) and the scale inhibitor consumption are discussed in this section. In the first set of experiments, Zn with and without Pb was mixed with ~ 22 ppm H_2S. Note that no pH adjustment was carried out in these experiments. PPCA, Zn and Pb concentrations were measured in the supernatant solutions of blank, 100 ppm SI-1 and SI-8 after 2 and 24 hours. The final pH and the concentrations of PPCA, Zn and Pb are shown in Table 7.3 and Figure 7.6. In the blank solution, the Zn levels dropped from 97 ppm to 56 ppm in the absence of Pb as shown in Figure 7.6. When 25 ppm and 50 ppm Pb were added to Zn before mixing with sulphide solutions, a smaller mass of ZnS precipitated as sulphide preferentially reacted with Pb and then Zn reacted with the remaining sulphide. Also, note that in the presence of the initial 50 ppm Pb, the supernatant solutions contained 74 ppm Zn and were completely stripped of Pb regardless of the reaction mechanism confirming that complete cations exchange has occurred.

In presence of 100 ppm SI-1, the final pH ranged between 4.11 and 4.6. As shown in Figure 7.7, Zn concentrations in the supernatant solutions were comparable to the initial Zn concentration *i.e.* 97 ppm; however, 17 ppm Zn was removed after filtration with a 0.2 μm filter. In comparison to the blank solution, 41 ppm Zn precipitated but note the difference in the final pH and therefore the decrease in the amount of ZnS could be

attributed to the increase in ZnS solubility, H_2S evolution and/or the scale inhibitor effect on particle size and this will be further discussed below.

100 ppm SI-1 was able to prevent the deposition of ZnS and PbS in 25 ppm Pb solution but there was a slight decrease in the inhibition efficiency for both ZnS and PbS at higher Pb concentration *i.e.* 50 ppm. It is interesting to note the adverse impact of the formation mechanism on the inhibition efficiency. Neither ZnS nor PbS deposition was prevented, as the Zn and Pb levels detected in SI-1 solutions were equivalent to the corresponding blank solutions. It is clear from Figure **7.8** that the scale inhibitor concentration decreased as a result of ZnS and PbS deposition. Also, filtering the inhibited solution caused the scale inhibitor concentration to decrease. 100 ppm SI-8, on the other hand, prevented the deposition of ZnS and furthermore PbS was inhibited when it formed by direct reaction between sulphide and Pb and extracting sulphide from ZnS (Figure 7.9).

Table 7.3 pH measurements of the supernatant solutions after 24 h

	Blank	**100 ppm SI-1**	**100 ppm SI-8**
0 ppm Pb	5.26	4.11	4.1
25 ppm Pb	6.23	4.39	4.62
50 ppm Pb	6.6	4.58	4.96
50* Pb	6.56	4.56	5
50* Pb	6.61	4.57	5.03

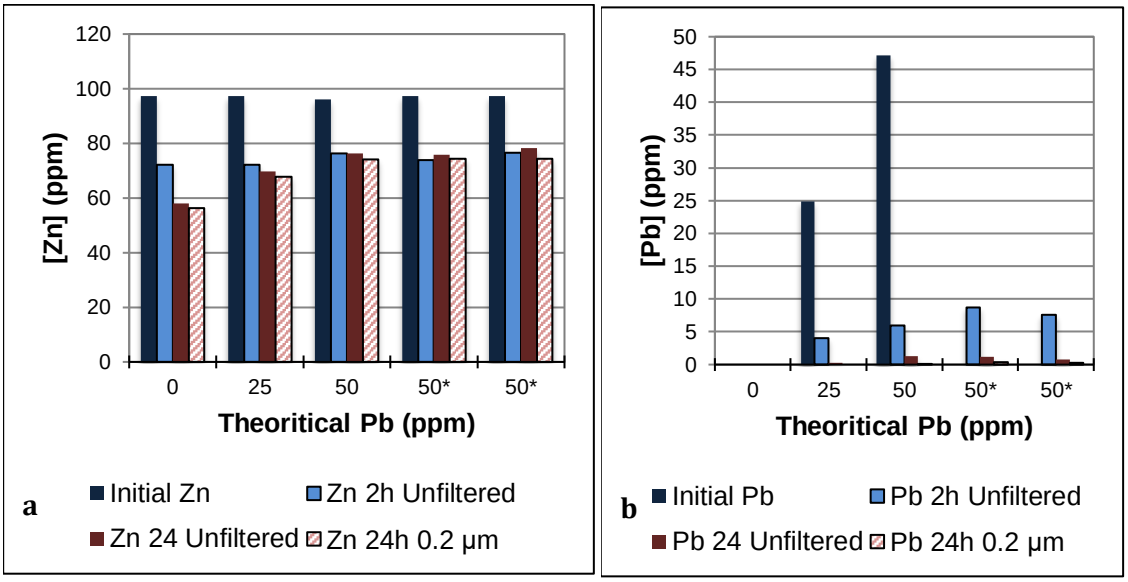

Figure 7.6 Zn and Pb concentrations in the ZnS and PbS supernatant solutions at 50°C in 3.5 wt% NaCl. H_2S is 22 ppm after mixing (based on Na_2S addition). 50*: Pb was added after ZnS had formed *i.e.* PbS formed by cation displacement.

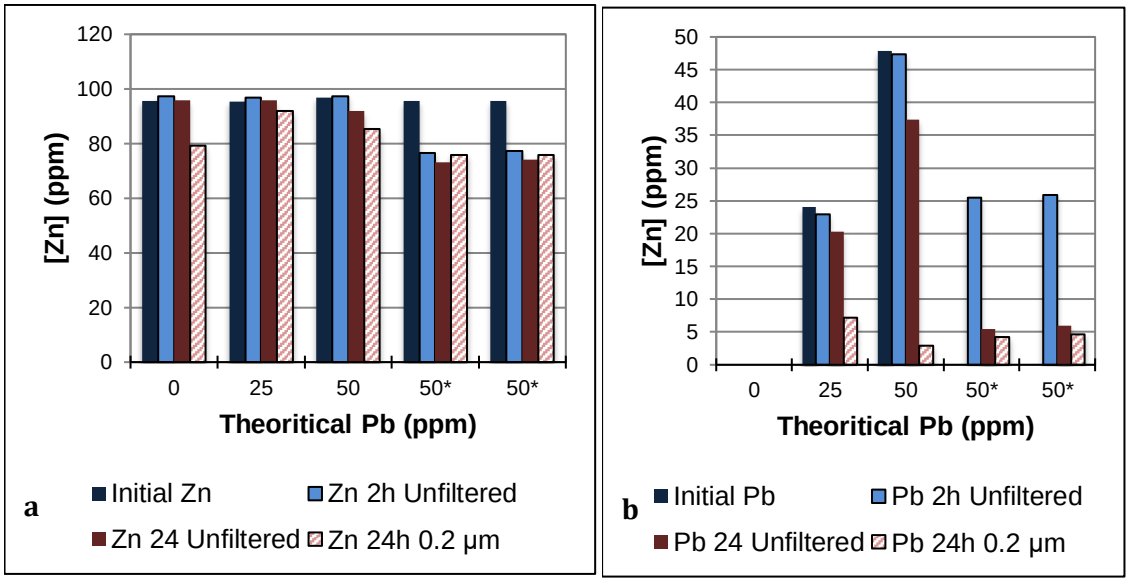

Figure 7.7 Zn and Pb concentrations in the ZnS and PbS supernatant solutions at 50°C in 3.5 wt% NaCl in presence of 100 ppm SI-1 (PPCA). H_2S is 22 ppm after mixing (based on Na_2S addition). 50*: Pb was added after ZnS had formed *i.e.* PbS formed by cation displacement.

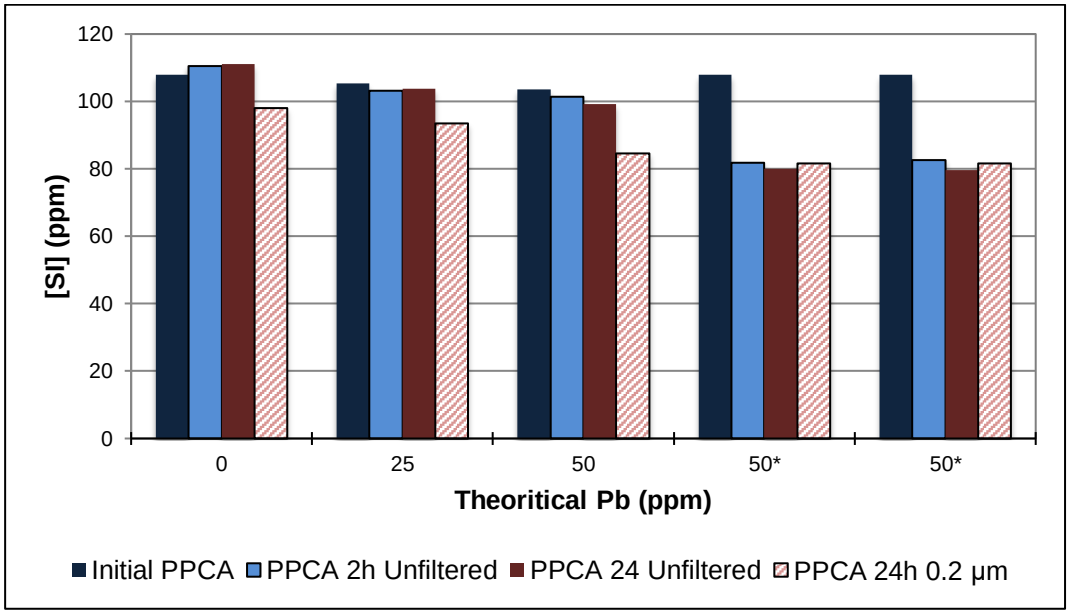

Figure 7.8 PPCA concentrations in the ZnS and PbS supernatant solutions at 50°C in 3.5 wt% NaCl in presence of 100 ppm SI-1 (PPCA). H_2S is 22 ppm after mixing (based on Na_2S addition). 50*: Pb was added after ZnS had formed *i.e.* PbS formed by cation displacement.

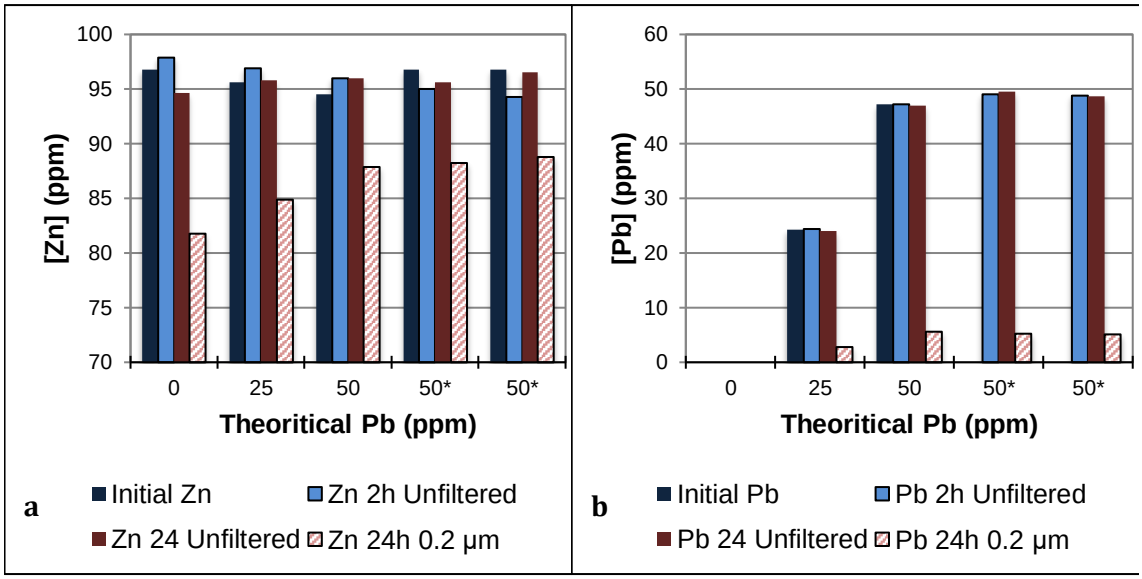

Figure 7.9 Zn and Pb concentrations in the ZnS and PbS supernatant solutions at 50°C in 3.5 wt% NaCl in presence of 100 ppm SI-8. H_2S was 22 ppm after mixing (based on Na_2S addition). 50*: Pb was added after ZnS had formed i.e. PbS formed via cation displacement.

7.3 Cation displacement in the presence of scale inhibitor (Fe, Zn, Pb and sulphide)

The interaction between Fe, Zn and Pb in sulphide solutions was investigated by the addition of Zn or Pb to preformed FeS containing samples. Figure 7.10 a) shows the Fe concentration in two blank solutions and in a 100 ppm SI-2 solution after 2 hours from mixing 100 ppm Fe with ~36 ppm H_2S *i.e.* sulphide is the limiting reactant; the Fe concentration would be 50 ppm if there was no FeS deposition. Figure 7.10 a) shows

that FeS precipitated in the blank and inhibited solutions but that the majority of the FeS particles in the 100 ppm SI-2 case were less than 0.45 μm in diameter *i.e.* the concentration was relatively unaffected by filtration.

Following the FeS formation (with and without inhibitor), different Zn solutions were added to the FeS solutions. Note that, there are three cases in this set of experiments in terms of scale inhibitor addition while Fe and Zn concentrations would be nearly 25 and 50 ppm, respectively, if there was no Fe and Zn precipitation. First, Zn solution (without scale inhibitor) was added to FeS solution (without scale inhibitor). Second, Zn solution (with scale inhibitor) was added to FeS solution (without scale inhibitor). In the third solution, Zn solution (without scale inhibitor) was added to FeS solution containing scale inhibitor. A 100 ml Zn solution was mixed with 90 ml FeS solution, thus the total Fe concentration would decrease from 50 ppm to 24 ppm due to dilution. 100 ppm Zn (without scale inhibitor) was added to Blank-1, which caused the complete exchange of FeS to ZnS with the associated liberation of Fe^{2+} into solution (Figure 7.10 b). A 100 ppm Zn and 200 ppm SI-2 solution was added to Blank-2, which caused FeS to completely redissolve while ZnS deposited as the preformed FeS was not inhibited. 100 ppm Zn was added to inhibited FeS solution 100 ppm SI (Figure 7.10(a)) and 50 ppm SI (Figure 7.10 (b)). When Zn solution was mixed with inhibited FeS solution, the FeS was completely redissolved and ZnS remained suspended in the solution indicated by the comparable Zn concentration in the stock solution and after 24 hours.

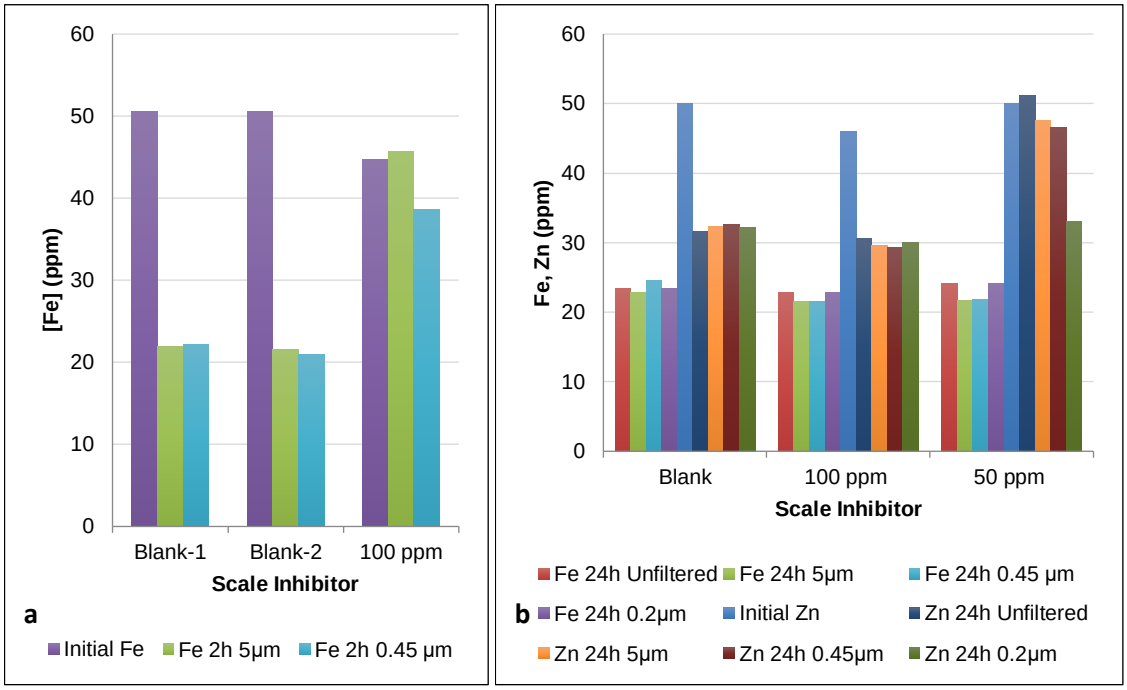

Figure 7.10 Zn interaction with FeS under anaerobic conditions at 23°C. 50 ml Fe solution was mixed with 50 ml H_2S solution (a), then 100 ml Zn solution was added to the FeS solution (b).

Similar behaviour was observed when Pb solutions were mixed with preformed FeS solutions, see Figure 7.11 a) and b). Therefore, PbS and ZnS can be prevented even when formed by cation displacement (equations 7 and 8), provided that the scale inhibitor is added to the initial Fe solution *i.e.* preformed FeS is inhibited/dispersed.

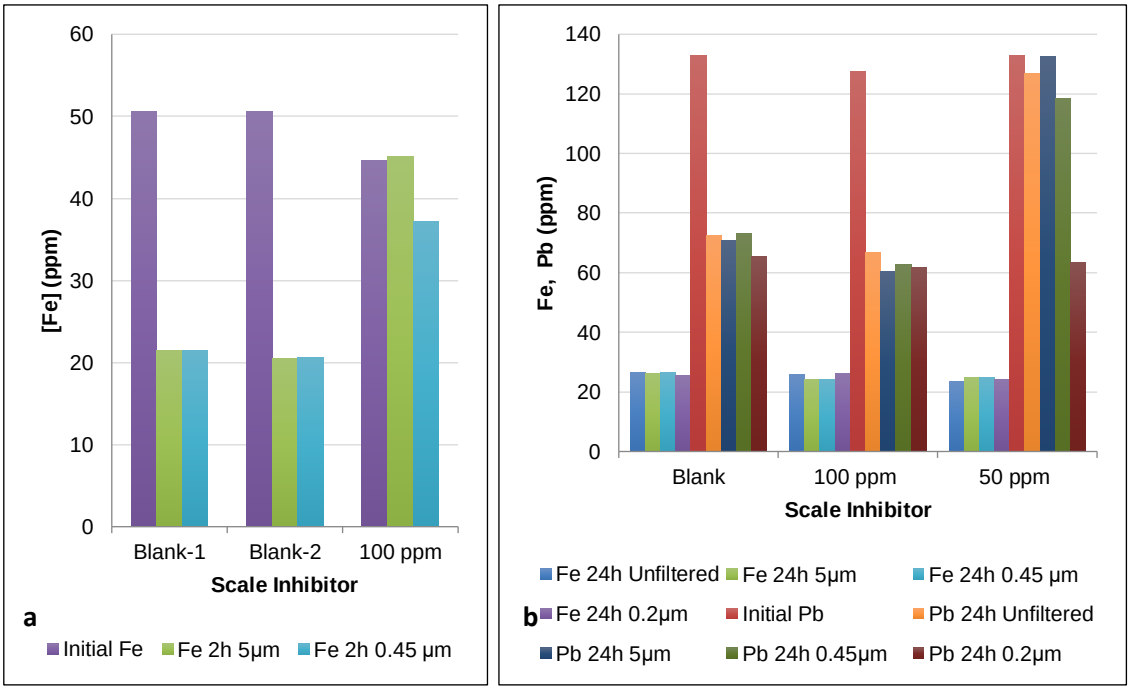

Figure 7.11 Pb interaction with FeS under anaerobic conditions at 23°C. 50 ml Fe solution was mixed with 50 ml H_2S solution (left), then 100 ml Pb solution was added to the FeS solution (right).

7.4 Fe, Zn and Pb interactions in sulphide solutions in the presence of SI

In addition to cation displacement reactions, the interaction between Fe, Zn and Pb in sulphide solutions was investigated by using another method where (1) Zn and Pb were added together to the sulphide solution containing the desired concentration of scale inhibitor, and then (2) Pb then Zn were added to the scale inhibitor containing sulphide solution. The resultant Zn and Pb concentrations would be the same regardless of the mixing method, as shown in Figure 7.12. In these experiments, the sulphide solutions were mixed with low pH solutions in order to reduce the final pH before adding the scaling cations, *i.e.* Zn and Pb. At low pH values, sulphide solutions are prone to H_2S evolution (Graham *et al.*, 2017), therefore blank solutions were used to ensure that the concentration of sulphide species was in excess to Zn and Pb, and thus that complete ZnS and PbS precipitation would occur.

As expected, Zn and Pb completely precipitated in the Blank solutions, however there was a significant impact of the precise mixing method on the inhibited samples. It was found that 10 ppm SI-2 provided more than 50% inhibition efficiency using Method 1, while Method 2 yielded very little inhibition. At 15 ppm SI-2, Method 1 resulted in almost complete inhibition of both zinc and lead sulphides but for Method 2, at least 20 ppm SI- 2 scale inhibitor was required to achieve the same result.

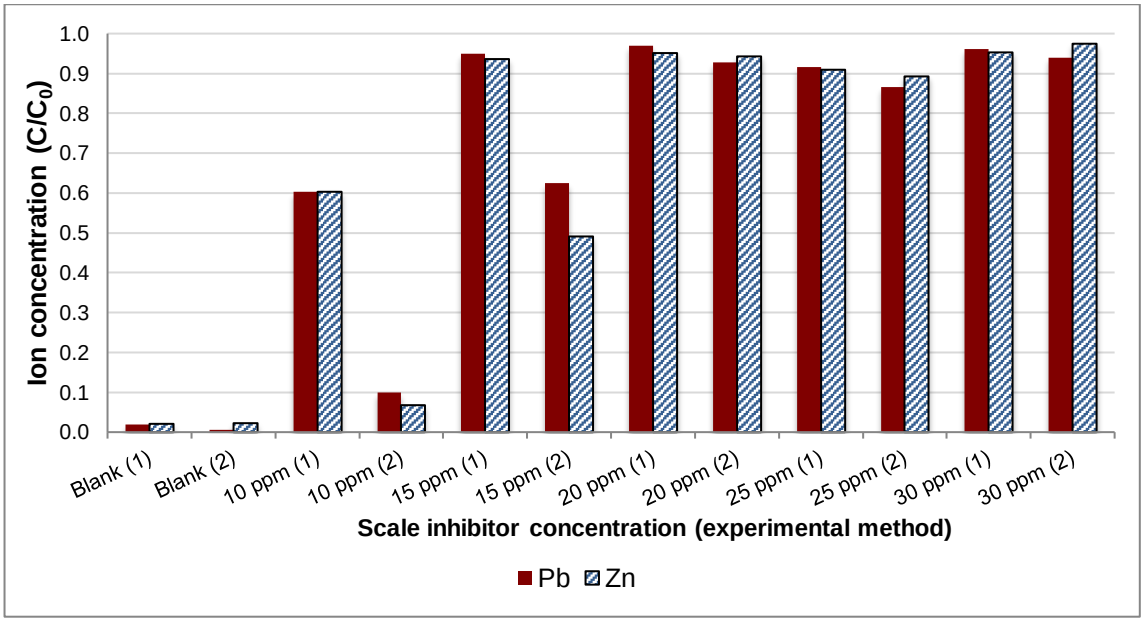

Figure 7.12 Zn and Pb interaction in sulphide solutions under aerobic conditions at 23°C using concurrent addition of Zn & Pb (Method 1) and sequential addition of Pb followed by Zn (Method 2). Initial Zn and Pb concentrations were 37 ppm and 36 ppm, respectively.

The test was repeated under the same conditions with the initial Pb concentration halved to 18 ppm. A similar trend was observed (Figure 7.13), i.e. the MIC for ZnS and PbS when Zn and Pb were concurrently mixed with sulphide, was less than when zinc was added to a mixture of pre-mixed lead, sulphide and inhibitor. The difference in the MIC might be attributable to the consumption of scale inhibitor during the inhibition of PbS, which would result in insufficient scale inhibitor remaining in solution to inhibit ZnS. In the future, this will be confirmed by measuring the scale inhibitor concentration at different times before and after the addition of PbS and ZnS to assay the amount consumed in the process.

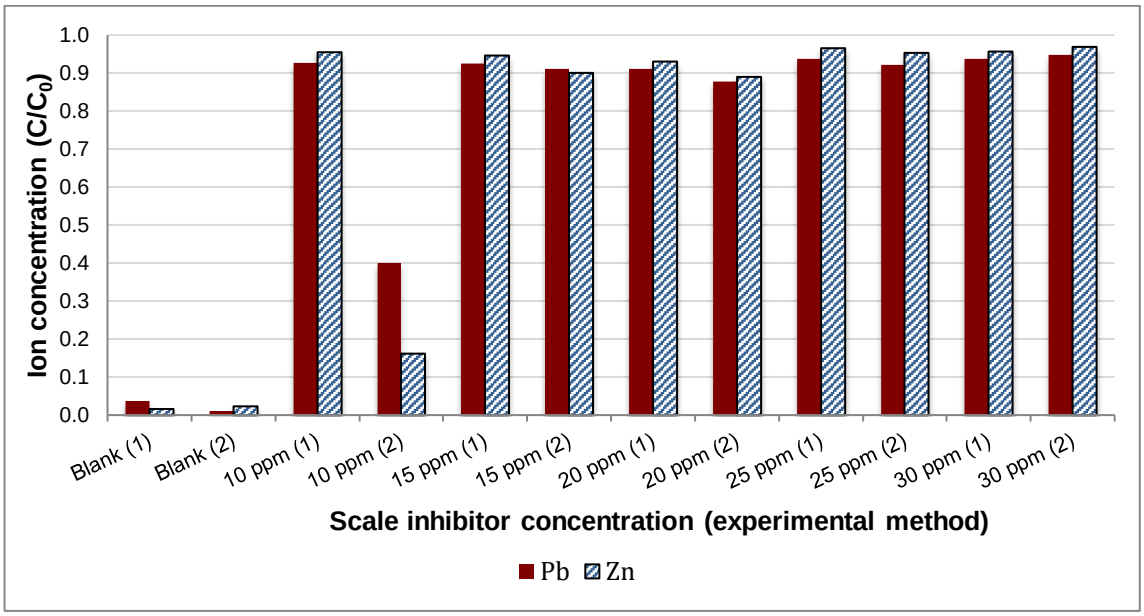

Figure 7.13 Zn and Pb interaction in sulphide solutions under aerobic conditions at 23°C using concurrent addition of Zn & Pb (Method 1) and sequential addition of Pb followed by Zn (Method 2). Initial Zn and Pb concentrations were 36 ppm and 18 ppm, respectively.

Figure 7.14 shows the Fe, Zn and Pb concentrations in the supernatant solutions after 24 hours when three mixing orders were used, as follows: (1) Fe, Zn and Pb were mixed concurrently with sulphide, (2) Zn/Pb were mixed with sulphide followed by the addition of Fe, (3) Fe was mixed with the sulphide solution, followed by the addition of a Zn/Pb mixture. For the Blank solution, Zn and Pb completely deposited, while a small amount of Fe remained in solution, due to the low solution pH. A concentration of 20 ppm SI-2 was sufficient to prevent the deposition of all sulphide scales, regardless of the mixing order. There were slight differences in the results between Methods 1 and 2 (mixing of Fe/Zn/Pb and addition of Zn/Pb to mixed Fe, scale inhibitor and sulphide solution). When ZnS and PbS were allowed to form before FeS, it was easier to inhibit all sulphide scales.

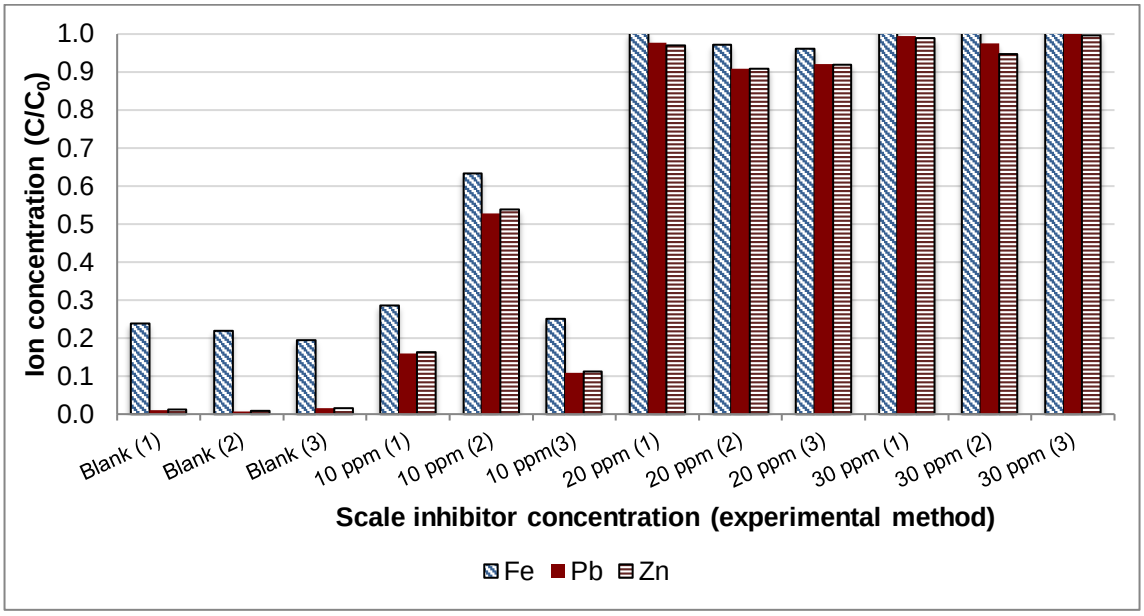

Figure 7.14 Fe, Zn and Pb interaction in sulphide solutions under anaerobic conditions at 23 °C using three mixing methods. Concurrent addition of Fe, Zn & Pb (Method 1), sequential addition of Pb/Zn mixture followed by Fe (Method 2) and sequential addition of Fe followed by Pb/Zn mixture (Method 3). Initial Fe, Zn and Pb concentrations were 36 ppm, 18 ppm and 17 ppm respectively.

50 ppm SI-1 was used to inhibit PbS and ZnS using the two mixing methods described above. In this test, 60 ppm H_2S was mixed with low pH 3.5 wt% NaCl in order to reduce the pH to a certain level prior to the addition of Pb and Zn solutions. After mixing, the H_2S concentration was 30 ppm (assuming there is no H_2S evolution) and pH was 7.98. In method 1, 0.4 ml of (500 ppm Pb and 500 ppm) was added to 10 ml of the low pH H_2S solution while in method 2, 0.2 ml of (1000 ppm Pb) was added to 10 ml of the low pH H_2S solution followed by addition of 0.2 ml (1000 ppm Zn). In both methods, the Pb and Zn concentrations would be the same if there were no PbS and ZnS precipitation, as shown in Figure 7.15 to Figure 7.17. After 24 hours, 50 ppm SI-1 was able to prevent the deposition of ZnS and indiscernible decrease in Pb concentration occurred. In contrast in method 2, the deposition of PbS was discernible as the Pb concentration decline from 19 ppm to 12 ppm. The particle size of inhibited ZnS and PbS was less 5 µm indicated by the comparable Zn and Pb concentrations in the filtered and unfiltered samples. However, after filtration with 0.2 µm filter significant reductions in the Zn and Pb concentrations were observed. Figure 7.16 shows the Pb and Zn concentrations in 100 ppm SI-1 solution at pH of 5.36 and 5.4 using method 1 and method 2, respectively. The inhibition efficiency of 100 ppm SI-1 for PbS and ZnS was high; however, in method 2 solution, Pb concentration decreased from 19 ppm to 15.5 ppm. Furthermore, after filtration with a 5 µm filter, there was no decrease in Zn and Pb concentration whereas both Zn and Pb concentrations were reduced in the 5 µm

filtered samples. In the 0.2 μm filtered samples, there was a slight reduction in Zn and Pb concentrations in method 1 solution while the method 2 solution were stripped of Pb. The test was repeated in 100 ppm SI-1 at pH values of 6.49 and 6.32 in method 1 and method 2, respectively. The overall trend was similar but at higher pH values there was further reduction in Zn and Pb concentrations in the 0.2 μm filtered samples. For example, the Zn concentration decreased from 16 ppm to 12.5 ppm, the Pb concentration decreased from 11 ppm to 9 ppm. It is known from the interaction and cation displacement experiments there would be no ZnS precipitation if there is dissolved Pb in the solution. It is interesting to note that there was a reduction in Zn concentration in both methods indicating that Pb was completely consumed. Despite PbS precipitation, there was a significant difference in Pb concentration particularly in the filtered samples.

Therefore, it is evident from these results the sequence of sulphide scale precipitation can have a significant impact on the inhibition efficiency using both the conventional scale inhibitor as well as the proprietary inhibitors. The tested scale inhibitors performed better when PbS and ZnS formed concurrently *i.e.* method 1 compared to method 2 where PbS formed prior to ZnS formation. Therefore, in the oilfield system, the minimum inhibitor concentration might be underestimated because it is common practice to evaluate the scale inhibitor performance using method 1. The increase of minimum inhibitor concentration in method 2 compared to method 1 can be attributed to the scale inhibitor consumption to inhibit the PbS before ZnS forms. Another explanation might be the preformed PbS particles act as a site and thus ZnS particles form on the PbS which lead to further growth and hence deposit of both PbS and ZnS. The subsequent scale formation might occur in the oilfield systems as a result of the gradual decrease in temperature and increase in pH as a consequence of CO_2 libration. As shown in Figure 7.18, PbS scale forms at lower pH values compared to ZnS and FeS and as the pH increases ZnS then FeS would form (Lewis 2010).

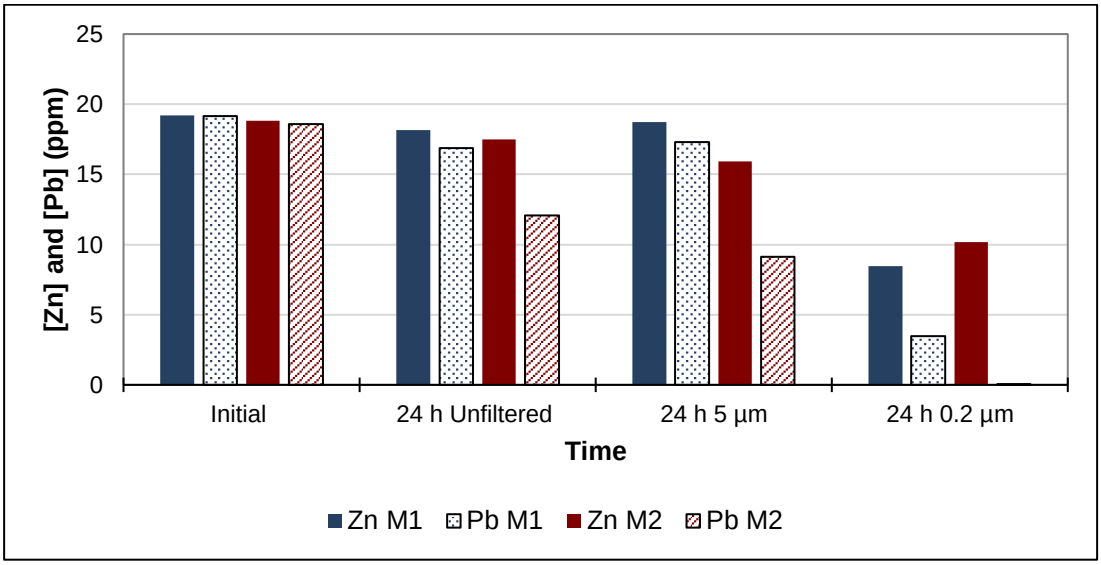

Figure 7.15 Zn and Pb interaction in sulphide solutions under aerobic conditions at 23°C using concurrent addition of Zn & Pb (Method 1) and sequential addition of Pb followed by Zn (Method 2). H_2S concentration was 30 ppm and SI-1 concentration was 50 ppm. pH of mixed H_2S-low pH brine was 7.98. pH of PbS/ZnS solutions (method 1&2) was 5.9 and 5.68, respectively.

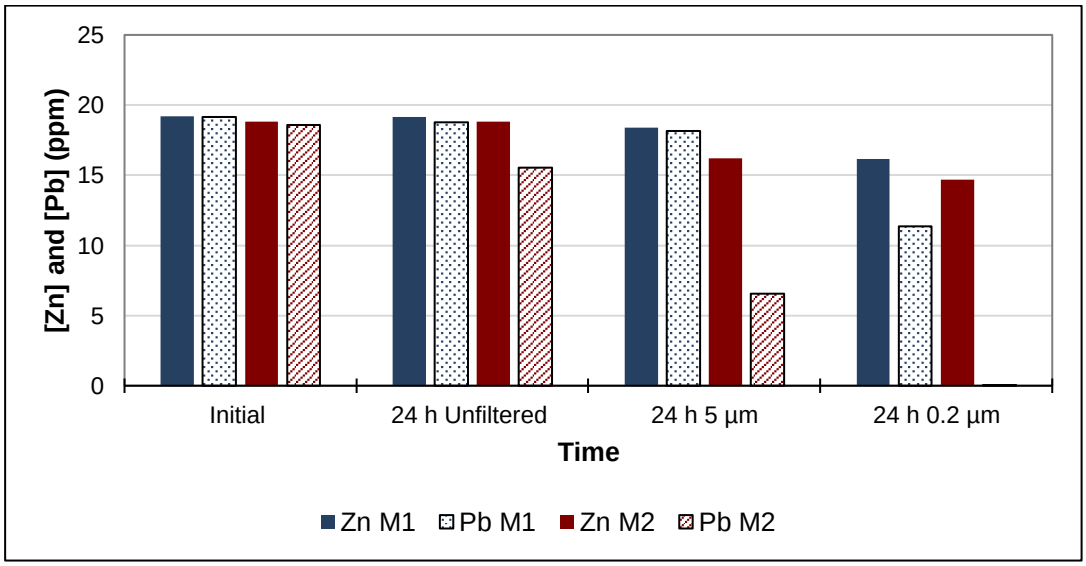

Figure 7.16 Zn and Pb interaction in sulphide solutions under aerobic conditions at 23°C using concurrent addition of Zn & Pb (Method 1) and sequential addition of Pb followed by Zn (Method 2). H_2S concentration was 30 ppm and SI-1 concentration was 100 ppm. pH of mixed H_2S-low pH brine was 7.31. pH of PbS/ZnS solutions (method 1&2) was 5.36 and 5.4, respectively.

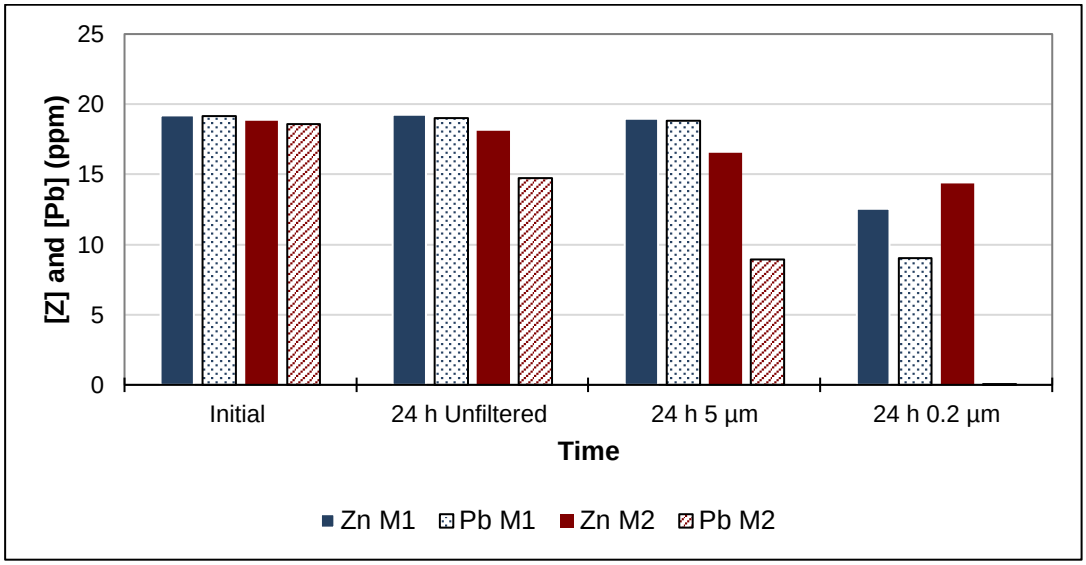

Figure 7.17 Zn and Pb interaction in sulphide solutions under aerobic conditions at 23°C using concurrent addition of Zn & Pb (Method 1) and sequential addition of Pb followed by Zn (Method 2). H_2S concentration was 30 ppm and SI-1 concentration was 100 ppm. pH of mixed H_2S-low pH brine was 9.31. pH of PbS/ZnS solutions (method 1&2) was 6.49 and 6.32, respectively.

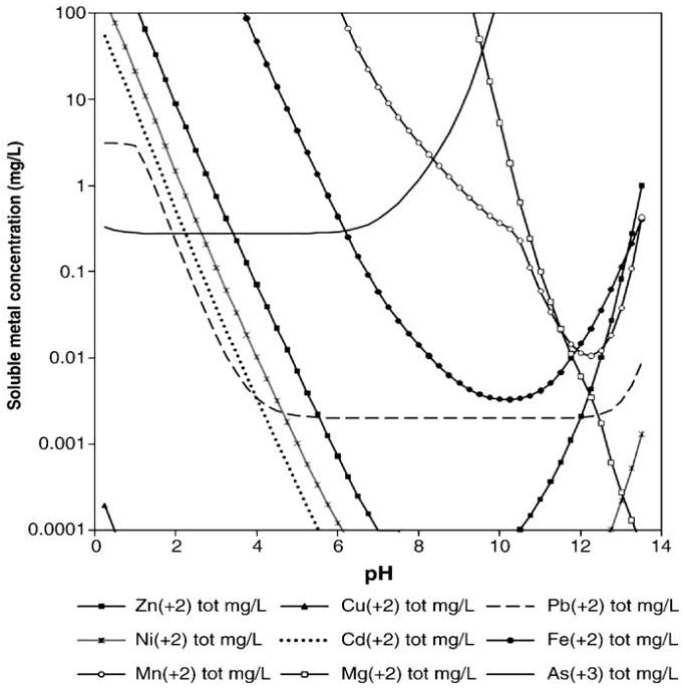

Figure 7.18 Solubilities of sulphide scales at different pH values (after Lewis 2010)

7.5 Conclusions

In this work, FeS, ZnS and PbS formation and inhibition tests were performed over a wide range of parameters. For the cation displacement experiments, the least soluble sulphide scale e.g. ZnS was allowed to form then Pb acetate was added to the pre-formed ZnS. In some experiments, scale inhibitors were added to the Zn solutions hence ZnS was inhibited, while in other sets of experiments the scale inhibitor was added to the Pb solution rather than the Zn solution. Similar experiments were performed for FeS/ZnS and FeS/PbS solutions. Another type of experiments was conducted in addition to investigate the impact of the ***sequence*** of scale formation on the inhibition efficiency. In these experiments, PbS was allowed to form first in the presence of scale inhibitor, then Zn solution was mixed with pre-formed PbS to precipitate ZnS as the H_2S was in excess to both Pb and Zn. Also, PbS/ZnS/FeS system was investigated using the same procedure. The main conclusions from this study are as follows:

Sulphide inhibitors SI-2 and SI-3 were remarkably effective against ZnS and PbS provided that the scale inhibitors are added to Zn and Pb containing brines prior to mixing with sulphide containing brine. On the other hand, when ZnS and PbS were allowed to form prior to scale inhibitors addition, they did ”reverse” the scale deposition. Furthermore, when ZnS had formed, then lead acetate/scale inhibitor solution was added to the preformed ZnS, neither SI-2 nor SI-3 were able to prevent PbS deposition by ionic displacement of Zn from ZnS by Pb^{2+} despite the fact that both scale inhibitors were effective against PbS under the same conditions using the conventional scale inhibition experiments.

100 ppm of SI-1 prevented the deposition of ZnS and ZnS alongside PbS. Unlike the 100 ppm SI-1 case, 100 ppm SI-8 prevented the deposition of ZnS and PbS regardless of the PbS formation mechanism.

In SI-2 solutions, the MIC for ZnS and PbS when Zn and Pb were concurrently mixed with sulphide, was less than when zinc was added to a mixture of pre-mixed lead, sulphide and inhibitor. The increase in the MIC for subsequent scale formation might be caused by scale inhibitor consumption in PbS system prior to ZnS formation.

In SI-1 solutions, it was easier to inhibit PbS and ZnS when they formed concurrently rather than forming PbS followed by ZnS. These results are in line with the difference in the MIC observed in SI-2 solutions.

Chapter 8

Scale Inhibitor Consumption in Sulphide Scale Formation

8.1 Introduction

Previously, various workers have examined the fate of the scale inhibitor (SI) during the scale inhibition process; this examines if the SI remains at its original dosage in solution or if it declines; i.e. the SI is "consumed" in the scale crystal lattice. An extensive survey of SI consumption in the inhibition of barite scale was published by Shaw and Sorbie (2013), however, to date no such results have been presented for sulphide scales. This chapter discusses inhibition of FeS and ZnS and for the first time presents results on scale inhibitor consumption in ***sulphide*** scale solutions.

It is shown that 100 ppm SI-1 prevented the deposition of ZnS in 3.5 wt% NaCl. Furthermore, increasing the pH of SI/ZnS solutions caused the particle size of ZnS to drop below 0.2 μm. In ZnS systems, there was a significant drop in the SI concentrations regardless whether ZnS was inhibited or not. Additionally, the addition of the scale inhibitor to preformed ZnS caused the scale inhibitor to precipitate. On the other hand, up to 100 ppm SI-1 did not prevent the deposition of FeS even when it was tested at comparable conditions to ZnS experiments; moreover, there was no decrease in the scale inhibitor concentration and hence no scale inhibitor consumption in the FeS solutions. In mixed FeS/ZnS systems, FeS had a negative impact on ZnS inhibition as ZnS partially deposited but there was a delay in the deposition of FeS. The explanation of this behaviour might be that the inhibited ZnS particles, which are sub-micron-sized, act as sites for FeS to deposit on but the accumulation of FeS led eventually to the deposition of both FeS and ZnS.

8.2 ZnS inhibition using SI-1 and SI-2 in 3.5 wt% NaCl

Figure 8.1 and Figure 8.2 show the Zn and SI concentrations (of SI-1 = PPCA and SI-4 = DETPMP) in the supernatant solutions after 24 hours in the presence of different sulphide concentrations. In these experiments, the initial Zn was kept constant at 50 ppm, while the sulphide concentration varied in order to test the inhibitors at different scaling tendency (saturation ratio, SR) levels. 10 and 100 ppm SI-1 prevented the ZnS deposition when 5 ppm H_2S was mixed with 50 ppm Zn. In these solutions, the scale inhibitor concentrations in the supernatant solutions were equal to the initial SI concentrations. As a consequence of increasing the sulphide concentration, and hence the amount of potential ZnS, the performance of 10 ppm SI-1 was impaired as the Zn concentration dropped from 50 ppm to 30 ppm. Furthermore, the scale inhibitor was

completely consumed, as indicated by the absence of SI in the supernatant solutions (Figure 8.2). 100 ppm SI-1 prevented the ZnS deposition at all tested sulphide concentrations and the SI was retained in the solution at its initial concentration level.

Up to 100 ppm SI-4 (DETPMP) had no effect on the ZnS scale, moreover, there was a discernible decline in the SI concentration (Figure 8.2). The 10 ppm SI-4 solutions were completely stripped of SI when ZnS precipitated. Another important observation is that the Zn concentration in the 100 ppm SI-4 solutions were less than that in the blank solutions suggesting that either (a) there is incompatibility between Zn and SI-4, or (b) that when the ZnS forms that some of the (relatively ineffective) SI-4 is consumed in the ZnS lattice. When the H_2S concentration was increased to 20 ppm, hence increasing the potential ZnS precipitate, the Zn concentration in the SI-4 and blank solutions were comparable. In addition, the scale inhibitor concentration in this solution was higher than that in the 5 and 10 ppm H_2S solutions. Therefore, the decrease in the scale inhibitor concentration could be attributed to precipitation of ZnS and incompatibility with the higher dissolved Zn concentrations.

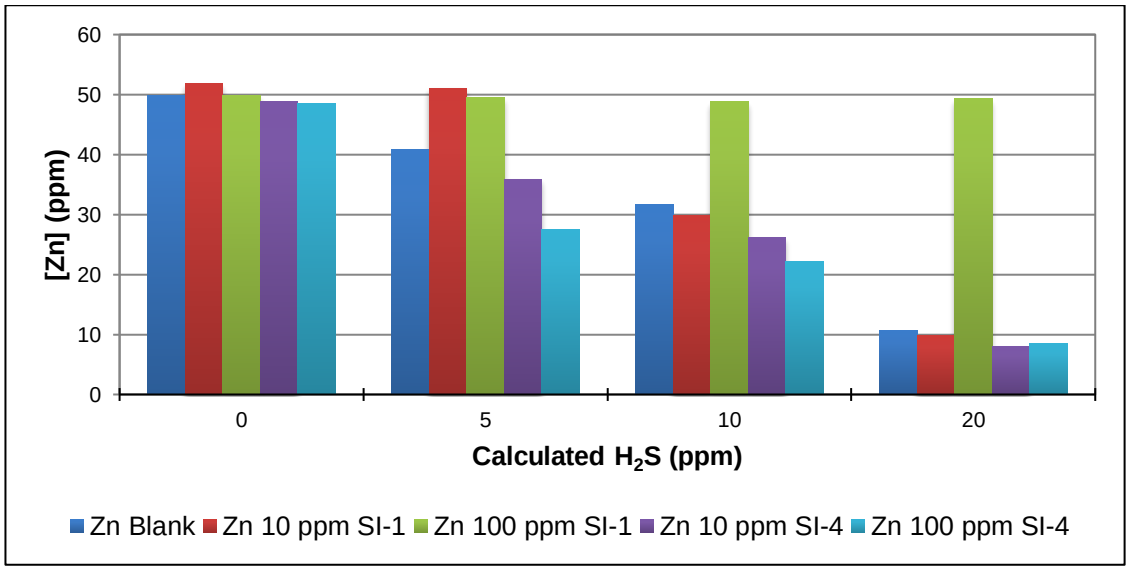

Figure 8.1 Zn concentrations in the ZnS supernatant solutions after 24 h without filtration at 50°C in 3.5 wt% NaCl in presence of SI-1 (PPCA) or SI-4 (DETPMP). H_2S concentrations are 5, 10 and 20 ppm after mixing (based on Na_2S addition).

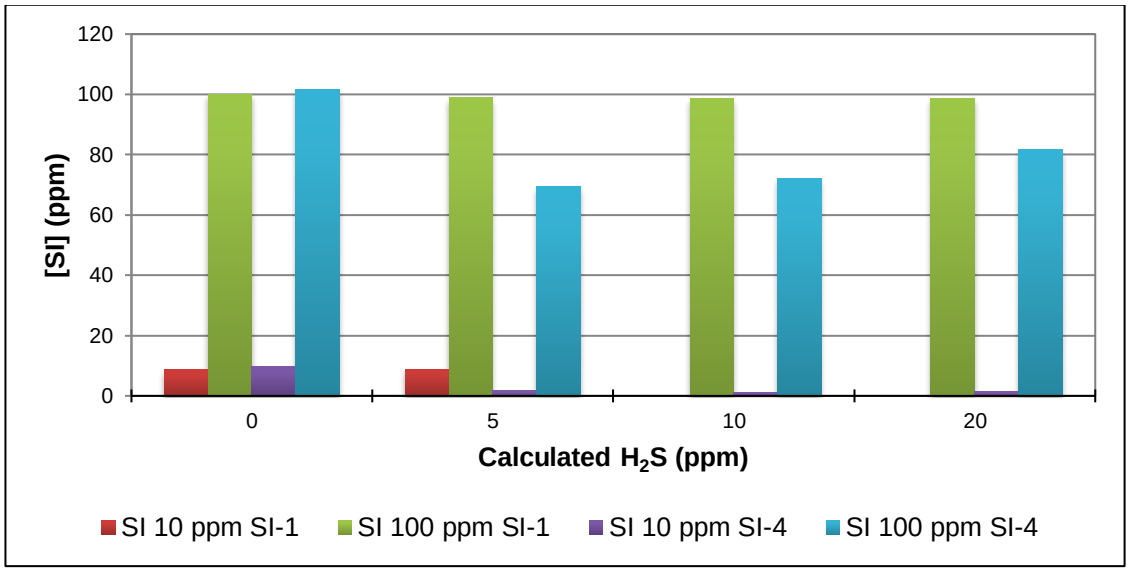

Figure 8.2 SI concentrations in the ZnS supernatant solutions after 24 h without filtration at 50°C in 3.5 wt% NaCl in presence of SI-1 (PPCA) or SI-4 (DETPMP). H_2S concentrations are 5, 10 and 20 ppm after mixing (based on Na_2S addition).

8.3 Compatibility between Zn and SI-1

The suspected compatibility between Zn and PPCA has been examined at different solution pH values and temperatures. Zn and PPCA concentrations were increased in the following set of experiments to nearly 200 ppm. The ICP results are plotted in Figure 8.3-Figure 8.5. At pH of 4.04, there was no decrease in the Zn and SI-1 concentrations at 23°C and 50°C, see Figure 8.3. Additionally, the solution was clear even when it was aged at 90°C for 24 h, (Photo 8.1). At higher pH values, the Zn and SI-1 precipitation was dependent on the temperature. For example, at 23°C there was no precipitation of Zn or SI-1; however, when the temperature was raised to 50°C, the Zn and SI-1 concentrations discernibly declined (refer to Figure 8.4). At pH 6.8, more Zn and SI-1 precipitated and furthermore increasing the temperature resulted in precipitating more Zn and SI-1 as shown in Figure 8.5.

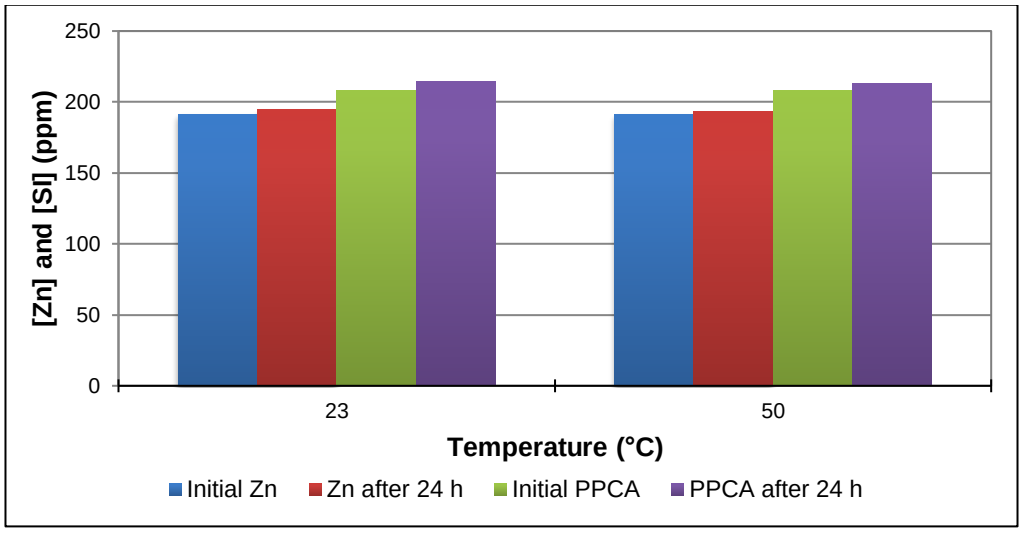

Figure 8.3 Zn and SI-1 concentrations after 24 h in 3.5 wt% NaCl without sulphide. Initial pH of Zn/SI-1 solution was 4.04.

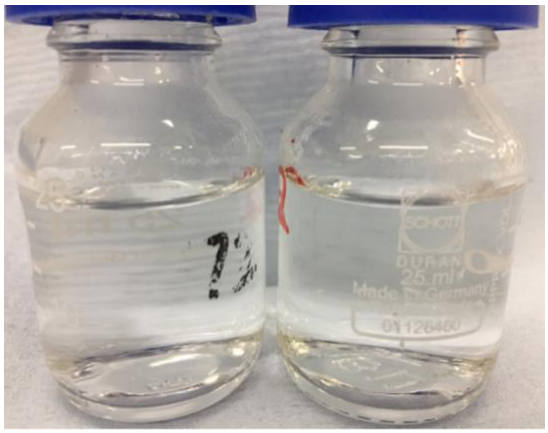

Photo 8.1 200 ppm Zn and 200 ppm SI-1 in 3.5 wt% NaCl without sulphide. Initial pH of Zn/SI-1 solution was 4.04.

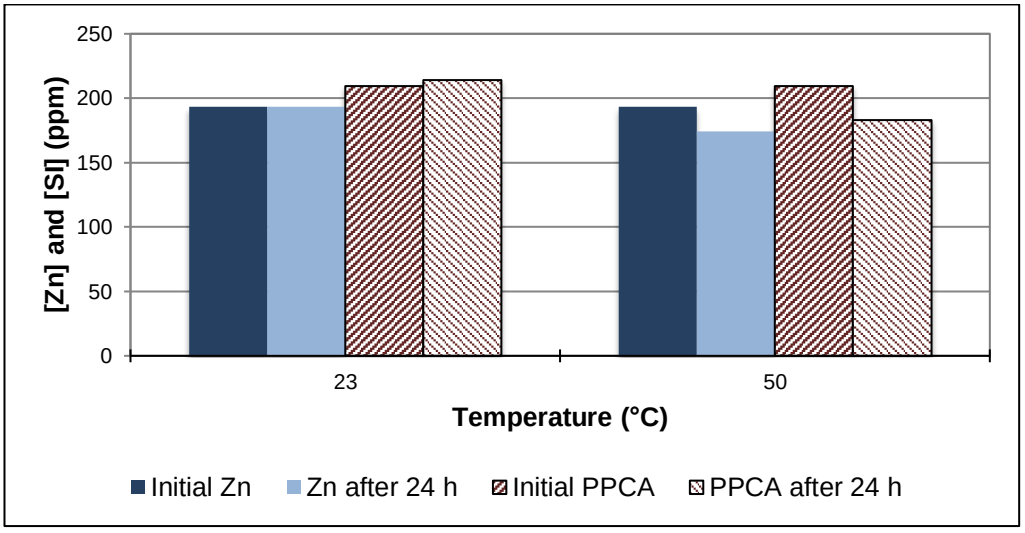

Figure 8.4 Zn and SI-1 concentrations after 24 h in 3.5 wt% NaCl without sulphide. The initial pH of Zn/SI-1 solution was 5.3.

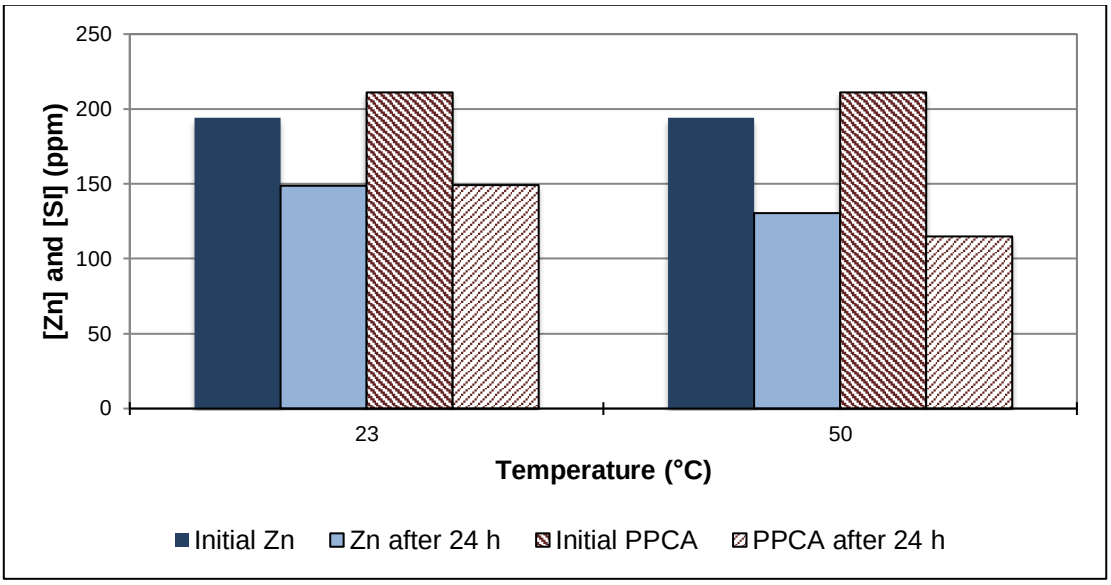

Figure 8.5 Zn and SI-1 concentrations after 24 h in 3.5 wt% NaCl without sulphide. The initial pH of Zn/SI-1 solution was 6.8.

8.4 ZnS inhibition using SI-1 at different pH values

Figure 8.6 shows the Zn concentrations in 3.5 wt% NaCl without sulphide *i.e.* initial Zn and in the ZnS supernatant solutions in the presence of 25 ppm H_2S and 100 ppm SI-1 (PPCA). The Zn solutions were pH adjusted to different values such that the final pH after mixing was pH ~ 4, 5.39 and 6.24. At pH 4, 100 ppm SI-1 managed to keep the ZnS particles suspended; however, after filtration with 0.2 μm filter, the Zn concentration decreased from 100 ppm to 77 ppm indicating that the particle size of inhibited ZnS is greater than 0.2 μm. Similar results were obtained when the test was conducted at pH 5.39. Despite SI-1 being able to delay the deposition of ZnS, significant drop in Zn concentration was observed after 24 hours as a consequence of increasing the pH to 6.24. 55 ppm Zn precipitated in this solution which is more than the expected Zn consumption due to ZnS precipitation *i.e.* 29 ppm Zn (assuming there was no decrease in sulphide concentration due to H_2S evolution). Therefore, the decrease in Zn concentration was attributed to both ZnS precipitation and incompatibility with SI-1 at high pH values. As shown in Figure 8.7, there was a decline in the SI-1 concentration in solutions with pH 4 and 5.39 and the decrease was more discernible for the pH 6.24 case. At pH 4 and 5.39, the SI-1 concentration decreased by ~14 ppm after filtration with 0.2 μm filter whereas 40 ppm SI-1 precipitated in the unfiltered and filtered samples (Figure 8.7).

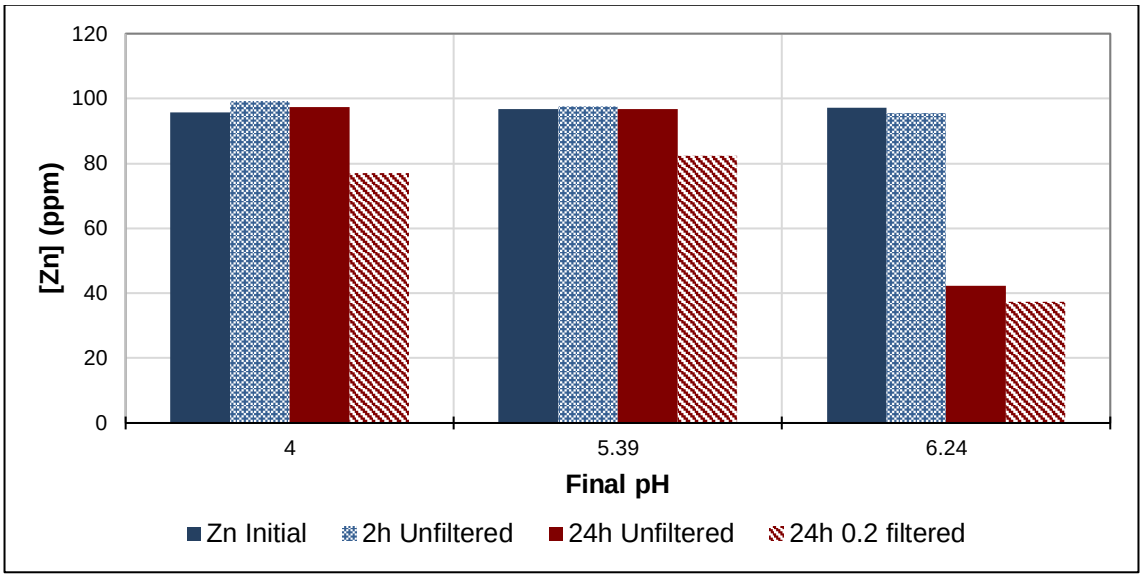

Figure 8.6 Zn concentrations in ZnS supernatant solutions at 50°C in 3.5 wt% NaCl in presence of 25 ppm H_2S.

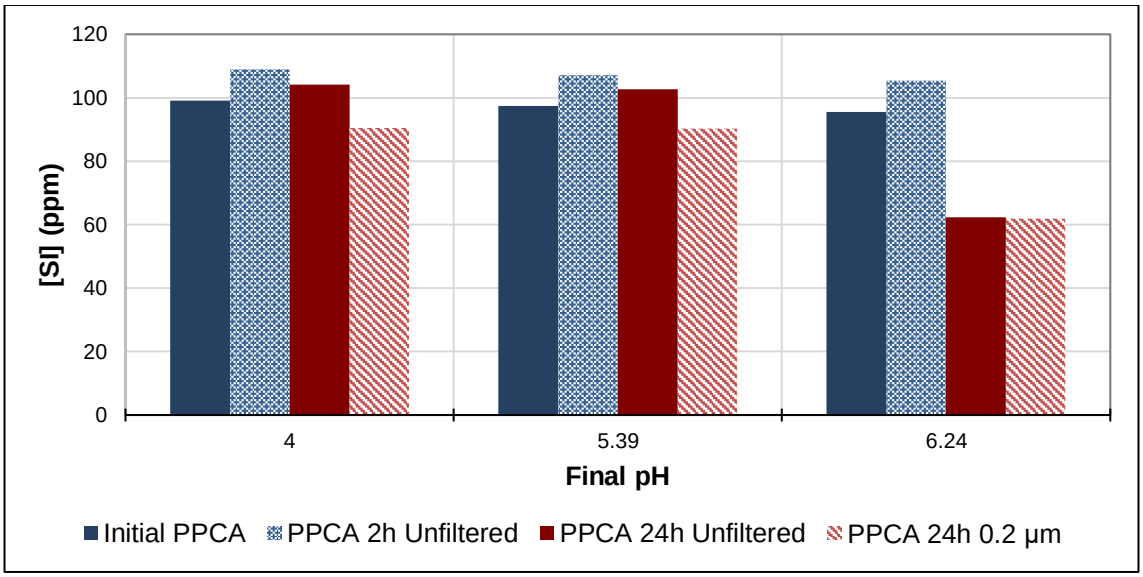

Figure 8.7 SI concentrations in ZnS supernatant solutions at 50°C in 3.5 wt% NaCl in presence of 25 ppm H_2S.

To study the impact of increasing the amount of ZnS on the performance of SI-1, the previous tests were repeated under the same conditions, except that 50 ppm H_2S was used instead of 25 ppm. The Zn and SI-1 concentrations are plotted in Figure 8.8 and Figure 8.9, respectively. In contrast to the 25 ppm H_2S experiments, SI-1 prevented the deposition of ZnS at all tested pH values. The inhibition efficiency of SI-1 in presence of 25 H_2S (pH 4.00 and 5.39) and 50 ppm H_2S (pH 4.16 and 5.9) is quite straightforward to explain in that 100 ppm was sufficient to inhibit the ZnS even in the presence of high sulphide concentration. On the other hand, at high pH values, the inhibition efficiency of SI-1 improved when the H_2S concentration was raised to 50 ppm. The increase in Zn consumption due to ZnS precipitation, hence reducing Zn-SI-1

interaction seems to be the most likely reason for the improvement in ZnS inhibition. In terms of SI consumption, comparable amounts of SI-1 were consumed at all tested pH values in presence of 50 ppm H_2S as shown in Figure 8.9.

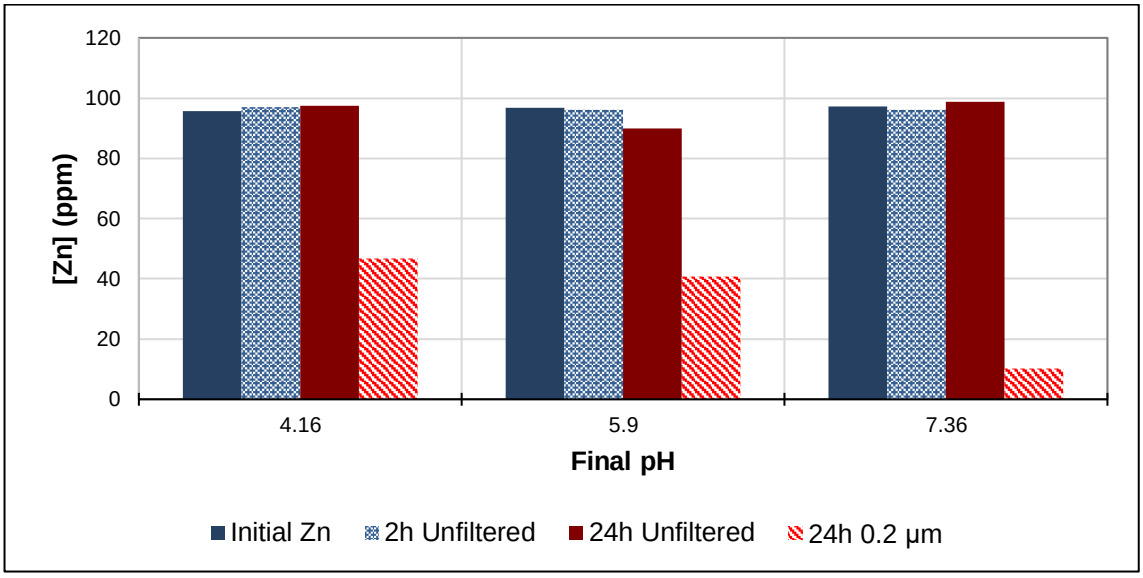

Figure 8.8 Zn concentrations in ZnS supernatant solutions at 50°C in 3.5 wt% NaCl in presence of 50 ppm H_2S.

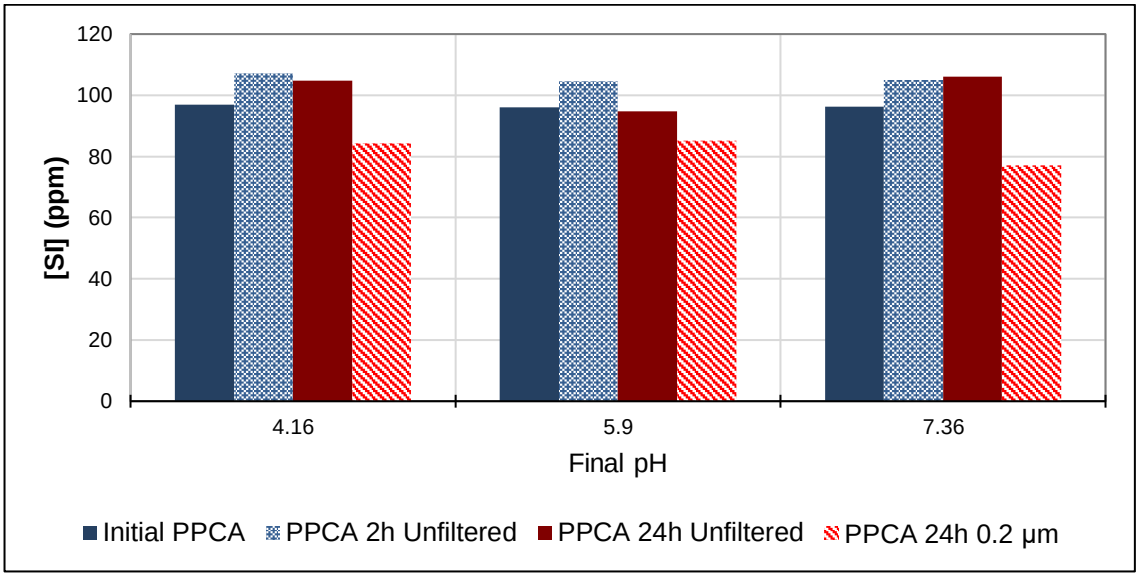

Figure 8.9 SI concentrations in ZnS supernatant solutions at 50°C in 3.5 wt% NaCl in presence of 50 ppm H_2S.

8.5 FeS inhibition using SI-1

Some scale inhibitors, such as PPCA (SI-1), showed reasonably good inhibition efficiency for ZnS but not FeS, as discussed in the previous chapters. However, the ZnS and FeS experiments were performed at different conditions including pH and temperature. So, in order to confirm the difference in the inhibition efficiency for ZnS and FeS, further tests have been conducted under the same conditions using SI-1. The

Fe and SI concentrations were measured to investigate the inhibition efficiency and the consumption of SI in FeS solutions. The results from these experiments are shown in Figure 8.10 and Figure 8.11.

It is clear from Figure 8.10 and Figure 8.11, that 100 ppm SI-1 did not inhibit the FeS deposition. Moreover, the SI concentration in the supernatant solutions with and without sulphide was comparable suggesting that there was essentially no interaction between Fe/FeS and SI-1. Note that, these experiments were conducted in 3.5 wt% sodium chloride solutions and therefore the interaction would be only between the scale inhibitors and scaling metals *i.e.* iron and zinc. In the presence of divalent cations such as calcium, Ca-SI and Mg-SI complexes and precipitation would occur depending on several factors such as the scale inhibitor type and concentration and pH (Jarrahian et al., 2019; Boak et al., 1999; Graham et al., 1997).

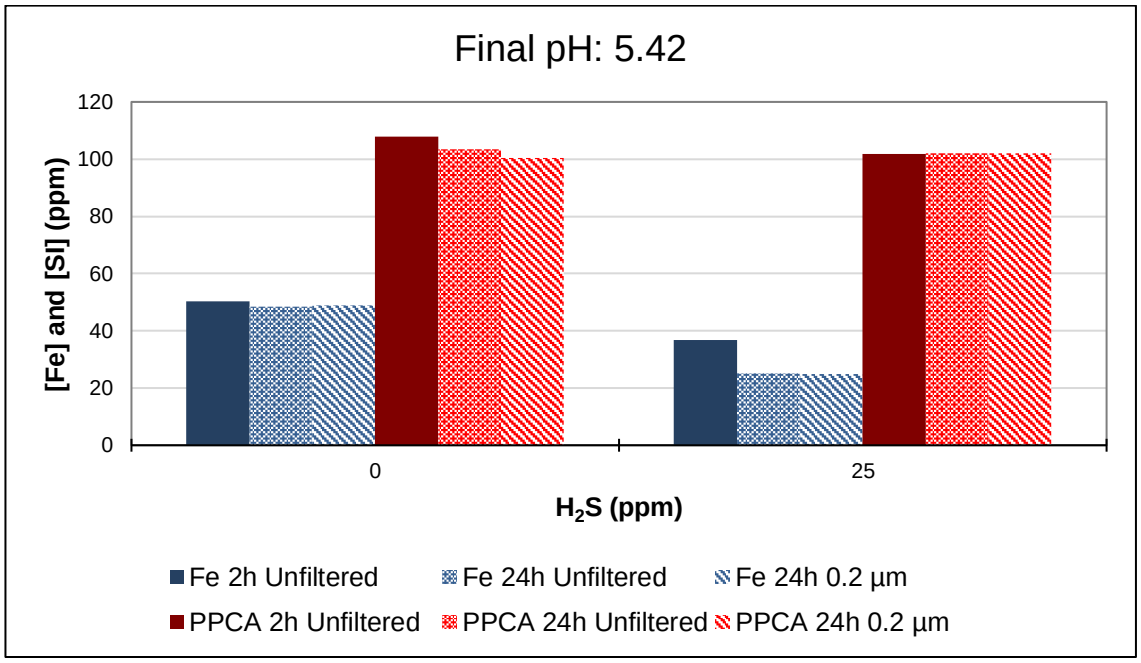

Figure 8.10 FeS inhibition in 3.5 wt% NaCl at 50°C at pH 5.42 in presence of 25 ppm H_2S

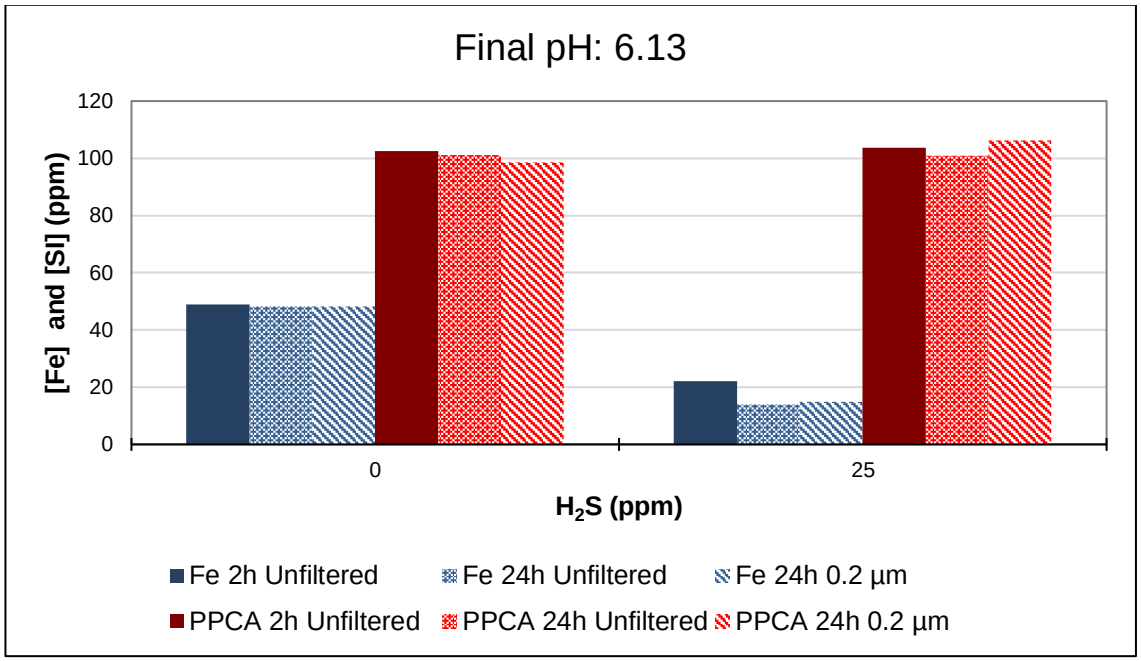

Figure 8.11 FeS inhibition in 3.5 wt% NaCl at 50°C at pH 6.13 in presence of 25 ppm H_2S

8.6 The impact of preformed ZnS on scale inhibitor consumption

In the following set of experiments, Zn solutions (without scale inhibitor) were mixed with sulphide solutions to precipitate ZnS. After that initial precipitation stage, certain amount of SI-1 was added to the ZnS solutions to examine the possible SI consumption. To calculate the initial SI concentration, similar amount of SI-1 was added to Zn solutions without sulphide. As shown in Figure 8.12 the Zn concentration dropped from 98 ppm to 37 ppm after 24 hours in the blank solutions as well as the blank solution mixed with SI-1. Figure 8.13 shows the SI-1 concentrations after 2 and 24 hours. The initial SI-1 concentration was 22.6 ppm. After 2 hours, almost 50% of the initial SI-1 remained in solutions when the sample was analysed without filtration. However, after filtration with a 0.2 µm filter, the SI-1 concentration decreased to 3.5 ppm and this is equivalent to the SI-1 concentration after 24 hours. Therefore, the SI-1 can be consumed not only by inhibiting the ZnS scale but also by interaction with pre-formed ZnS.

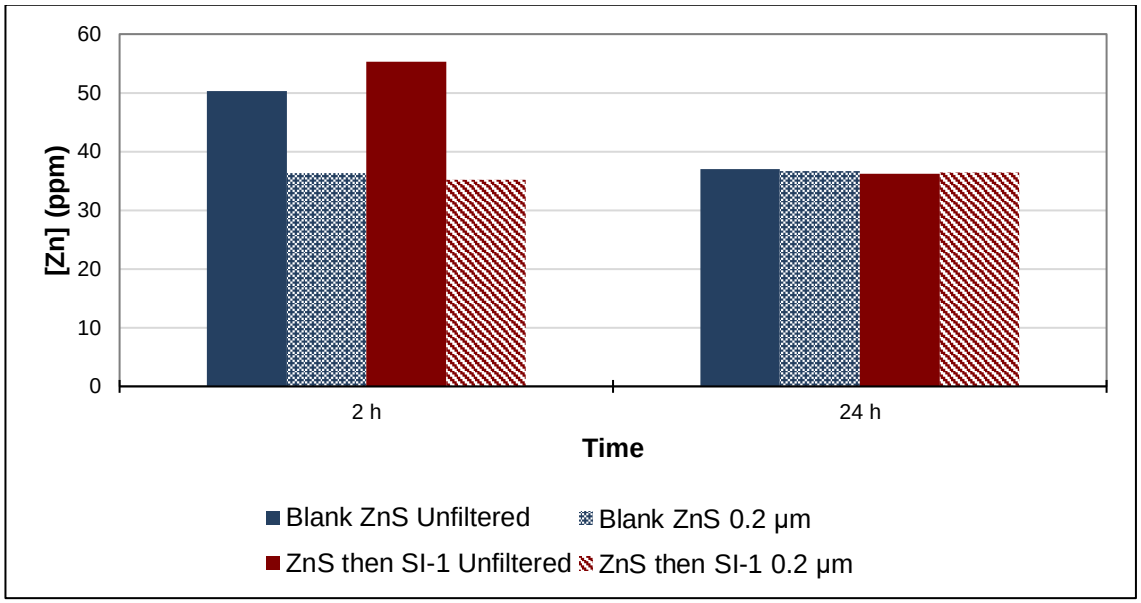

Figure 8.12 Zn concentrations in the supernatant solutions after 2 and 24 h. Scale inhibitor was added to some solutions after ZnS formation. The initial Zn concentration was 98 ppm.

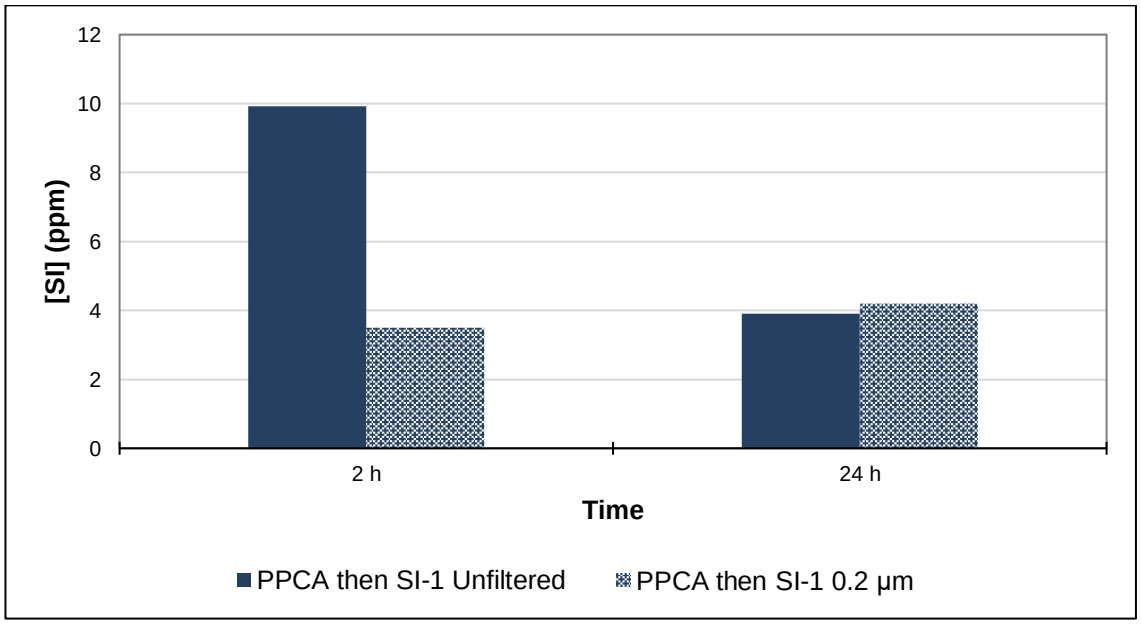

Figure 8.13 SI concentrations in the supernatant solutions after 2 and 24 h. Scale inhibitor was added to some solutions after ZnS formation. The initial SI concentration was 22.6 ppm.

The tests were repeated in presence of 50 ppm SI-2 (a high molecular weight sulphonated co-polymers) and ICP results are plotted in Figure 8.14 and Figure 8.15. It is clear from Figure 8.14 that 50 ppm SI-2 prevented the deposition of ZnS. The addition of nearly 20 ppm SI-1 resulted in a slight increase in the Zn concentration in the filtered sample. This might be attributed to the decrease in the pH and hence the solubility of ZnS. It is interesting to note that 10 ppm SI was detected in the SI-2 solutions therefore the SI-2 can be monitored by measuring phosphorous using ICP. After the addition of SI-1, the SI concentration increased to 35.8 ppm and remained

constant in the unfiltered samples. By contrast, when the samples had been filtered through 0.2 µm filter, the SI concentration dropped to zero in SI-2 solutions and to 9.5 ppm in SI-1/SI-2 solutions.

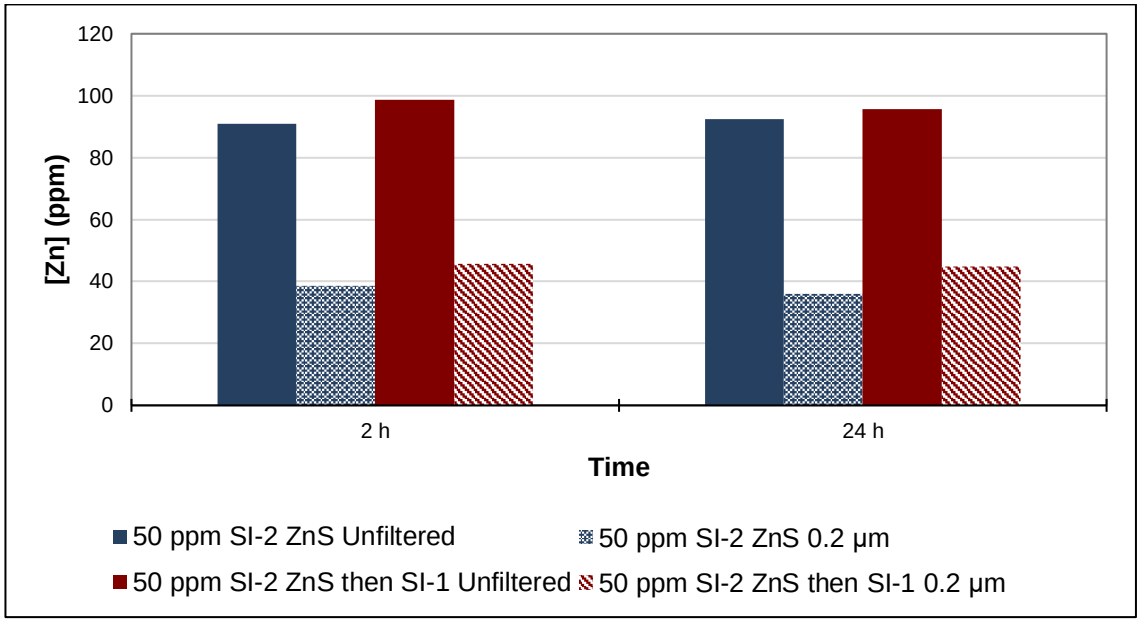

Figure 8.14 Zn concentrations in the supernatant solutions after 2 and 24 h. Scale inhibitor was added to some solutions after ZnS formation. The initial Zn concentration was 94.4 ppm.

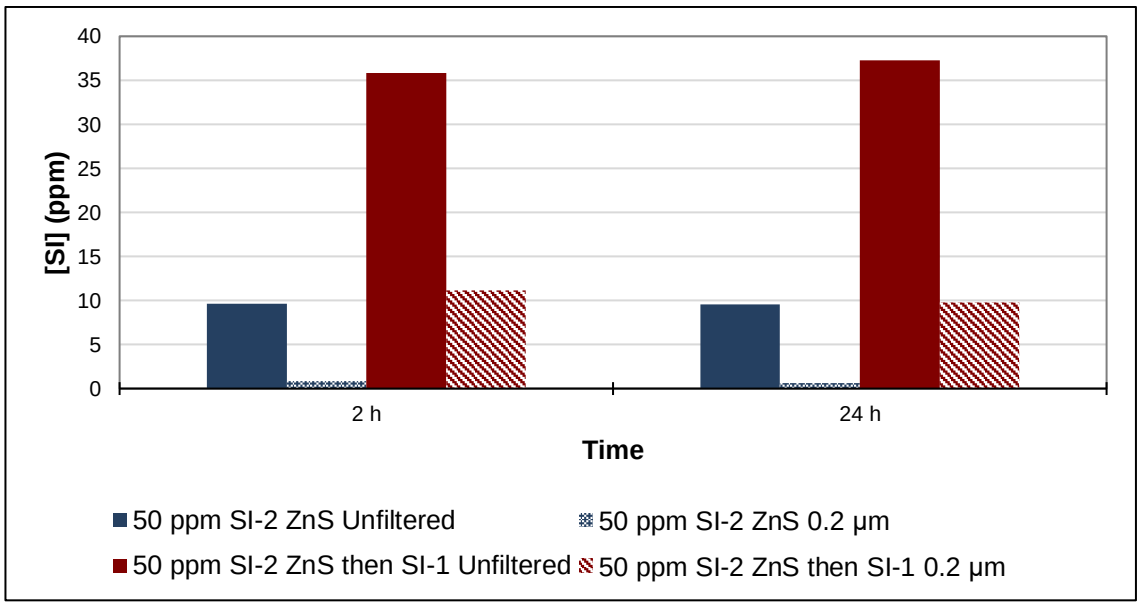

Figure 8.15 SI concentrations (SI-1 + SI-2) in the supernatant solutions after 2 and 24 h. Scale inhibitor was added to some solutions after ZnS formation. The initial SI concentration was 10.1 ppm. After SI-1 addition, the SI concentration was 35.8 ppm.

8.7 The impact of pH on ZnS and FeS inhibition at 23°C

Different concentrations of SI-1 namely 10, 50 and 100 ppm were used to inhibit ZnS in presence of 25 ppm H_2S and 100 ppm Zn in 3.5 wt% NaCl at 23°C at different pH values. Both Zn and SI-1 concentrations were monitored after 2 and 24 hours in order

to examine the inhibition efficiency and the scale inhibitor consumption. It is clearly shown in Figure 8.16 10 ppm SI-1 was not sufficiency to prevent the deposition of ZnS. Additionally, significant amount of the scale inhibitor was consumed as the scale inhibitor dropped to 1 ppm in the supernatant solutions. Similarly, 50 ppm of SI-1 did not prevent the deposition of ZnS and nearly 37 ppm of the scale inhibitor deposited with the ZnS, see Figure 8.17.

When the scale inhibitor concentration was increased to 100 ppm, the inhibition efficiency for ZnS was significantly improved as evidently shown in Figure 8.18. This set of experiments was conducted at 23°C and thus the H_2S decrease due to evolution is expected to be minimal. However, the Zn concentrations detected in the 100 ppm SI-1 after filtration was higher than that in 10 and 50 ppm SI-1 at comparable pH values *i.e.* 34 ppm Zn was detected in the 10 and 50 ppm solutions while 45 ppm Zn was measured in the 100 ppm SI-1. In terms of the scale inhibitor consumption, the SI-1 concentrations remained almost the same in the unfiltered samples; however, after filtration it decreased from 95 ppm to 62 ppm. Hence, 33 ppm SI-1 was consumed which is comparable to the deposited amount of SI-1 in 50 ppm SI-1 solution.

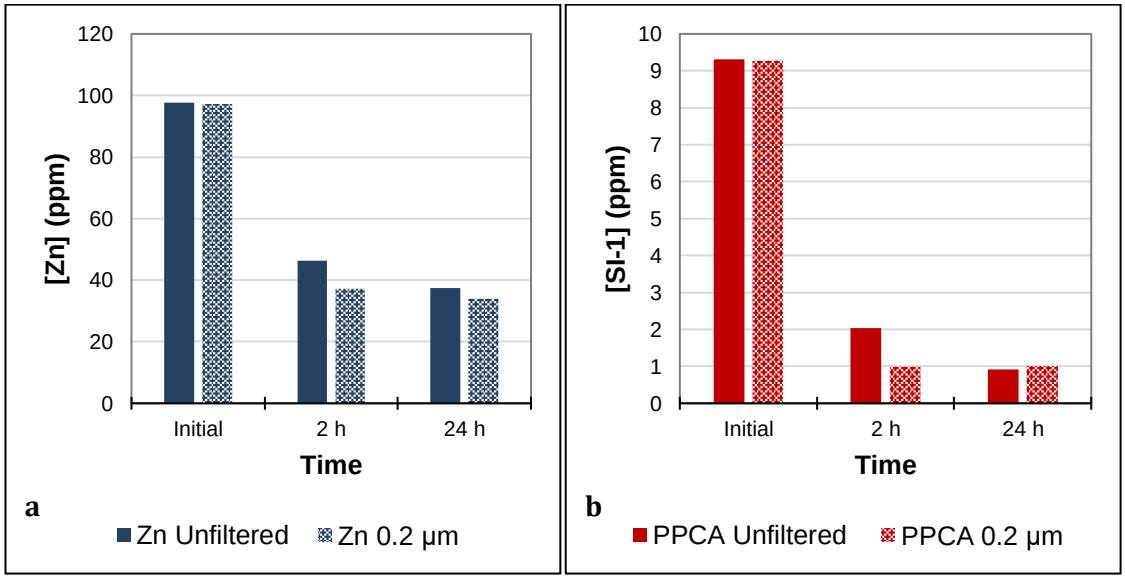

Figure 8.16 Zn and SI-1 concentrations in the supernatant solutions in presence of 25 ppm H_2S at 23°C in 3.5 wt% NaCl. The final pH was 4.59.

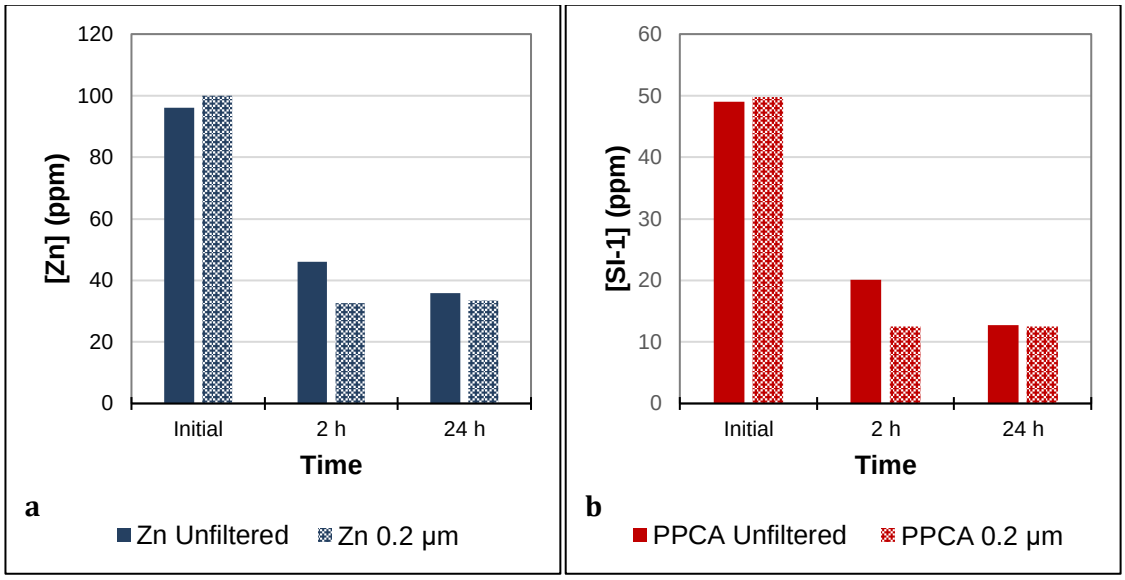

Figure 8.17 Zn and SI-1 concentrations in the supernatant solutions in presence of 25 ppm H_2S at 23°C in 3.5 wt% NaCl. The final pH was 4.14.

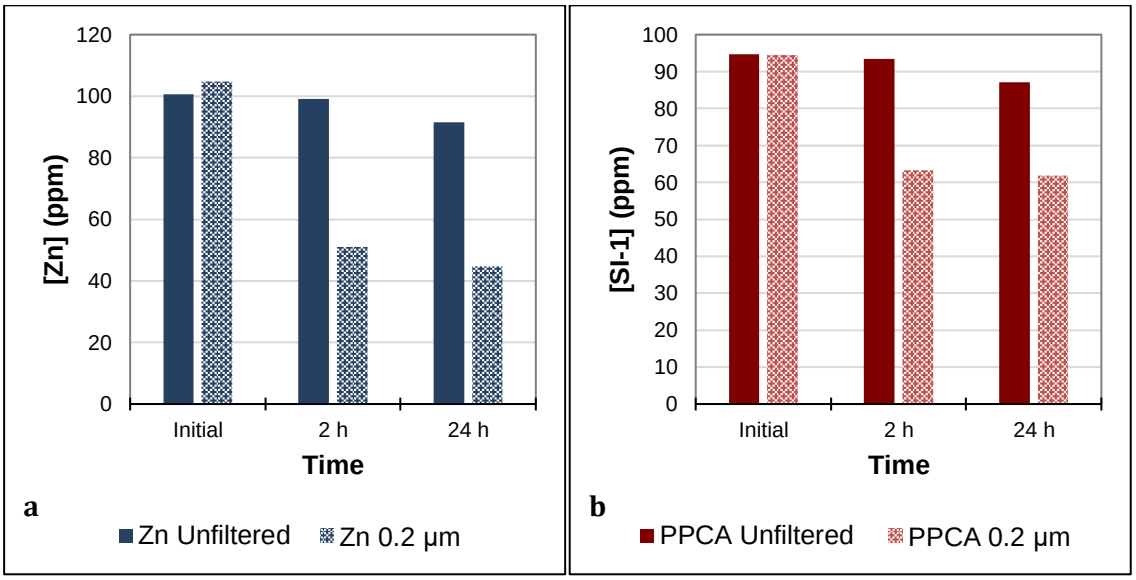

Figure 8.18 Zn and SI-1 concentrations in the supernatant solutions in presence of 25 ppm H_2S at 23°C in 3.5 wt% NaCl. The final pH was 4.08.

From the previous results, 100 ppm SI-1 was sufficient to prevent the deposition of ZnS and the scale inhibitor was partially consumed. In the following tests, a mixture of 100 ppm SI-1 and 50 ppm SI-2 was tested for ZnS inhibition and scale inhibitor consumption. It is evident from Figure 8.19 that the mixture prevented the deposition of ZnS and moreover the drop in scale inhibitor concentration was comparable to the 100 ppm SI-1 and the mixture of 100 ppm SI-1 and 50 ppm SI-2. Further work will be conducted to examine the consumption of SI-2 in sulphide scale solutions.

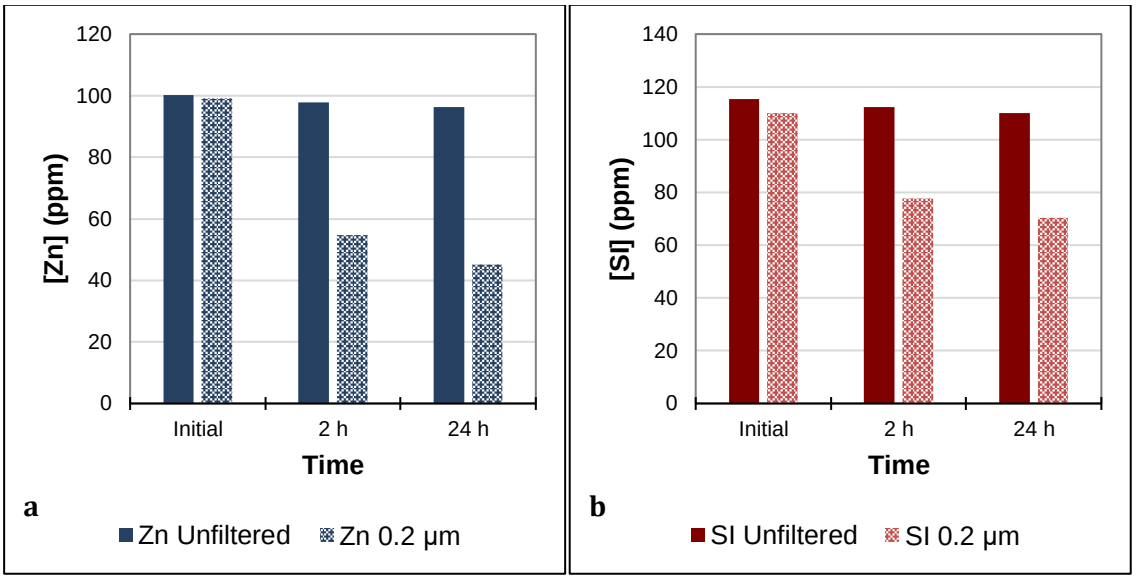

Figure 8.19 Zn and SI concentrations in the supernatant solutions in presence of 25 ppm H_2S at 23°C in 3.5 wt% NaCl. The final pH was 4.08. Mixture of 100 ppm SI-1 and 50 ppm SI-2.

In order to investigate the impact of the pH on the inhibition efficiency of SI-1, the pH of Zn/SI-1 solutions were adjusted such that the final pH increased to 5-6. As shown in Figure 8.20, increasing the pH had no impact on the inhibition efficiency for ZnS in 10 ppm SI-1 solution. By contrary, in 50 ppm SI-1, the deposition of ZnS was delayed as the Zn and SI-1 concentrations after 2 hours were comparable to the initial concentrations, see Figure 8.21. When the reaction time was extended to 24 hours, complete precipitation of ZnS occurred and the final concentrations were similar at the two tested pH values.

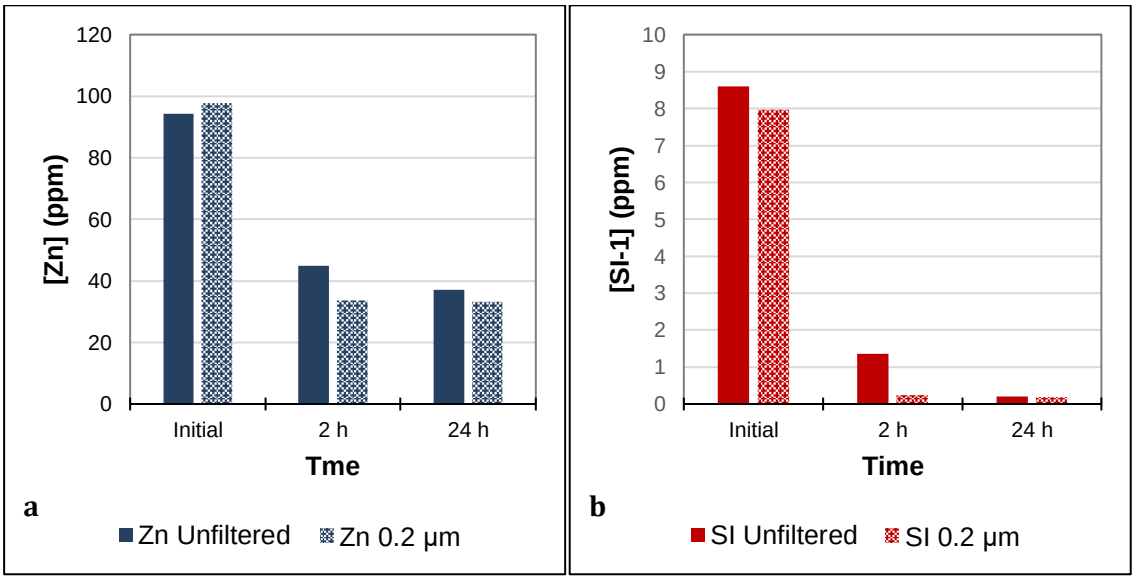

Figure 8.20 Zn and SI-1 concentrations in the supernatant solutions in presence of 25 ppm H_2S at 23°C in 3.5 wt% NaCl. The final pH was 5.18.

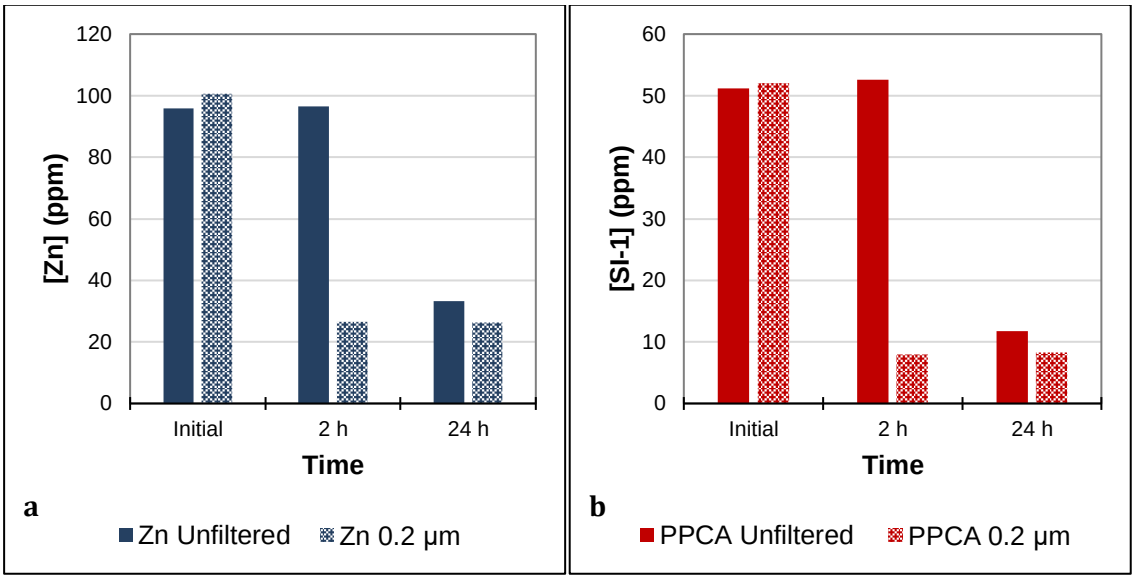

Figure 8.21 Zn and SI-1 concentrations in the supernatant solutions in presence of 25 ppm H_2S at 23°C in 3.5 wt% NaCl. The final pH was 5.63.

To confirm the previous observation that no scale inhibitor would be consumed in FeS solutions, the following set of experiments were conducted. Figure 8.22 shows the Fe and SI-1 concentrations when 100 ppm Fe and 20 ppm SI-1 solution was mixed with 44 ppm H_2S. FeS partially deposited in the first two hours and when the time was extended to 24 hours, FeS completely deposited. Despite the FeS deposition, the scale inhibitor concentration did not decrease. In presence of 100 ppm SI-1, there was no FeS inhibition or scale inhibitor consumption at pH of 5.45 and 6.9, see Figure 8.23 and Figure 8.24. The difference in the Fe decline *i.e.* FeS precipitation was due to the difference in the pH and hence FeS solubility. Figure 8.25 shows Fe, Zn and SI-1 concentrations in the supernatant solutions when Zn, Fe and SI-1 solutions were mixed with H_2S solutions. No FeS deposition occurred in the first two hours but nearly 5 ppm Fe precipitated as FeS after 24 hours. Similarly, Zn concentration declined in the 24 hour supernatant solutions. The tests were repeated using SI-1 (PPCA) and SI-8 (Acrylic sulphonated non-ionic Terpolymer) in the presence of 25 ppm H_2S, and the Zn concentration was increased to 18 ppm instead of 10 ppm. From the ZnS and PbS inhibition results shown in Figure 7.16 and Figure 7.17, it is seen that 100 ppm SI-1 was sufficient to prevent the deposition of ZnS even in presence of 18 ppm Pb. In contrast, the formation of FeS had a negative impact on the inhibition of ZnS despite the fact that 100 ppm SI-1 and 100 ppm SI-8 were very effective against ZnS when it formed as a single scale or alongside PbS. In presence of 100 ppm SI-1, nearly 20 ppm Fe precipitated as FeS when there was no Zn in the solutions, see Figure 8.26. In presence of ZnS, the amount of FeS deposition was reduced since the sulphide was partially

consumed to precipitate ZnS and furthermore the deposition of FeS was delayed. After 24 hours, 10 ppm Fe deposited and 8 ppm Zn of the initial 18 ppm deposited as ZnS. Similar behaviour was obtained in 100 ppm SI-8 solutions as shown in Figure 8.27. Note the difference in the amount of FeS precipitation in SI-8 compared to SI-1 solutions which can be attributed to the difference in pH of these solutions *i.e.* the final pH of SI-1 and SI-8 solutions were 5.94 and 7.9, respectively. This confirms the importance of pH monitoring to avoid misinterpretation of inhibition results. Therefore, none of the tested conventional scale inhibitors managed to inhibit FeS despite the fact that they were effective against ZnS and PbS. The failure of these scale inhibitors to prevent FeS might be attributed to the point of zero charge (PZC) as the PZC of ZnS and PbS is around 4 where PZC of FeS is 7.5.

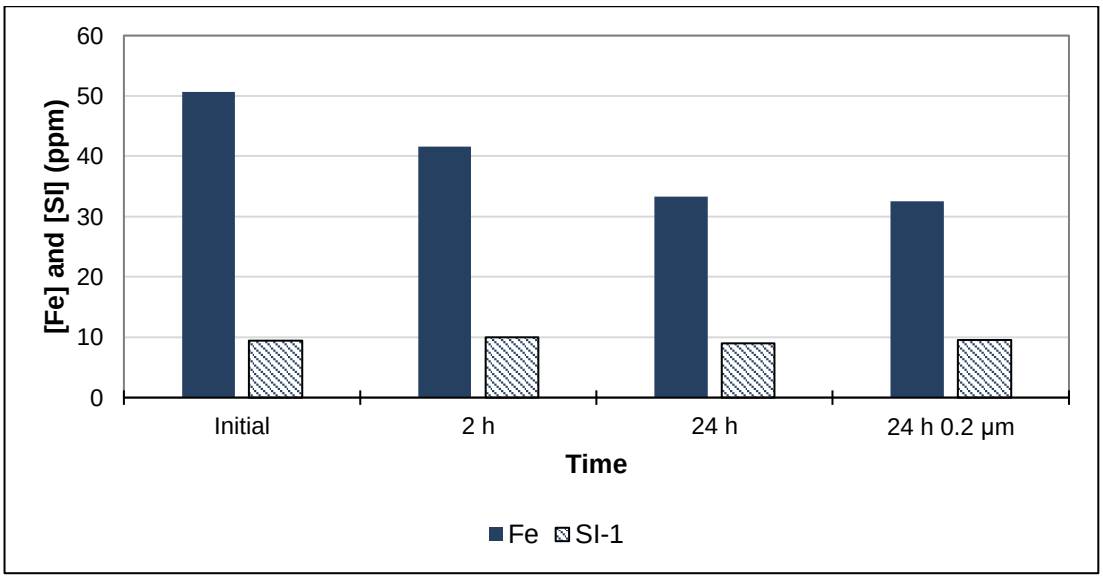

Figure 8.22 Fe and SI-1 concentrations in the supernatant solutions in presence of 23 ppm H_2S at 23°C in 3.5 wt% NaCl. The final pH was 6.62 .

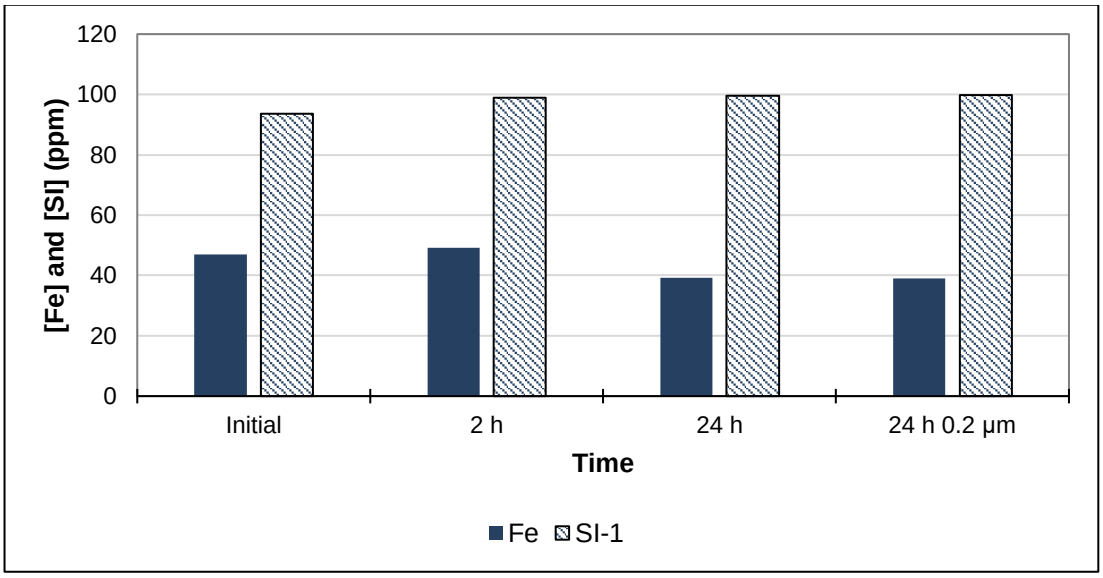

Figure 8.23 Fe and SI-1 concentrations in the supernatant solutions in presence of 23 ppm H_2S at 23°C in 3.5 wt% NaCl. The final pH was 5.45.

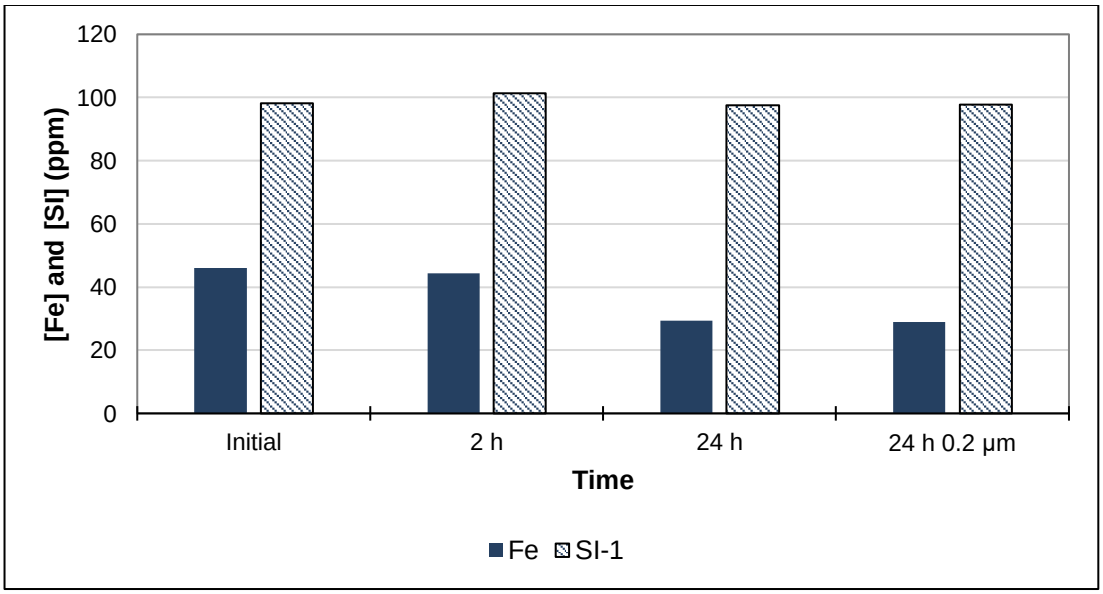

Figure 8.24 Fe and SI-1 concentrations in the supernatant solutions in presence of 23 ppm H_2S at 23°C in 3.5 wt% NaCl. The final pH was 6.9.

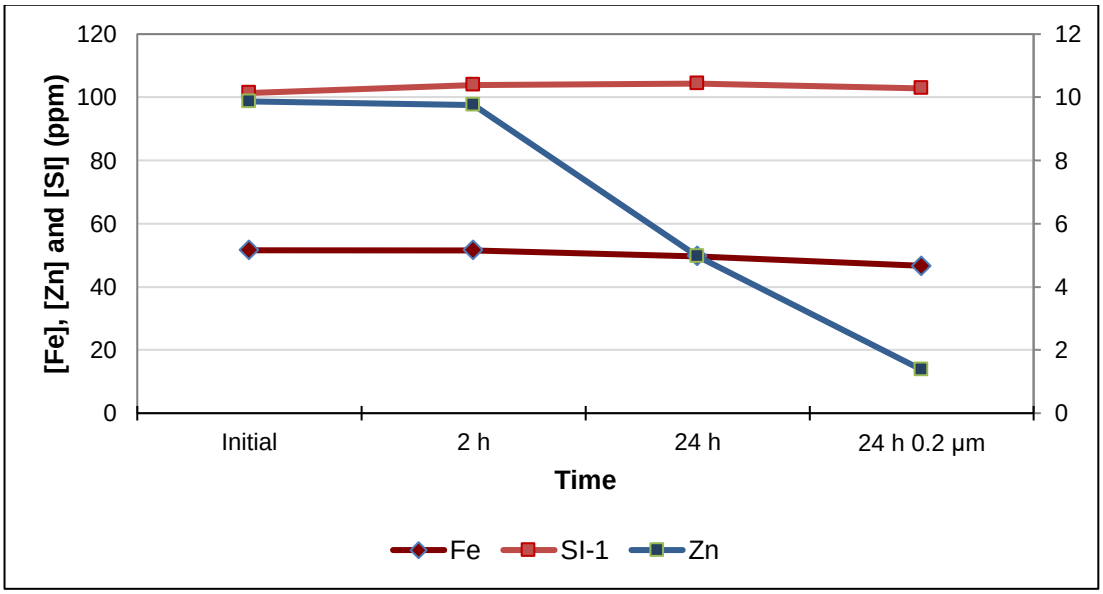

Figure 8.25 Zn, Fe and SI-1 concentrations in the supernatant solutions in presence of 23 ppm H_2S at 23°C in 3.5 wt% NaCl. The final pH was 5.44.

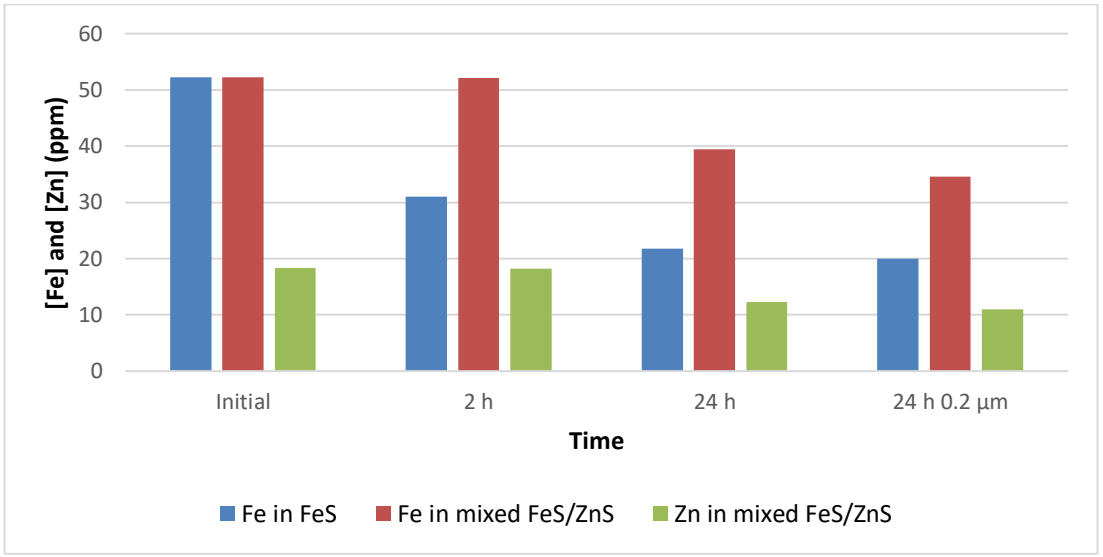

Figure 8.26 Zn, Fe and SI-1 concentrations in the supernatant solutions in presence of 25 ppm H_2S at 23°C in 3.5 wt% NaCl. The final pH was 5.94.

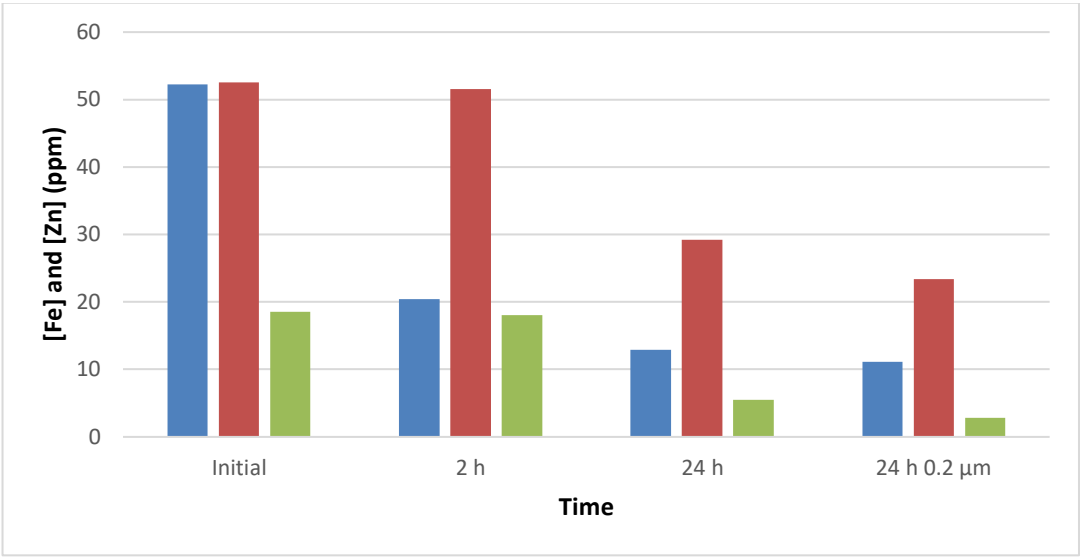

Figure 8.27 Zn, Fe and SI-8 concentrations in the supernatant solutions in presence of 25 ppm H_2S at 23°C in 3.5 wt% NaCl. The final pH was 7.9.

8.8 Conclusions

Compatibility between Zn and PPCA was examined at different conditions including temperature and pH values. This was achieved by adding 200 ppm Zn and 200 ppm PPCA in 3.5 wt% NaCl and then these solutions were heated and pH adjusted to the desired values. The inhibition efficiency for ZnS and FeS in 3.5 wt% NaCl at different temperatures and pH values was also studied. For the first time, the scale inhibitor consumption in ZnS and FeS was investigated. The interaction between ZnS and FeS in the presence of scale inhibitor was also examined. The main conclusions from this study are as follows:

1. At natural pH of 200 ppm Zn and 200 ppm PPCA solutions *i.e.* pH ~ 4, there was no precipitation. However, at higher temperature and pH values the solutions turned cloudy and a white precipitate *i.e.* Zn-SI complex deposited. ICP results revealed that significant decrease in Zn and PPCA concentrations occurred as a consequence of increasing the temperature and pH. Therefore, some scale inhibitors cannot be used in presence of high Zn concentration even for inhibiting other scales as the increase in pH might lead to Zn-SI precipitation.

2. 100 ppm SI-1 prevented the deposition of ZnS in 3.5 wt% NaCl. At conditions similar to the ZnS tests, 100 ppm SI-1 did not inhibit FeS. Therefore, it is easier to inhibit ZnS despite the fact that the solubility of FeS is higher than that of ZnS.

3. While SI-1 (PPCA) concentration decreased in the supernatant of the ZnS solutions, no similar drop was observed in FeS solutions. The concentration of SI-1 decreased even when added to a pre-formed ZnS containing solution. So, it is clear from these observations the scale inhibitor, in this case PPCA, was consumed in ZnS whereas there was no interaction between Fe/FeS and the scale inhibitor. Different scales including sulphide and conventional scales usually form together and therefore the scale inhibitor consumption in ZnS can affect the performance of the scale inhibitor for other scales.

4. When 10 ppm SI-1 (PPCA) and SI-4 (DETPMP) were tested on ZnS, complete precipitation of ZnS and SI occurred. This confirms the scale inhibitor consumption in ZnS solutions using the commonly available polymeric and phosphonate scale inhibitors *i.e.* PPCA and DETPMP respectively.

5. In mixed FeS and ZnS solutions, two distinct types of behaviour were observed. First, ZnS inhibition was affected by FeS formation as ZnS partially deposited within few hours. On the other hand, FeS deposition was delayed as a result of ZnS formation. Formation of inhibited ZnS sub-micron sized particles may act as sites for FeS and this may explain the delay in FeS deposition in mixed FeS/ZnS systems.

Chapter 9
Filter-Blocking Tests for Sulphide Systems

9.1 Introduction

This chapter summarises the steps taken to achieve repeatable testing of iron and zinc sulphide scale inhibitors using a dynamic filter-blocking rig. Furthermore, the inhibition efficiencies of different inhibitors for FeS and ZnS scale control were evaluated over a wide range of parameters using the established methodology. One of the main advantages of dynamic *i.e.* filter-blocking or tube-blocking tests, is that they can be used to evaluate the performance of scale inhibitors at elevated temperatures (>100°C) and pressures (up to 2500 psig) and to determine the impact of flow on the system. However, there are some drawbacks such as the short mixing/residence time experienced by the incompatible scaling brines.

Traditional tube blocking tests (dynamic scale loops) are based on the pre-heating of two incompatible brines in flowing pipes with the subsequent mixing, precipitation and adherence of the formed scale in/onto a coiled length of pipe, known as the test coil. However, some sulphide scales are known to be "soft" scales and consequently these materials may not adhere to the tubing wall, as would be expected for calcium carbonate or barium sulphate scale. This can lead to false inhibition results, since the tube does not "block" in the test time. This limitation has been overcome by replacing the test coil with a filter of defined mesh size in combination with a length of tube to allow pre-filter mixing (Figure 9.1).

Some work has been carried out to achieve repeatable scaling times for iron or zinc sulphide scales using the filter sizes that are commercially available *i.e.* 7, 15 or 40 µm. The limited granularity, combined with the extremely low solubility of the sulphide scales, presents challenges for achieving scaling times that are appropriately short (to allow repeated testing) but also appropriately long (so as to avoid unreliable results). In this study, our definition of the scaling time is the time would take the pressure across the filter to increase 5 psi. These challenges will be addressed below.

As in the static experiments described in previous chapters, the sulphide solution was prepared by adding a specified mass of sodium sulphide nonahydrate ($Na_2S.9H_2O$) to a pre-prepared brine to give the desired sulphide concentration. Iron and zinc solutions were prepared by adding iron chloride tetrahydrate ($FeCl_2.4H_2O$) or zinc chloride ($ZnCl_2$), respectively. The scale inhibitor was added to the scaling metal solutions.

Iron sulphide experiments present a greater experimental challenge due to the potential for iron oxidation, therefore the brines were N_2 sparged, and the iron and sulphide solutions were prepared in an anaerobic chamber before being transferred to the filter-blocking rig. The H_2S concentration was monitored to ensure that the H_2S evolution was negligible and thus the desired sulphide concentration was injected. The length of the pre-heat coils was sufficient to heat the solutions to the desired temperature. The pressure drop cross the filter (dP) was measured by a differential transducer with high accuracy.

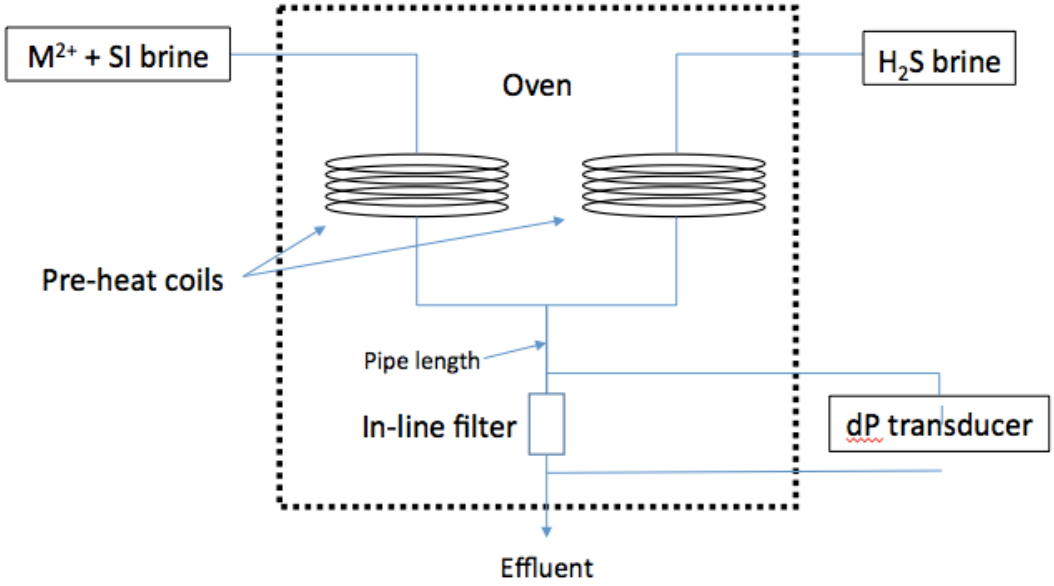

Figure 9.1 Diagram of filter-blocking rig.

One of the main objectives of this period of study was to compare the results from the static inhibition tests with the dynamic tests. As noted in previous chapters, the particle size of the inhibited scales was seen to decrease with increasing scale inhibitor concentration, therefore this phenomenon was further examined in relation to scaling time. Since SIs affect the size of sulphide particles, then the size of the filter mesh will have a significant bearing on what we define as "inhibited" or "non inhibited" sulphide systems.

9.2 Experimental work

9.2.1 Establishing filter size

In the first set of experiments, the tests were conducted at mild conditions *i.e.* 23°C or 50°C, and 3.5 wt% NaCl to determine the repeatability of scaling times and also to establish the ability of 5% nitric acid (HNO_3) to reliably clean the filter between runs.

200 ppm H_2S and 100 ppm Fe solutions were injected at 5 ml/min each and therefore the total flow rate was 10 ml/min with mixed 100 ppm H_2S and 50 ppm Fe. It is worth mentioning that at low flow rates the scaling time was high and the repeatebity was unsatifactory and hence 10 ml/min was used in this study. The filter size in these experiments was 7 µm. The FeS formation tests were repeated five times and results were plotted (Figure 9.2).

The scaling time ranged between 2.50 min to 2.75 min, which is equivalent to a 9% variance. The same conditions were used again with a 15 µm filter instead of the 7 µm filter and the scaling time increased as a result however the variation in scaling time was higher than 50% when the tests were repeated (Figure 9.3). It was therefore decided to use 7 µm because of the repeatability and to compare the results with the static tests where the filter size was 5 µm. As shown in Figure 9.4, increasing the filter size to 40 µm resulted in a very long scaling time *i.e.* the increase in the differential pressure was 2 psi in 50 min which was experimentally impractical. These results confirmed the importance of selecting the appropriate filter size to avoid misinterpretation of the inhibition results.

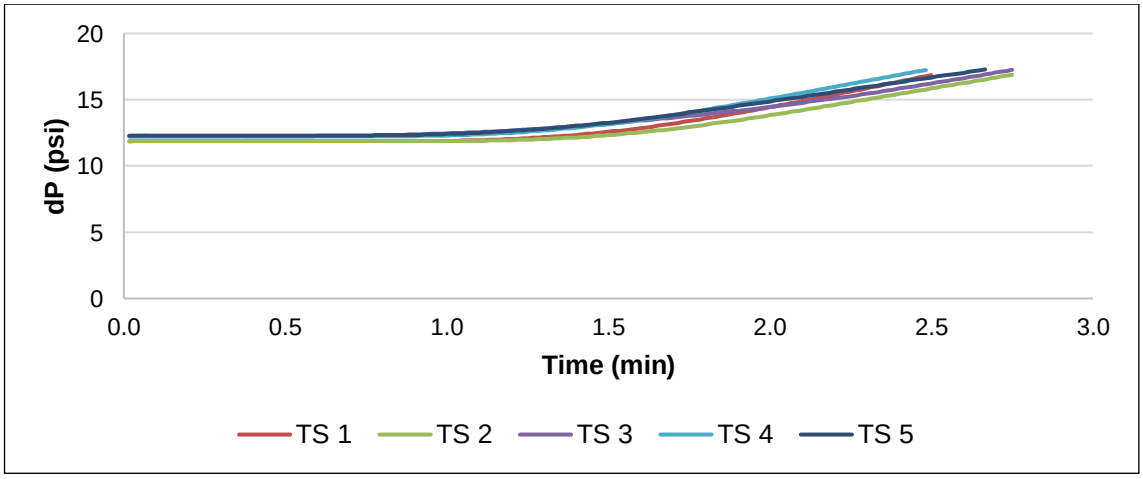

Figure 9.2 Differential pressure (psi) vs time, Test scale times Q_{total} = 10 mL/min 55°C, 500 psi, 7 µm filter & 100 mm pipe in presence of 100 ppm H_2S and 50 ppm Fe.

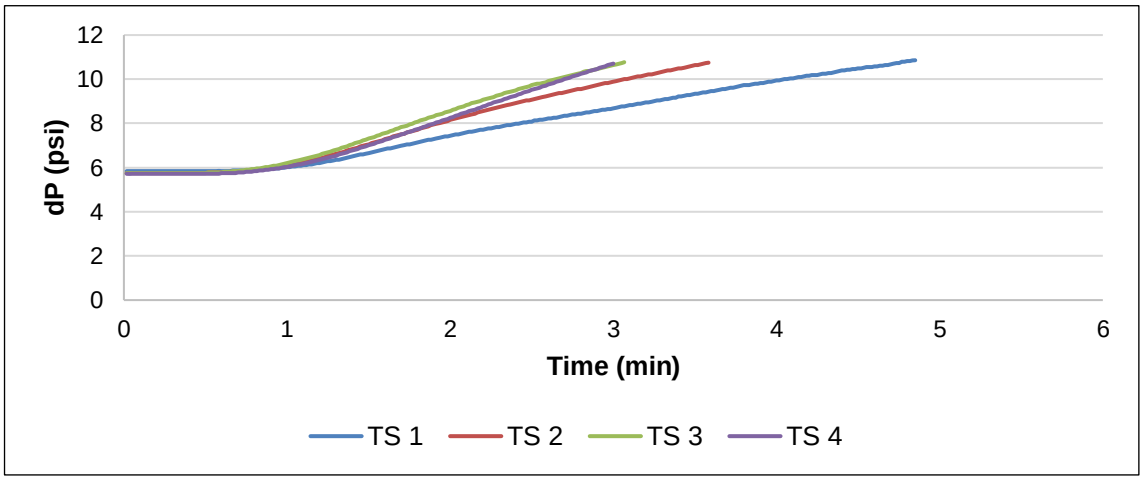

Figure 9.3 Differential pressure (psi) vs time, TS times Q_{total} = 10 mL/min 55°C, 500 psi, 15 µm filter & 100 mm pipe in presence of 100 ppm H_2S and 50 ppm Fe.

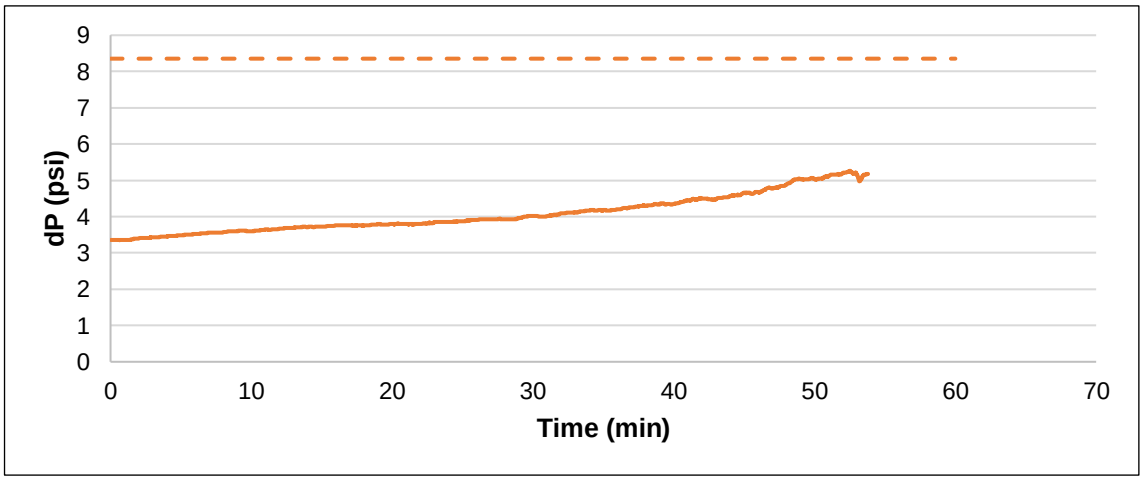

Figure 9.4 Differential pressure (psi) vs time, TS times Q_{total} = 10 mL/min 40 µm filter & 50 mm pipe in presence of 100 ppm H_2S and 50 ppm Fe at 55 °C and 500 psi. The solid line represents the the experimental pressure drop while the dotted line represent the 5 psi increase in the pressure drop.

9.2.2 FeS inhibition by SI-2

Different concentrations of SI-2 were tested for FeS inhibition using filter-blocking tests. The experiments were conducted at 55°C and 500 psi with a 7 µm filter and a combined flow rate of 10 ml/min. After mixing, H_2S and Fe concentrations were 100 ppm and 50 ppm, respectively.

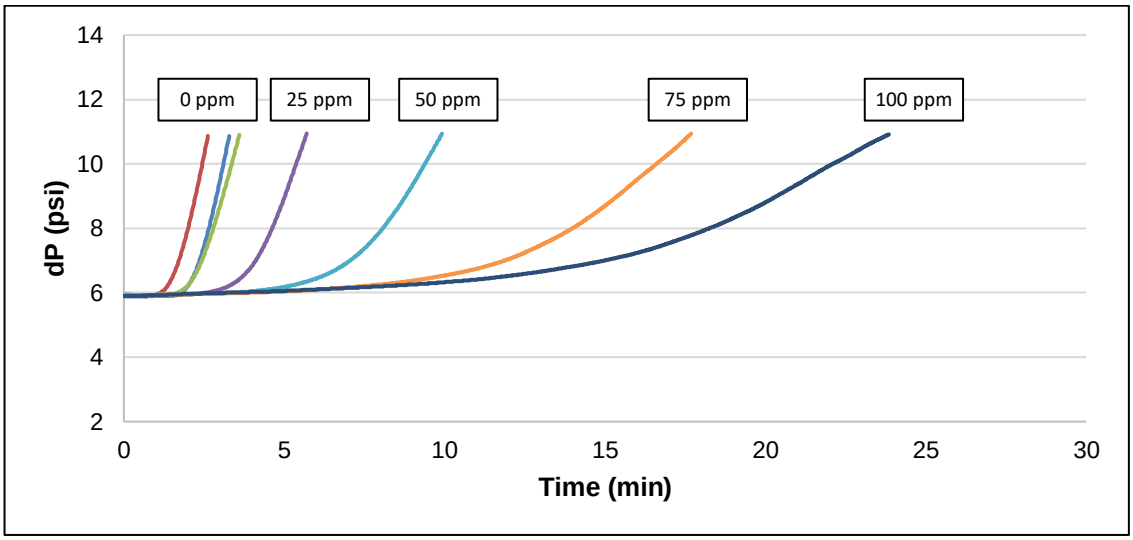

Figure 9.5 FeS inhibition by SI-2 T = 55°C P = 500 psi 7 µm filter Q_{total} = 10 mL/min. 3.5 wt% NaCl, 100 ppm H_2S and 50 ppm Fe.

The scaling time for the Blank (no inhibitor) test was nearly 3 minutes Figure 9.5 and this time was extended to 5.4 min by the addition of 25 ppm SI-2. Increasing the scale inhibitor concentration to 50 ppm resulted in an extension of the scaling time to 9.5 min. The scaling times of 75 ppm and 100 ppm SI-2 were 17 min and 23 min respectively. Based on the pass/fail criteria selected for the filter-blocking experiments *i.e.* extending the scaling time to three times the test scale time, the MIC was between 25 ppm and 50 ppm (closer to 25 ppm). This is in-line with the MIC and the observed particle size reduction in the static tests (Figure 6.10 and Figure 6.11).

As previously discussed, SI-2 does not stop the formation of FeS, it does however suspend the formed precipitate so as to prevent deposition and resultant adhesion of the scale. Extending the scaling time from the filter blocking tests was further evidence that with increasing scale inhibitor concentration there was further reduction in the size of the scale particles formed.

9.2.3 ZnS inhibition - method development

Two brines, namely 3.5 wt% NaCl and Khuff formation water (TDS = 192,000 ppm), were used to study the impact of salinity on the inhibition efficiency of SI-2 for ZnS scale control. The filter size for these tests was 15 µm and the initial scaling ion concentrations were 200 ppm H_2S and 100 ppm Zn. In 3.5 wt% NaCl without scale inhibitor, a 5 psi rise in differential pressure was observed at 6.6 min (Figure 9.6), *c.f.* approximately 3 min for FeS. When the test was repeated with 100 ppm SI-2, the scaling time significantly increased to 26 min.

Figure 9.6 shows that when the tests were repeated in Khuff formation water (much higher salinity) there was a significant impact on both the blank and the inhibited solutions. The 5 psi increase occurred in 6.6 min in the 3.5 wt% NaCl and 3 min in the Khuff formation water and 100 ppm SI-2 was seen to have a negligible positive impact on the scaling time.

This result ran contrary to the static inhibition results, in which SI-2 was effective even when tested at high temperatures (90°C) and high salinity (GFW and KFW) for all common sulphide scales *i.e.* FeS, ZnS and PbS. Hence, the significant drop in the scaling time is not attributed to the poor inhibition performance.

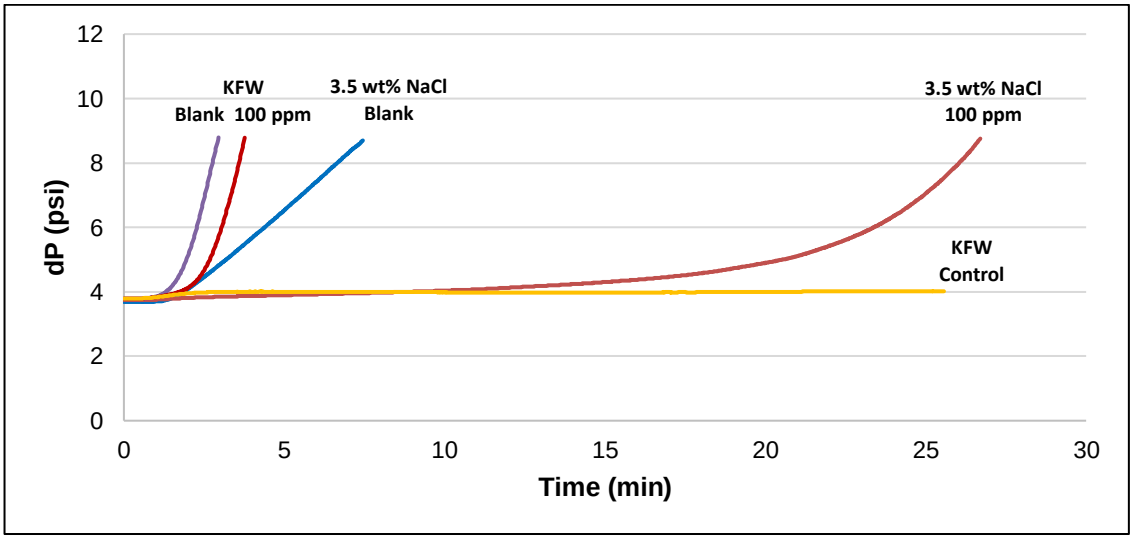

Figure 9.6 ZnS inhibition by SI-2 (T = 50°C; P = 500 psi; 15 µm filter; Q_{total} = 10 mL/min)

The Control experiment performed using the Khuff formation water *i.e.* a test run without the addition of sulphide or zinc to the system, showed no increase in differential pressure. However, when the conventional method was used *i.e.* natural pH H_2S brine (~pH 12) and low pH cation brine (without scaling metal), the pressure gradually increased despite the fact that there was no sulphide scale or conventional scales (the formation water did not contain sulphate, bicarbonate or scaling metals (Figure 9.7)

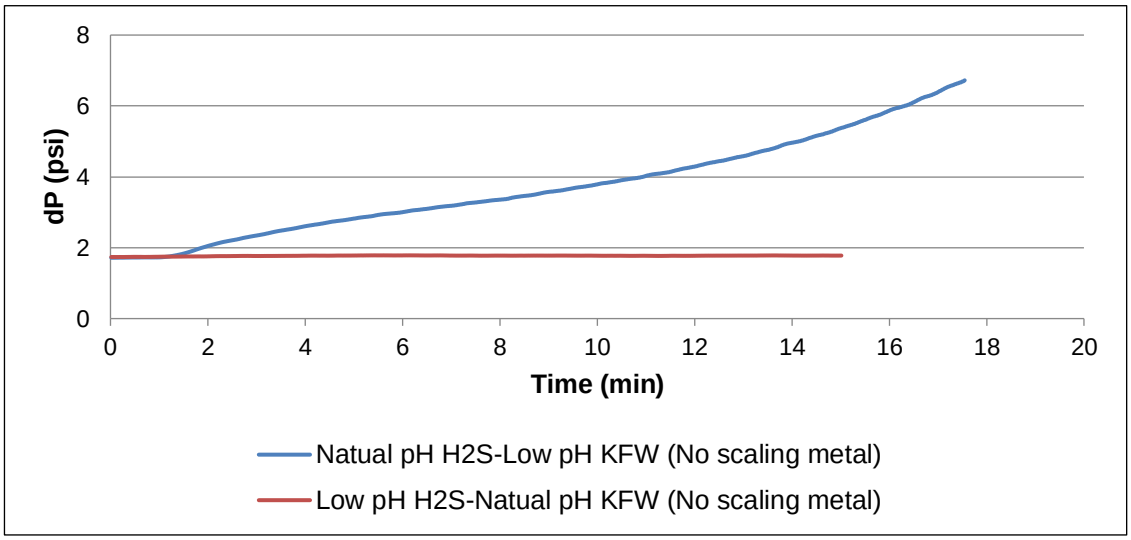

Figure 9.7 T = 120°C P = 500 psi 7 µm filter Q_{total} = 10 mL/min.

To understand whether this incompatibility was driven by the difference in pH between high pH and low pH brines in the mixing stage, the pH of the H_2S brine was reduced prior to injection (Figure 9.7; red line). This procedure was seen to remove the risk of pH-driven incompatibility causing erroneous (non-sulphide scale) pressure rises.

In the modified procedure, the pH of H_2S brine was reduced and therefore there was a risk of H_2S evolution. Consequently static tests were conducted, which proved that all Fe was stripped from solution therefore H_2S was in excess throughout the tests. Figure 9.8 confirms the repeatability of the scaling times using the modified procedure in 3.5 wt% NaCl.

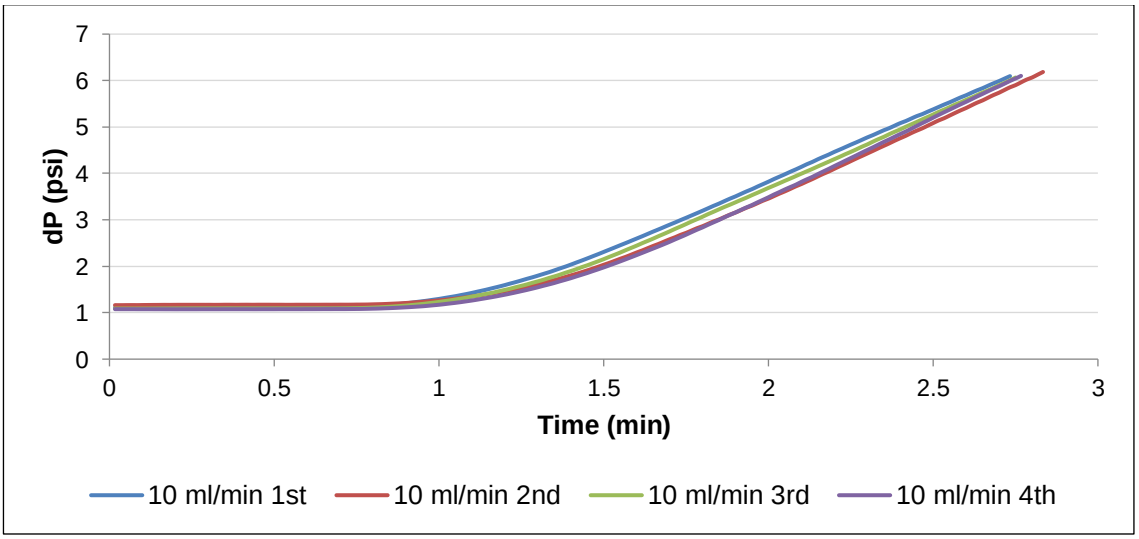

Figure 9.8 FeS formation using the modified pH adjustment procedure. T = 120°C; P = 500 psi; 7 µm filter; Q_{total} = 10 mL/min. Final pH 6.9.

When the test was conducted in Khuff FW, the scaling time was increased when the test was repeated under the same conditions using the same filter (Figure 9.9). In the first

test, the scaling time was 4 min, which subsequently extended to 8 min and then 16 min. The increase in the scaling time for the subsequent tests was attributed to filter degradation of the stainless steel 316 filter.

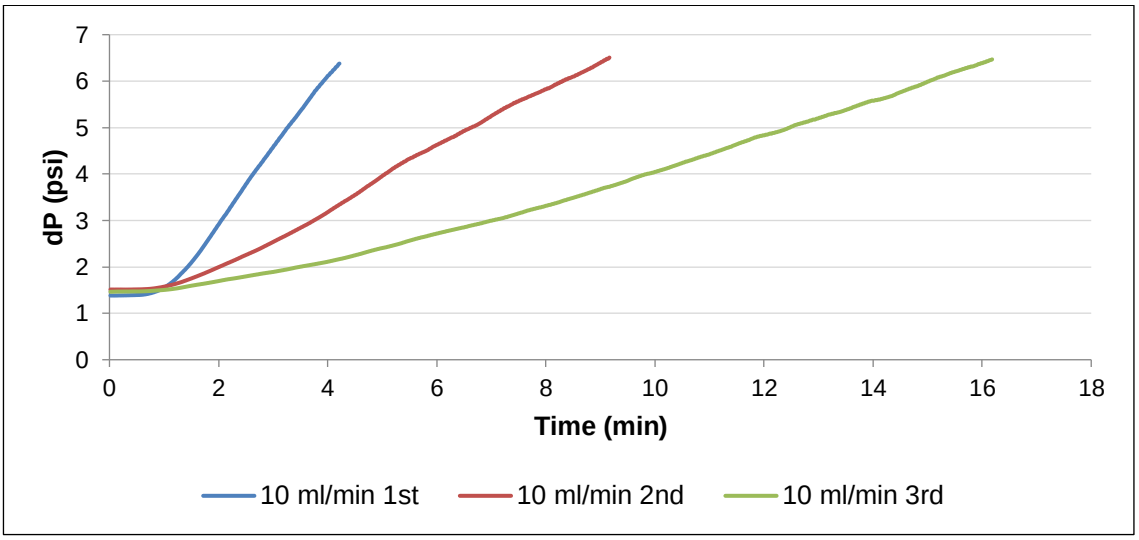

Figure 9.9 FeS formation using modified pH adjustment of H_2S brine. Khuff FW at T = 120°C P = 500 psi 7 µm filter Q_{total} = 10 mL/min. Final pH 6.7.

9.2.4 ZnS inhibition – static and dynamic comparison

A series of ZnS formation and inhibition tests were carried out in 3.5 wt% NaCl to compare the behaviour in static and dynamic environments. Figure 9.10 to Figure 9.14 show the Zn concentrations in the supernatant solutions after 2 and 24 h in blank and inhibited solutions. The initial Zn and H_2S concentrations after mixing were 100 ppm and 30 ppm, respectively. As shown in Figure 9.10 the Zn concentration in the Blank solution at pH 4.5 decreased from 100 ppm to 64 ppm and 47 ppm after 2 and 24 h, respectively. At pH 4.97, the Zn concentration declined to 58 ppm and 43 ppm when the samples were collected after 2 and 24 h without filtration. The slight increase in the amount of ZnS precipitation was attributed to the increase in the pH and hence the decrease in ZnS solubility.

In comparison to the Blank solutions, all tested scale inhibitors delayed or prevented the deposition of ZnS. Figure 9.11 shows the Zn concentrations in the presence of 100 ppm SI-1 (PPCA) at different pH values. At pH 4.05, the deposition of ZnS was delayed; however, a significant mass of ZnS deposited after 24 h and in addition further decrease in the Zn concentration was observed in the filtered sample. On the other hand, when the tests were performed under the same conditions but at higher pH values, the deposition were prevented and moreover the particle size of the inhibited ZnS was less

than 0.2 µm indicated by the comparable Zn concentrations in the unfiltered and filtered samples.

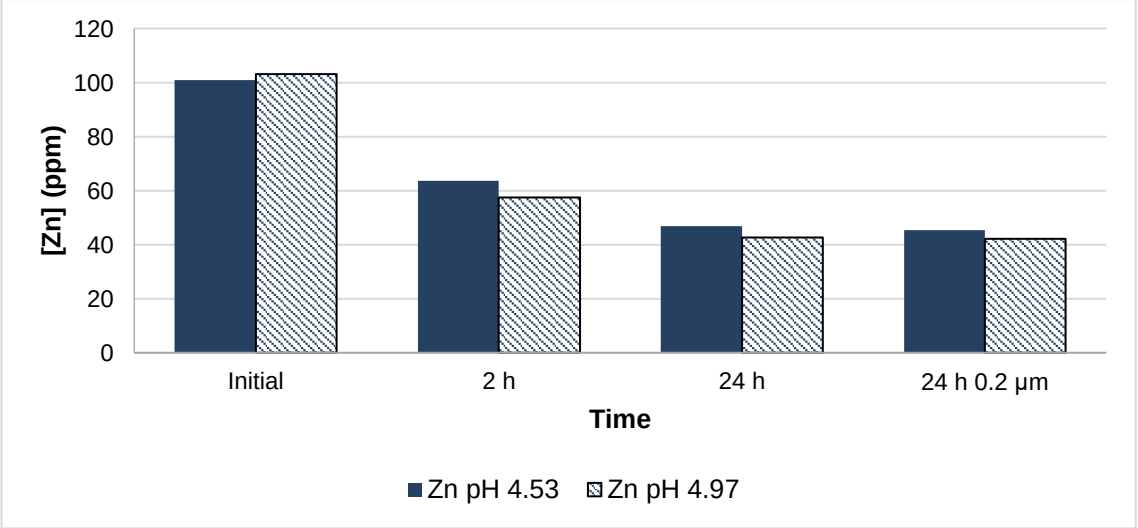

Figure 9.10 Zn concentrations for uninhibited ZnS formation in 3.5 wt% NaCl at 23°C. Initial Zn = 100 ppm; initial H_2S = 30 ppm.

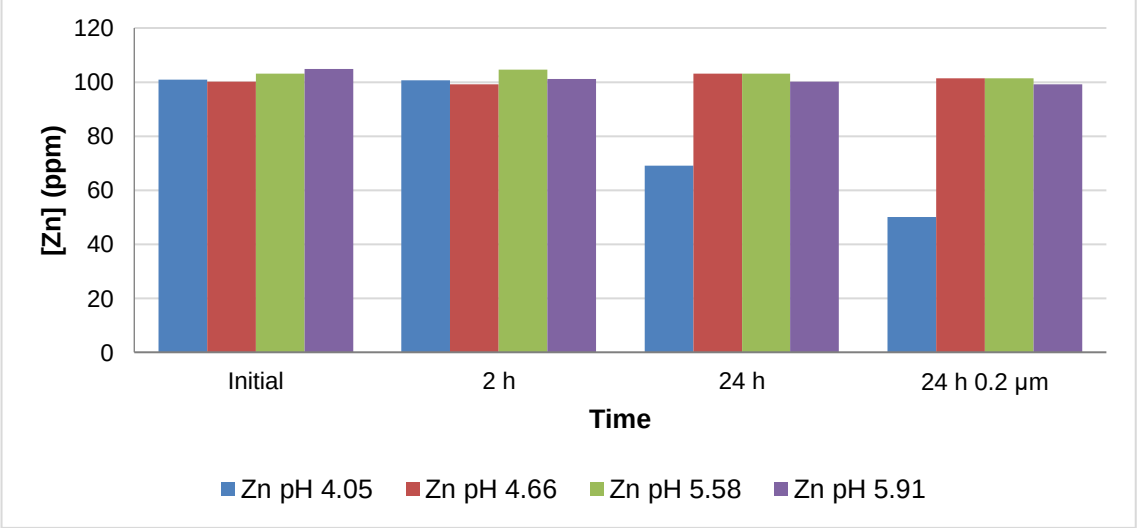

Figure 9.11 Zn concentrations in the 100 ppm SI-1 solutions in the presence of 30 ppm H_2S at 23°C in 3.5 wt% NaCl.

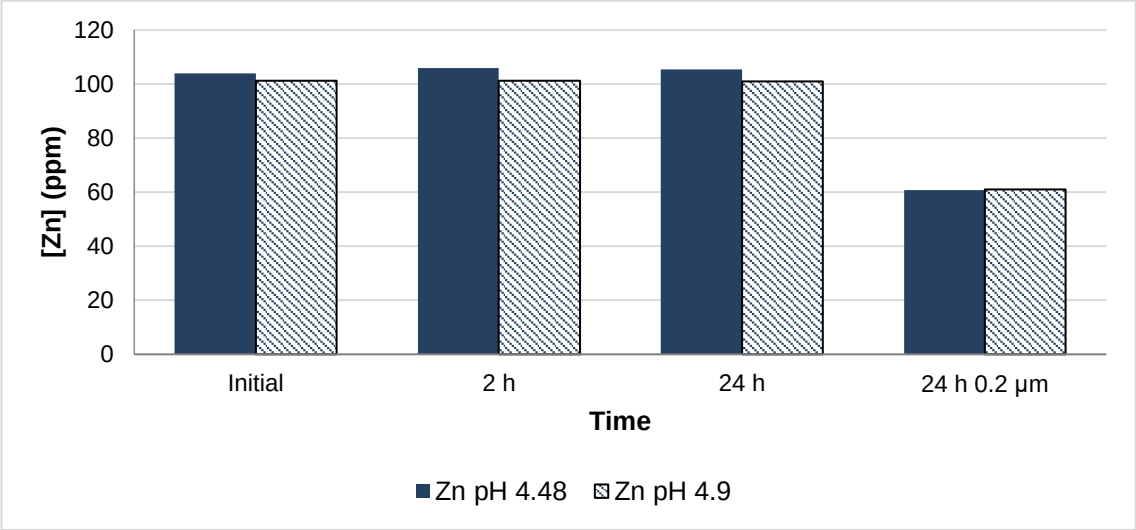

Figure 9.12 Zn concentrations in the 100 ppm SI-2 solutions in the presence of 30 ppm H_2S at 23°C in 3.5 wt% NaCl.

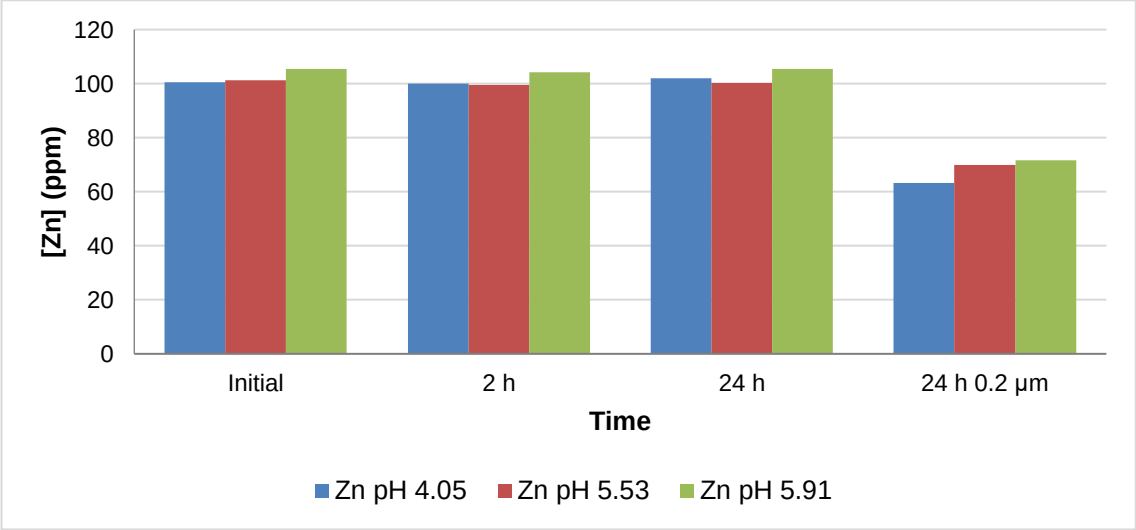

Figure 9.13 Zn concentrations in the 100 ppm SI-3 solutions in the presence of 30 ppm H_2S at 23°C in 3.5 wt% NaCl.

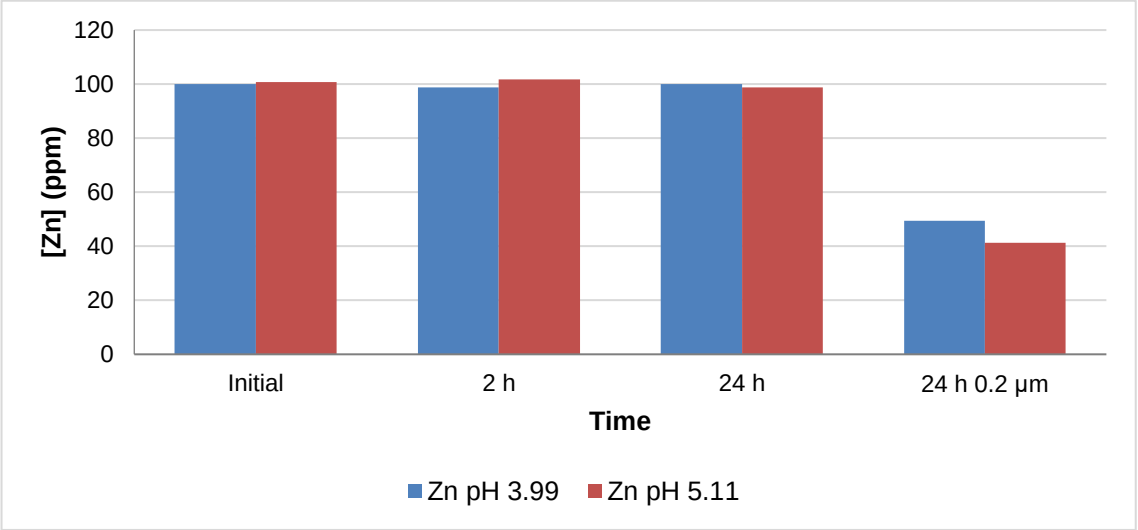

Figure 9.14 Zn concentrations in the 100 ppm SI-8 solutions in the presence of 30 ppm H_2S at 23°C in 3.5 wt% NaCl.

Filter-blocking tests were conducted under the same conditions for the scale inhibitors used in the static tests. These scale inhibitors were selected because they showed high inhibition efficiency and represent different chemistries. The scaling time for the Blank solution at pH 4.5 was around 5.4 min (Figure 9.15). The addition of 100 ppm SI-1 at pH 4.04 extended the scaling time to 9.2 min despite the fact that there was ZnS deposition in the static tests. 100 ppm SI-1 pH caused the particle size to drop below 0.2 µm and yet the scaling time was 8 min *i.e.* less than the low pH SI-1 solution.

Although SI-2 was very effective against ZnS, the scaling time using 100 ppm SI-2 (3.7 min) was less than that observed in the Blank solution. The decrease in the scaling time, in spite of previously observed high inhibition efficiency, might be attributed to the formation of Zn-SI complexes or the viscosity of high concentration of high molecular weight SI. Both 100 ppm SI-3 and 100 ppm SI-8 prevented the deposition of ZnS at all tested pH values and extended the scaling time in the dynamic tests. In terms of inhibition efficiency based on scaling time, the most effective scale inhibitors were SI-1 and SI-8 followed by SI-3 while SI-2 caused the scaling time to decrease compared to the Blank solution.

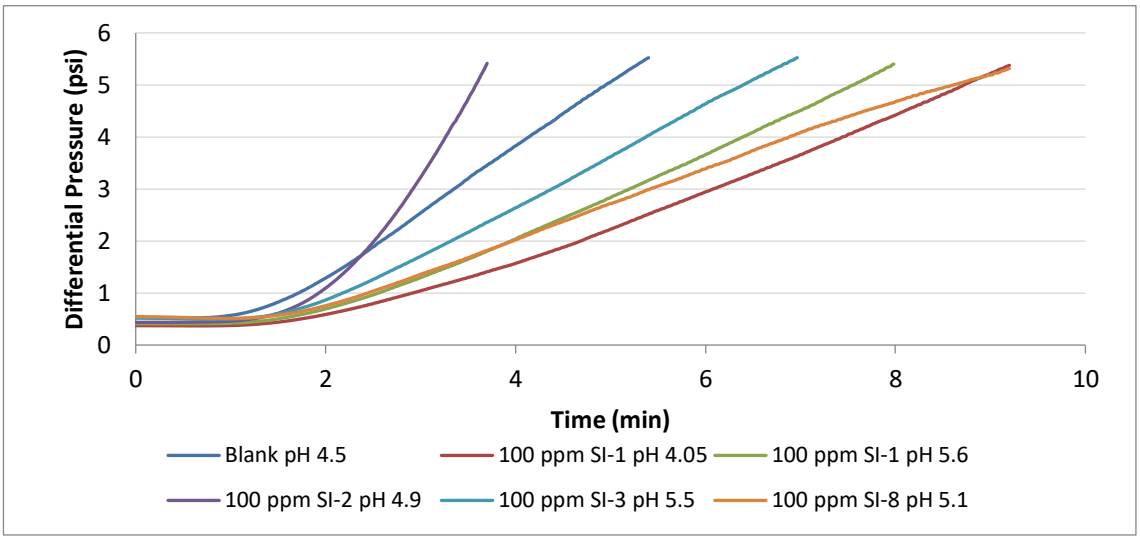

Figure 9.15 ZnS inhibition by different SIs T = 23°C P = 500 psi 7 µm filter Q_{total} = 10 mL/min. 3.5 wt% NaCl, 30 ppm H_2S and 100 ppm Zn.

9.3 Summary and conclusions

In this study, a filter-blocking rig was used to evaluate the inhibition efficiency of different scale inhibitors against FeS or ZnS. As explained above, one of the main advantages of dynamic testing is the ability to evaluate the performance of scale inhibitors at elevated temperatures and pressures that cannot be tested using the conventional static tests.

In a conventional tube blocking rig, a pressure increase is noted when a significant amount of the scale has formed by the comingling of two pre-heated brines and has adhered to the inner surface of a metal coiled tube (the test coil). Due to the nature and mass of the sulphide scales expected to form in these tests, it was decided to use filter-blocking rather than tube-blocking tests. The impact of scale type, filter size and salinity with and without scale inhibitor was studied at mild conditions. The impact of the scale inhibitor type and concentration on the scaling time was also examined. The procedure was modified to overcome the problem associated with mixing low-pH KFW with high pH H_2S KFW.

The main conclusions from this work are:

1. There are several factors affecting the scaling time including the type of the scale, the filter size and the injection flow rate. The scaling times for FeS were shorter than that for ZnS solutions under the same conditions, which has been attributed to the difference in the resultant particle sizes, as well as the nature of

FeS. This latter explanation was based on the agglomeration of FeS noted in the static tests at similar conditions.

2. Preliminary experiments showed that good repeatability was achieved when using a 7 μm and a total flow rate of 10 ml/min (5 ml/min cation brine and 5 ml/min sulphide brine). It was found that rig metallurgy was vitally important to repeatable results. When experiments were carried out at high temperature/salinity and high H_2S concentrations the stainless steel 316 filter was seen to be incompatible and was replaced by a Hastelloy alternative.

3. The dispersive nature of sulphide scale inhibitors was observed during the filter-blocking tests *i.e.* increasing the scale inhibitor concentration caused the particle size to decrease as observed by scaling time extension. As with the static tests, it may be possible to keep formed sulphide scales in suspension even at low inhibitor loading (25 ppm SI-2 doubled the scaling time of the Blank solution at 7 μm) however if operational requirements dictate smaller particle size then higher concentrations SI may be needed.

4. The change in the scaling time can be affected by not only the inhibition efficiency but also metal-SI complexes. This is important to consider when testing conventional scales in presence of heavy metals such as Pb, Zn and Fe even if there was no H_2S.

Chapter 10

Conclusions, Recommendations and Future Work

10.1.1 Introduction

Iron sulphide (FeS), zinc sulphide (ZnS) and lead sulphide (PbS) have been outstanding problems in many oil and gas producer wells in reservoirs around the World. The formation of sulphide scales can pose safety hazards and have serious economic consequences. There are two ways to mitigate the sulphide scale problems namely scale removal by chemical or mechanical means and through prevention using scale inhibition. The mechanical removal is not cost effective, while the chemical treatment option is associated with several drawbacks including the high corrosion rate, H_2S generation or limited scale dissolving power. Therefore, efficient scale inhibition is preferred to scale removal in most cases. There are many publications which discuss the inhibition of sulphide scales; however, there is a lack of deep understanding of the factors that affect sulphide scale formation and inhibition. In this work, sulphide scale formation and inhibition have been systematically investigated to understand the factors governing the formation of the three sulphide scales (FeS, ZnS and PbS) both as single scales and when formed concurrently or consecutively.

10.1.2 Summary

This thesis presents a systematic investigation of the formation and inhibition of iron sulphide (FeS), zinc sulphide (ZnS) and lead sulphide (PbS) scales over a wide range of parameters including temperature, pH, salinity and initial concentrations of Fe, Zn, Pb and sulphide species.

The formation of these sulphide scales as single scales and/or combined scales was studied to understand the interactions between Fe, Zn and Pb in sulphide solutions prior to conducting inhibition experiments. Several scale inhibitors were then tested for their inhibition efficiency against ZnS and PbS under aerobic conditions and for FeS under mainly anaerobic conditions. In addition, iron hydroxide inhibition was studied as an extension of the aerobic FeS experiments

The chosen inhibitors included a selection of commonly used “conventional” scale inhibitors (phosphonates and polymers) as well as two proprietary high molecular weight sulphonated co-polymers (SI-2 and SI-3). The experimental procedures were then modified to study the effect of ion displacement and scale formation sequence (concurrent or consecutive sulphide formation) on inhibition efficiency. An extensive

series of ZnS and FeS inhibition experiments was conducted using PPCA (denoted SI-1 throughout the thesis) to study the inhibition efficiency in addition to the scale inhibitor consumption. A filter-blocking rig was also used to evaluate the inhibition efficiency of polymeric and phosphonate scale inhibitors against FeS and ZnS. Also, the impact of filter size and the type of scale on the scaling time was examined in these filter blocking experiments. The mixing procedure was slightly modified to overcome the unexpected pressure increase which was attributed to some solution incompatibilities.

10.1.3 Conclusions

The formation of both ZnS and PbS are effectively instantaneous and moreover the reactions between Zn^{2+} and S^{2-}, and Pb^{2+} and S^{2-} were both seen to be fully quantitative at oilfield representative pH values. It is therefore true to say that for PbS and ZnS experiments where the sulphide species are in high excess to initial Pb and Zn concentrations, essentially complete precipitation of Pb and Zn would occur.

The solubilities of FeS, ZnS and PbS are all extremely low, however there still exists a differential solubility between these species *i.e.* PbS is less soluble than ZnS and FeS is most soluble of all (but FeS is still very insoluble). This solubility hierarchy was observed experimentally by the fact that the more soluble cation (Fe or Zn) would not form unless *all* of the less soluble cation (Zn or Pb) had precipitated from solution. Indeed, the relative solubility products were the driving force for complete cation exchange when lead was added to pre-formed $ZnS_{(s)}$. Similarly, full FeS dissolution was observed after the addition of Pb^{2+} or Zn^{2+}, with the concurrent formation of lead or zinc sulphide. For scale removal design, the difference in solubility between the scales should be considered as any exchange, even on the outer layer, would act as a barrier that prevents the dissolution of the other scales.

For PbS and ZnS inhibition experiments, the performance of the scale inhibitors can be directly evaluated based on the concentrations of Pb and Zn detected in the supernatant solutions. On the other hand, the well-documented pH sensitivity of FeS was seen to complicate the interpretation of the "apparent inhibition" of tested chemistries. At the conditions tested, FeS solids were only formed at pH values greater than or equal to 4.5, therefore any inhibition results must also account for the underlying solubility of the scale. It was found that the use of a 0.2 µm in-line filter was able to remove even the

smallest FeS particles from test solutions, therefore allowing for the differentiation of aqueous Fe (from pH-driven solubility) from suspended FeS (from the inhibitor).

From the chemistries studied within this thesis and from the literature available to date, there are *no* scale inhibitors capable of retaining iron, zinc or lead sulphide in solution at sub-stoichiometric concentrations. This "ineffectiveness" is driven by the extremely low solubility of all three sulphide scales. The "apparent inhibition" of sulphide scales observed throughout this study was, in fact, driven by the suspension of precipitated scale solids and therefore the delay, in some cases indefinitely, of the deposition of the scale particles.

SI-2 and SI-3 were the only inhibitors to successfully prevent the deposition of FeS, ZnS and PbS scales regardless of the final pH of the supernatant solutions. SI-2 outperformed all of the other inhibitors for mitigating FeS, ZnS and PbS deposition at all tested conditions *i.e.* 95°C, high salinity brines and pH range 3 to 7. Although SI-3 showed some efficacy, increasing the pH and salinity had a negative effect on the performance against FeS, ZnS and PbS inhibition.

The mode of action for SI-2 was studied and our results revealed a significant decrease in the size of the resultant precipitate to below the size of the uninhibited FeS, ZnS and PbS. This effect was increased by increasing the scale inhibitor concentration. Therefore, if the operational needs require the reduction of sulphide scale particles below certain sizes, *e.g.* 0.45 or 0.2 µm, then higher concentrations of inhibitor will be required for the smaller particle sizes. In this work, inhibited test solutions passed thought the 0.45 µm size criterion, but none passed through the 0.2 µm filter. This size filter *i.e.* 0.2 µm retained inhibited FeS, ZnS and PbS particles and so can be used to remove sulphide scales to differentiate between the truly dissolved metal ions and colloidal sulphide scale, to obtain accurate SI measurements using Hyamine and sulphide measurements using UV-Vis spectrophotometric analytical methods.

The phenomenon of metal displacement driven by the greater affinity of another metal has been used extensively in the mining industry. In this thesis, for the first time the impact of this phenomenon on the inhibition efficiency was investigated. When ZnS and PbS were allowed to form prior to scale inhibitors addition, they did "reverse" the scale deposition. Furthermore, when ZnS had formed, then lead /scale inhibitor solution was added to the preformed ZnS, neither SI-2 nor SI-3 were able to prevent PbS deposition

by ionic displacement of Zn from ZnS by Pb^{2+} despite the fact that both scale inhibitors were effective against PbS under the same conditions using the conventional scale inhibition experiments. Therefore, before implementing the scale treatment, any suspended or deposited sulphide scale must be efficiently removed from the production system otherwise the least soluble sulphide scale would deposit on the preformed scale.

Some scale inhibitors reduced the particle size of the deposited ZnS scale. Therefore, this phenomenon might delay the deposition of sulphide scale in dynamic systems or they might be further developed or mixed with other scale inhibitors such as SI-2 to improve the inhibition efficiency.

SI-1 (PPCA) was found to be incompatible with Zn ions when the conditions were slightly changed (T = 50°C and pH > ~ 5.5) although the solutions were clear at more benign conditions *i.e.* 23°C and pH 4. 100 ppm SI-1 prevented the deposition of ZnS and PbS in 3.5 wt% NaCl. At conditions similar to ZnS and PbS tests, 100 ppm SI-1 did not inhibit FeS. Therefore, it is easier to inhibit ZnS and PbS despite the fact that the solubility of FeS is higher than that those of ZnS and PbS. In addition, there was an improvement in the inhibition efficiency at higher pH values and the inhibited ZnS became less than 0.2 µm. In mixed ZnS/FeS solutions, both ZnS and FeS deposited despite the fact that SI-1 was effective against ZnS under the same conditions. Hence, the presence of FeS had a negative impact on the inhibition efficiency for ZnS and more likely similar effect would occur in FeS/conventional scales systems.

For the first time, the fate of scale inhibitor in sulphide scale solutions was investigated by carrying out "SI consumption" experiments. The scale inhibitor was consumed in ZnS and PbS forming experiments. For example, in the presence of 10 ppm SI-1 in ZnS solutions, the scale inhibitor was completely consumed and in 50 ppm SI-1/ZnS solutions, around 40 ppm was consumed. On the other hand, there was no reduction in the scale inhibitor concentration in FeS solutions, despite the complete precipitation of FeS. The reduction in the scale inhibitor concentrations due to either incompatibility issues as explained above or consumption in sulphide scale solutions should be considered when designing scale inhibitor treatments, as this might lead to underestimating the MIC.

We slightly modified the experimental procedure to allow one sulphide scale *e.g.* PbS to form prior to another one *e.g.* ZnS. In these experiments, all sulphide scales formed by

direct reaction between sulphide and the scaling metal as the sulphide was in excess to the total Pb and Zn ions. In SI-2 solutions, the MIC for ZnS and PbS when Zn and Pb were concurrently mixed with sulphide, was less than when zinc was added to a mixture of pre-mixed lead, sulphide and inhibitor. In SI-1 solutions, it was easier to inhibit PbS and ZnS when they formed concurrently rather than forming PbS followed by ZnS. These results are in line with the difference in the MIC observed in SI-2 solutions. `In the oilfield system, PbS and ZnS precipitate due to the increase in the pH and decrease in the temperature and PbS would be expected to precipitate before ZnS because of the difference in the solubility. In addition, unlike PbS and ZnS, the solubility of FeS is lower at high temperature, therefore the sequence of sulphide scales deposition in a production system might be different from what occurs in conventional scale inhibition tests and consequently the scale inhibitor concentration required to inhibit sulphide scale may also change accordingly.

10.2 Future Work

It is recognised by the author that the range of tests that could be performed, even on the limited number of current sulphide scale inhibitors, is effectively endless. However, it is recognized that there is a significant potential for nearly all producing oil wells to sour over time, including those already experiencing the formation of the common inorganic scales *i.e.* barite and calcite. It would therefore appear most pressing to investigate the interactions between sulphide scales and conventional scales and to explore the effect of co-formation on the inhibition chemistries that have shown potential against sulphide scales.

Experimentally, it is common practice to mix scaling cations with scaling anions in one stage, however this will not be the case in dynamic production streams. Further method and equipment development is required to approach a more field-representative analogue of this process, especially to accommodate high pressures and temperatures. Also, it is recommended to investigate scale formation and inhibition using different filter sizes and formation rock instead of the filter. Our preliminary work presented in this thesis has shown that the precise mechanism and sequence of sulphide scale formation affects how much SI is required to inhibit the process.

From this study, SI-1 (PPCA) was consumed during ZnS and PbS inhibition tests but not for FeS. It is therefore recommended that more work should be undertaken to

examine the scale inhibitor consumption of different scale inhibitor chemistries and to generally gain a greater appreciation of the "final destination" of the inhibitor molecules used for sulphide scale control. The final fate of the SIs is important both for practical and theoretical reasons.

The most promising inhibitor chemistry studied herein was a high-molecular-weight sulphonated co-polymer, which showed a significant ability to suspend formed sulphide scale particles over a wide range of conditions. Such high molecular weight polymers may be susceptible to shear degradation (breakage of the polymer backbone due to mechanical stress). These mechanical stresses are common during the injection processes used for scale inhibitor injection. It would therefore be of interest to examine the viscosity, molecular weight distribution and effective MIC values as a function of applied shear stress for these types of chemistries.

References

Al-Khaldi, M.H., Al-Juhani, A.M., Al-Mutairi, S.H. and Gurmen, M.N. 2011. New Insights into the Removal of Calcium Sulphate Scale. SPE European Formation Damage Conference. Noordwijk, the Netherlands, 7-10 June.

Allaga, D.A., Wu, G., Sharma, M.M. and Lake, L.W. 1992. Barium and Calcium Sulphate Precipitation and Migration Inside Sandpacks. SPE Formation Evaluation 79-86.

Baba, A.A. and Adekola, F.A. 2012. A Study of Dissolution Kinetics of a Nigerian Galena Ore in Hydrochloric Acid. Journal of Saudi Chemical Society. 16, 4, 377-386.

Baraka-Lokmane S., Hurtevent C., Tillement O., Simpson, C. and Graham, G. M., 2015. Development and Qualification of New Zinc and Lead Sulphide Scale Inhibitors for Application under Harsh Conditions. SPE International Symposium on Oilfield Chemistry. Society of Petroleum Engineers, The Woodlands, Texas, USA, 13-15 April.

Baraka-Lokmane, S., Hurtevent, C., Rossiter, M., Bryce, F., Lepoivre, F., Marais, A., Tillement, O., Simpson, C. and Graham G.M. 2016. Design and Performance of Novel Sulphide Nanoparticle Scale Inhibitors for North Sea HP/HT Fields. SPE International Oilfield Scale Conference and Exhibition. Society of Petroleum Engineers, Aberdeen, UK, 11-12 May.

Barrett, T. J. and Anderson, G. M.: "The solubility of Sphalerite and Galena in 1-5M NaCl solutions to 300°C", Geochina et Cosmochima Acta (1988) 52, 813.

Barthorpe, R.T. 1993. The Impairment of Scale Inhibitor Function by Commonly Used Organic Anions. SPE International Symposium on Oilfield Chemistry. New Orleans, LA, USA, 2-5 March.

Berry, S. L., Boles, J. L., Singh, A. and Hashim, I. 2012. Enhancing Production by Removing Zinc Sulphide Scale from an Offshore Well: A Case Histroy. SPE Production and Operations, 318-326.

Biggs, K., Allison, D. and Ford, W. G. F., 1992. Acid Treatment Removes Zinc Sulphide Scale Restriction. Oil and Gas Journal.

Bittner, S.D., Zemlak, K.R. and Korotash, B.D. 2000. Coiled Tubing Scale Removal of Iron Sulphide- A Case Study of the Kaybob Field in Central Alberta. SPE/ICoTA Coiled Round Table. Houston, Texas, 5-6 April.

Chase, M. W., Davies, C. A., Downey, J. R., Frurip, D. R., McDonald, R. A. and Syverud, A. N. 1985. JANAF Thermochemical Tables. J Phys Chem Ref Data 14 (1): 1-1856.

Chen, T., Montgomerie, H., Chen, P., Hagen, T. H. and Kegg, S. J. 2009. Development of Environmentally Friendly Iron Sulphide Inhibitors for Field Application. SPE International Symposium on Oilfield Chemistry, The Woodlands. Texas, USA, 20-22 April.

Chen, T., Chen, P., Hagen, T., Montgomerie, H. and Heath, S. 2013. Scale Squeeze Treatments in Short Perforation and High Water Production ESP Wells – Applcation of Oilfield Scale Management Toolbox. International Petroleum Technology Conference. Beijing, China, 26-28 March.

Chen, T., Wang, Q., Chang, F.F. and Al-Janabi, Y.T. 2016. New Develpments in Iron Sulphide Dissolvers. International NACE Corrosion Conference and Expo.

Chenglong, Z. and Youcai, Z., 2009. Mechanochemical Leaching of Sphalerite in an Alkaline Solution Containing Lead Carbonate. Hydrometallurgy 100, 56-59.

Chenglong, Z., Youcai, Z., Cuixiang, G., Xi, H. and Hongjiang, L.., 2008. Leaching of zinc sulphide in alkaline solution via chemical conversion with lead carbonate. Hydrometallurgy 90, 19–25.

Clever, H. L. and Johnston, F. J.: "The Solubility of Some Sparingly Soluble Lead Salts: An Evaluation of the Solubility in Water and Aqueous Electrolyte Solution", *J. Phys. Chem. Ref. Data* (1980) Vol. **9**, No. 3, 751-784.

Boak, L.S., Graham, G.M. and Sorbie, K.S. 1999. The Influence of Divalent Cations on the Performance of $BaSO_4$ Scale Inhibitor Species. SPE International Symposium on Oilfield Chemistry. Houston, Texas, 16-19 February.

Collins, I.R., Cowie, L.G., Nicol, M. and Stewart, N.J. 1999. Field Application of a Scale Inhibitor Squeeze Enhancing Additive. SPE Production and Facilities 14 21-29.

Collins, I. R. and Jordan, M. M. 2001. Occurrence, Prediction, and Prevention of Zinc Sulphide Scale Within Gulf Coast and North Sea High-Temperature and High-Salinity Production Wells. SPE International Symposium on Oil Field Scale, Aberdeen, UK, 30-31 January.

Dyer, S., Solutions, S., Orski, K., Menezes, C., Total, E., Heath, S., Macpherson, C., Simpson, C., Graham, G., 2006. Development of Appropriate Test Methodologies for the Selection and Application of Lead and Zinc Sulphide Inhibitors for the Elgin/Franklin Field. Solutions 1–15.

El-Hajj, H., Peng, Y., Fan, C., AlBuraikan, R., Leal, J. and Chang, F. 2015. A Systematic Approach to Dissolve Iron Sulphide Scales. The SPE Middle East Oil and Gas Show and Conference, Manama, Bahrain, 8-11 March.

Elkatatny, S. 2017. New Formulation for Iron Sulphide Scale Removal. The SPE Middle East Oil and Gas Show and Conference, Manama, Bahrain, 6-9 March.

Emmons, D. and Chesnut, G. R. 1988. Hydroxyethylacrylate/Acrylate Coplymers as Zinc Sulphide Scale Inhibitors. US Patent 4,762,626.

Ford, W.G.F., Walker, M.L., Halterman, M.P., Brawley, D.G. and Fulton, R.G. 1992. Removing a Typical Iron Sulphide Scale: The Scientific Approach. SPE Rocky Mountain Reginal Meeting, SPE-24327-MS. Casper, Wyoming, USA.

Franco, C.A., Solares, J.R., Al-Marri, H.M., Mukhles, A.E., Ramadhan, N.H. and Saihati, A.H. 2010. Analysis of Deposition Mechanism of Mineral Scales Precipiating in the Sandface and Production Strings of Gas-Condensate Wells. SPE Production and Operations 161-171.

Frigo, D.M., Jackson, L.A., Doran, S.M. and Trompert, R.A. 2000. Chemical Inhibition of Halite Scaling in Topsides Equipment. International Symposium on Oildfield Scale, Aberdeen, UK, 26-27 January.

Gdanski, R. 2008. Formation Mineralogy Impacts Scale Inhibitor Squeeze Designs. SPE Europe/EAGE Annual Conference and Exhibition. Rome, Italy, 9-12 June.

Gougler Jr, P. D., Hendrick, J. E. and Coulter, A. W. 1985. Field Investigation identifies Source and Magnitude of Iron Problems. SPE Production Operations Symposium, Oklahoma, USA, 10-12 March.

Graham, A.J., Al-Harbi, B.G., Singleton, M.A., Collins, I. R. and Sorbie, K. S., 2017. Cation Exchange in Sulphide Scales. the Chemistry in the Oil Industry symposium, Manchester, UK, 6-8 November.

Graham, G.M., Boak, L.S and Sorbie, K.S. 1997. The Influence of Formation Calcium on Effectiveness of Generically Different Barium Sulphate Oilfield Scale Inhibitors. SPE International Symposium on Oilfield Chemistry. Houston, Texas, 18-21 February.

Hafiz, T., Hoegerl, M., AlSuwaij, A. and Almathami, A. 2017. Synethetic Iron Sulphide Scale and Polymeric Scale Dissolvers. The SPE Middle East Oil and Gas Show and Conference, Manama, Bahrain, 6-9 March.

Hartog, F. A., Jonkers, G., Schmidt, A. P., and Schuiling, R. D., 2002. Lead Deposits in Dutch Natural Gas Systems. *SPE Prod. Facil.*, 122-128.

Ho, K., Chen, T., Chen, P., Hagen, T., Montgomerie, H. and Benvie, R. 2014. Development of Novel Test Methodology to Understand the Mechanisms of Halite Inhibition and Enviromentally Acceptable Halite Scale Inhibitors for High Temperature Application. SPE International Oilfield Scale Conference and Exhibition. Aberdeen, Scotland, UK, 14-15 May.

Holdich, R. G. and Lawson, G. J. (1987) The Solubility of Aqueous Lead Chloride Solutions, *Hydrometallurgy*, 19(2), pp.199-208.

Jarrahian, K., Sorbie, K.S., Singleton, M.A., Boak, L.S. and Graham, A.J. 2019. The Effect of pH and Mineralogy on the Retention of Polymeric Scale Inhibitors on Carbonate Rocks for Application in Squeeze Treatments. SPE Production and Operations, 344-360.

Jordan, M. M., Sjursaether, K., Edgerton, M.C. and Bruce, R. 2000. Inhibition of Lead and Zinc Sulphide Scale Deposits Formed during Production from High Temperature Oil and Condensate Reservoirs. SPE Asia Pacific Oil and Gas Conference and Exhibition. Society of Petroleum Engineers, Brisbane, Australia, 16-18 October.

Jordan, M.M. and Williams, H. 2016. Insights on the Impact of Fluid Cooling on High Temperature Conditions (175°C) for Carbonate and Sulphate Scale Dissolver Performance. NACE Corrosion Conference and Expo.

Kan, A.T., Fu, G., Al-Saiari, H., Tomson, M.B. and Shen, D. 2009. Enhanced Scale-Inhibitor Treatments With the Additive of Zinc. SPE Journal 617-626

Kan, A.T., Fu, G. and Tomson, M.B. 2005. Prediction of Scale Inhibitor Squeeze and Return in Calcite-Bearing Formation. SPE International Symposium on Oilfield Chemistry. Houston, Texas, USA, 2-4 February.

Kasnick, M. A., and Engen, R. J., 1989. Iron Sulphide Scaling and Associated Corrosion in Saudi Arabian Khuff Gas Wells. SPE Middle East Oil Technical Conference and Exhibition, Manama, Bahrain, 11-14 March.

Keogh, W., Boakye, G.O., Neville, A., Charpentier, T., Olsen, J.H., Eroini, V., Nielsen, F.M., Ellingsen, J., Bache, O., Baraka-Lokmane, S. and Bourdelet, E. 2018. Lead Sulphide (PbS) Scale Behavior and Deposition as a Function of Polymeric Sulphide Inhibitor Concentration in Multiphase. Nace

Kerver, J.K. and Heilhecker, J. K. 1969. Scale Inhibition by the Squeeze Technique. Journal of Canadian Petroleum Technology. V8 i01 p15-23.

Kerver, J.K., Kaiser Jr, A.D., Heilhecker, J.K. and Mckinney, J.M. 1969. Treatment of Solids Plugged Wells with Reversibly Adsorbable Inhibitor. US Patent 3481400A.

Kharaka, Y.K., Maest, A. S., Carothers, W. W., Law, L. M., Lamothe, P. J. and Fries, T. L. 1987. Geochemistry of metal-rich brines from central Mississippi Salt Dome basin, U.S.A. Applied Geochemistry, 2(5-6): 543–561.

King, G.E. and Warden, S.L. 1989. Introductory Work in Scale Inhibitor Squeeze Performance: Core Tests and Field Results. SPE International Symposium on Oilfield Chemistry. Houston, Texas 8-10 February. SPE 18485

Kvarekval, J., Nyborg, R. and Choi, H. 2003. Formation of Multilayer Iron Sulphide Films During High Temperature CO_2/H_2S Corrosion of Carbon Steel. NACE International, NACE-03339. San Diego, California, USA: NACE 2003.

Leal, J. A., Solares, J. R., Nasr-El-Din, H. A., Franco, C. A., Garzon, F. O., Al-Marri, H. M., Al-Aqeel, S. A. and Izquierdo, G. A. 2007. A Systematic Approach to Remove Iron Sulphide Scale: A Case History. SPE Middle East Oil and Gas Show and Conference, 11-14 March, Manama, Bahrain.

Lehmann, M. and Firouzkouhi, F. F. 2008. A New Chemical Treatment to Inhibit Iron Sulphide Deposition and Agglomeration. SPE International Oilfield Scale Conference, Aberdeen, UK, 28-29 May.

Lewis, A.E. 2010. Review of Metal Sulphide Precipitation. Hydrometallurgy, 104 222-234.

Li, W., Ruan, G., Bhandari, N., Wang, X., Liu, Y., Dushane, H. and Tomson, M. 2018. Development of Novel Iron Sulfide Scale Control Chemicals. Society of Petroleum Engineers. SPE International Oilfield Scale Conference and Exhibition, 20-21 June, Aberdeen, Scotland, UK

Lopez, T. H., Yuan, M., Williamson, D.A. and Przybylinski, J. L. 2005. Comparing Efficacy of Scale Inhibitors for Inhibition of Zinc Sulphide and Lead Sulphide Scales. SPE International Symposium on Oil field Scale, Aberdeen, UK, 11-12 May.

Mackay, E.J. and Jordan, M.M. 2003. SQUEEZE Modelling: Treatment Design and Case Histories. SPE European Formation Damage Conference. The Hauge, the Netherlands, 13-14 May.

Mahmoud, M. A., Kamal, M., Bageri, B. S. and Hussein, I. 2015. Removal of Pyrite and Different Types of Iron Sulphide Scales in Oil and Gas Wells without H2S Generation. International Petroleum Technology Conference, 6-9 December, Doha, Qatar.

Mathis, J., Actis Goretta, E., Saubidet, M.L., Castineriras, T., Funes, A., Figini, F., Wang, X. and Economides, M.J. 2013. Formation Damage Caused by Pipe Dope and Its Remediation. SPE Production and Operations Symposium. Oklahoma City, Oklahoma, USA, 23-26 March.

McCartney, R. A., Brice, S. and Chalmers, A. 2016. High Pb and Zn Concentrations in Formation Water from the Culzean Field: Real or Artefact?. SPE International Oilfield Scale Conference and Exhibition. Society of Petroleum Engineers, Aberdeen, UK, 11-12 May.

Miles, L. 1970. A New Concept in Scale Inhibitor Formation Squeeze Treatments. SPE Rocky Mountain Regional Meeting. Casper, Wyoming 8-9 June. SPE2909

Mirza, M.S. and Prasad, V. 1999. Scale Removal in Khuff Gas Wells. Middle East Oil Show and Conference, SPE-53345-MS (Bahrain: SPE 1999), p. 8

Nasr-El-Din, H.A., Lynn, J.D., Hashem, M.K., Bitar, G.E. and Al-Ali, A.A. 2002. Lessons Learned from Descaling Wells in a Sandstone Reservoir in Saudi Arabia. SPE Oilfield Scale Symposium. Aberdeen, UK, 30-31 January.

Nasr-El-Din, H.A., Al-Mutairi, S.H. and Al-Driweesh, S.M. 2002. Lessons Learned from Acid Pickle Treatments of Deep/Sour Gas Wells. SPE International Symposium and Exhibition on Formatio Damage Control. Lafayette, Louisiana, USA, 20-21 February.

Nasr-El-Din, H.A., Al-Saiari, H.A., Al-Hajj, H.H., Samy, M., Garcia, M., Frenier, W. and Samuel, M. 2004. A Single-Stage Acid Treatment to Remove and Mitigate Calcium Carbonate in Sandstone and Carbonate Reservoirs. International Symposium on Oilfield Scale. Aberdeen, UK, 26-27 May.

Nasr-El-Din, H.A., Al-Mutairi, S.H., Al-Hajji, H.H. and Lynn, J.D. 2004. Evaluation of a New Barite Dissolver: Lab Studies. SPE International Symposium and Exhibition on Formation Damage Control. Lafayette, Louisiana, USA, 18-20 February.

Nasr-El-Din, H.A., Fadhel, B.A., Al-Humaidan, A.Y., Frenier, W.W. and Hill, D. 2000. An Experimental Study of Removing Iron Sulphide Scale from Well Tubulars. The international Symposium on Oilfield Scale. Aberdeen, UK,

Nasr-El-Din H. A., and Al-Humaidan, A. Y. 2001, Iron Sulphide Scale: Formation, Removal and Prevention. SPE International Symposium on Oilfield Scale, Aberdeen UK, 30-31 January.

Oddo, J.E., Kan, A.T., He, S., Gerbino, A.J. and Tomson, M. 1997. Method for Scale Inhibitor Squeeze Application to Gas and Oil Wells. US Patent 5655601.

Oddo, J.E., Smith, J.P. and Tomson, M.B. 1991. Analysis of and Solutions to the CaCO3 and CaSO4 Scaling Problems Encountered in Wells Offshore Indonesia. SPE

Annual Technical Conference and Exhibition, Dallas, Texas, USA, 6-9 October. SPE 22782.

Okocha, C and Sorbie, K. S. 2013. Scale Prediction for Iron, Zinc and Lead Sulphides and Its Relation to Scale Test Design. SPE 164111. International Symposium on Oilfield Chemistry, The Woodlands, Texas, USA, 8-10 April.

Okocha, C., Sorbie, K.S., Hurtevent, C., Baraka-Lokmane, S. and Rossiter, M., 2014. Sulphide Scale (PbS/ZnS) Formation and Inhibition Tests for a Gas Condensate Field with Severe Scaling Conditions. SPE International Oilfield Scale Conference and Exhibition. Society of Petroleum Engineers, Aberdeen, UK, 14-15 May.

Okocha, C. and Sorbie, K.S. 2014. Sulphide Scale Co-Precipitation with Calcium Carbonate. SPE International Symposium and Exhibition on Formation Damage Control. Lafayette, Louisiana, USA, 26-28 February.

Okocha, C., Kaiser, A., Underwood, S., Samaniego, W. and Wylde, J. 2018. New Generation Squeezable Sulphide Inhibitor Successfully Averts Challenging Sulphide Scale Depostion in Permian Basin. SPE International Oilfield Scale Conference and Exhibition. Aberdeen, Scotland, UK, 20-21 June.

Orski, K., Grimbert, B., Menezes, C.A. and Quin, E. 2007. Fighting Lead and Zinc Sulphide Scales on a North Sea HP/HT Field. European Formation Damage Conference. Society of Petroleum Engineers, Scheveningen, The Netherlands, 30 May-1 June.

Peng, Y., Yue, Z., Ozuruigbo, C. and Fan, C. 2015. Carbonate Scale Control under High Level of Dissolved Iron and Calcium in the Bakken Formation. SPE International Symposium on Oilfield Chemistry. Society of Petroleum Engineers, The Woodlands, Texas, USA, 13-15 April.

Przybylinski, J. L. 2001. Iron Sulphide Scale Deposit Formation and Prevention under Anaerobic Conditions Typically Found in the Oil Field. International Symposium on Oilfield Chemistry, Houston, Texas, 13-16 February.

Russek, J., Flores, N. and Brooks, J. 2018. A Novel Evaluation of Scale Inhibitor Performance Against Calcium Carbonate Scaling in the Presence of Iron Sulphide. SPE

International Oilfield Scale Conference and Exhibition, Aberdeen, Scotland, UK, 20-21 June.

Saidoun, M., Mateen, K. Baraka-Lokmane, S. and Hurteven, C. 2016. Prediction of Sulphide Scales-Improvement of Our Understanding of Heavy Metal Sulphide Solubility. SPE International Oilfield Scale Conference and Exhibition. Society of Petroleum Engineers, Aberdeen, UK, 11-12 May.

Salman, M., Qabazard, H. and Moshfeghani, M. 2007. Water Scaling Case Studies in a Kuwaiti Oil Field. Journal of Petroleum Science and Engineering. 55 (48-55).

Savin, A. J., Adamson, B., Wylde, J. J., Kerr, J. R., Kayser, C. W., Trallenkamp, T., Fischer, D. and Okocha, C. 2014. Sulphide Scale Control: A High Efficacy Breakthrough Using an Innovative Class of Polymeric Inhibitors. SPE International Oilfield Scale Conference and Exhibition. Society of Petroleum Engineers, Aberdeen, UK, 14-15 May.

Shaw, S. S. and Sorbie, K. S. 2012. The Effect of pH on Static Barium Sulphate Inhibition Efficiency and Minimum Inhibitor Concentration (MIC) of Generic Scale Inhibitors. SPE International Conference on Oilfield Scale, 30-31 May, Aberdeen, UK

Shaw, S. S. and Sorbie, K. S. 2013. Scale-Inhibitor Consumption in Long-Term Static Barium Sulphate Inhibition Efficiency Tests. SPE Production and Operations.

Shen, D., Shcolnik, D., Perkins, R., Taylor, G. and Brown, M. 2012. Evaluation of Scale Inhibitors in Marcellus High-Iron Waters. SPE Oil and Gas Facilities: 34-42.

Shuler, P. J., Daniels, E. J., Burton, L. and Chen, H. J., 2000. Modeling of Scale Deposition in Gas Wells with Very Saline Produced Water. NACE International, Orlando, Florida, USA.

Smith, C. F., Crowe, C. W. and Nolan, T. J. 1969. Seconday Deposition of Iron Compounds Following Acidizing Treatments. Journal of Petroleum Technology.

Smith, J.K. and Przybylinski, J.L. 2006. The Effect of Common Brine Constituents on the Efficacy of Halite Precipitation Inhibitors. Corrosion NACExpo 2006.

Sorbie, K. S. and Laing, N. 2004. How Scale Inhibitors Work: Mechanisms of Selected Barium Sulphate Scale inhibitors Across a Wide Temperature Range. SPE International Symposium on Oilfield Scale, 26-27 May, Aberdeen, United Kingdom.

Sutherland, L. and Jordan, M. 2016. Enhancing Scale Inhibitor Squeeze Retention With Additives. SPE International Oilfield Scale Conference and Exhibition, Aberdeen, Scotland, UK, 11-12 May.

Sutherland, L. and Jordan, M. 2018. Enhancing Scale Inhibitor Squeeze Retention in Carbonate Reservoirs. SPE International Oilfield Scale Conference and Exhibition, Aberdeen, Scotland, UK, 20-21 June.

Taylor, K. C., Nasr-El-Din, H. A. and Al-Alawi, M. J. 1999. Systematic Study of Iron Control Chemicals Used During Well Stimulation. SPE Journal, 19-24.

Todd, M., Strachan, C., Moir, G. and Goulding, J. 2013. Process for inhibition of sulphide scales. WO 2013/152832

Tortolano, C., Chen, T., Chen, P., Montgomerie, H., Hagen, T., Benvie, R. and Zou, L. 2014. Mechanisms, New Test Methodology and Enviromentally Acceptable Inhibitors for Co-deposition of Zinc Sulphide and Calcium Carbonate Scales for High Temperature Application. SPE International Oilfield Scale Conference and Exhibition. Society of Petroleum Engineers, Aberdeen, UK, 14-15 May.

Vazquez, O., Mackay, E., Sorbie, K. and Jordan, M.M. 2009. Impact of Mutual Solvent Preflush on Scale Squeeze Treatments: Extended Squeeze Lifetime and Improved Well Clean-up Time. SPE European Formation Damage Conference, Scheveningen, the Netherlands, 27-29 May. SPE121857

Verri, G., Sorbie, K. S., Singleton, M. A. *et al*., 2017. Iron Sulphide Scale Management in High-H_2S and CO_2 Carbonate Reserviors. SPE Production & Operations, 305-313.

Walker, M.L., Dill, W.R., Besler, M.R. and McFatridge, D.G. 1991. Iron Control in West Texas Sour-Gas Wells Provides Sustained Production Increases. Journal of Petroleum Technlolgy 43, 05 (SPE 1991)

Wang, B., Chen, T., Chen, P., Montgomerie, H., Hagen, T., Liu, X., Yang, X. 2012. Development of Test Method and Environmentally Acceptable Inhibitors for Zinc

Sulphide Deposited in Oil and Gas Fields. SPE International Conference on Oilfield Scale. Society of Petroleum Engineers, Aberdeen, UK, 30-31 May.

Wang, Q., Zhang, Z., Kan, A. and Tomson, M. 2014. Kinetics and Inhibition of Ferrous Sulphide Nucleation and Precipitation. SPE International Oilfield Scale Conference and Exhibition. Society of Petroleum Engineers, Aberdeen, UK, 14-15 May.

Wang, Q., Ajwad, H., Shafai, T. and Lynn, J.D. 2013. Iron Sulphide Scale Dissolvers: How Effective Are They?. SPE Saudi Arabia Section Annual Technical Symposium and Exhibition. Khobar, Saudi Arabia, 19-22 May.

Wang, Q., Leal, J., Syafii, I., Mukhules, A.E., Chen, T., Chang, F. and Espinosa, M. 2016. Iron Sulphide and Removal in Scale Formation Sour Gas Wells. SPE International Oilfield Scale Conference and Exhibition. Aberdeen, UK, 11-12 May.

Wang, Q., Chen, T., Chang, F., Al-Nasser, W. and Liang, F. 2018. Searching for Iron Sulphide Scale Dissolver for Downhole Applications. International NACE Corrosion Conference and Expo.

Wilkin, R.T. and Barnes, H.L. 1996. Pyrite Formation by Reactions of Iron Monosulphides with Dissolved Inorganic and Organic Sulphur Species. Elsevier Science Geochimica et Cosmochimica Acta 60, 21 (1996) 4167-4179

Williams, H., Tortolano, C. and Adenuga, T. 2015. Mechanisms of Environmentally Acceptable Inhibitors for Zinc Sulphide Inhibition. SPE International Symposium on Oilfield Chemistry. Society of Petroleum Engineers, The Woodlands, Texas, USA, 13-15 April.

Wylde, J.J. and Slayer, J.L. 2013. Halite Scale Formation Mechanisms, Removal and Control: A Global Overview of Mechanical, Process and Chemical Strategies. SPE International Symposium on Oilfield Chemistry. The Woodlands, Texas, USA, 8-10 April.

Wylde, J.J., Okocha, C., Smith, R., Mahmoudkhani, A. and Kelly, C.J. 2016. Dissolution of Sulphide Scale: A Step Change with a Novel, High Performance, Non-Mineral Acid Chemical. SPE International Oilfield Scale Conference and Exhibition. Aberdeen, Scotland, UK, 11-12 May.

References

Yap, J., Fuller, M. J., Schafer, L. A. and Kelkar, S. 2010. Removing Iron Sulphide Scale: A Novel Approach. The International Petroleum Exhibition and Conference, Abu Dhabi, UAE, 1-4 November.